FINITE ELEMENT MODELING OF MICROPILES AND THE INFLUENCE OF STEEL CASING ON LOAD TRANSFER MECHANISMS

By Daniel Barron

5/17/2016

A thesis submitted to the

Faculty of the Graduate School of

State University of New York at Buffalo

In partial fulfillment of the requirements for the degree of

Master of Science

Department of Civil, Structural and Environmental Engineering

Geomechanics and Geotechnical Engineering

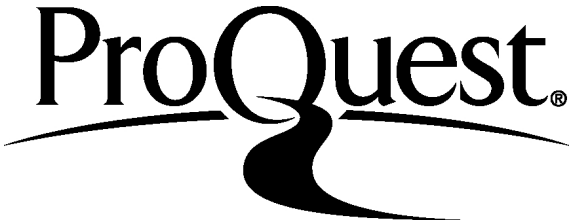

Acknowledgements

To my Father,

Your knowledge and passion for the construction industry is inspiring.

I will never forget all the great work we have done together.

To my Mother,

From you comes my creativity.

Thank you for always supporting my innovative endeavors.

Buffalo Drilling Company, Inc.

Barron and Associates, P.C.

Buffalo Well Products

I would like to thank all of the employees for supporting my research in any way possible over the years, especially James Barron for giving me to opportunity to learn the geotechnical industry. Also, I would like to thank Brad Smith for teaching me the unique science of geology, which has been a large part of my success.

The University at Buffalo

The professional and innovative atmosphere at UB has been a great place to learn over the last few years. I am proud to be a part of such a successful engineering program. I would like to thank both Dr. Sabanayagam Thevanayagam and Dr. Anthony Tessari for always having your doors open. Both of you have been fundamental in guiding me both academically and professionally.

List of Tables

List of Figures

Abstract

Micropiles made their debut as a cost effective way to retrofit existing historical structures. Recently, micropiles have increased in popularity all over the world and are being used for bridges, buildings, slope stability, antenna towers, and residential construction. Micropiles excel in difficult drilling conditions where other deep foundation methods are not plausible and consist of any combination of grout, rebar, hollow bar, steel pin, and steel casing. Due to their slender nature, defined less than 300 mm in diameter and lengths up to 100 feet, micropiles offer a distinct challenge in quantifying load transfer behaviors. Research at the University at Buffalo investigated the load transfer behavior of a single micropile and the influence of steel casing in soil using the finite element software ABAQUS. Soil models of sand, clay, and rock were fabricated. Simulated load testing determined micropile axial and lateral capacities for various cased length ratios, the cased length to micropile length, and were compared to field load tests. For both the clay and sand models an increase in cased length ratio resulted in lower axial capacities and higher lateral capacities. For the lateral case, diminishing returns on lateral capacities are observed for cased length ratios over 1:2. An increase in axial capacity was observed when casing to shale rock. The results are compared to various case studies, typical construction practices, and current design methodologies.

1. Introduction

1.1 Definition of a Micropile

A micropile is defined by the Federal Highway Administration as a drilled pile being equivalent to or less than 300 mm in diameter. They are slender in nature, having a low diameter to length ratio, resulting in a majority of load transfer to the soil from to skin friction. The borehole is grouted along with reinforcing steel, such as steel pipe, steel rod, rebar, or a specialized hollow bar. Many times micropile boreholes are advanced using temporary or permanent casing to prevent the hole from collapsing. Micropiles are known to suitably hold both compression and tension loads. Micropiles can be designed in groups attached via a pile cap or mat to increase the overall load capability of the system. Some driven piles are considered small enough to be labeled as micropiles, however driven micropiles will not be covered in this paper. The micropile can be installed on a batter and is known to be effective in difficult drilling conditions. Micropiles are also commonly called minipiles, pin piles, root piles, needle piles, and friction piles (FHWA, 2005).

1.2 History of the Micropile

Micropiles originated in Europe mainly to stabilize historic or sensitive structures. As the understanding of geomechnanics continued to develop, a greater need for micropiles was recognized. Micropile technology is credited to begin in Italy during the 1950's by Fernando Lizzi, but was not seen in the United States until the 1980's (Bruce & Juran, 1997). Since then, much collaboration and research has been done in the area of micropile design and construction. Today, micropiles are effectively utilized in various scenarios including building underpinning, environmental remediation, excavation stabilization, and slope stability.

A growing understanding of soil mechanics and the seismic effects on foundations has given rise to the use of micropiles. Deteriorating and ageing buildings require foundation retrofitting to withstand the continuing loads from the environment and structure. The versatility of micropile construction has allowed effective stabilization of many older structures. Micropiles have been an integral part of the restoration of monuments in Europe (Lizzi, 1982). The interest in protecting delicate historic structures from serious seismic events has led to the growth of micropiles. Technological innovation in drilling equipment has given micropiles the ability to be constructed in almost every soil and site condition. Specialized drilling rigs and modern materials make micropile capacities possible of reaching more than 500 kN (Bruce & Juran, 1997). Micropiles can be placed at various angles, constructed where minimal vibration is required, and in places with limited space.

An investigation will be made into the various design methods available from different literatures and the commonality among them. A finite element model will compare the differences between theoretical design and field load tests. Design considerations are largely based on the type of soil present. The capacity of the micropile is a combination of skin friction, end bearing resistance, and structural capacity. Varying soil characteristics in clay, sand, and rock offer different assumptions to design a micropile most effectively to hold design loads within deflection restrictions. Construction methods associated with micropiles will also be discussed considering construction techniques, load testing, and instrumentation. The focus of the paper is on the soil-structure interaction of the micropiles specifically investigating the influence various casing lengths has on load transfer mechanisms. Additionally, case studies will be discussed at the end of the paper focusing on each unique micropile application. The case

studies cover construction projects using micropiles for underpinning and new bridge foundations.

1.3 Evolution of Micropile Classification

There exist many different uses for micropiles in the construction, civil, and environmental industry. Micropiles can be used ranging from slope stability to new foundation projects. Each individual design is based on the type of loads the micropile is expected to carry. Some low capacity micropiles are designed solely using grout without any structural steel. However, mostly the micropile design consists of steel counterparts. The structural steel is typically pipe, H-beam, hollow bar, or a steel rod. Grout used can be mixed on or off site, and strength depends on the water to cement ratio used (Shong & Chung, 2003). Larger aggregate may be placed when filling larger diameter bored holes. Commonly, micropiles are classified by their design purpose, structural components, soil stratums encountered, and construction methodology.

The Federal Highway Administration (FHWA) sets forth a classification scheme using two methodologies. FHWA first breaks down the classification of micropiles based on the fundamental theory of how the load is transferred to the soil. Case 1 micropiles are stated as directly loaded piles. Loaded in the axial and/or lateral direction, case 1 micropiles transfer the load directly into competent stratum and are mainly supported by the soil directly surrounding the micropile. Almost all micropiles constructed in North America and 90 percent of international micropiles are identified as Case 1 (FHWA, 2005).

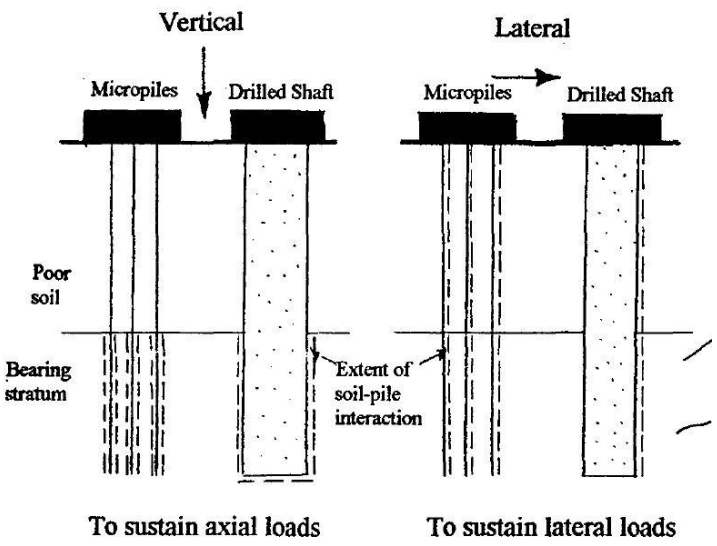

Figure 1-1. Case 1 micropiles transfer direct vertical and lateral loads to competent bearing stratum (Bruce & Juran, 1997)

On the other hand, Case 2 micropiles, developed by Dr. Lizzi focuses on constructing a three-dimensional network of root piles fully bonded over the entire length (Lizzi, 1982). As seen in Figure 1-2, the micropiles are arranged in a way to lower the center of gravity of the structure (FHWA, 2005). Due to the intertwining nature of the micropiles a composite block is constructed below the structure. These micropiles are generally not reinforced or only contain a steel rod in the center to maintain cost effectiveness.

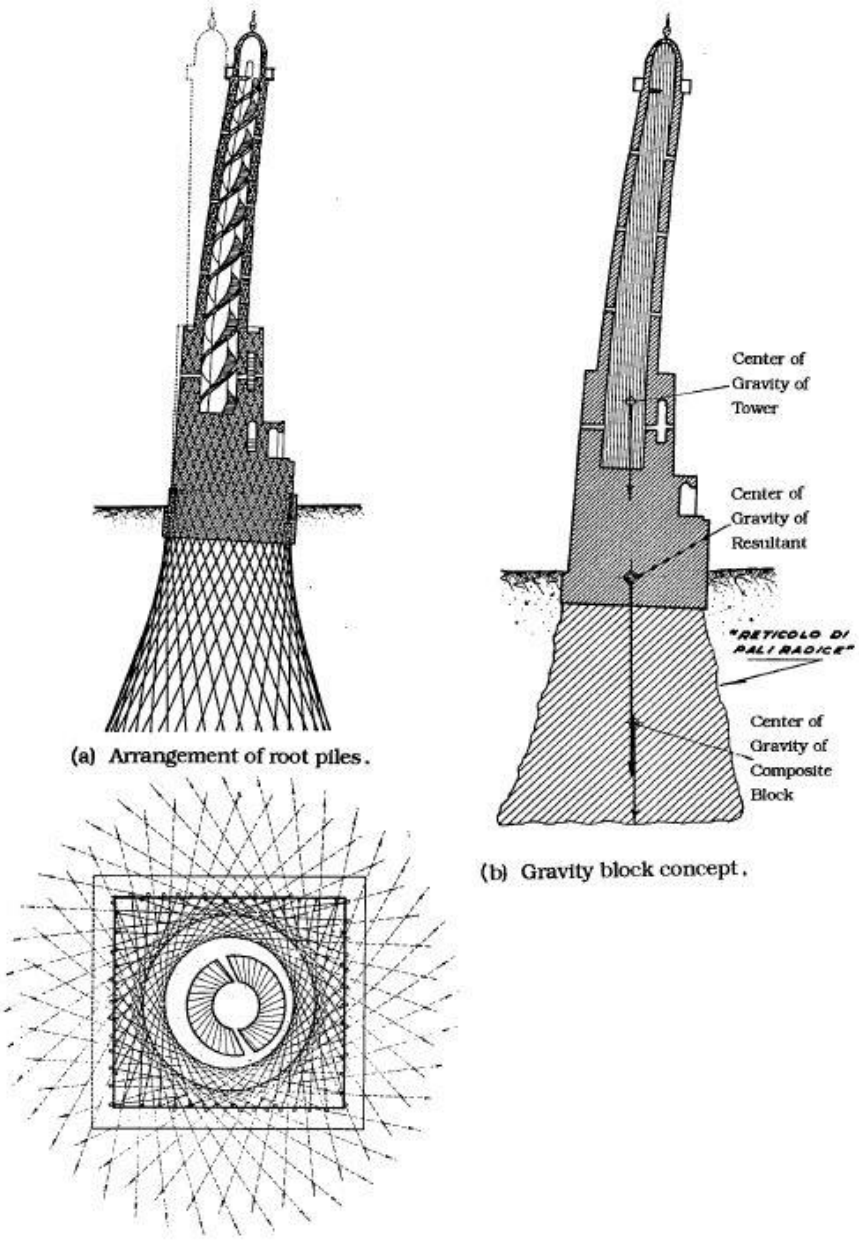

Figure 1-2. Case 2 micropile system utilizes a composite block of micropiles and soil to stabilize the structure (Bruce & Juran, 1997)

In addition, the micropile is classified by the grouting mythology used for placement. As seen in Figure 1-3, grout can be placed four different ways deemed as Type A, Type B, Type C, or Type D.

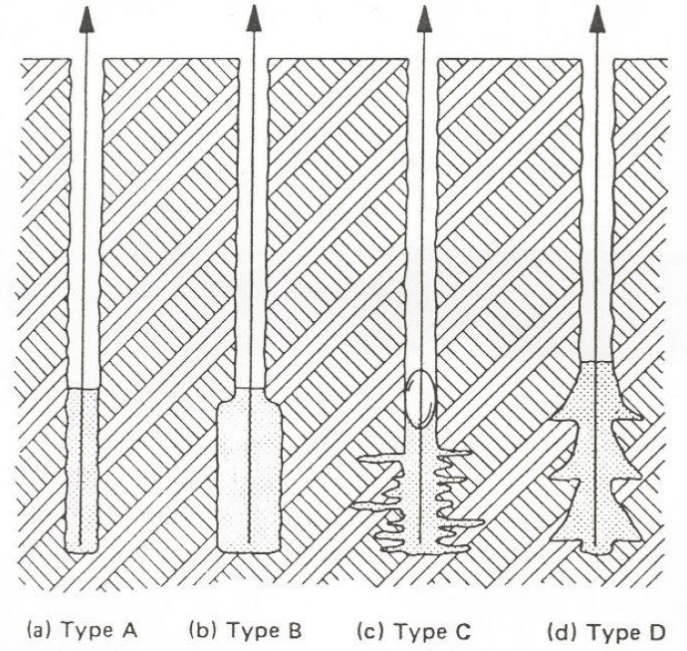

Figure 1-3. Micropiles classified by the method of grout placement (Shong & Chung, 2003)

Type A the grout is placed under gravity causing the grout to form to the general shape of the drilled hole. For a Type B micropile grout is pressurized from 0.5 to 1 MPa and injected into the hole as the casing is withdrawn forcing grout into voids spanning past the drilled borehole shape. Type C required two steps, first primary grout is placed under a pressure of 1 to 2 MPa followed by secondary grout injection 15 to 25 minutes later using a specialized sleeved grout pipe. Type C micropiles are most commonly seen in France. Lastly, Type D micropiles require a two-step process consisting of primary and secondary grouting. The secondary grout is injected with a pressure 2 to 8 MPa with most of the time followed by a packer (Shong & Chung, 2003).

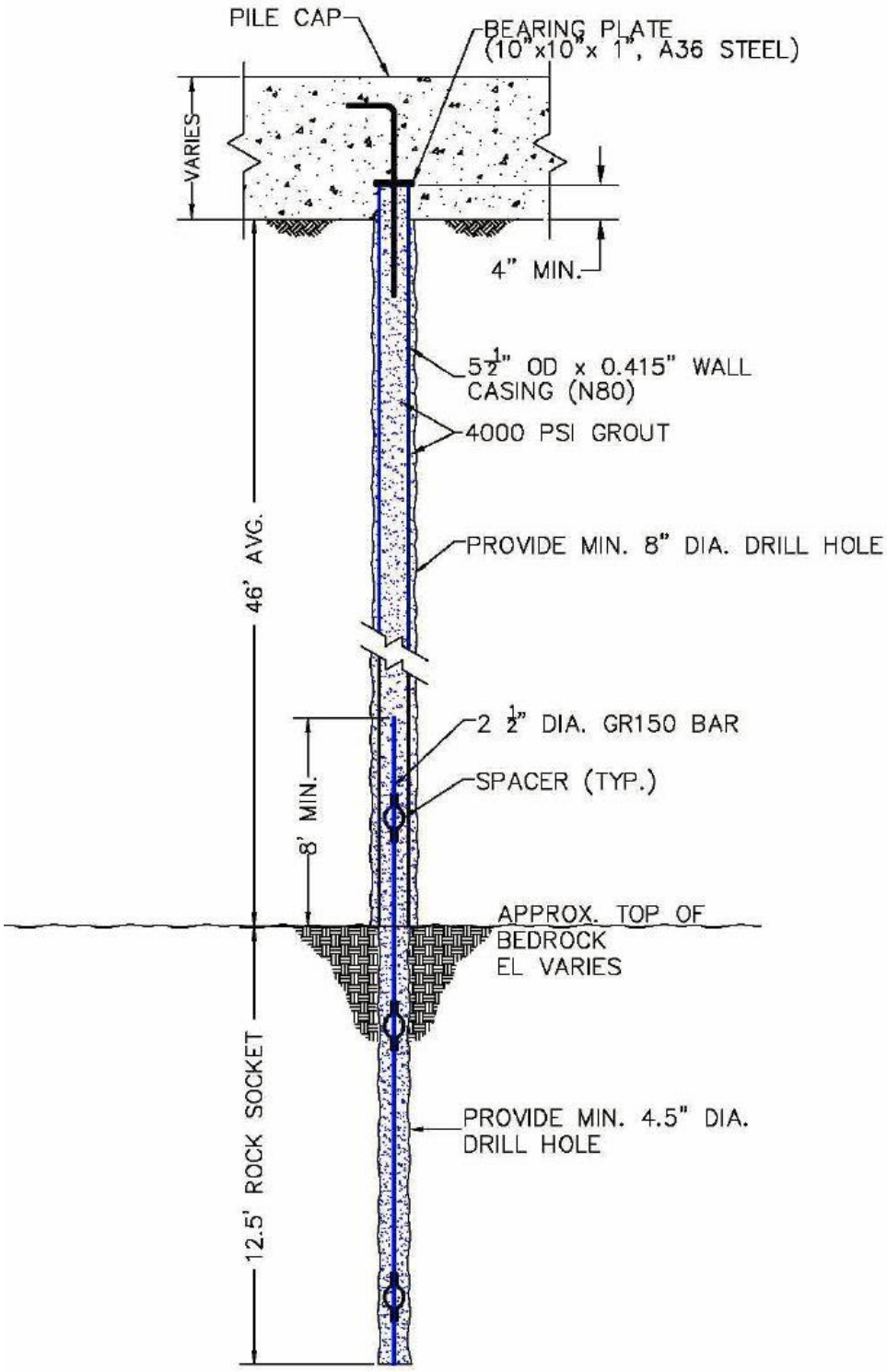

Figure 1-4. A typical micropile design cased through the overburden soil with a rock socket (FHWA, 2005)

Micropiles have been placed in a vast variety of soil bearing scenarios. Ranging from karst terrain, to expansive clay, to limestone. Micropiles can be placed in almost any competent soil strata from depths ranging from 5 to over 50 feet. Design methods for micropiles consider the varying characteristics of the soil present. The three main soil types considered in design are sand, clay, and rock. Hybrid design methodologies are used for silt, gravel, large voids, running sands and other geology features (Hussin & Cook, 2010).

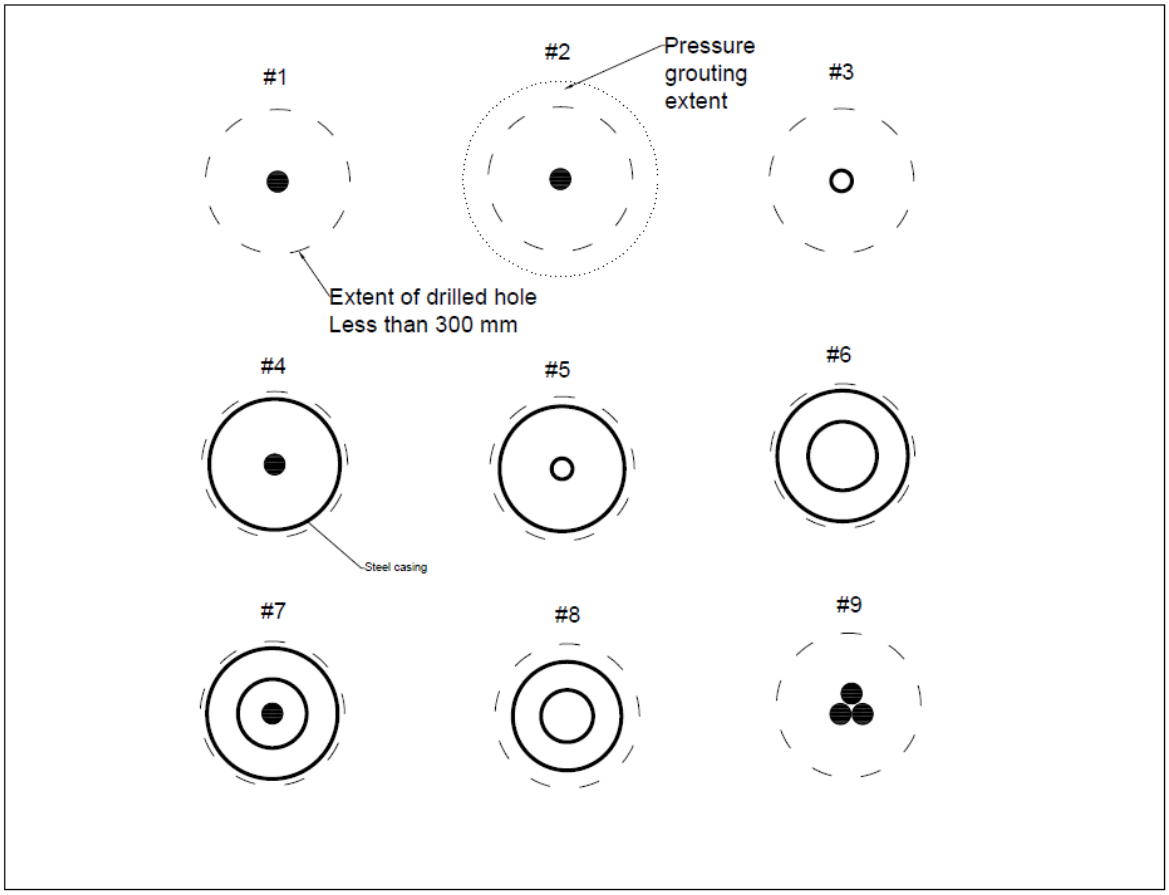

Figure 1-5. Typical micropile cross sections

1.4 Applications of the Micropile

As mentioned previously the application of the micropile can vary and is mostly utilized in difficult drilling conditions, tight spaces, and when large caissons or pile driving is not necessary. Since their use became more popular in the 1980's they can now be seen in many new construction projects such as bridges, commercial building, residential structures, break walls, wind turbines, and antenna towers. Especially when rocky soils are present that prevent efficient driving of piles or drilling of large diameter shafts (Shong & Chung, 2003). Micropiles can be placed in tight places and micropile drill rigs can be much smaller than other typical construction equipment as seen in Figure 1-6. The small diameter of the micropile can utilize more expensive materials in the drill bits requiring a less downward pressure from the drill rig.

Figure 1-6. Techno Drill 610 compact drill rig

Micropiles were first used to retrofit existing monuments and continue to fill a niche in adding capacity and reducing settlements among existing foundations. The explosion of 4G networks and existing antenna towers adding additional equipment has made micropile design and construction a booming enterprise. Micropiles are often used to prevent additional settlement were problems have been recognized. These projects typically require tight drilling areas and connection components to an existing foundation. Another micropile retrofit application consists of earthquake retrofits where a structure is deemed inadequate to handle a design earthquake in the area. Micropiles add additional stability where shallow foundations may be expected to settle, punch through the existing bearing grade, or overturn when strong ground motion is applied to the structure. Historic structures that have old and fragile foundation components utilize the non-intrusive nature of micropiles to add stability and increase the lifetime of the structure.

The quick and effective nature of micropiles gives engineers and contractors a viable solution in difficult conditions. Due to this an interest has developed in using micropiles for slope stability projects ranging from slopes, walkways, roads, and tunneling. Since various grouting procedures utilize some ground improvement as well many successful micropile slope stability projects have been seen.

FHWA outlines a general design process for the micropile as follows:

1. Requirements of the micropile such as loads, location, and micropile layout
2. Geotechnical data available, design parameters, and geological profile
3. Micropile type and construction process

4. Evaluate grout-soil or steel-soil interface bond values
5. Design embedment and bond length
6. Select types of steel reinforcement
7. Check buckling, bending, bursting, inclined loading, and punching shear of soil
8. Design pile-structure connection components
9. Design adequate corrosion protection of the micropile

As the use of the micropile continues to grow the need for research, case studies, and design procedures become more critical to practicing engineers and contractors. This research report is aimed to continue to grow the knowledge of micropile design and construction so that they may be used in the most efficient ways possible. A challenge of micropile design and construction is determining when micropiles are more cost effective than other deep foundation techniques. Identifying loads and geologic conditions most suitable for micropiles can be difficult and many projects use micropiles where other deep foundation methods should be used and vice versa. This paper aims to provide the reader with tools necessary to determine efficient use of the various cross sections on the micropile.

1.3.1 New Foundation Micropile Construction

As bridge construction continues to be a major part of updating the aging infrastructure in the United States (U.S.) micropiles will continue to be an important tool in bridge construction and rehabilitation. Below as seen in Figure 1-7 and Figure 1-8 is one micropile design for a bridge abutment. The design utilizes both vertical and battered piles to secure the bridge abutment to rock placed on site. The use of casing adds additional lateral strength to the micropile system (Elaziz & Naggar, 2015). With this type of system the abutment is typically poured onto the micropiles creating a hybrid foundation system (Luna, Dixon, Kershaw, & Siegel, 2015).

Micropiles are typically used for bridge abutments when shallow rock is present. This serves to seat the bridge abutments into competent rock. Quick installation and the ability to include a rock socket has made micropiles an effective foundation for bridges over the use of caissons or driven piles (Larsson & Jog, 2014). Load testing of micropiles is almost always required for bridge construction (Splitstone, Stonecheck, Dodson, & Fuller, 2010). A case study present at the end of the paper outlines the design-test-construction process for micropiles used to support bridge abutments.

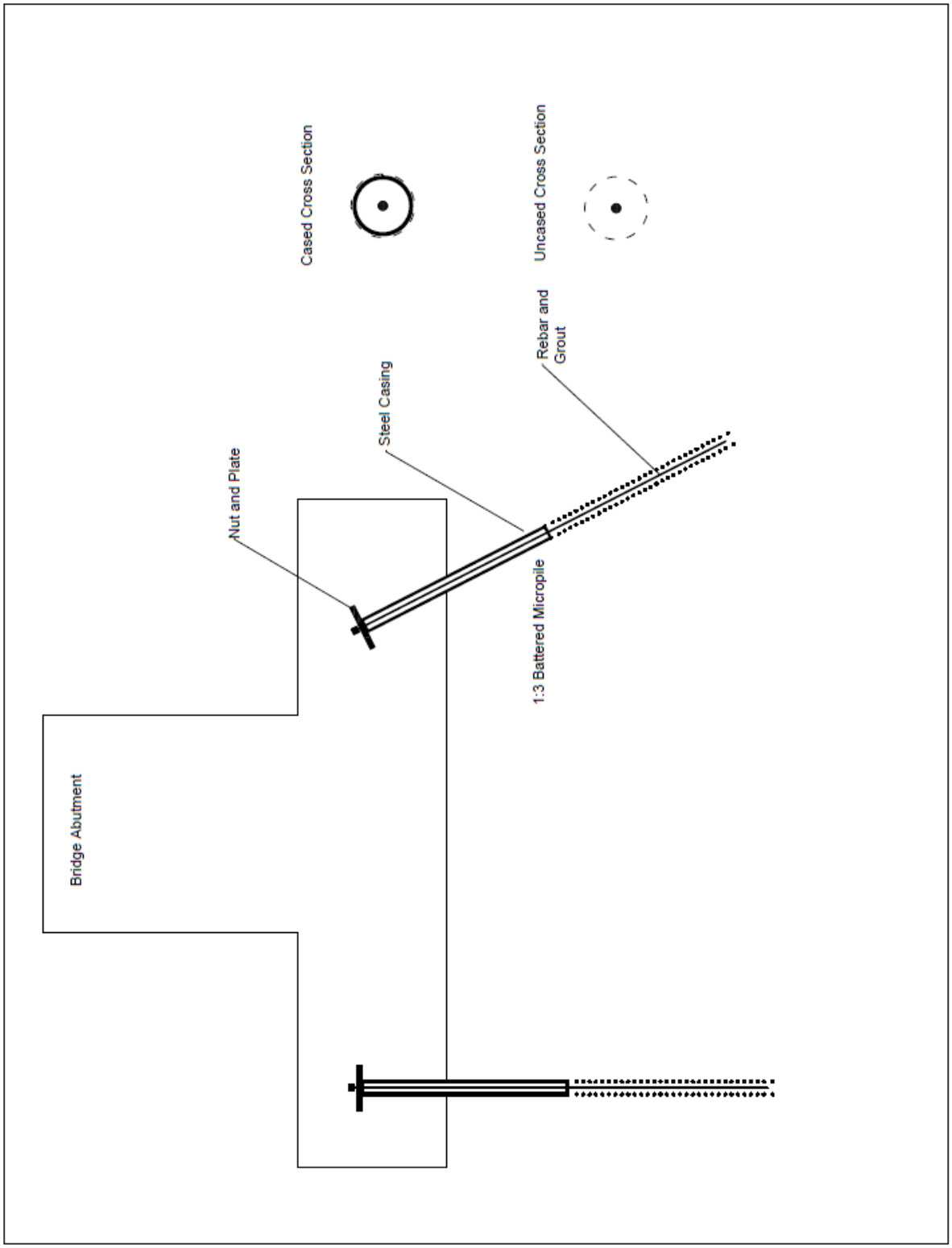

Figure 1-7. Bridge abutment micropile cross section ("Grove Road Bridge Replacement," 2014)

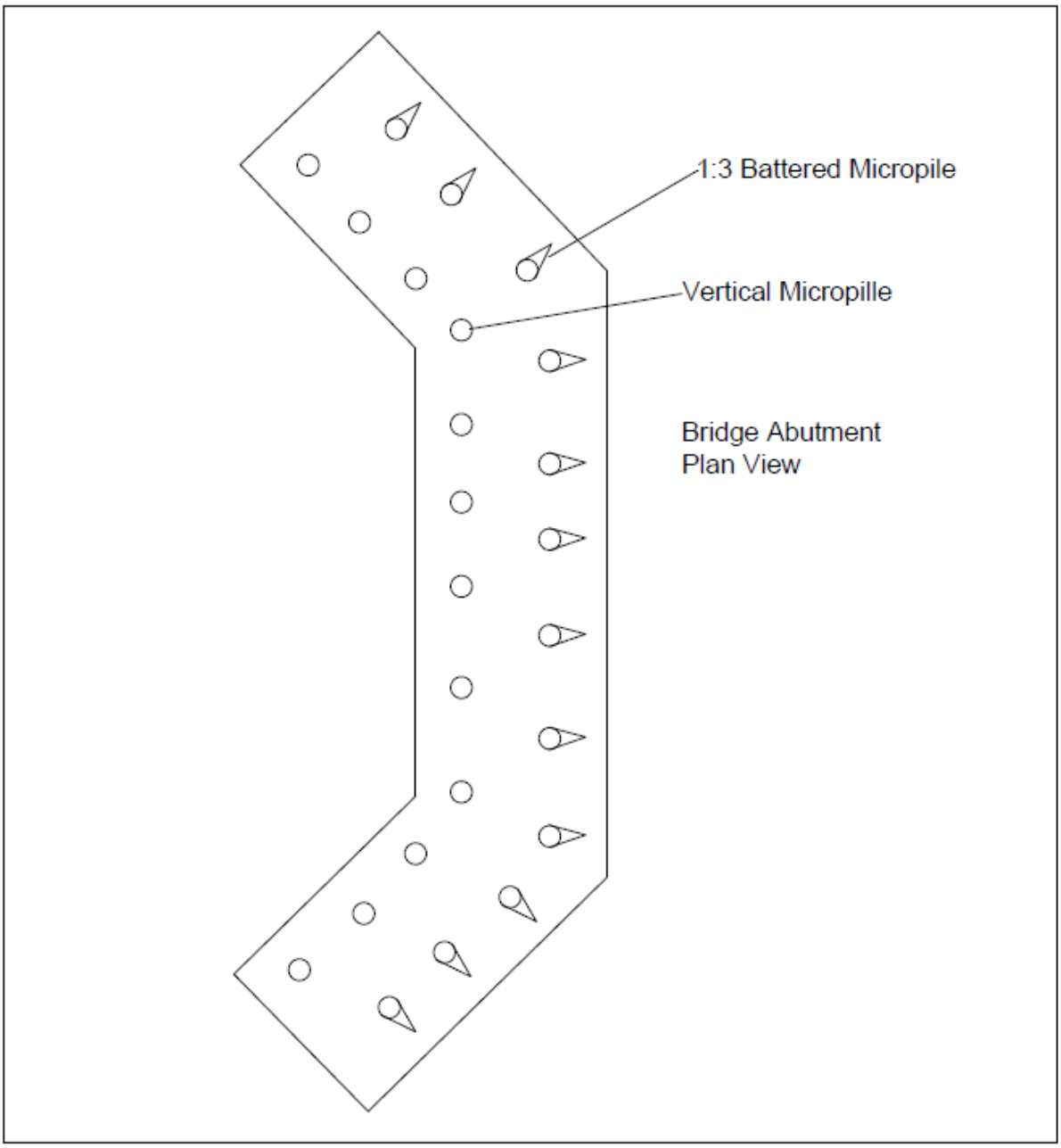

Figure 1-8. Bridge abutment micropile plan view ("Grove Road Bridge Replacement," 2014)

The communication industry and antenna tower construction saw a boom when cell phones became popular. Once again, with the development of smart phones, existing antenna towers are

adding addition antennas. Micropiles are emerging as the chosen foundation technology to add capacity and stability to existing antenna towers ("Monopole Reinforcement and Retrofit Project," 2014). Seen below in Figure 1-9 and Figure 1-10 are micropile designs for an existing antenna tower.

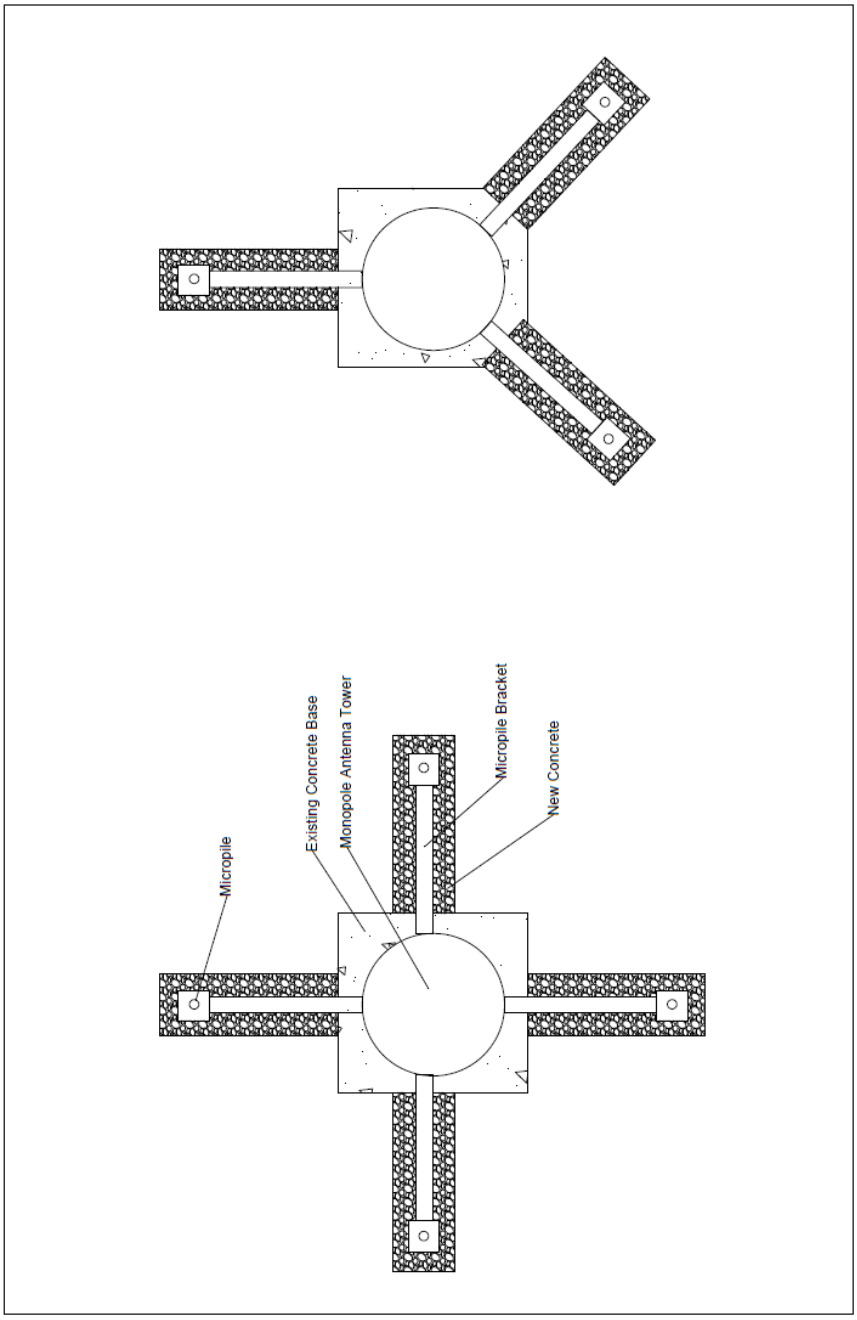

Figure 1-9. Plan view of antenna tower 4-leg and 3-leg micropile retrofit

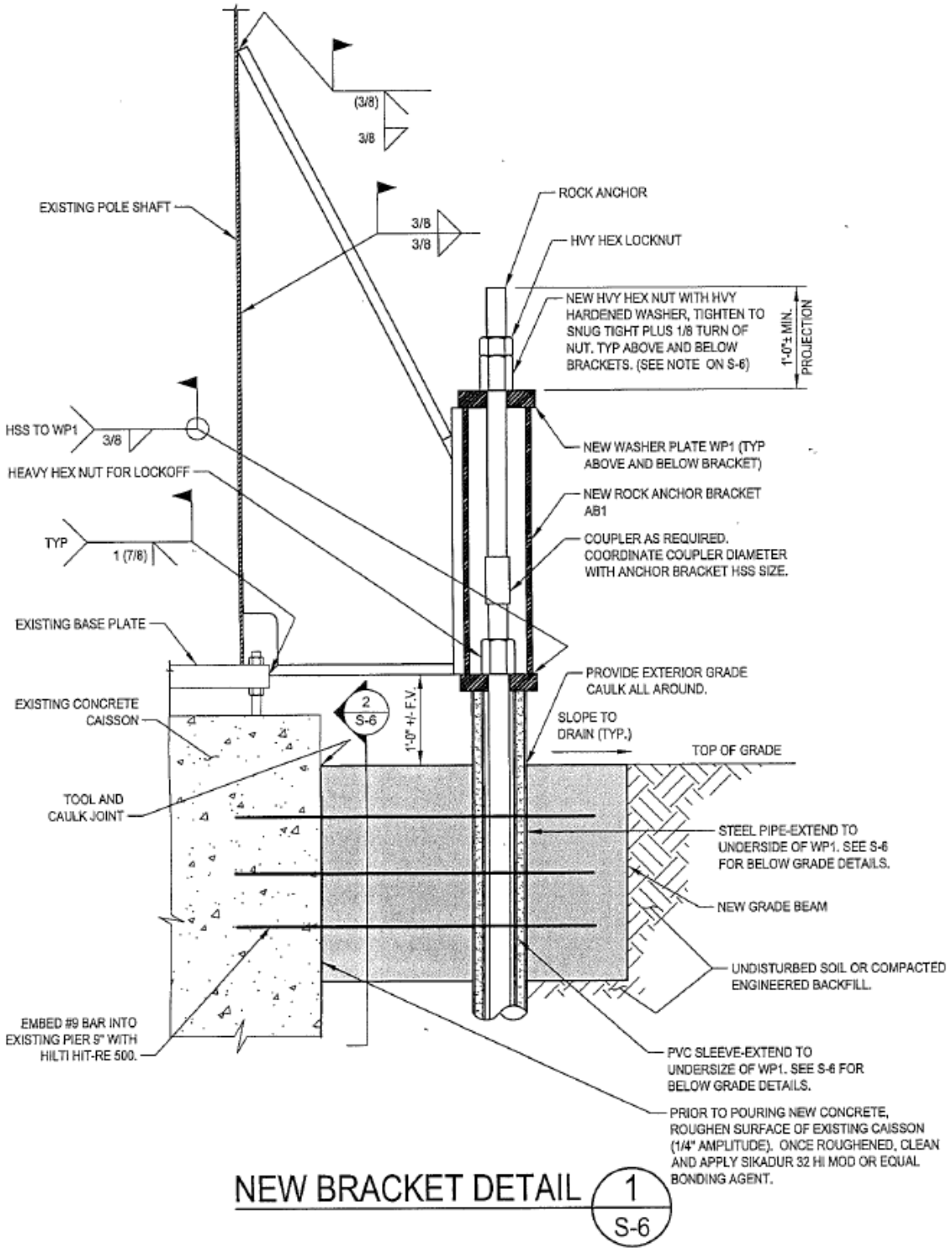

Figure 1-10. Typical micropile connection detail for antenna tower retrofit projects ("Monopole Reinforcement and Retrofit Project," 2014)

Note that the connection details are an integral part of these types of projects and can be difficult to design and construct. This design has the micropile down into rock which is sometimes called a rock anchor (FHWA, 2005). Antenna tower companies and contractors utilize both the compression and tension capabilities of these types of systems.

Another difficult part of the antenna retrofit process, not shown in the above example, is coring through an existing foundation element (Bruce & Juran, 1997). Contractors are wary of doing so due to hitting rebar often not in the same place as shown in plans. This can compromise the foundation system and require additional retrofit work. Antenna tower layouts can consist of 3 or 4 micropiles equally spaced around the existing tower ("Monopole Reinforcement and Retrofit Project," 2014).

The wind turbines industry is starting to realize the potential micropiles have for small to medium sized wind turbines (1 kW to 100 kW). Hybrid foundation systems, typically utilizing a ring of micropiles around the perimeter, can prevent overturning and reduce the required footing size. These types of hybrid foundations can reduce a foundation area up to 75%, provide a 40% reduction in concrete consumption, and provide a 70% reduction in reinforcing steel (Aschenbroich).

Figure 1-11. Overturned shallow foundation of a wind turbine (Aschenbroich)

Large moment loads on the foundations make these systems effective. However, they have not been seen replacing the large monopole foundations typically seen for large wind turbines (greater than 1 MW) (Aschenbroich).

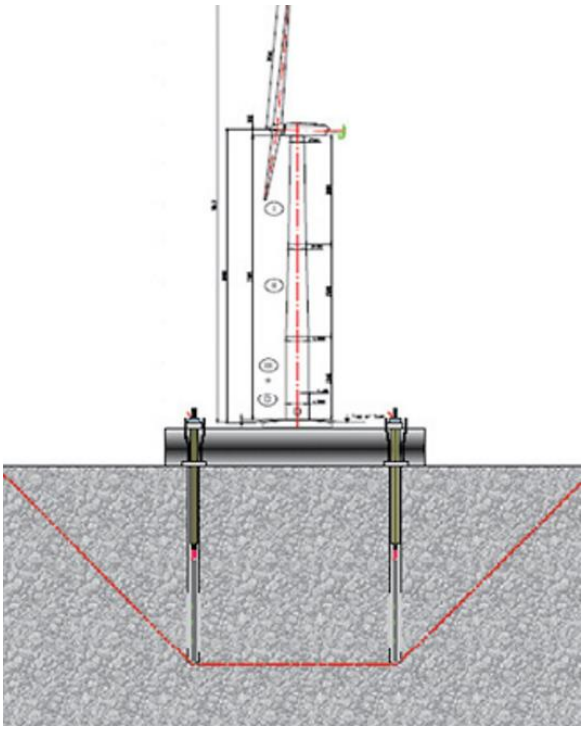

Figure 1-12 and Figure 1-13. Micropile anchor design and construction for a wind turbine (Aschenbroich)

The above figures show the construction process for the wind turbine foundation. The footing is poured around the polyvinylchloride (PVC) pipe which, in this instance is considered a groutable void form (GVF). The GVF allows them to pretension the micropile and then grout the voided area specifying a certain downward pressure on the hybrid foundation system (Aschenbroich). The micropile is seeing new uses in new foundation construction every day. Due to inexpensive testing and ease of installation more and more engineers are utilizing the benefits of micropiles. As design methods, installation methods, and materials continue to advance the use of micropiles for new foundation construction will continue to grow.

1.3.2 Existing Foundation Micropile Renovations and Rehabilitation

Micropiles made their debut underpinning historic buildings, primarily Case 1, by a concept developed by Fernando Lizzi. Historic buildings that were weakened by war, unforeseen loadings, improper design, and other factors required a retrofit to the foundation to prevent additional structural damage. Only micropiles offered an economical solution for tight spaces without compromising the integrity of the existing structure. Many times the facility can remain open during construction and once finished the micropiles are quickly mobilized to carry loads.

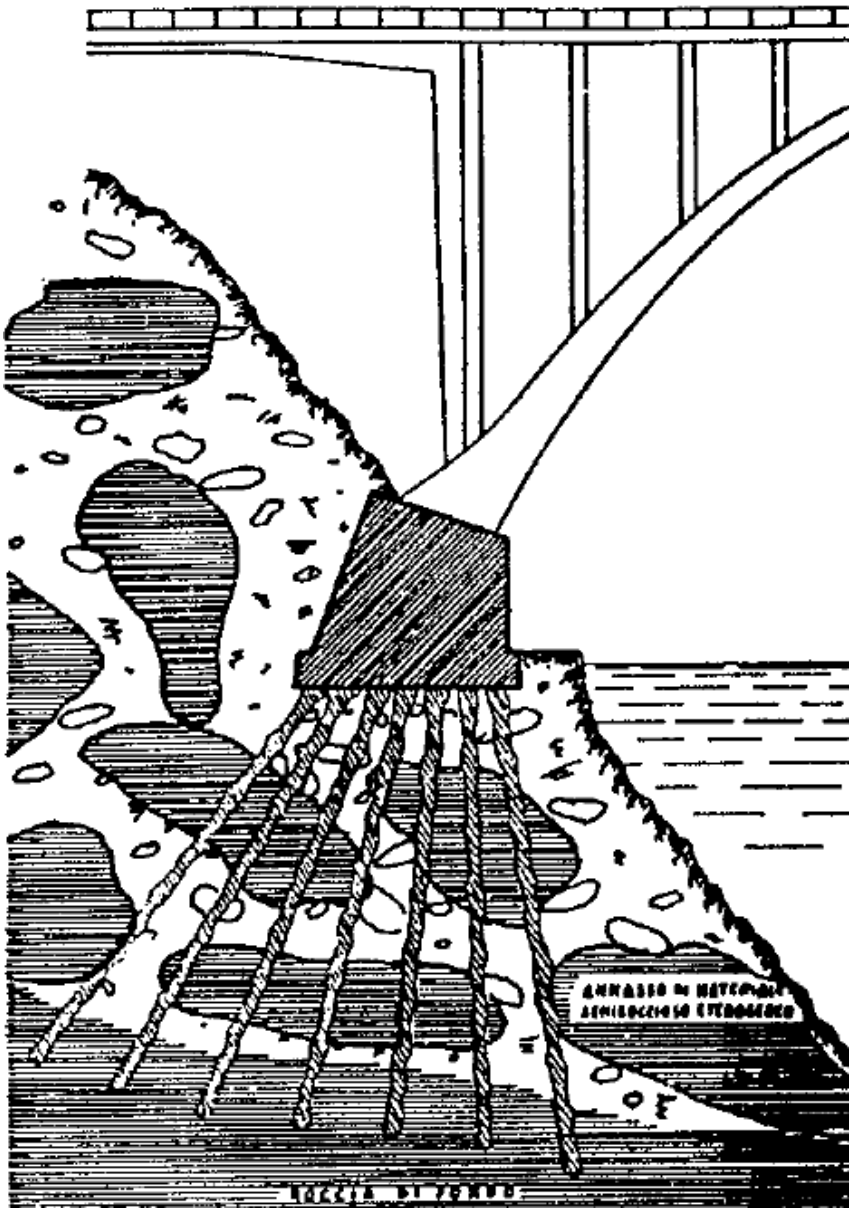

Figure 1-14. Widening of the thruway between Milan and Bergamo, Italy (Lizzi, 1982)

Lizzi uses micropiles in Figure 1-15 to increase the load bearing capacity of a bridge pier in Italy that underwent widening of a bridge deck (Lizzi, 1982). Being able to access tight spaces while not disturbing the existing structure made micropiles an easy sell for Lizzi. He never suggested to preload the piles because he believed this lowers their overall load carrying capacity.

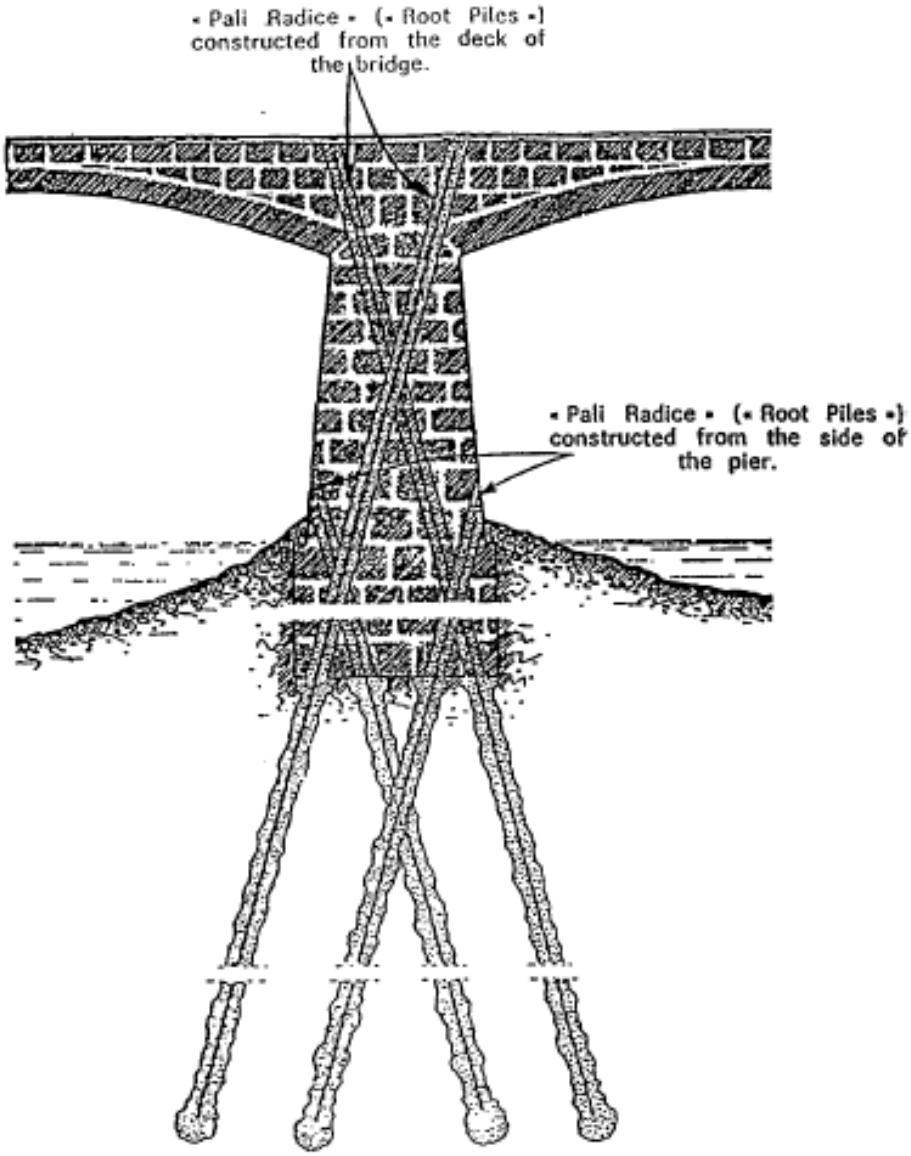

Figure 1-15. Underpinning of a bridge pier in Italy by root piles (Lizzi, 1982)

The underpinning of monuments has been attributed to the creation of the micropile. Fernando Lizzi developed a small diameter pile that was used to underpin structures holding loads of about 10 tons. At the time of its inception many did not believe that such a small component could hold such loads. However, inexpensive load tests proved the root piles or pali radice, micropiles fully bonded to the soil, could hold 10 tons of load with 2-3 mm of settlement.

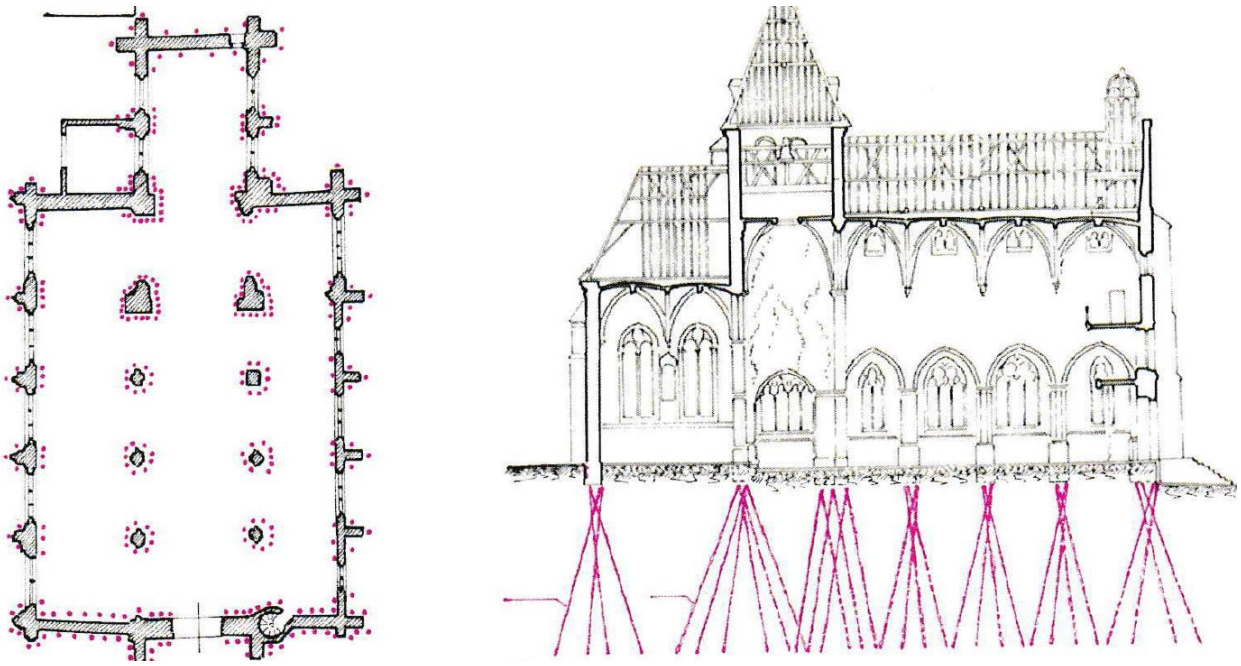

Figure 1-16. . Underpin plans for the Monumental Church of Tourny located in Eure, France (Lizzi, 1982)

Soon monument owners all over Europe began to utilize the effectiveness of micropiles. The main attraction was the complementary function the micropiles had for the exisiting foundations. The fully bonded micropiles were quickly mobilized under slight settlements of the structure. Therefore, the micropiles would interact with the existing foundation and carry loads where settlements occurred. The more movement from the structure the more mobilized the micropiles become and carry additional load. The micropile continue to take the load of the structure until the entire structure is supported by the micropiles (Lizzi, 1982)

Figure 1-17. Viaduct pali radice construction done in Teruel, Spain (Lizzi, 1982)

Minimum vibrations from drilling equipment used for micropiles assures that no additional damage will occur during installation. Renovating these historic monumental structures requires extreme care and diligence by the engineers involved. A majority of large foundation restoration projects are carried out over various stages and require immense investigation into the existing structures and forces acting upon the foundation.

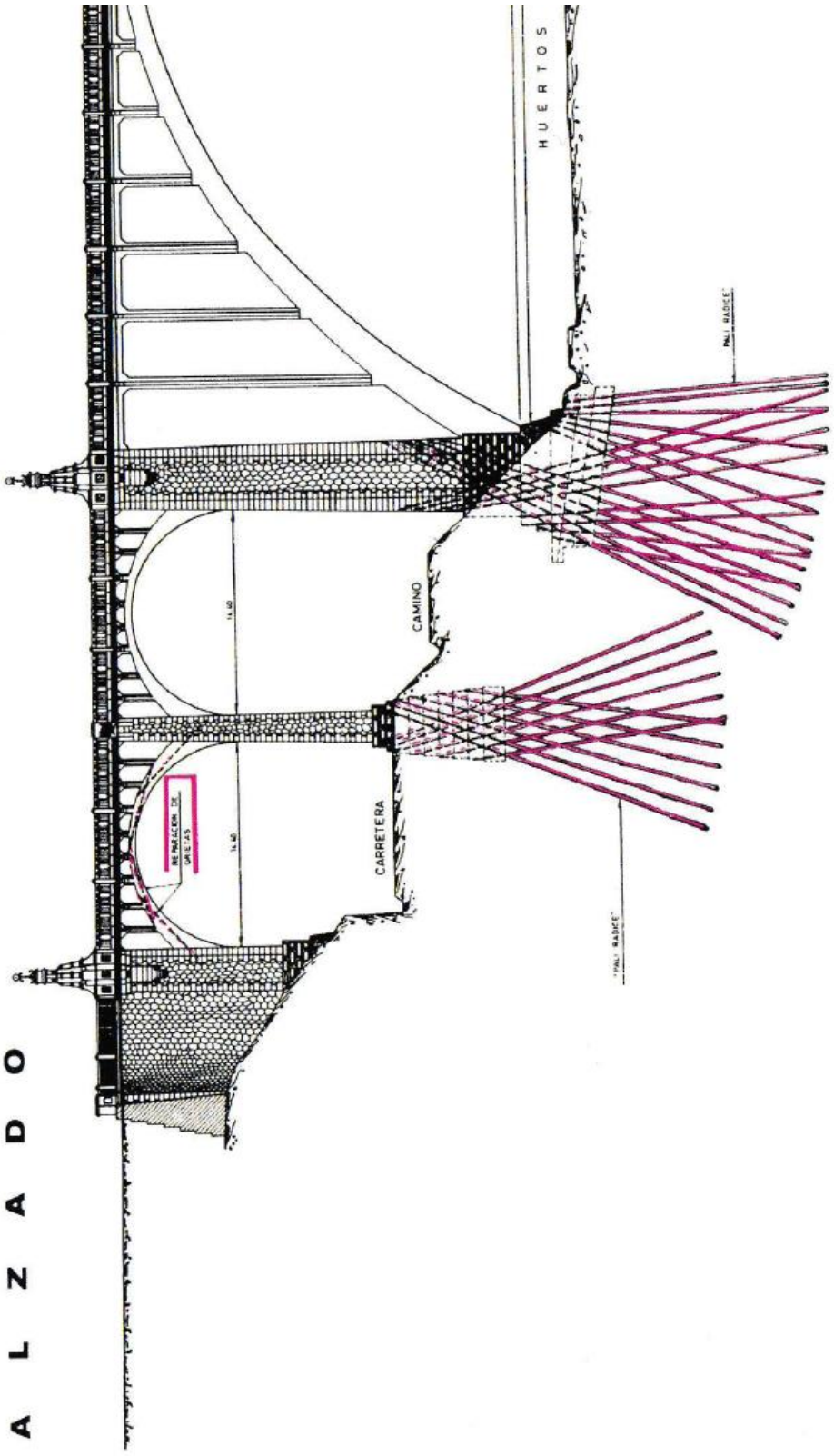

Figure 1-18. Underpinning plans of the viaduct using case 2 root piles (Lizzi, 1982)

The Cathedral of Agrigento was built upon a soft limestone layer on top of clay. Over time the church settled and a large crack formed throughout the entire length of the floor. Differential settlement was believed to be caused by the compressibility of the clay combined with slope failure from the land sliding over time.

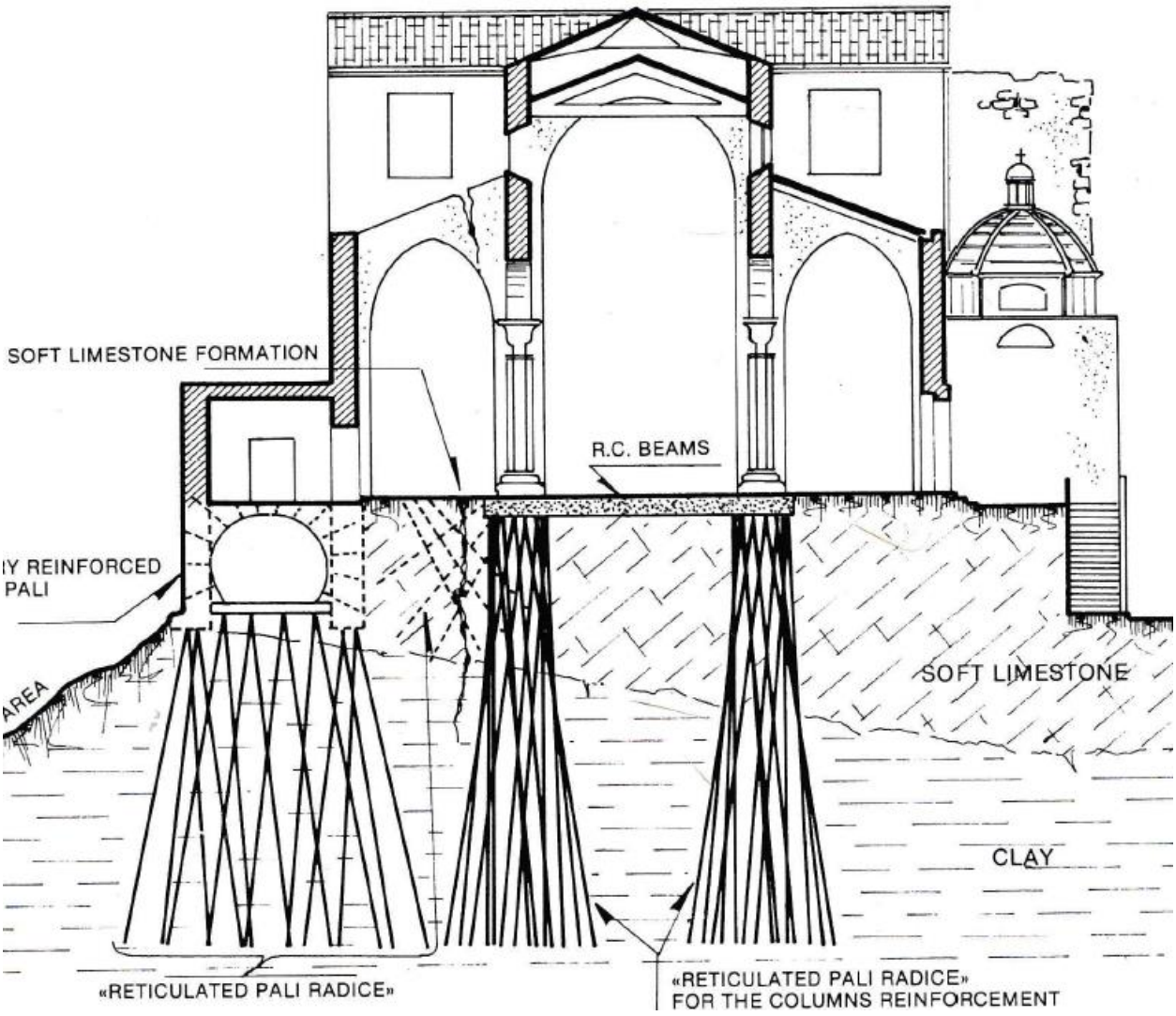

Figure 1-19. Cathedral of Agrigento using pali radice for underpinning (Lizzi, 1982)

Initially, root piles were installed to prevent further slope failure for the part of the church next to the sloped area. After seeing a reduction in movement the church planned to install more

micropiles for the church columns. All of the micropiles were grouted under pressure and an additional beam was added to securely connect the church foundation system to the newly installed pile system (Lizzi, 1982).

Two case studies are covered at the end of the report describing the use of micropiles to underpin a building with settlement problems at Suranaree University of Technology (SUT) in Thailand and also underpinning an existing building in New York State to allow excavation adjacent to the building.

In underpinning projects great care must be taken not to risk the integrity of the existing foundation. Pressure grouting is preferred to treat the surrounding soil and prevent any settlement during construction. Various coupling options including but not limited to plates, rebar, dowels, and additional concrete are used to connect the micropile to the existing foundation (Bruce & Juran, 1997).

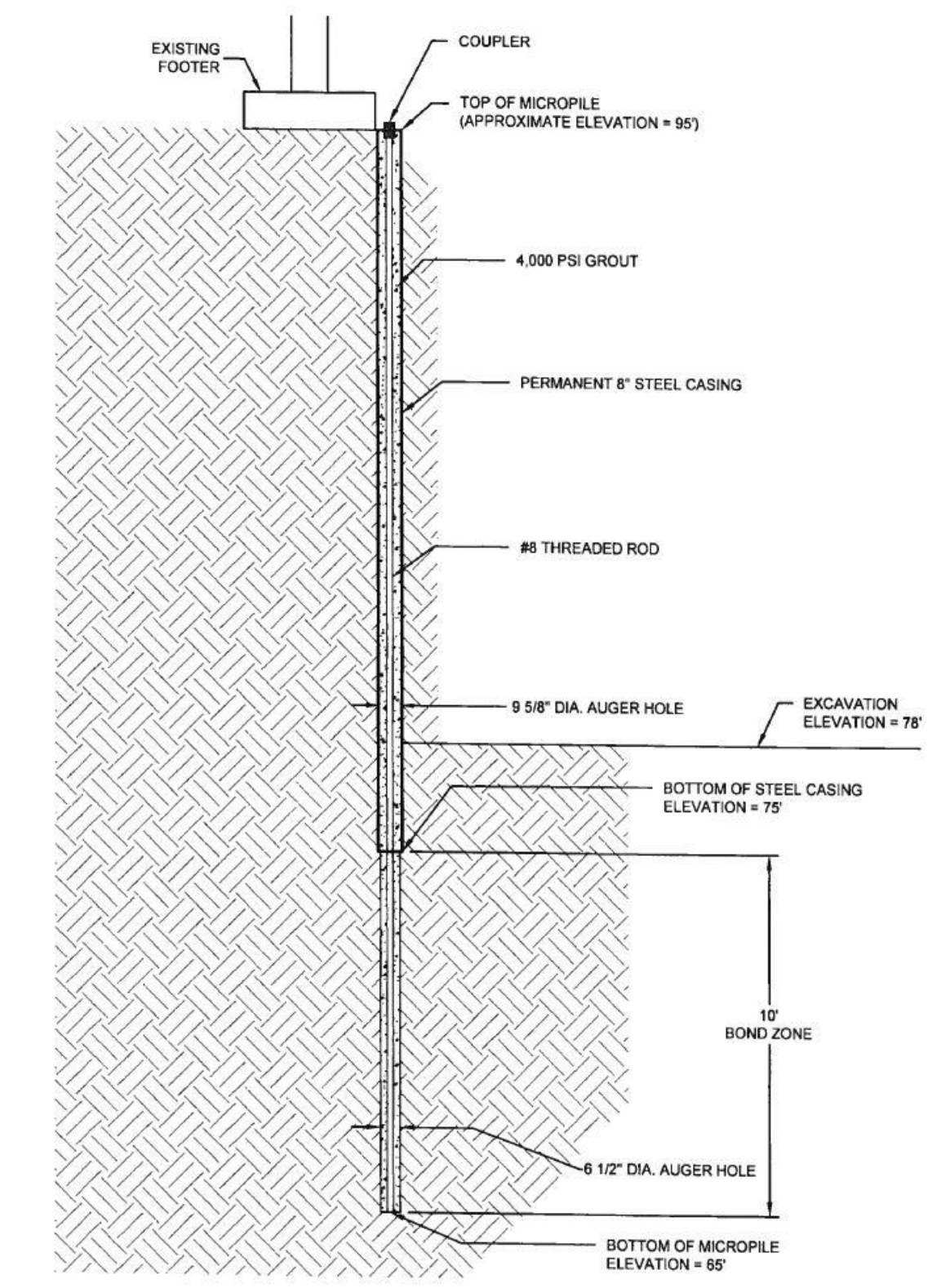

Figure 1-20. Typical underpinning of an existing foundation using micropiles for Hartwick College, New York.

2. Design Equations for the Micropile

The micropile is capable of withstanding both axial and lateral loads. Determining the axial and lateral capacity of the micropile is dependent of geotechnical and structural elements. Axial capacity is dependent on a combination of shaft and end bearing resistance. Micropiles, due to their slender nature, depend largely on the shaft resistance. Lateral capacity can be determined from the pile stiffness and the expected lateral soil reaction from the mobilized soil (Reese & Van-Impe, 2011). Typical pile design procedures are covered, however only the bond stress method was developed solely for the micropile (FHWA, 2005),

2.1 Axial Capacity of the Micropile

A simple representation of the axial capacity of a single micropile is as follows,

$$Q = Q_p + Q_s \quad \text{(Eq. 2.1)}$$

Where:

Q = ultimate micropile capacity

Q_p = end bearing resistance

Q_s = shaft resistance

Shaft resistance can be broken down further as follows,

$$Q_s = \pi D \sum_{i=1}^{m} f_{si}\ dl_i \quad \text{(Eq. 2.2)}$$

Where:

f_{si} = ultimate unit skin friction for layer *i*

D = diameter of the micropile

m = number of soil layers

dl_i = depth of considered layer

Equation 2.2 outlines the basis that shaft resistance is a sum of the skin friction about the perimeter of the pile. The summation allows different shaft resistance values for different soil layers encountered by the micropile. The alpha method and the beta method described below use this formulation to determine ultimate micropile capacity (*Canadian Foundation Engineering Manual, 3rd Edition,* 1992). A majority of other methods exist to determine micropile capacity stem from the basis of Equation 2.1 and Equation 2.2. Note should be taken that when determining uplift capacity, only skin friction is considered. Also, water pressure and the pile weight are contributing factors when calculating pile uplift capacity (*Canadian Foundation Engineering Manual, 3rd Edition,* 1992).

2.1.1 Alpha Method

The alpha method utilizes an adhesion factor, α, as a ratio of the unit skin friction to the undrained shear strength of clay. Thus, the alpha method is evaluated as a total stress analysis due to using the cohesion of clay to determine the shaft resistance (Lindeburg, 2012). The value of alpha is determined by the cohesion of the clay and typical values can be seen in Table 2-1 below. Skin friction is often taken as a uniform per soil layer for the shaft sections of the micropile, due to laboratory testing usually providing one shear strength value per layer of clay. However, shear strength tends to increase with depth. Also, it is common practice for cohesive

soil to neglect skin friction at the top 1.5 meters of the pile (*Canadian Foundation Engineering Manual, 3rd Edition*, 1992). The unit skin friction is then determined by Equation 2.3 below.

$$f_s = \alpha\, c \qquad \text{(Eq. 2.3)}$$

Where:

f_s = unit skin friction (kPa or lbf/ft^2)

α = adhesion factor

c = undrained shear strength (cohesion, kPa or lbf/ft^2)

Table 2-1. Adhesion factors for the Alpha Method (Lindeburg, 2012)

Cohesion, c lbf/ft^2 (kPa)	α (range of values)	Average Value
500 (24)	1.0	1.0
1000 (48)	0.56 – 0.96	0.83
2000 (96)	0.34 – 0.83	0.56
3000 (144)	0.26 – 0.78	0.43

When using the alpha method, to determine the end bearing capacity of the micropile the following equation is commonly used.

$$Q_p = 9A_p c \qquad \text{(Eq. 2.4)}$$

Where:

Q_p = end bearing resistance (kN or kips)

A_p = area of pile tip (m^2 or ft^2)

c = cohesion of soil at pile tip (kPa or kips/ft^2)

2.1.2 Beta Method

The beta method is an effective stress analysis done to determine the geotechnical capacity of a micropile. Common with granular material, however it can be used with cohesive material as well. In the beta method, the frictional shaft resistance is taken as a fraction of the effective vertical stress. When determining the effective vertical stress, the Canadian Foundation Manual uses the concept of "critical depth" in which at a certain depth the pile the effective vertical stress used to calculate capacity becomes constant (*Canadian Foundation Engineering Manual, 3rd Edition*, 1992). This critical depth is a certain multiple of the pile diameters, depends on the type of material, and is only applicable to sand (Sivakugan, 2010). The difference shown with using critical depth can be seen in Figure 2-1.

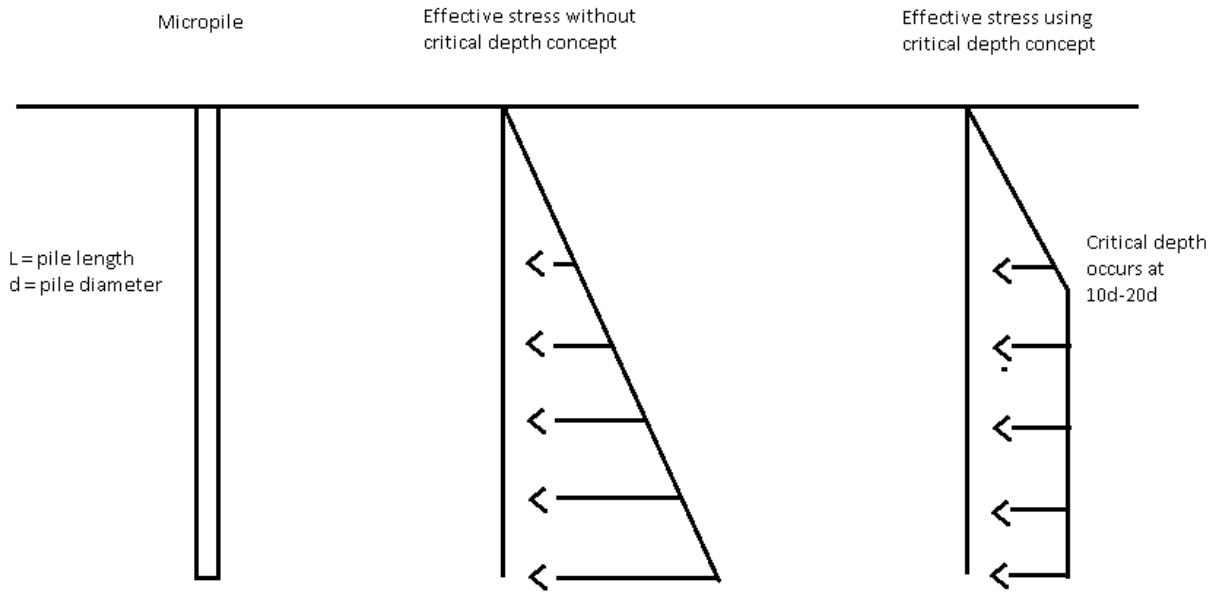

Figure 2-1. Diagram showing the concept of critical depth

Using critical depth gives more conservative results for micropile capacity. The skin friction of the micropile can be calculated using the Beta Method as follows.

$$Q_s = \beta \pi D L \sigma' \qquad \text{(Eq. 2.5)}$$

Where:

Q_s = total skin friction resistance (kN or kips)

β = fractional factor (See Table 2-3)

D = pile diameter (m or ft)

L = pile length (m or ft)

σ' = effective vertical stress (kPa or kips/ft^2)

For the beta method Equation 2.6 can be used to determine the tip bearing resistance. This equation is primarily used when dealing with cohesionless soils.

$$Q_p = A_p \sigma' N_t \quad \text{(Eq. 2.6)}$$

Where:

Q_p = total bearing resistance (kN or kips)

A_p = area of pile tip (m^2 or ft^2)

N_t = bearing capacity factor (See Table 2-2)

σ' = vertical effective stress at pile base (kPa or kips/ft^2)

Table 2-2. Range of Nt values for cohesionless soils (*Canadian Foundation Engineering Manual, 3rd Edition*, 1992)

SOIL TYPE	CAST-IN-PLACE PILES	DRIVEN PILES
Silt	10 - 30	20 - 40
Loose sand	20 - 30	30 - 80
Medium sand	30 - 60	50 - 120
Dense sand	50 - 100	100 - 120
Gravel	80 - 150	150 - 300

In the absence of test loading, a factor of safety of at least 3 should be applied to any theoretical computation.

Table 2-3. Range of β coefficients for cohesionless soils (*Canadian Foundation Engineering Manual, 3rd Edition*, 1992)

SOIL TYPE	CAST-IN-PLACE PILES	DRIVEN PILES
Silt	0.2 - 0.30	0.3 - 0.5
Loose sand	0.2 - 0.4	0.3 - 0.8
Medium sand	0.3 - 0.5	0.6 - 1.0
Dense sand	0.4 - 0.6	0.8 - 1.2
Gravel	0.4 - 0.7	0.8 - 1.5

There exists a variety of methods available to calculate micropile capacity. It is imperative to cite reference manuals when designing micropiles. Computing various methods and comparing the results is essential to determine an effective design. A majority of the time pile load tests are implemented to verify if the micropile can handle the designated loads. Seen in the Appendix are example calculations for the methods described. These capacity and design values are compared to other methods as well as simulated load tests developed by finite element models.

2.1.3 Bond Stress Method

The FHWA Micropile Design and Construction Manual outline the geotechnical capacity of the micropile in a manner of bond strength. This bond strength is the grout to ground bonding interaction. A designated bond zone is determined to withstand the expected tension and/or compression loading. For certain soil deposits the bonding is unsuitable and geotechnical engineers should use extra care when bonding to these types of soils. Organic soils and cohesive soils with a liquid limit greater than 50, average plastic index greater than 20, and average liquidity index greater than 0.2, additional safety factor should be used (FHWA, 2005). This is

typically due to the low hydraulic conductivity of the soil preventing flow of the grout into the soil. The allowable maximum compression or tension load for design calculated using Equation 2.7 below.

$$P_{G-allowable} = \frac{\alpha_{bond}}{FS}(\pi D_b L_b) \quad \text{(Eq. 2.7)}$$

Where:

$P_{G\text{-allowable}}$ = compression or tension load for design (kN or kips)

α_{bond} = grout to ground ultimate bond strength (kPa or kips/ft^2)

FS = factor of safety (recommended 2-2.5)

D_b = diameter of micropile drilled hole (m or ft)

L_b = bond length designated for micropile (m or ft)

Table 2-4. Summary of typical grout-to-ground values for micropile design (FHWA, 2005)

Soil / Rock Description	Grout-to-Ground Bond Ultimate Strengths, kPa (psi)			
	Type A	Type B	Type C	Type D
Silt & Clay (some sand) (soft, medium plastic)	35-70 (5-10)	35-95 (5-14)	50-120 (5-17.5)	50-145 (5-21)
Silt & Clay (some sand) (stiff, dense to very dense)	50-120 (5-17.5)	70-190 (10-27.5)	95-190 (14-27.5)	95-190 (14-27.5)
Sand (some silt) (fine, loose-medium dense)	70-145 (10-21)	70-190 (10-27.5)	95-190 (14-27.5)	95- 240 (14-35)
Sand (some silt, gravel) (fine-coarse, med.-very dense)	95-215 (14-31)	120-360 (17.5-52)	145-360 (21-52)	145-385 (21-56)
Gravel (some sand) (medium-very dense)	95-265 (14-38.5)	120-360 (17.5-52)	145-360 (21-52)	145-385 (21-56)
Glacial Till (silt, sand, gravel) (medium-very dense, cemented)	95-190 (14-27.5)	95-310 (14-45)	120-310 (17.5-45)	120-335 (17.5-48.5)
Soft Shales (fresh-moderate fracturing, little to no weathering)	205-550 (30-80)	N/A	N/A	N/A
Slates and Hard Shales (fresh-moderate fracturing, little to no weathering)	515-1,380 (75-200)	N/A	N/A	N/A
Limestone (fresh-moderate fracturing, little to no weathering)	1,035-2,070 (150-300)	N/A	N/A	N/A
Sandstone (fresh-moderate fracturing, little to no weathering)	520-1,725 (75.5-250)	N/A	N/A	N/A
Granite and Basalt (fresh-moderate fracturing, little to no weathering)	1,380-4,200 (200-609)	N/A	N/A	N/A

Type A: Gravity grout only
Type B: Pressure grouted through the casing during casing withdrawal
Type C: Primary grout placed under gravity head, then one phase of secondary "global" pressure grouting
Type D: Primary grout placed under gravity head, then one or more phases of secondary "global" pressure grouting

The basic theory behind Equation 2.7 is that unit bond strength, determined empirically and shown in Table 2-4 based on the soil type, is multiplied by the surface area of the bond zone. Often end bearing is not considered, thus including another factor of safety. The bond zone may only include grout to soil contact, meaning any cased part of the pile may not be included in the bond zone. However, it is expected that the steel to ground will mitigate some load. Many contracts specify the minimum bond length and maximum unit bond strength used for each soil layer. Equation 2.7 may also be manipulated, if the allowable design load is known, to determine the required bond length of the micropile. This simple design method has been proven effective in many construction projects especially when paired with micropile load tests.

2.1.4 U.S. Army Corps of Engineers

Much of the history of micropile design exists using empirical data to construct equations that give conservative ultimate capacity values. However, researchers have developed different load-displacement formulas for various soil and pile conditions. The U.S. Army Corps of Engineers released a report discussing various load-transfer formulas. The majority of the report focused on axial loadings dealing with *f-w* curves for side friction and *q-w* curves for end bearing (Mosher & Dawkins, 2000). These relationships represent load-deformation curves in which more soil resistance is mobilized with increased deformation. A schematic representation of this methodology is presented by Figure 2-2.

The soil-pile system is considered radially symmetric located in a vertically homogeneous elastic medium to arrive at a relationship between side friction and axial pile displacement. Shear stresses are also assumed to decline a distance radially away from the pile. Using various work done by Kraft, Ray, Kagawa, Poulos, Davis, Randolph, and Wroth the U.S. Army Corps of Engineers sets forth the following relationship presented below in equation 2.8.

$$w = \frac{fR}{G} \ln\left(2L\rho \frac{1-v}{R}\right) \qquad \text{(Eq. 2.8)}$$

Where:

w = axial displacement of the pile

f = side friction between soil and pile

R = pile radius

G = soil shear modulus of elasticity

L = embedded length of pile

$\boldsymbol{\rho}$ = depth factor for soil modulus

v = Poisson's ratio of the soil

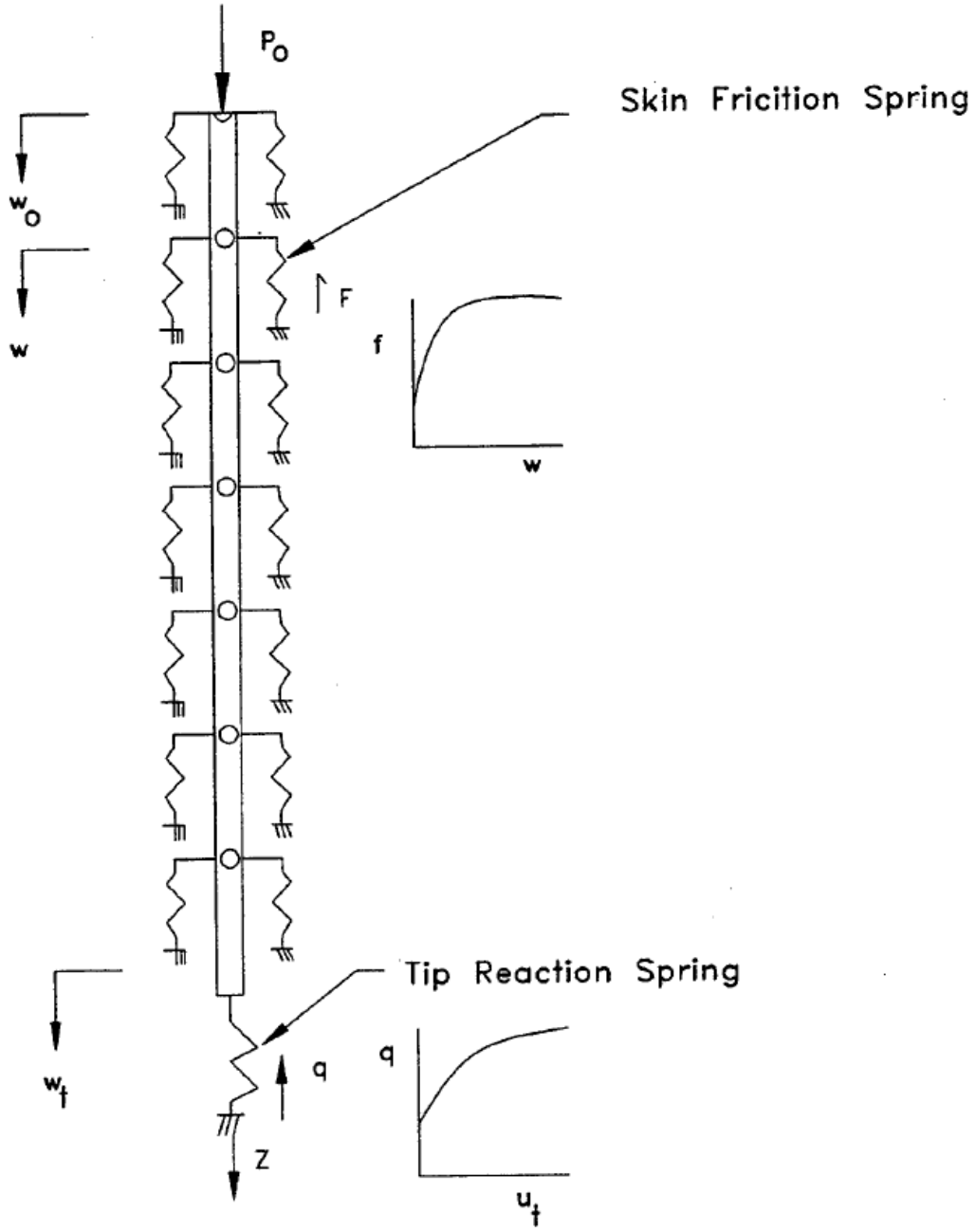

Figure 2-2. Soil-spring model for axially loaded pile (Mosher & Dawkins, 2000)

2.1.5 Structural Considerations for Axial Compression-Tension

When analyzing the structural components of the micropile the combination of steel and grout determines the axial capacity. Compression design can be calculated by the following equation.

$$Q_w = g\, f_c^1\, A_c + s\, f_y A_y \qquad \text{(Eq. 2.9)}$$

Where:

Q_w = design ultimate axial load

g and s = partial factors depending on material (depends on ASD or LRFD method)

f_c^1 = unconfined compressive strength of grout

A_c = area of micropile grout

f_y = yield stress of reinforcing steel

A_y = area of steel reinforcement

Essentially, this equation relates the areas of each material and their yield strength. The steel can be a combination of rod and pipe. If they have different yield stress values the term needs to be broken into two parts. This equation is for the axial capacity of the pile and doesn't consider structural buckling. Buckling may occur over any length. This is due to the lack of lateral confinement of the pile. These conditions can exist in soil such as karst terrain or liquefied soil. During structural design, if there exists casing in the final micropile design, buckling should be evaluated for any free length if any void areas or weak soil strata are encountered (Mosher & Dawkins, 2000). This scenario can essentially be treated as a beam constrained at both ends. The

structural capacities of micropiles are essential in effective design. Geotechnical engineers and structural engineers need to have open communication during micropile design (FHWA, 2005).

To determine possible buckling of a micropile a simple approach is to assume an unsupported length and do a column buckling analysis. This analysis is shown below in Figure 2-3 below. This void can also be considered for very weak soils and for locations in which liquefaction may occur during extreme earthquake shaking.

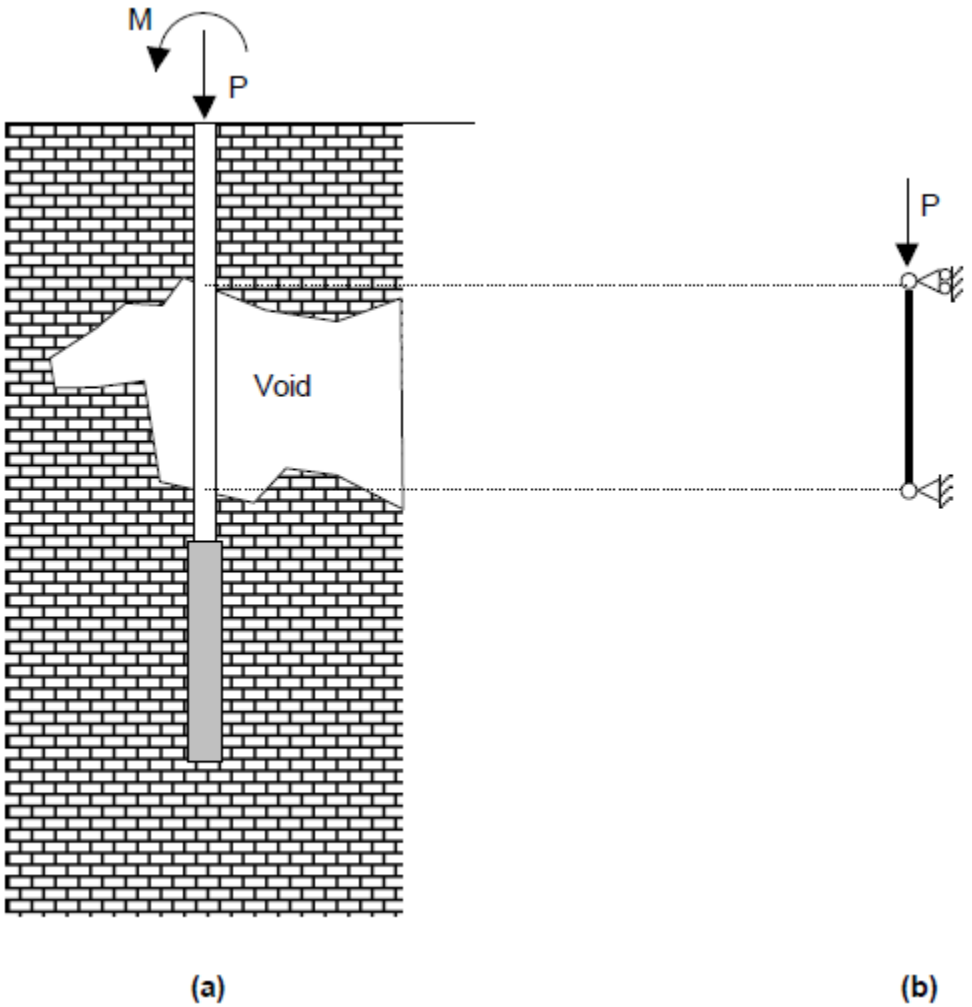

Figure 2-3. Micropile through a void in karst terrain (a) and buckling capacity model (b) (Cadden & Gomez, 2002)

2.2 Lateral Capacity of the Micropile

The soil-structure-interaction between the micropile and soil during lateral loading is a much more involved and difficult situation to model compared to the axial case. Purely elastic models fall short of characterizing the plastic behavior that inevitably occurs at the low soil pressures occurring near the ground surface. The nature of the load transfer mechanisms from lateral load transfers forces to the top portions of the soil which in turn yields. As the load is increased the soil yielding begins to occur further down the pile (Reese & Van-Impe, 2011). Due to this case, steel casing is an integral part of effectively transferring lateral loading to deeper stronger soils.

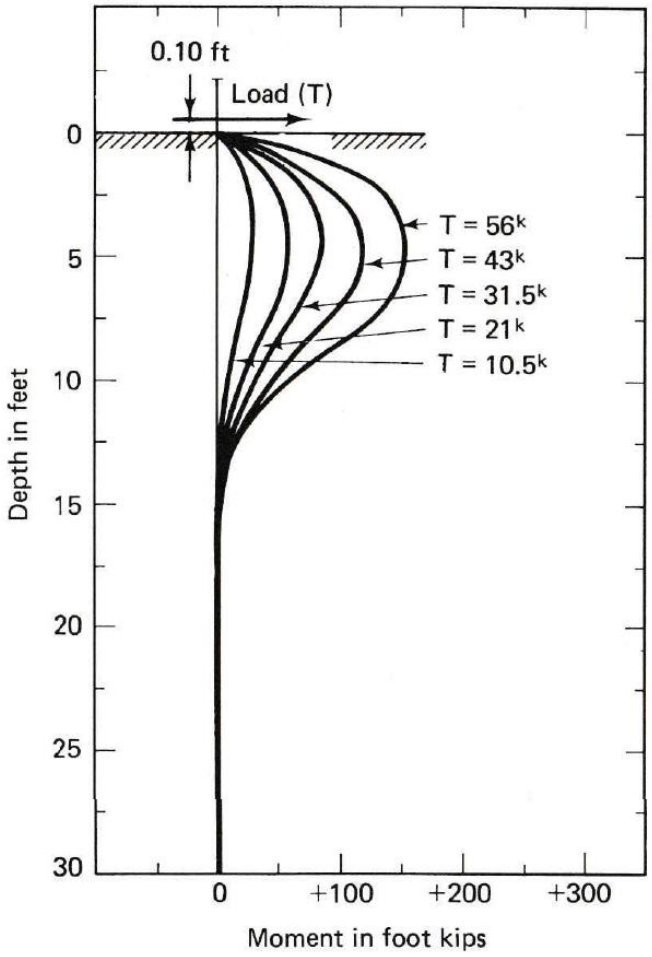

Figure 2-4. Moment vs. depth of a laterally loaded pile during load testing (Scott, 1981)

2.2.1 Winkler Spring Approach

A Winkler foundation system is presented. In this case the micropile, modeled as a beam, is rigid and placed upon a bed of Winkler springs. The load *P* is applied at the pile tip and no tensile stresses are allowed to develop between the subgrade and the pile. This scenario can be seen in Figure 2-5 below.

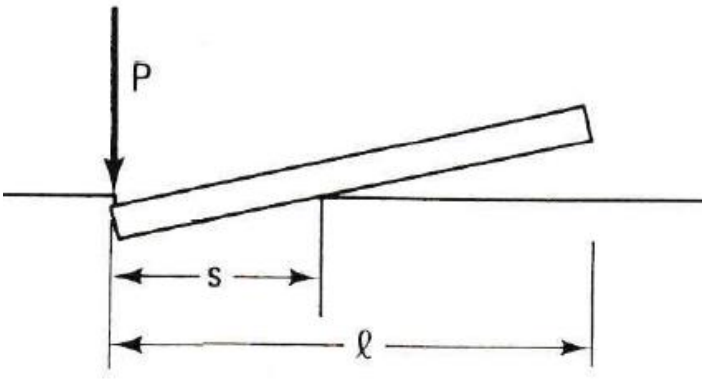

Figure 2-5. Winkler foundation under load *P* (Scott, 1981)

Taking force equilibriums among the beam equations are constructed by Scott to determine the beam deflection and moment at any given section. These equations are shown below.

$$w = \frac{2P}{kl}\left(-3\frac{x}{l} + 2\right) \qquad \text{(Eq. 2.10)}$$

$$M = Pl\left(-\left(\frac{x}{l}\right)^3 + 2\left(\frac{x}{l}\right)^2 - \frac{x}{l}\right) \qquad \text{(Eq. 2.11)}$$

Where:

w = beam deflection

P = load applied

k = subgrade reaction

l = length of pile

x = location along pile beginning at pile top

M = moment in the pile at a specific location

Various additions can be done to the Winkler model to emulate more precise field conditions. Such as below, a rigid beam now has tensile resistance at the bottom of the pile, this model would more appropriately fit the context of laterally loaded micropiles. However, this solution becomes much more complicated than the system presented above.

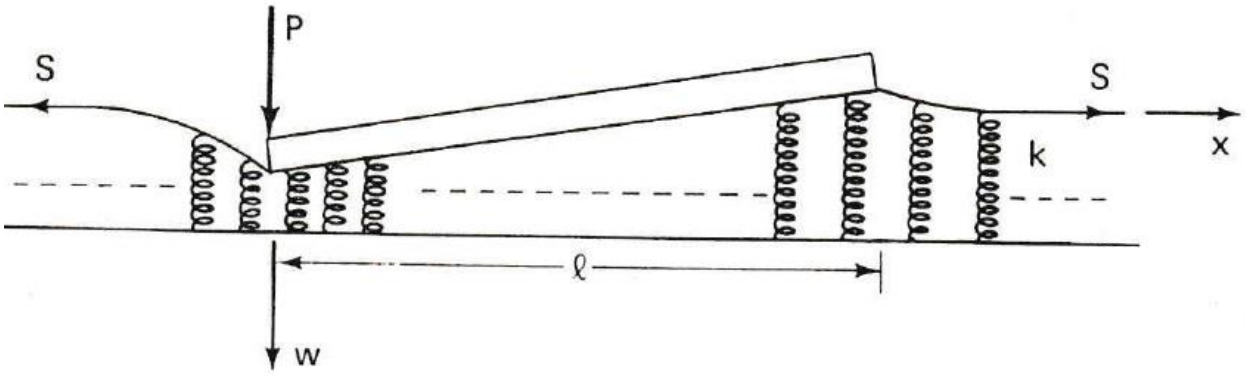

Figure 2-6. Point loading of a Winkler foundation allowing the subgrade to act in tension (Scott, 1981)

2.2.2 Beam Theory and *p-y* Soil Interaction

As the concern for the behavior of laterally loaded piles grew so did the availability of *p-y* curves. These curves represent the resulting soil reaction pressure per length, *p*, due to how much the soil has been mobilized, *y*. With these empirical graphs researchers were able to solve complex differential equations. Solutions to the beam theory and soil-structure-interaction can be found by placing various boundary conditions on the system. The fundamental differential equation present by Reese and Van Impe relating the soil reaction, pile stiffness, and pile loading can be seen below.

$$E_p\, I_p \frac{d^4y}{dx^4} + P_x \frac{d^2y}{dx^2} - p + W = 0 \qquad \text{(Eq. 2.12)}$$

Where:

E_p = pile modulus of elasticity

I_p = pile moment of inertia

y = pile deflection

x = distance from pile top

P_x = axial load on pile

p = soil reaction per unit length

W = distributed force along the length of the pile

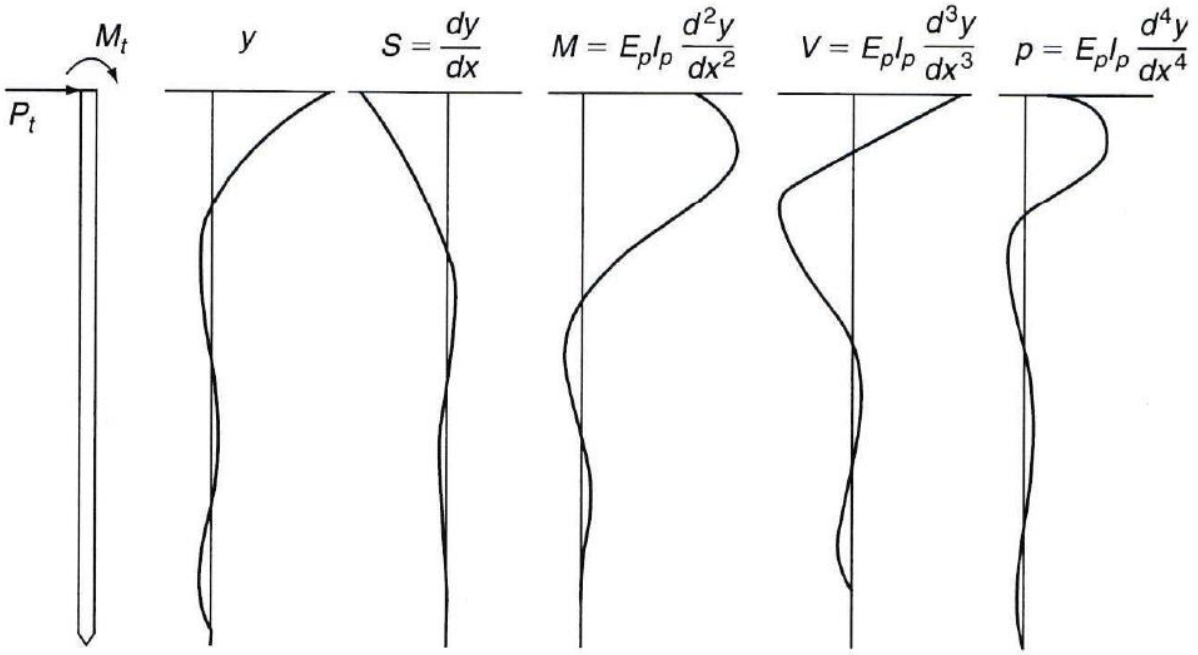

Figure 2-7. Deflection, moment, shear, and soil reaction for the beam theory solution (Reese & Van-Impe, 2011)

A solution to the differential equation can be seen in Figure 2-7 above using a lateral load and applied moment at the pile top. These numerical solutions allow the validation of many design theories used. The finite difference method can also be used with the *p-y* curves to obtain similar results. A *p-y* curve demonstrates the vast increase in strength present in the soil further down from the ground surface (Reese & Van-Impe, 2011).

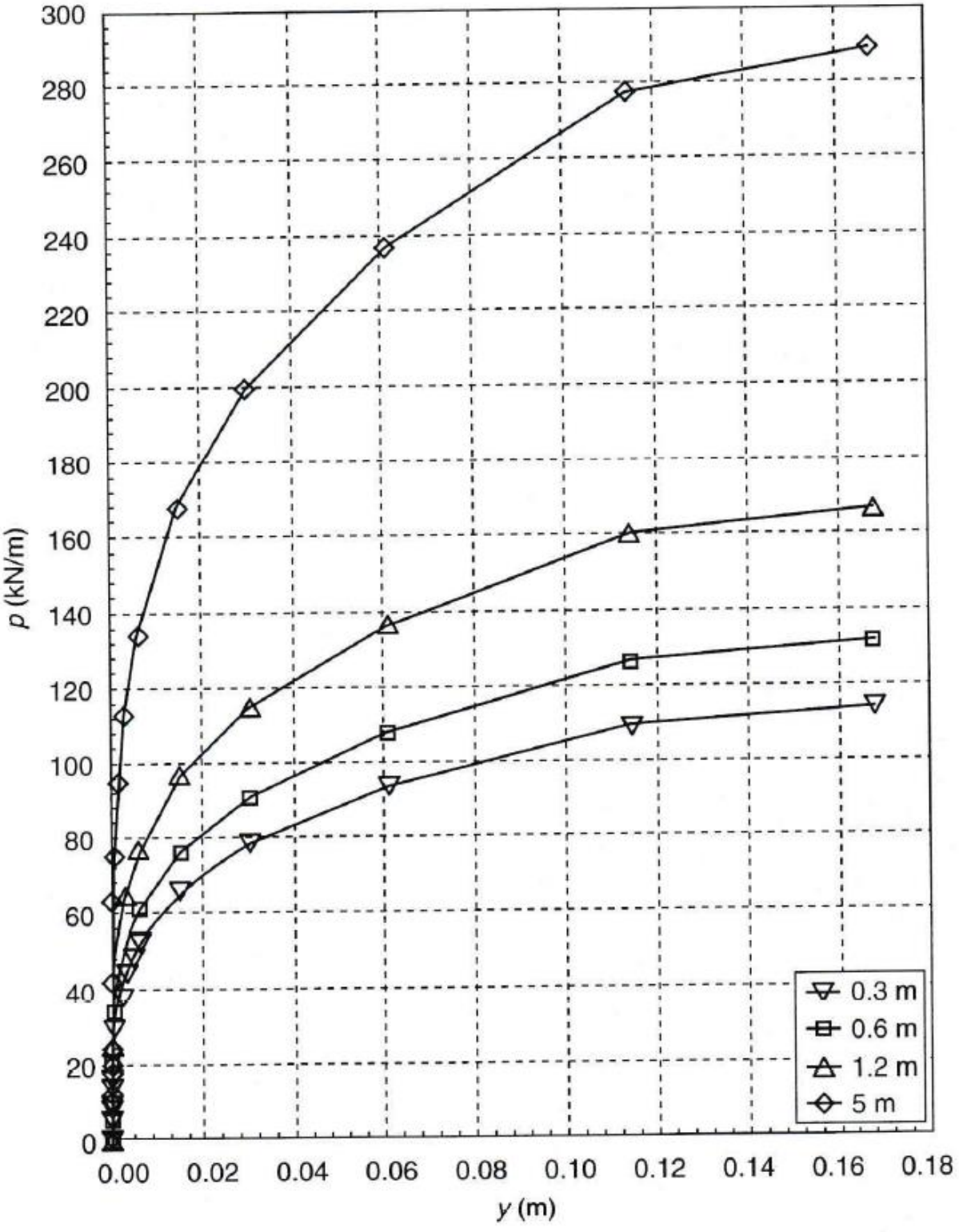

Figure 2-8. Example *p-y* curve developed for clay after load testing (Reese & Van-Impe, 2011)

2.2.3 Structural Considerations for Lateral Loading

The greatest concern for the structural components of a micropile when subjected to lateral loading in the bending stresses that occur. Since the micropile is considered to be a very slender pile, having a low pile diameter to length ration, large bending stresses can cause bending failure.

$$M_y = S\,\boldsymbol{\sigma_y} \qquad \text{(Eq. 2.13)}$$

Elastic section modulus (S) and plastic section modulus (Z) can be used to determine the yield moment of the micropile due to the yield stress of the micropile materials. Load factor resistance design (LRFD) is required for the design of structural bending in micropiles.

3. Micropile Construction Techniques

The type of drilling method used is largely dependent on the site conditions. Access, soil conditions, and the micropile application often determine the construction process. Often, overburden drilling is followed by rock drilling. In this case two different drilling methods might be necessary, one for overburden soil and another for rock excavation. Below Figure 3-1 shows some of the more common generic drilling methods used for micropile construction. When underpinning a structure or using micropiles for foundation retrofitting, it is also common to penetrate an existing structure.

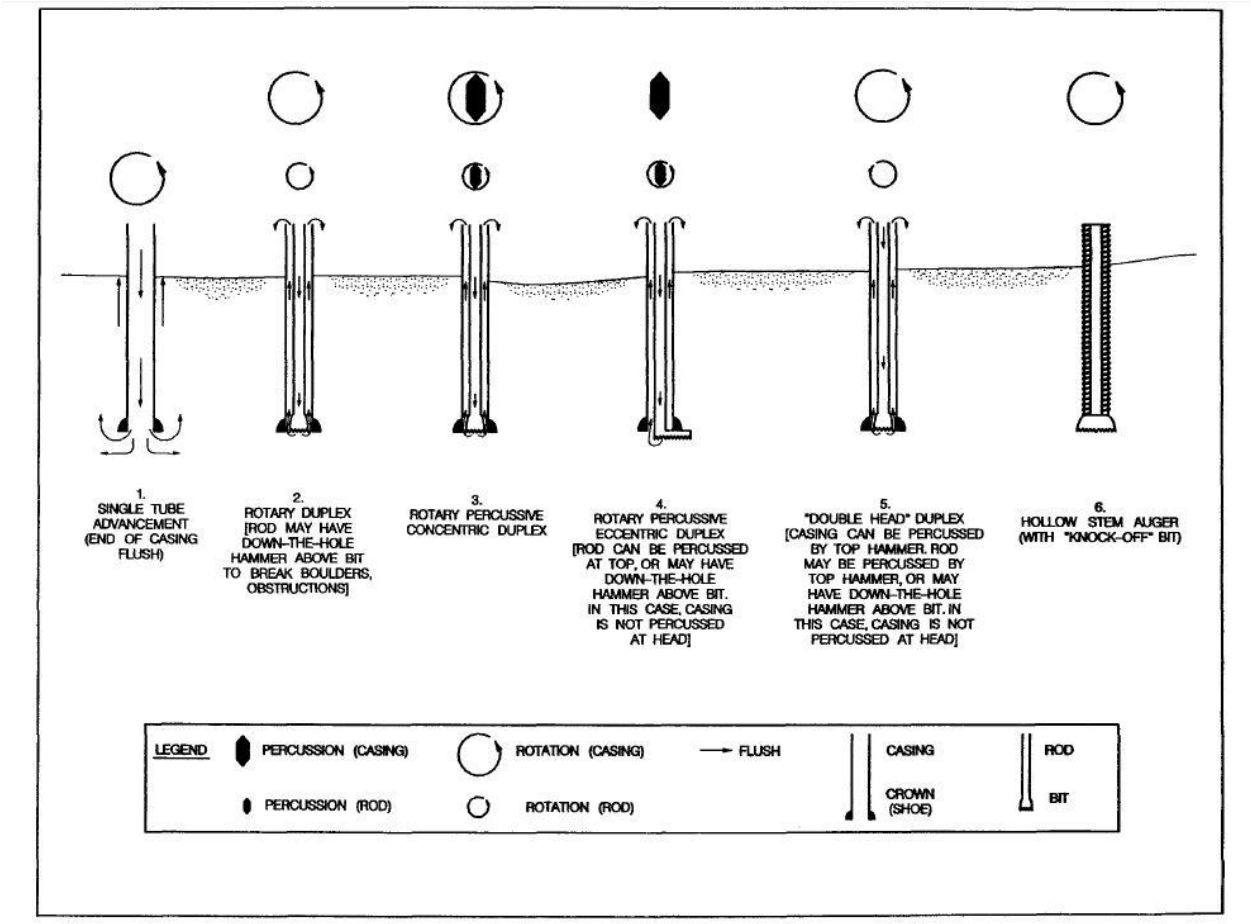

Figure 3-1. Schematic representation of the six generic overburden drilling methods (Bruce & Juran, 1997)

Micropile drill rigs are considered on the smaller part of the drilling rig spectrum, but range in size depending on the application. A typical micropile rig can be seen in Figure 3-2. While drilling is taking place, water is used to provide cooling and flushing. Flushing the borehole consists of removing the drilled soil resulting in a clean hole. Other methods such as foam and air are also used when drilling micropiles (Bruce & Juran, 1997). Foam and air also provide cooling while cleaning the drilled hole. The most common drilling method for overburden soils is single tube advancement, while the most common drilling method for rock excavation is rotary percussion. These two drilling methods are discussed in detail below.

Single tube advancement involves adding drill teeth or a casing bit to the end of the casing. As the casing is advanced, addition pieces are added to lengthen the hole. Rotating the casing breaks apart the soil, which is then flushed out. This method is advantageous because the drill bit is advances as the casing keeps the hole stabilized (Bruce & Juran, 1997). It must be noted that if the casing is to be removed, it should be done within a 24 hour period or there is risk of the casing becoming stuck. This drilling method is capable of drilling almost any type of overburden soil and some softer rock. Generally, if the micropile is designed to rest on bedrock, the casing bit will grind on top of the rock for a period of time. This ensures a competent bearing stratum.

Rotary percussion, also known as a rock hammer, uses abrupt oscillations and rotation to excavate rock (Shong & Chung, 2003). The rock hammer can be placed down the hole, where the casing is resting on bedrock, and advanced. Once bedrock is reached, the kelly bar of the rig is detached and a rock hammer is installed. The rock socket during drilling is almost always restricted by the inside diameter of the casing. Drilling time for the rock greatly depends on the

type of rock encountered, but generally is much costlier and time consuming than overburden drilling. Rock hammers are loud and required immense amount of foam or water to prevent the bit from becoming stripped.

Figure 3-2. Davey Kent 725 drill rig used for micropile construction

Once the drilling is complete, grouting and steel placement begins. Most commonly the grout is mixed on site and placed under gravity or pressure, depending on the micropile type. Threaded steel bar and steel pipe are then placed in the hole, if required, and then grouted. Depending on the size of these components a crane may be necessary. Sometimes the engineer requires the

casing in the hole as the steel pipe reinforcement. Micropile specifications also are known to require grout placed on the outside of the steel pipe for a greater concrete-to-soil bond, and ensure any voids surrounding the micropile are filled (NYSDOT, 2015).

Each drilling contractor has slightly different methods for the process outlined above. Load tests are prevalent among construction projects that use micropiles. The load tests provide important data concerning load capacity and settlement while ensuring quality control of the micropile. This provides the owner and contractor with empirical knowledge of the micropile and whether the design is sufficient. It should be noted that the drilling operator is highly skilled and often designated as the supervisor responsible for the safety of his laborers. Micropile construction for one hole requires 2-4 workers: a drilling operator and various laborers. As the drilling operator manages the drill rig, the laborers mix grout, move supplies, add casing, change bits, and provide additional eyes for the driller. The time required for each micropile is controlled by hole depth, rock socket depth, hole diameter, weather conditions, and schedule.

4. Load Testing of Micropiles

To assure the micropile design is adequate to hold loadings required for a structure a load test is typically performed. This allows the owner, contractor, and engineer to verify the soil-structure system behaves as they expect and modify any design if necessary. Load testing of a micropile prior to construction is often performed as part of a value engineering process. Often the test results provide the engineer assurance that predicted soil conditions are appropriate. Also, it provides the owner an opportunity to try less conservative designs that may provide significant savings. Due to the uncertainty in geotechnical soil characteristics micropile designs tend to be overly conservative. Load testing gives all parties involved to see the true behavior of the micropile compared to theoretical design calculations. Moreover, load deformation information can be crucial for structural engineers to correctly design connections and deformations in the structure. This section of the paper is included because load testing data is essential in the refinement of theoretical micropile capacity calculations. Simulated load tests were set up in ABAQUS to most accurately demonstrate a field load test. This allowed effective comparison to field load tests and simulated load tests for the load transfer research conducted.

Figure 4-1. Micropile static load test setup prior to applying tensile load

Sacrificial micropiles are loaded until a failure criteria is met laid out by the engineer. These micropiles are load tested next to the main site and then cut off the ground elevation. Production piles can also be load testing, but loaded up to the expected working load to avoid damaging the pile. Load testing production piles can save money, however may be risky if failure occurs. If a production pile load test fails and damage is visible additional design work is required. Failure criteria can be set forth in many different ways. The most common failure criteria seen are maximum deflection at ultimate loading, loading at which creep exceeds allowable movement,

maximum slope of the loading curve, and Davisson's loading criteria. Other load test failure criteria can be specified in the contract documents per the engineer.

Figure 4-2. Sacrificial hollow bar micropile prior to load testing

4.1 Compression and Tension Axial Load Testing

A majority of micropiles are designed to handle axial compressive or tensile loads. These loads are from the weight of the structure and any expected live loadings. Tensile loads are of more concern for uplift cases typically from overturning. The New York State Department of Transportation releases a Static Pile Load Test Manual that outlines static pile test methods. They specify a failure load defined by the load vs. gross deflection curve reached a slope of 1/32" per kip of applied load (*Geotechnical Control Procedure: Static Pile Load Test Manual*, 2015).

The GCP-18 as laid out by the NYSDOT specifies multiple types of static load tests including quick load test, incremental static load test, and constant rate of penetration test. These tests consist of loading the micropile through two cycles and up to failure criteria. On the first cycle the quick load test requires the micropile to be loaded up to 200% of the design load and then up to failure criteria for the second cycle. Example results from an incremental static load test can be seen in Figure 4-3 below.

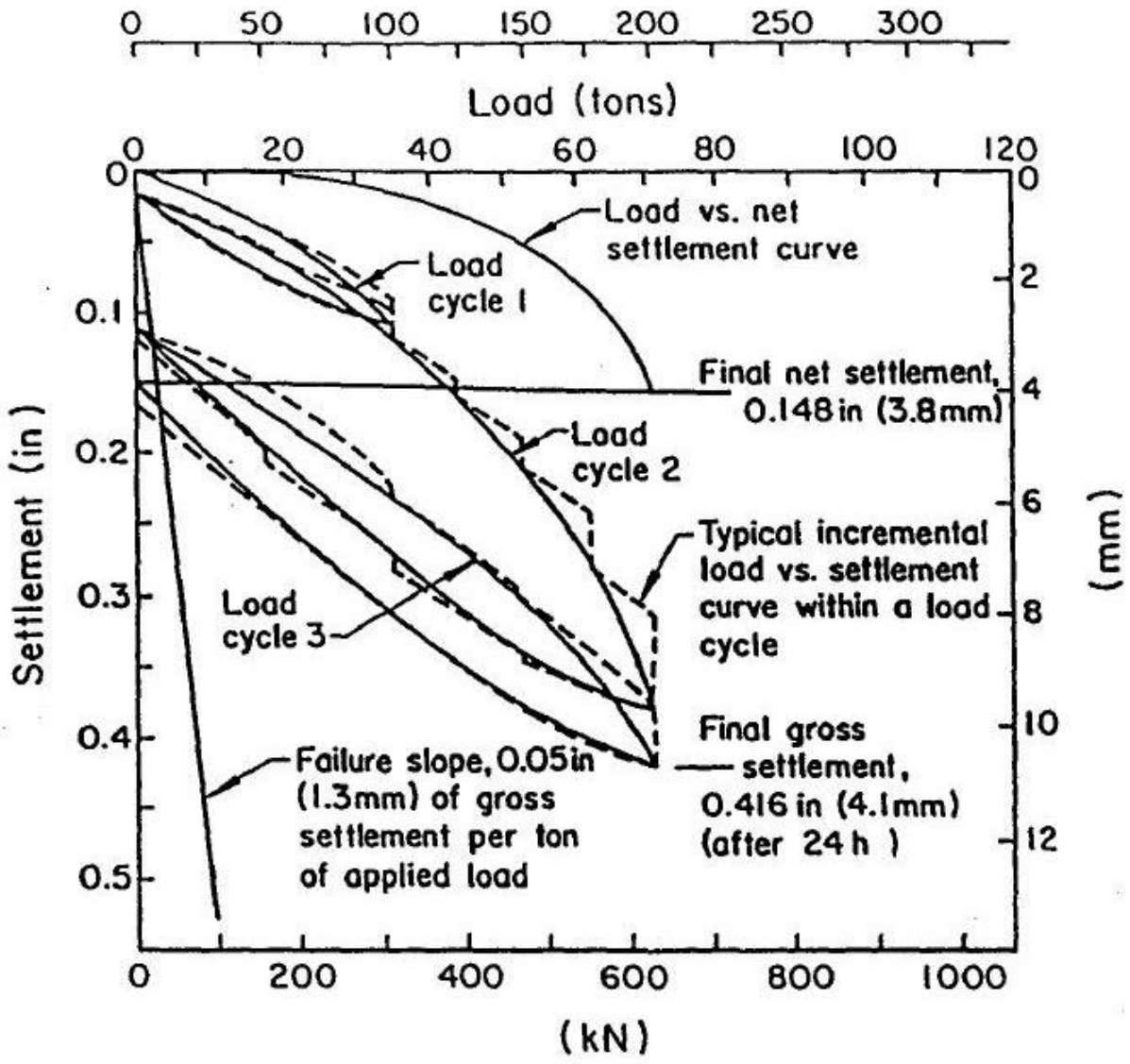

Figure 4-3. Load deformation graph of an incremental load test (*Geotechnical Control Procedure: Static Pile Load Test Manual*, 2015)

Another commonly used load test standard in the American Society for Testing and Materials ASTM D1143. The Standard Test Method for Piles Under Static Axial Compressive Load outlines similar testing procedures and load frame setup as presented in the NYSDOT GCP-18. Important sections include loading apparatus, measurement setup, loading procedures, safety, and report.

Two types of axial load testing include compression load testing and tensile load testing. Micropiles are known to have similar capacities in the axial and tensile load case. However, there are differences. Tensile load cases only mobilize side friction, which in the slender case of the micropile can be inconsequential. Due to this reason tensile load tests can be carried out to assure the compressive capacity of a micropile. In rare cases such as high capacity micropiles and for cases where micropile bucking is of concern compression load testing is required. The load frames for a compression load test and a tensile load test differ in the ways in which the reactionary loads are transferred to the ground.

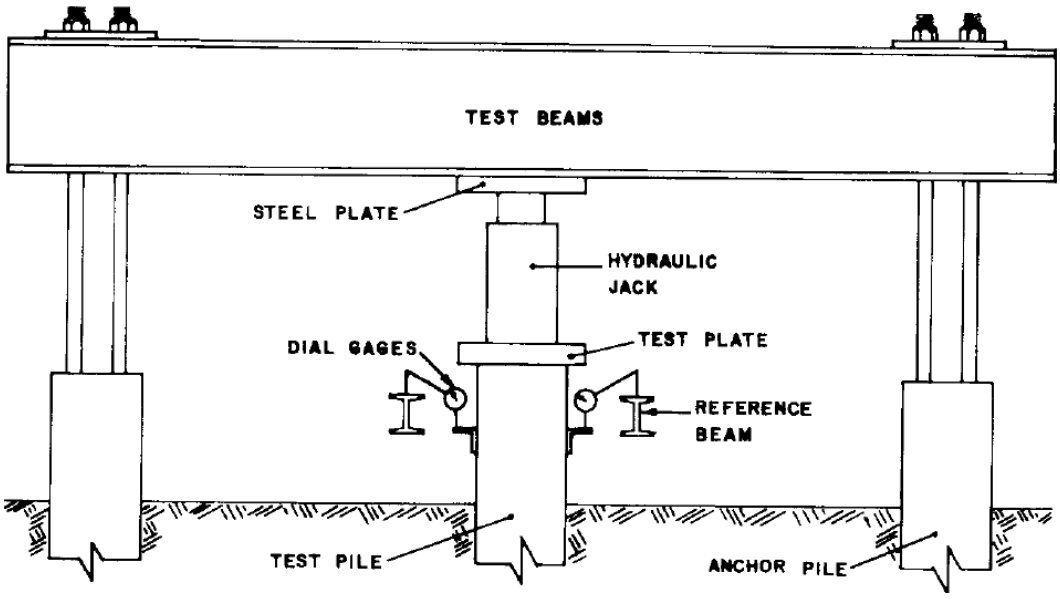

Figure 4-4. Load Test Frame setup for a compression load test (ASTM, 1994)

The reason tensile load tests are commonly conducted is the reduced cost compared to compression load tests. A compression load test frame can be seen in Figure 4-4 and a tensile load test frame can be seen in Figure 4-5. A compression load applied by a hydraulic jack requires reaction forces opposite of the forces applied to the pile, thus reaction anchor piles are

required. These additional piles increase the cost of the load test dramatically compared to a tensile load test where cribbing can be used to transfer the reactionary forces to the ground.

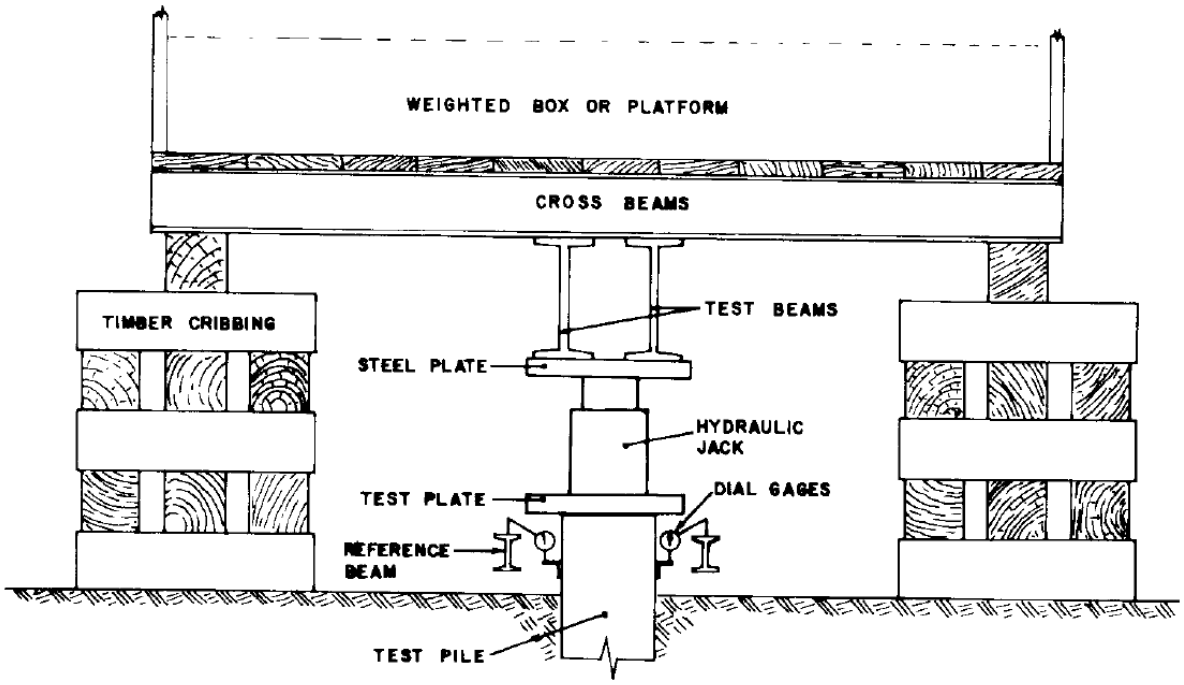

Figure 4-5. Load Test Frame setup for a tensile load test (ASTM, 1994)

Load test data is invaluable to an engineer designing micropiles. One of the reasons ABAQUS was chosen for this research was the ability to most accurately simulate micropile load tests. The ability to simulate an axial load test with various casing lengths is a cost effective way to further understand load transfer mechanisms. Replicating field load tests as close as possible allows a more realistic calibration of the computer models.

4.2 Lateral Load Testing

Unlike axial load testing of micropiles, the lateral load testing of micropiles is much less common. Micropiles are designed to resist high lateral loads in specific circumstances such as high wind loads, wave loadings, earthquake loadings, and to resist expected overturning of the structure. Same concept applies for lateral load testing in that a load frame needs to accommodate the reactionary forces from the applied load. The ASTM3966 Standard Test Methods for Deep Foundations Under Lateral Loads outlines a few basic load frame principles that is recommended for engineer and contractors to use. Three of those load frame setups can be seen in the various figures located below. Figure 4-6 utilizes additional piling and a pile cap to resist the lateral loading applied to the test pile. This would be necessary for large lateral loadings where a weighted platform is not adequate to resist the load as seen in Figure 4-7.

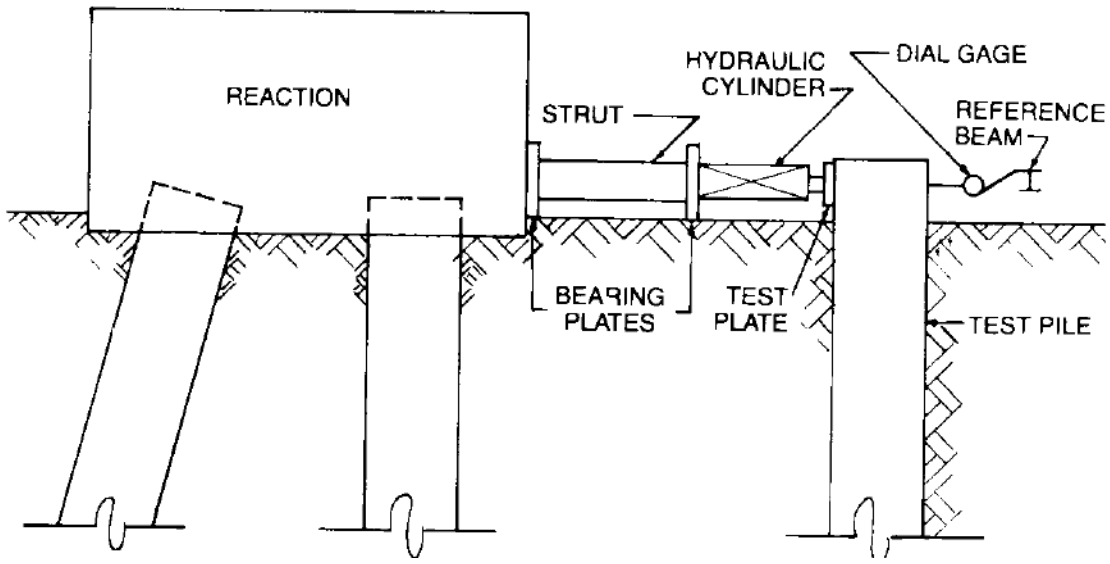

Figure 4-6. Reaction pile system for lateral load test (ASTM, 1995)

Any additional micropiles or poured concrete required for a lateral load test can significantly increase the cost of testing. For this reason engineers and contractors typically try and use temporary load frames when possible. Due to high potential cost of lateral load testing in some instances the owner prefers a conservative design to avoid this additional cost ("Micropile Installations Dutchess Rail Trail (Stage 4) Poughkeepsie, New York," 2012).

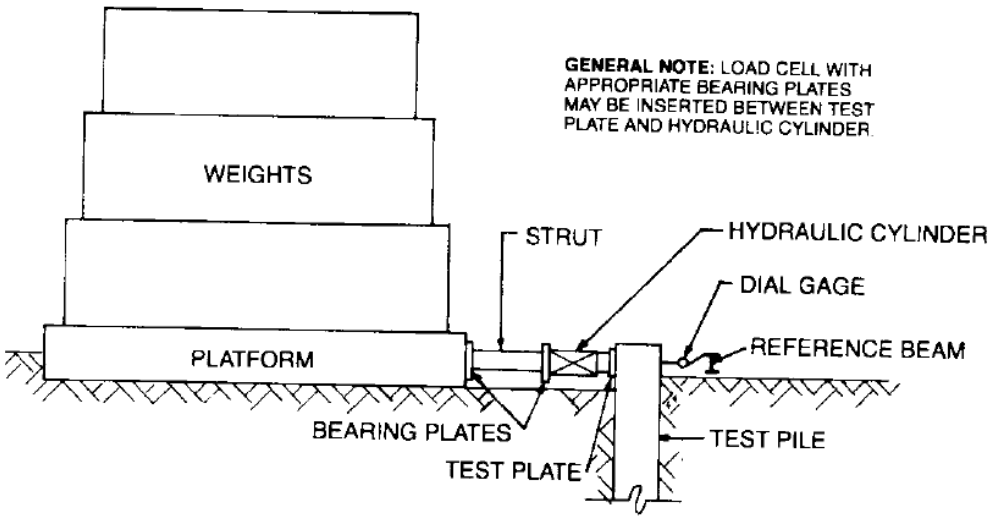

Figure 4-7. Weighted platform system for lateral load test (ASTM, 1995)

Testing two piles simultaneously allows the engineer to provide a reactionary force and see the performance of two piles at the same time. As seen in Figure 4-8 this method of lateral load testing utilizes the test piles providing the necessary reactionary forces. Separate reference beams gives the engineer data about each pile individually while the same load is being applied to each pile (ASTM, 1995). However, if one of the piles fail prior to acceptable test loads the data may become void for both piles.

Lateral load tests were also simulated using the program ABAQUS. Results indicated the casing is an important aspect of the lateral capacity of micropiles and should always be included when high lateral capacities are required.

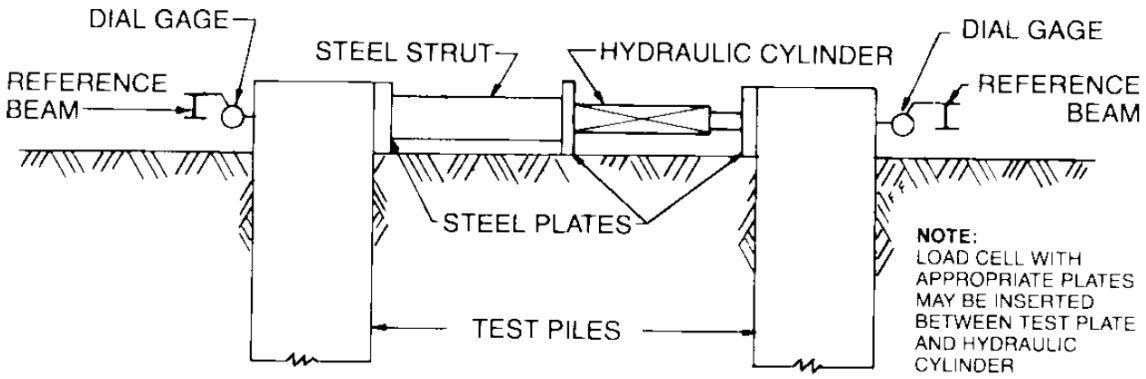

Figure 4-8. Lateral load testing of two piles simultaneously (ASTM, 1995)

Micropiles can be designed to withstand both lateral and axial forces at the same time. However, when large lateral loads are expected a lateral load test can be conducted. Certain circumstances require knowing the exact behavior of the micropile when subjected to both axial and lateral loads at the same time. Seen in Figure 4-9 is a setup that tests the pile for a combined axial and lateral load. The combined load can induce additional moments throughout the micropile. The combined loading test may be the most realistic way to model the loading conditions of the micropile in the field. A downside to this test is intricate load frame and is only feasible for large scale projects, high capacity micropiles, or difficult site conditions.

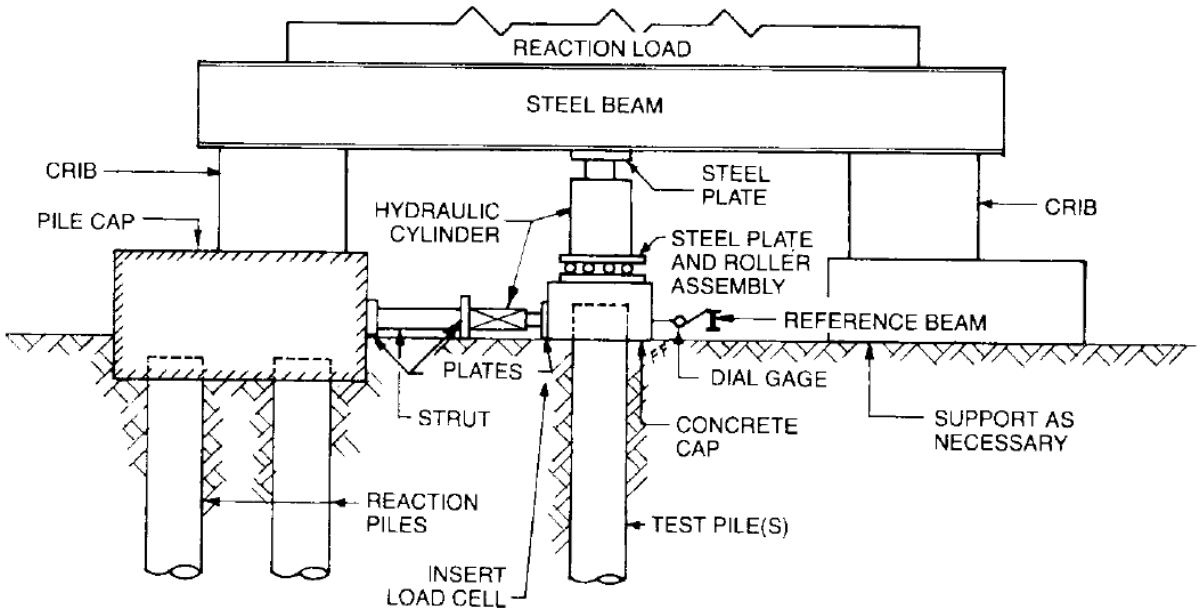

Figure 4-9. Load test frame for a combined lateral and axial compressive load (ASTM, 1995)

Understanding the relationship between axial and lateral capacities of the micropile is difficult, but load test data can provide engineers certainty in their design. We have seen potential in using available load test data and sophisticated load test modeling to better understand the soil structure interaction between the micropile and soil during load.

4.3 Instrumentation and Data Analysis

Essential data documented from a micropile load test consists of percentage of design load applied, duration of load applied, and deformation of the pile. Depending on the specifications set forth by the engineer and the type of test conducted more advanced testing techniques may be required. The recent use of strain gauges, digital telltales, accelerometers, and other advanced sensing technologies has allowed a greater understanding of the load transfer mechanisms of micropiles. Although these advanced sensing technologies are mostly used in an academic or a research environment, more contractors and engineers are seeing the value engineering in using these sensors to better understand the performance of micropiles (Bruce & Juran, 1997).

Instrumentation of micropiles has determined that end bearing provides small resistance compared to the skin friction resistance provided by a micropile. This is due to the slenderness ratio (micropile diameter/micropile length) of the micropile. Results have also shown that micropiles are capable of transferring large loads to rock sockets by utilizing steel casing (Seo, Prezzi, & Salgado, 2013). Using sensing technology to understand the load transfer mechanisms for various field conditions will aid to progress the theoretical understanding of micropile behavior. Instrumented field test data and computer modeling can aid micropile design engineers to develop more accurate design equations and theories.

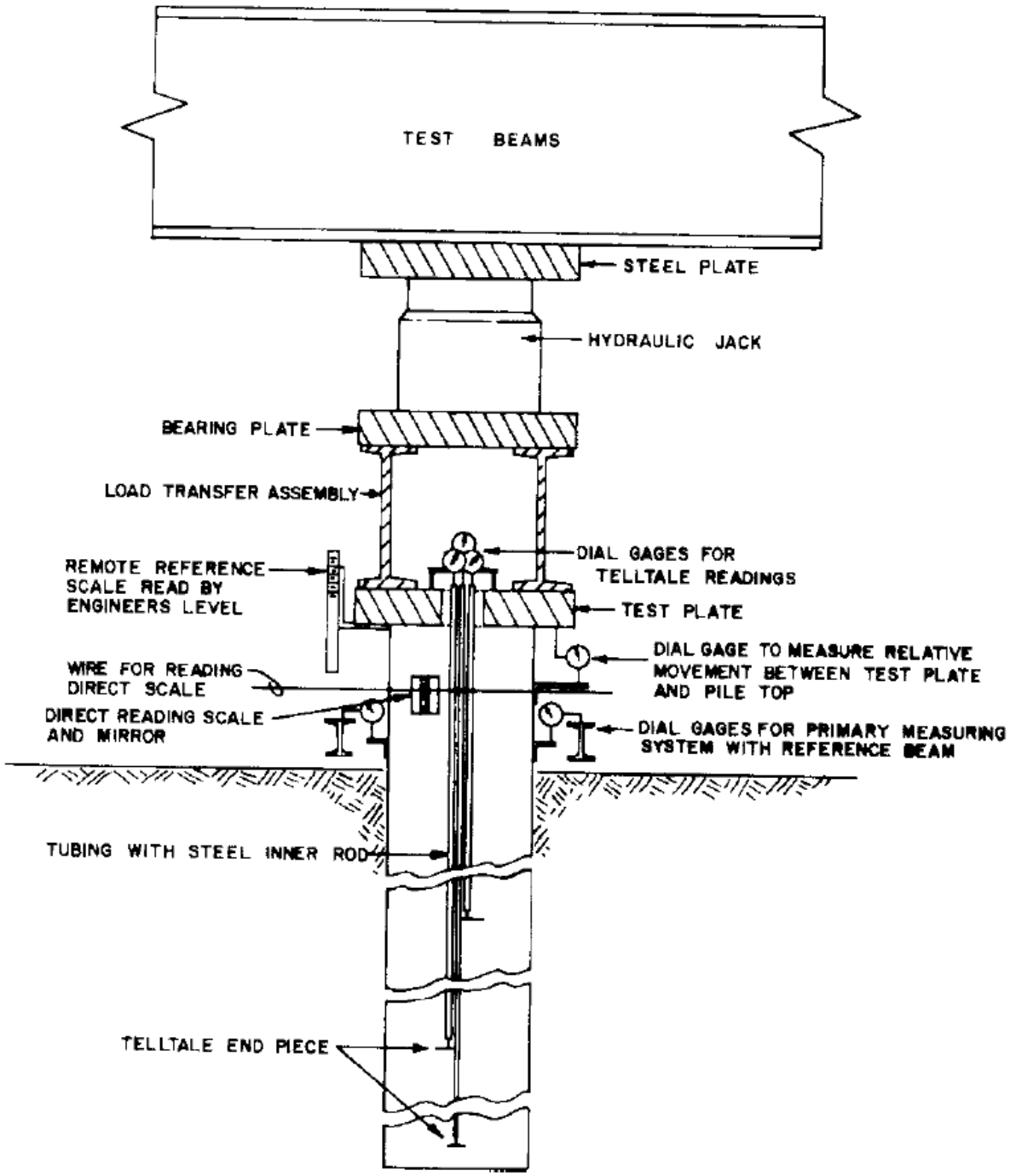

Figure 4-10. Typical instrumentation for a micropile load test (Bruce & Juran, 1997)

In Figure 4-10 above shows a typical load test instrumentation setup to acquire data to determine whether the micropile is adequate to hold the design loading. Dial gauges measure the relative movement to a reference beam providing the engineer with settlement readings. During this time load values are also being recorded from a hydraulic jack or other loading device (ASTM, 1994). Further instrumentation beyond typical load tests, as seen in Figure 4-11, includes strain gauges at various points along the pile. This allows the engineer to interpret how the load transfer mechanism of the micropile are interacting with the ground.

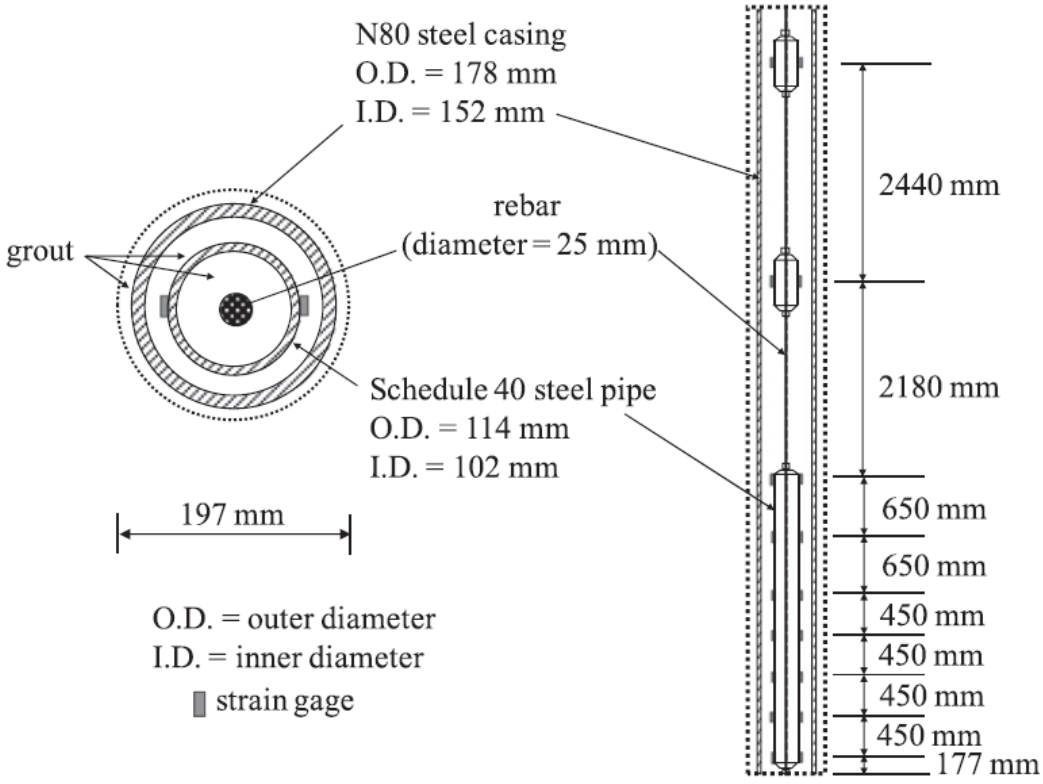

Figure 4-11. Instrumentation details for a rock-socketed micropile (Seo et al., 2013)

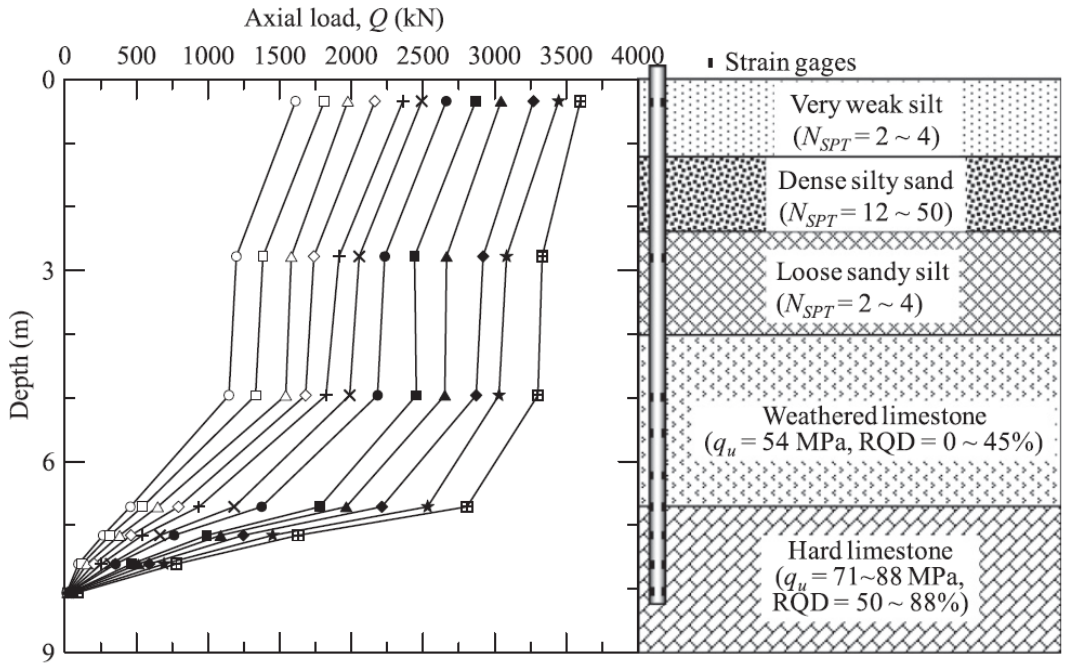

Figure 4-12. Distribution of axial load for an instrumented rock-socketed micropile (Seo et al., 2013)

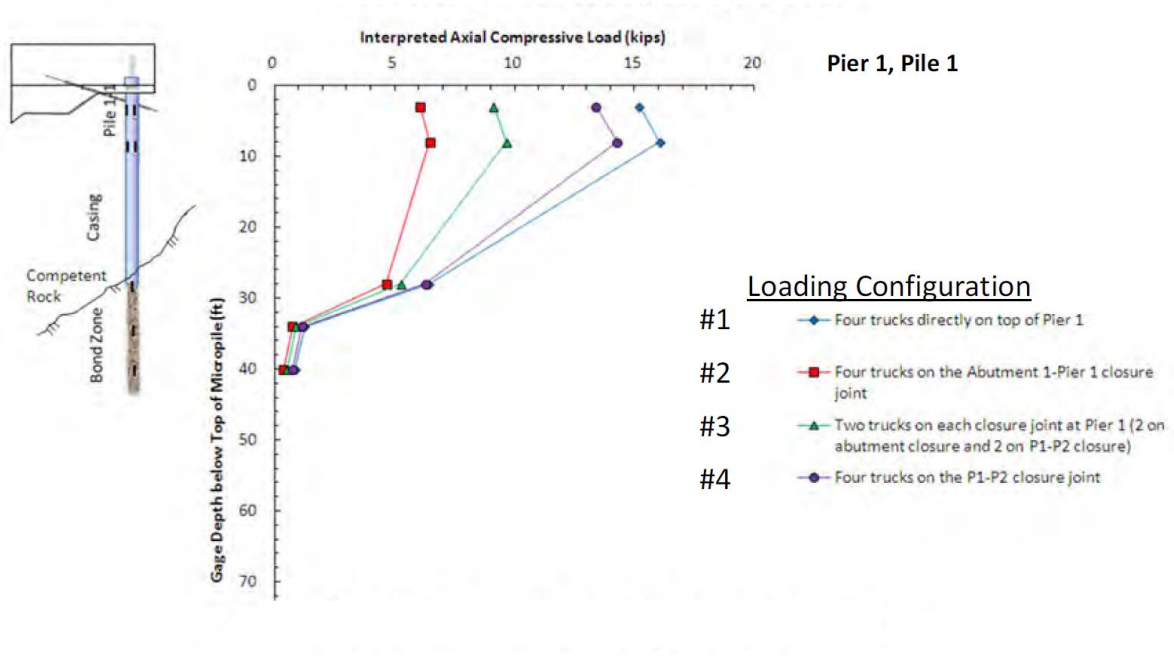

Figure 4-13. Instrumented micropile for Bridge No. 2 of the Foothills Parkway in eastern Tennessee (Luna et al., 2015)

Results for instrumented load tests can be seen above in Figure 4-12 and Figure 4-13. As simulated in the FEM the casing provides some friction for the micropile but acts more unbonded. Casing to rock provides immense capacity for the micropile as seen up to 3500 kN (Seo et al., 2013). Much of the axial loading is both cases presented above is transferred between the rock socket and the micropile.

Many large scale projects utilize strain gauges and other instrumentation to better understand the load transfer behavior of the micropile design. Due to the ease of installation and load testing makes the micropile a candidate for instrumented load tests to become more popular. Especially for high capacity micropiles cased to rock, instrumented load tests provide data on the exact load transfer mechanisms and ensure the micropile can adequately handle the loads required. Previous field tests and instrumented micropile results were compared to the current FEM to ensure expected capacities and typical load transfer behaviors.

5. Finite Element Analysis of a Micropile

In order to understand further the behavior of a loaded micropile a finite element model was constructed. Finite Element Analysis (FEA) uses boundary conditions to determine approximate solutions for a system by solving a system of many equations. Providing material characteristics, a geometric model, and loadings the finite element software can determine the behavior of the system. For this project ABAQUS was used as the finite element software.

Numerical modeling can be beneficial for complex scenarios where traditional analysis methods become too time consuming and impractical. FEA can offer insight as to how the system behaves and then verified with using traditional engineering techniques. Running models such as this provides the engineering community with insight of the soil-structure-interaction (Hussin & Cook) of the micropile components and the soil. Bond strength, material characteristics, loading type, and structure design all impact the behavior of a soil-structure micropile system. The system was sequentially made more complex, with hand calculation checks along the way, to ensure the soil system was modeled properly. The main isolated variable, casing length, was chosen to show the geotechnical community the importance and impact casing design may have. This variable change is referred to as the cased length ration or CLR. Due to the slender nature of the micropile bending stresses can quickly cause plastic deformation if the load is not adequately transferred to competent soil or rock. The load transfer mechanisms present in steel casing for high capacity micropiles and laterally loaded designs prompted the further research. The Geomechanics and Geotechnical Engineering group at the University at Buffalo planned and implemented a micropile research model in ABAQUS.

Initially, two main types of soil, sand and clay, were used to analyze the behavior of the micropile. This is because the geotechnical design field focuses on developing design equations to deal with these two types of soils. Sand, a more granular material, depends on developing effective stress as depth increases. Clay, a cohesive material, is highly dependent on historic geologic loadings for its stiffness. As typically seen in the field the soil increases in strength as depth increases. Three soil layers are used in the model with each layer containing a higher strength. When designing the finite element model a process was followed to ensure quality and accuracy of the model. A flowchart outlining the process can be seen in Figure 5-1.

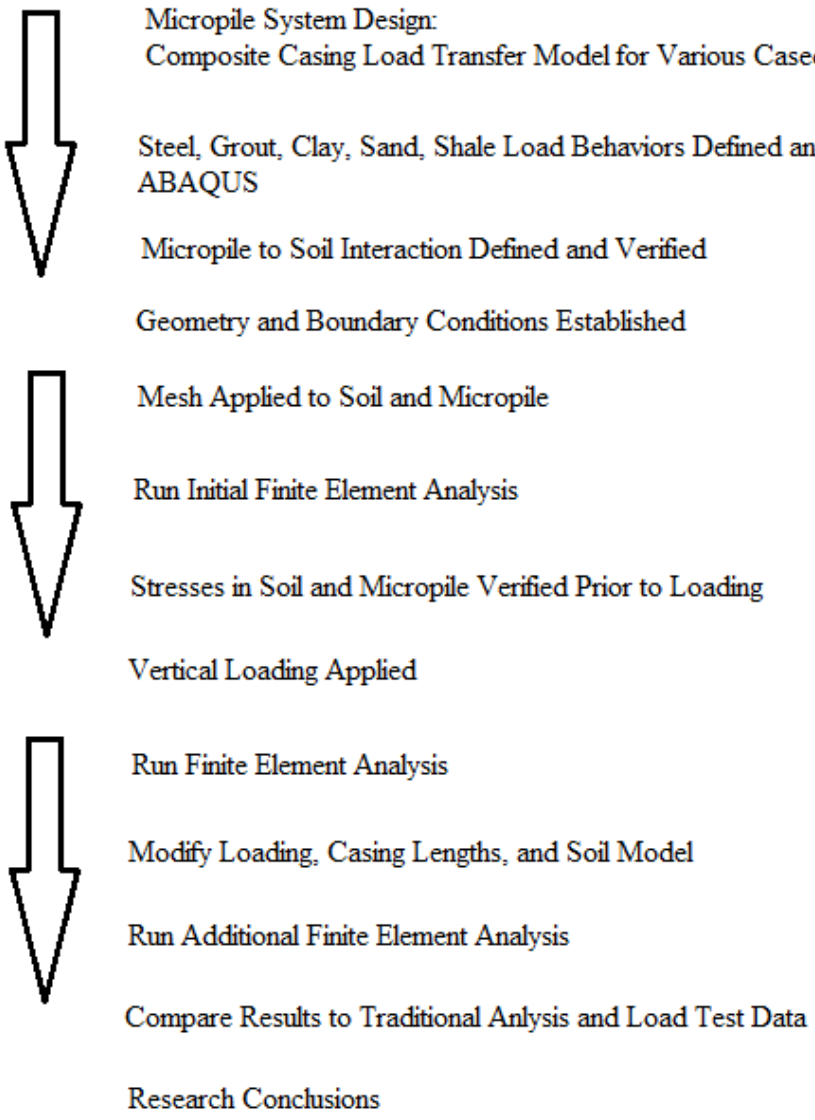

Figure 5-1. Finite Element Modeling Design Process

The history of the software ABAQUS dates back to 1978 at the dawn of the modern computer. Initially made for the mechanical engineering applications such as aerospace, automotive, and industrial machines ABAQUS has grown to be used all over the world for a multitude of problems (Helwany, 2007).

5.1 Finite Element Model Material Properties

Material properties are one of the most important aspects of finite element modeling to ensure accuracy. Many design equation in the geotechnical construction industry correspond to the elastic region of soils. This is to ensure safety of the public and keep geotechnical design conservative. However, in order to design more effectively elasto-plastic models need to be researched and further understood. For each material an elastic region was defined using an elastic modulus, poisons ratio, and density. Then for each material a plastic region was defined in a manner in which the material is expected to fail. The failure mechanisms of steel and concrete are fairly well understood. In this model strain hardening was used to emulate the plastic region of the steel and the stress-strain behavior can be seen in Figure 5-2.

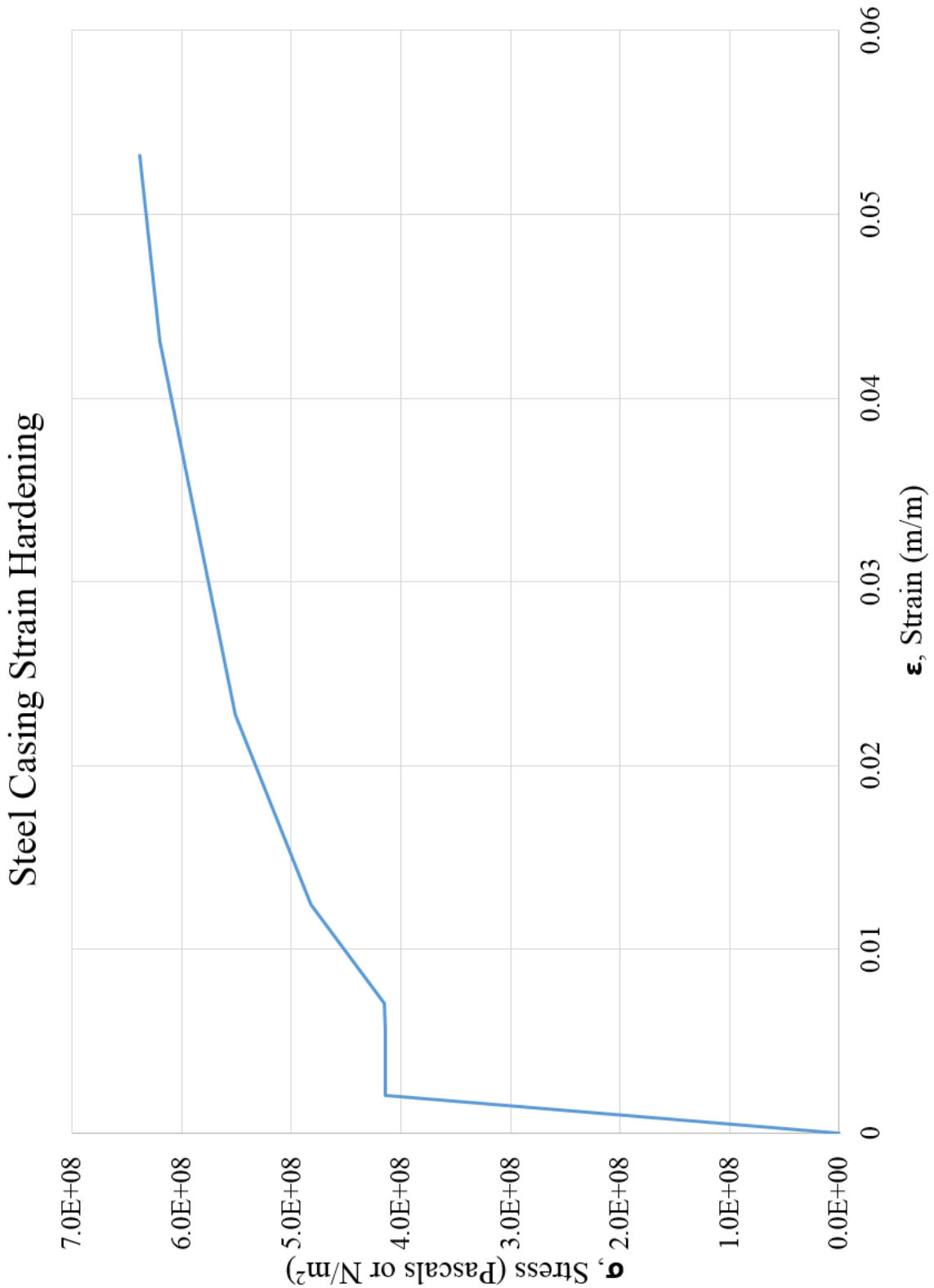

Figure 5-2. Stress-strain behavior of steel

For concrete, a Concrete Damaged Plasticity model was used to emulate compressive crushing and tensile cracking of the concrete. Since concrete behaves differently is compression and tension it is important to model these two instances differently. ABAQUS defines the behavior of Concrete Damaged Plasticity with the relationships seen in Figure 5-3. The variables E_o, ε_t, ε_c, d_t, and d_c represent the elastic modulus of concrete, strain variable in tension, strain variable in compression, damage variable in tension, and damage variable in compression. Essentially when a limit state is reached in compression the concrete has the ability to carry additional load before severe deformation. However, when concrete is in tension, such as bending of the micropile, concrete cracking can cause severe deformation and significant loss of strength. ABAQUS requires some user defined stress-strain behavior which can be seen in Figure 5-4 and Figure 5-5 then takes the various damage parameters and smooths the curves to math something similar seen in Figure 5-3.

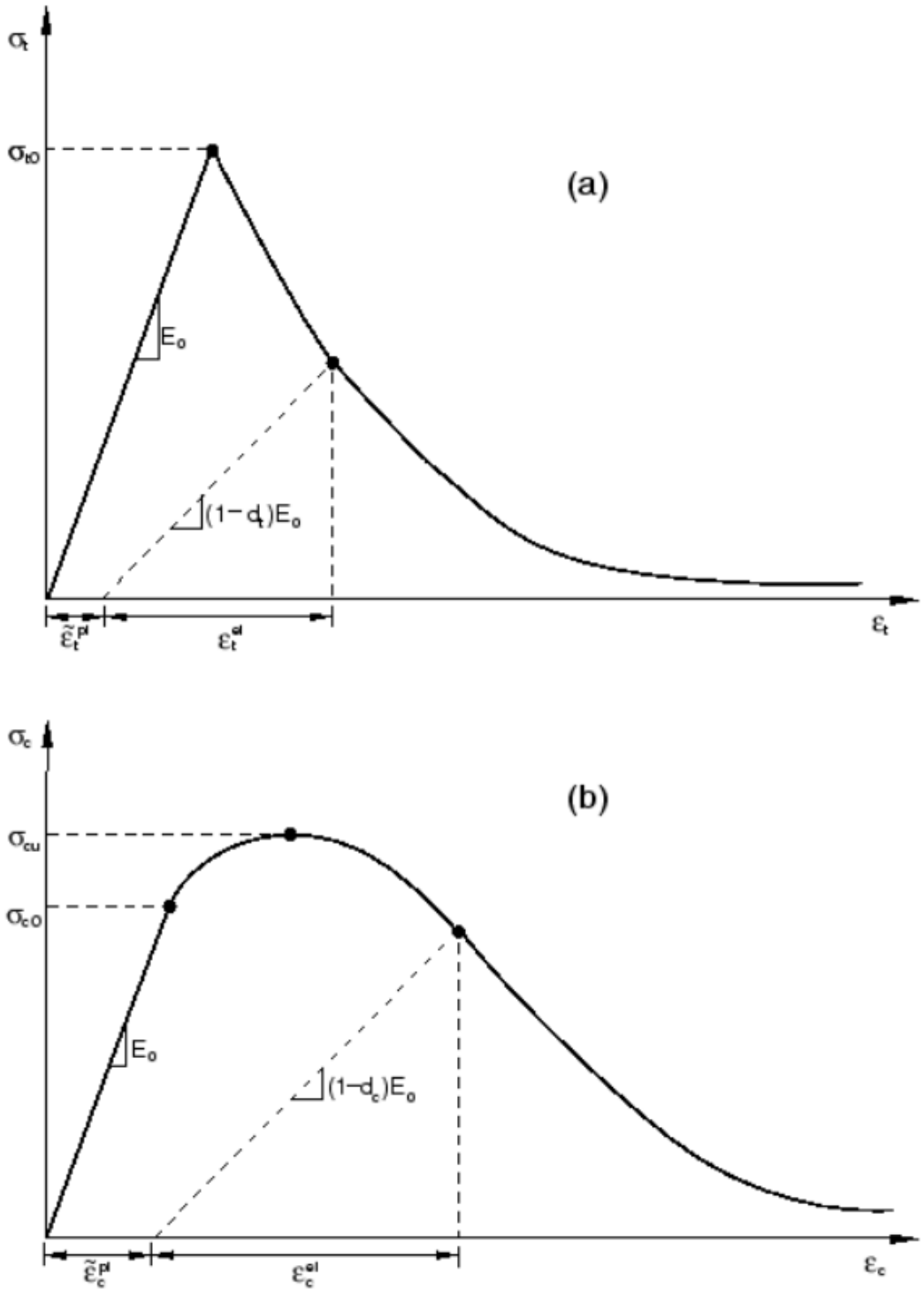

Figure 5-3. Response to uniaxial concrete loading in tension (a) and compression (b)

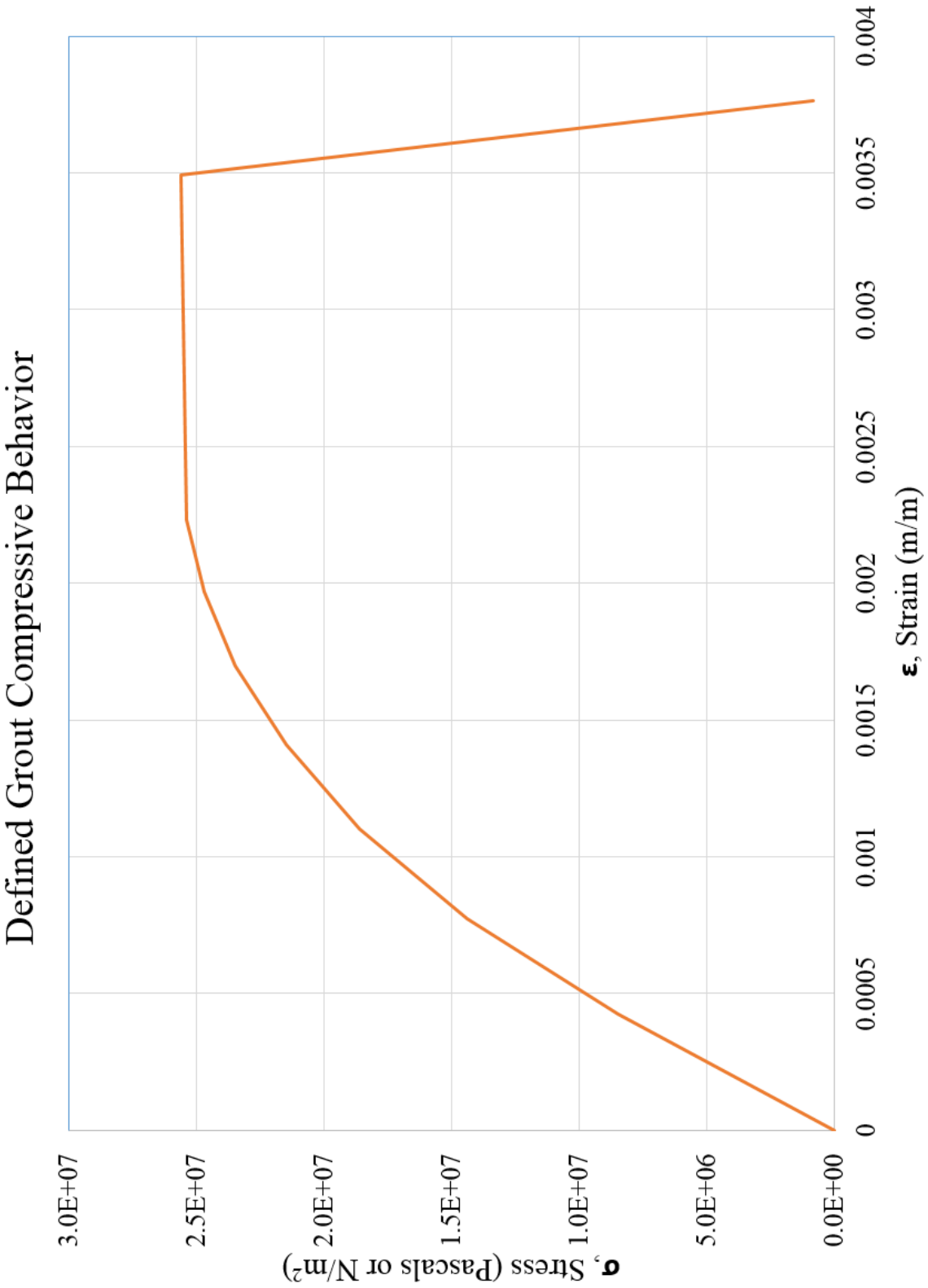

Figure 5-4. User define concrete crushing in compression

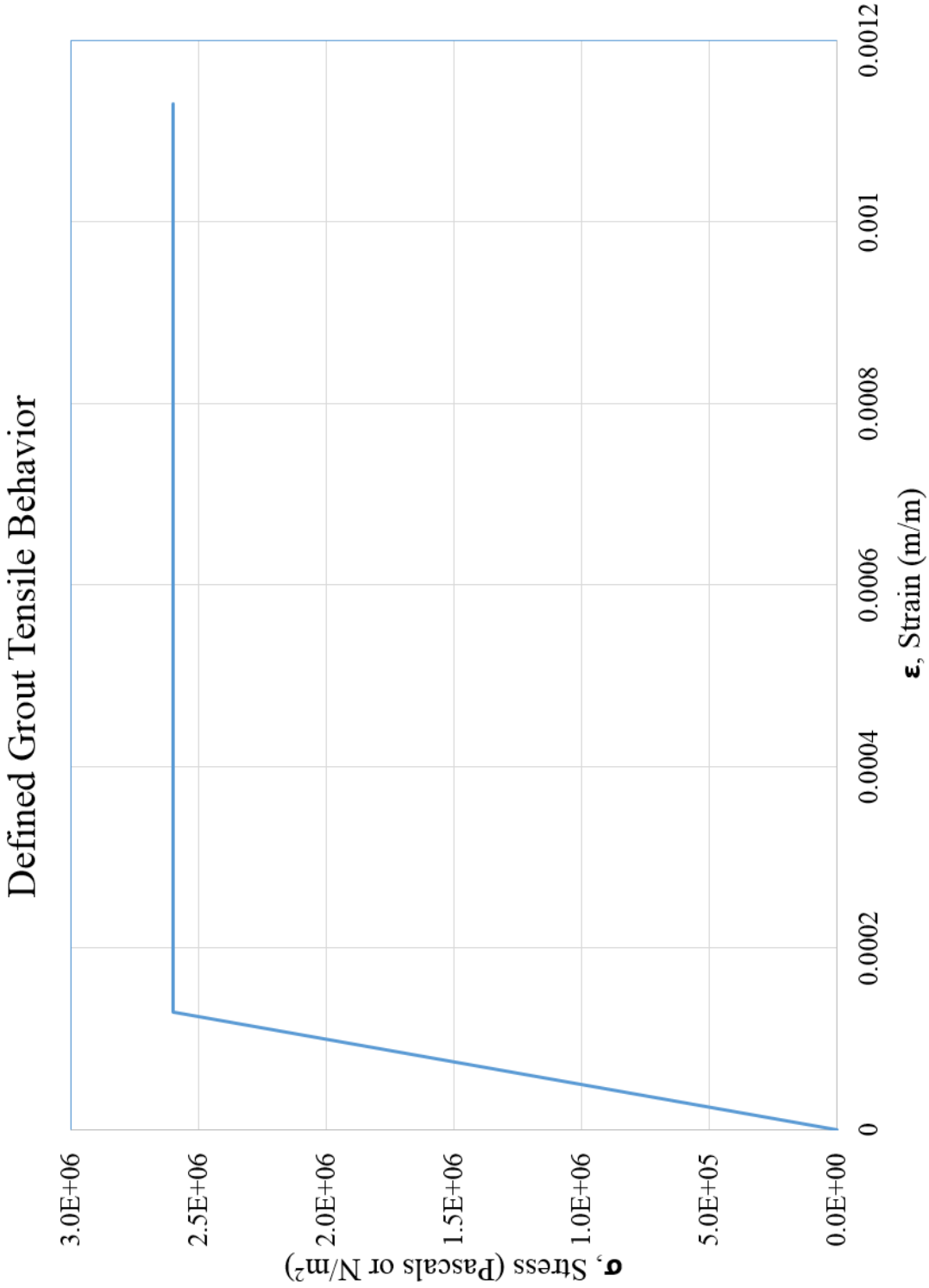

Figure 5-5. User define concrete tension cracking

The plastic flow of geomaterials, specifically cohesive-frictional materials, has experienced extensive progress in the form of research and triaxial testing. However, discrepancy still occurs between theoretical models and in-situ soil behavior (Houlsby, 1991). For this model Mohr-Coloumb Plasticity was used to emulate the plastic yielding of the soil. This theoretical model was chosen due to its applications for both cohsive and frictional soils. In Mohr-Coloumb model a combination of normal and shear stresses determine the yield limit of the material. A graph showing a soil material containing both an angle of internal friction and cohesion can be seen in Figure 5-6. For the model developed in ABAQUS, the clay was only given cohesive properties while the sand was soley given an internal angle of friction. Although in-situ soils rarely exhibit this ideal behavior identifying the difference in the soil-structure interation among these two soil properties leads to a greater understanding among the geotechnical industry.

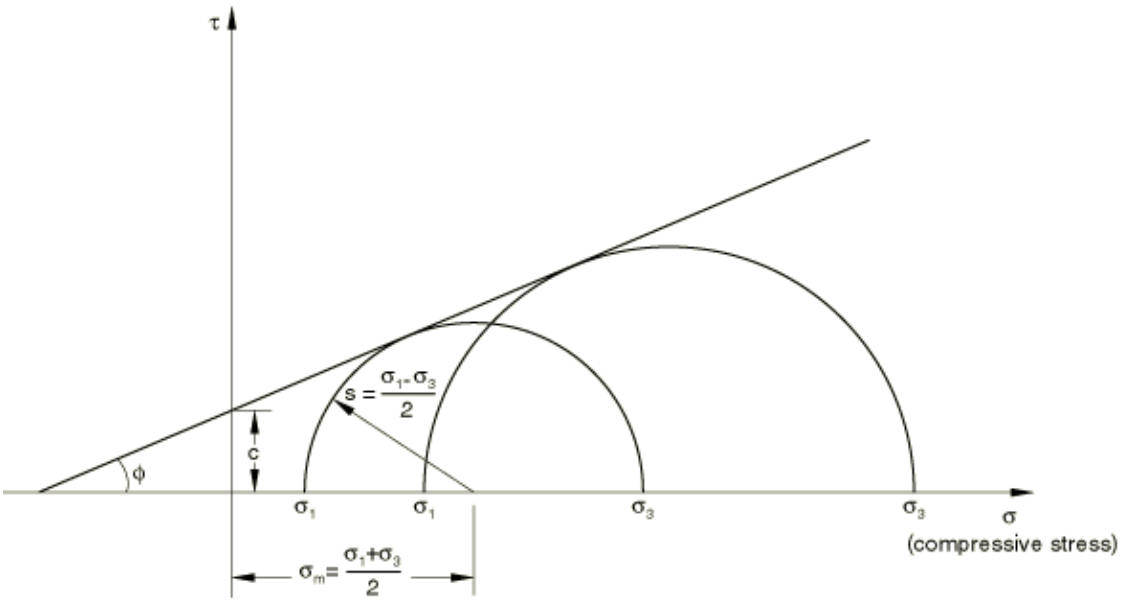

Figure 5-6. Mohr-Coulomb yield surface (Helwany, 2007)

The Mohr-Columb shear strength model is defined by the following equation.

$$\tau = c - \sigma \tan \phi \qquad \text{(Eq. 5.1)}$$

Mohr coloum plastic flow equations are written in terms of three stress invariants.

$$F = R_{mc} q - p \tan \phi - c \qquad \text{(Eq. 5.2)}$$

Where the stress invariants are defined as follows:

$$p = -\frac{1}{3} trace(\boldsymbol{\sigma}) \qquad \text{(Eq. 5.3)}$$

The equivalent pressure stress

$$q = \sqrt{\frac{3}{2} (\boldsymbol{S} : \boldsymbol{S})} \qquad \text{(Eq. 5.4)}$$

Mises equivalent stress

$$r = \left(\frac{9}{2} \boldsymbol{S} \cdot \boldsymbol{S} : \boldsymbol{S}\right)^{\frac{1}{3}} \qquad \text{(Eq. 5.5)}$$

Is the third invariant of deviatoric stress

$$\boldsymbol{S} = \boldsymbol{\sigma} + p \boldsymbol{I} \qquad \text{(Eq. 5.6)}$$

Is the deviatoric stress

A close comparison between clay and sand of similar strength characteristics was a main goal of the research. The various soil variables used in the model can be seen in Table 5-1 below. To simulate a majority of field conditions the soil strengthens and increases in density with respect to depth.

Table 5-1. Soil characteristics used in model

Soil Classification	Modulus of Elasticity MPa	Poisson's Ratio	Density (kg/m^3)	Friction Angle	Cohesion (kPa)	Side Friction Coefficient on Steel	Side Friction Coefficient on Concrete
very loose SAND (Splitstone et al.)	10	0.4	1400	20	0	0.237	0.25
medium dense SAND (Splitstone et al.)	25	0.3	1550	30	0	0.363	0.45
very dense SAND (Splitstone et al.)	50	0.25	1750	38	0	0.473	0.65
very soft CLAY (CL)	10	0.4	1400	0	25	0.237	0.25
medium stiff CLAY (CL)	25	0.3	1550	0	50	0.363	0.4
very stiff CLAY (CL)	50	0.25	1750	0	100	0.473	0.6
Shale Rock	5000	0.25	2000	-	500	0.473	0.6

A basic soil model was chosen for the research on part to better understand the model before introducing more complex soil behavior. Time dependency, water pressures, voids, and other soil characteristics are planned to be added for future research.

5.2 Finite Element Model Geometry and Boundary Conditions

The geometry of the soil and the micropile can be seen in Figure 5-7 and Figure 5-8 below. The aim was to simulate the most generic micropile possible thus a diameter of 0.2 meter and a length of 16.5 meters was chosen. The soil layers are split into three separate sections to represent the increase in strength typically associated with depth.

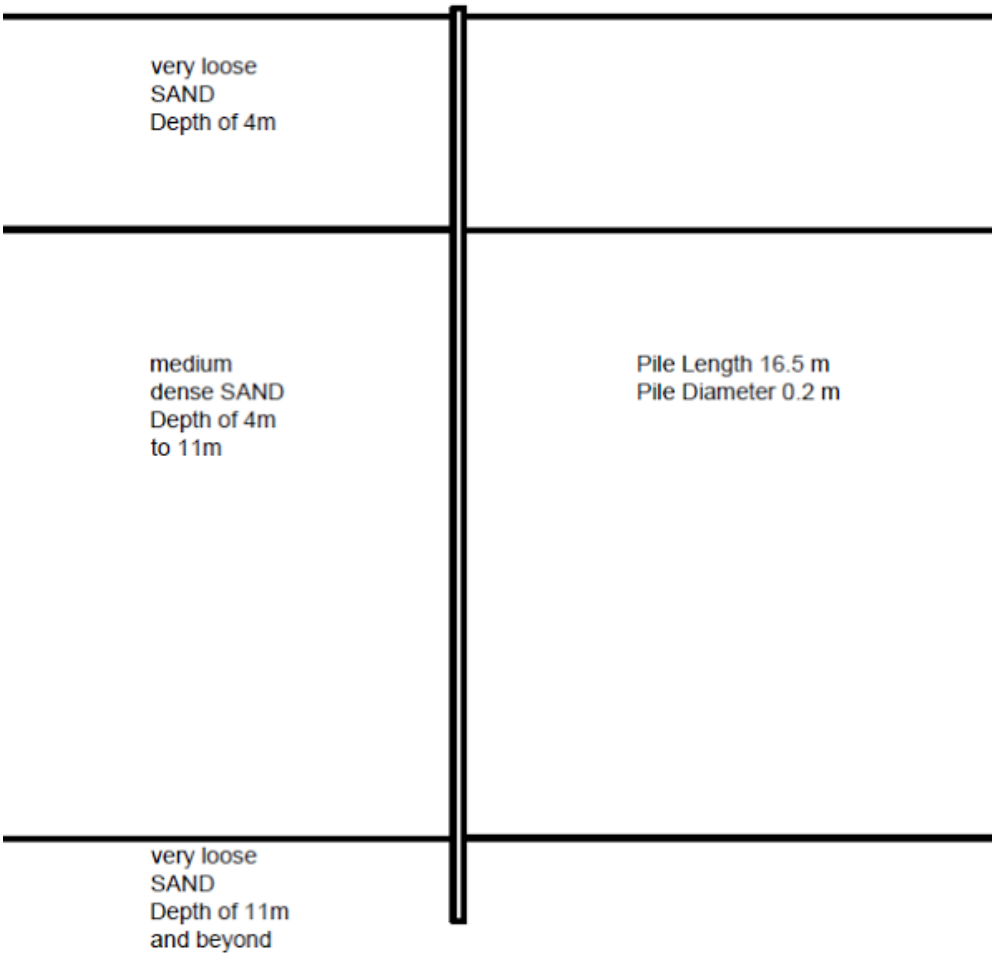

Figure 5-7. Schematic of the micropile finite element model

The micropile was initially designed to accommodate various casing lengths and the existence of a steel pin. Since the research was determined to focus on the direct results of various casing lengths the pin was never inserted. To emulate various casing length the casing was split into four section along the length of the pile. These sections were changed to represent grout or steel depending on whether the micropile simulated was to have no casing, one quarter length casing, half-length casing, three quarter length casing, and full length casing. The steel to steel connections were continuous in the model. Therefore, the steel section remained constant throughout the cased lengths.

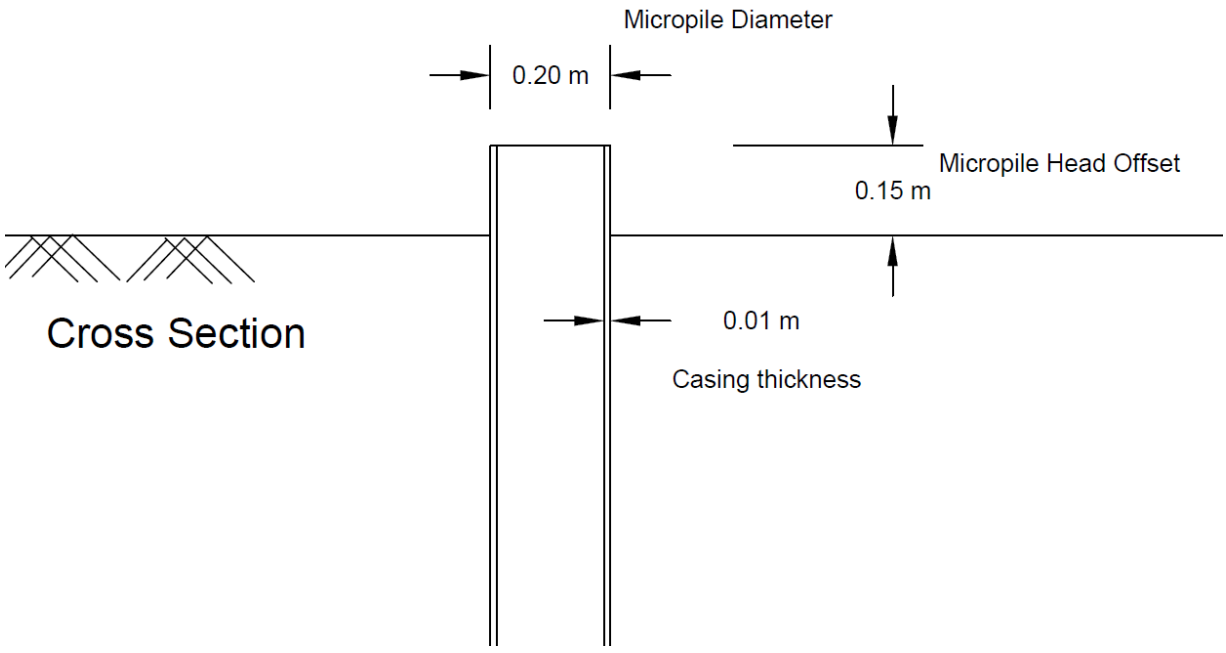

Figure 5-8. Cross section at the top of the micropile

Once the geometery was designed boundary conditions were added to the model. At the bottom of the soil block the boundary was constrained to not allow any movement or rotations in any direction. The sides of the soil model were constrained in the horizontal direction to prevent any outward movement of the soil. However, the sides of the soil model were allowed to move in the vertical direction to allow for vertical stresses to develop in the soil due to gravity.

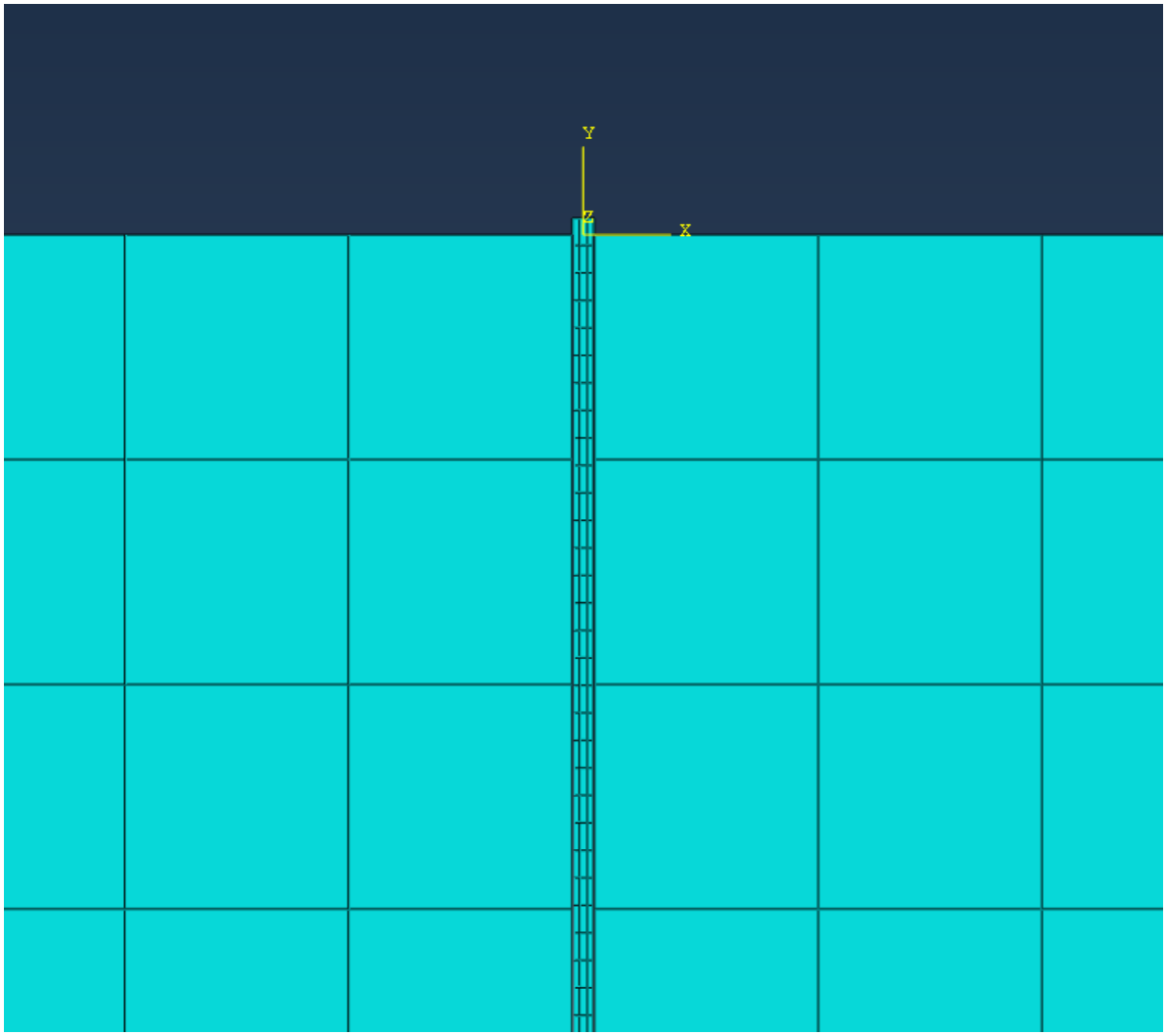

Figure 5-9. Close up view of the micropile mesh and soil mesh

The interaction between the soil and the micropile structure was designed based on friction values. Frictional values were assigned based on steel-soil and grout-soil expected bonding values. The sand tends to have a higher bond to soil than clay. Also, steel casing is smooth thus a smaller coefficient of friction was used for any cased part of the micropile. In practice, it is a general principle to neglect any axial resistance provided by the casing (FHWA, 2005).

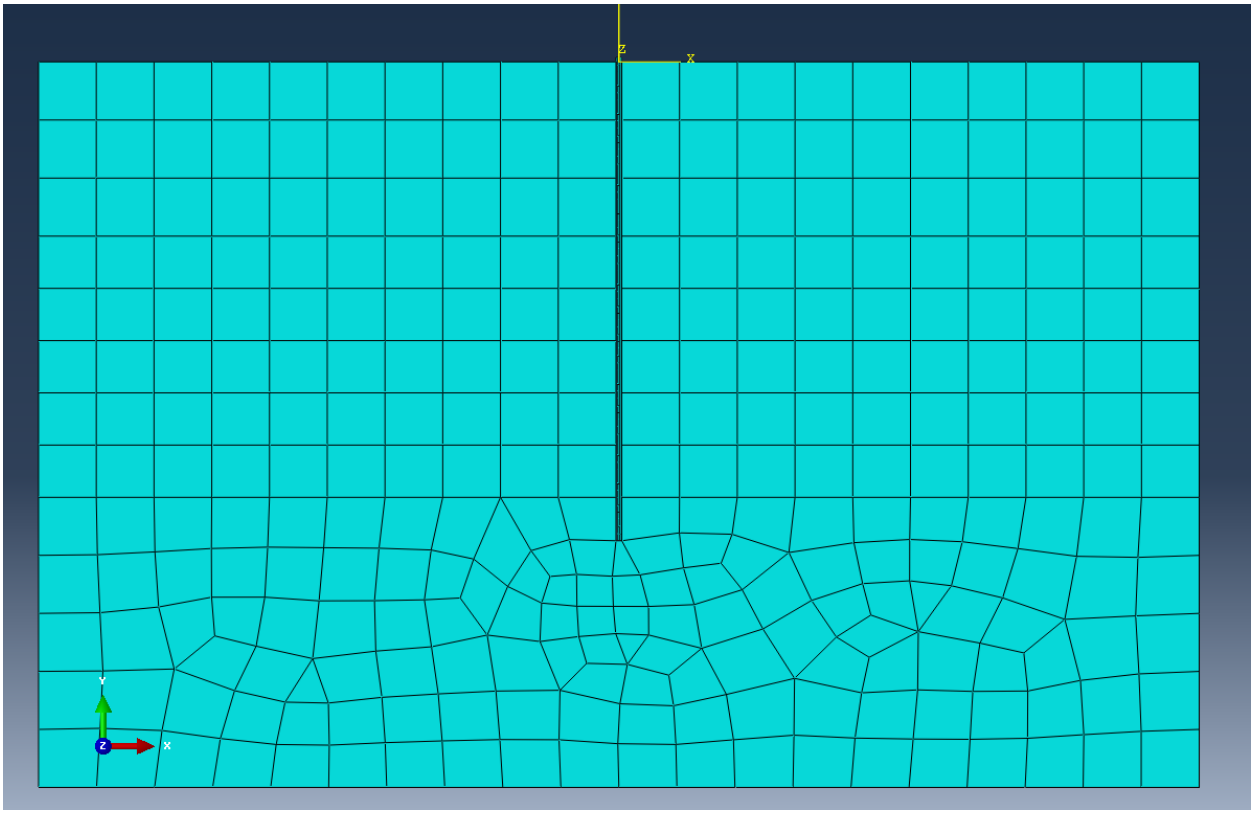

Figure 5-10. Complete meshed model

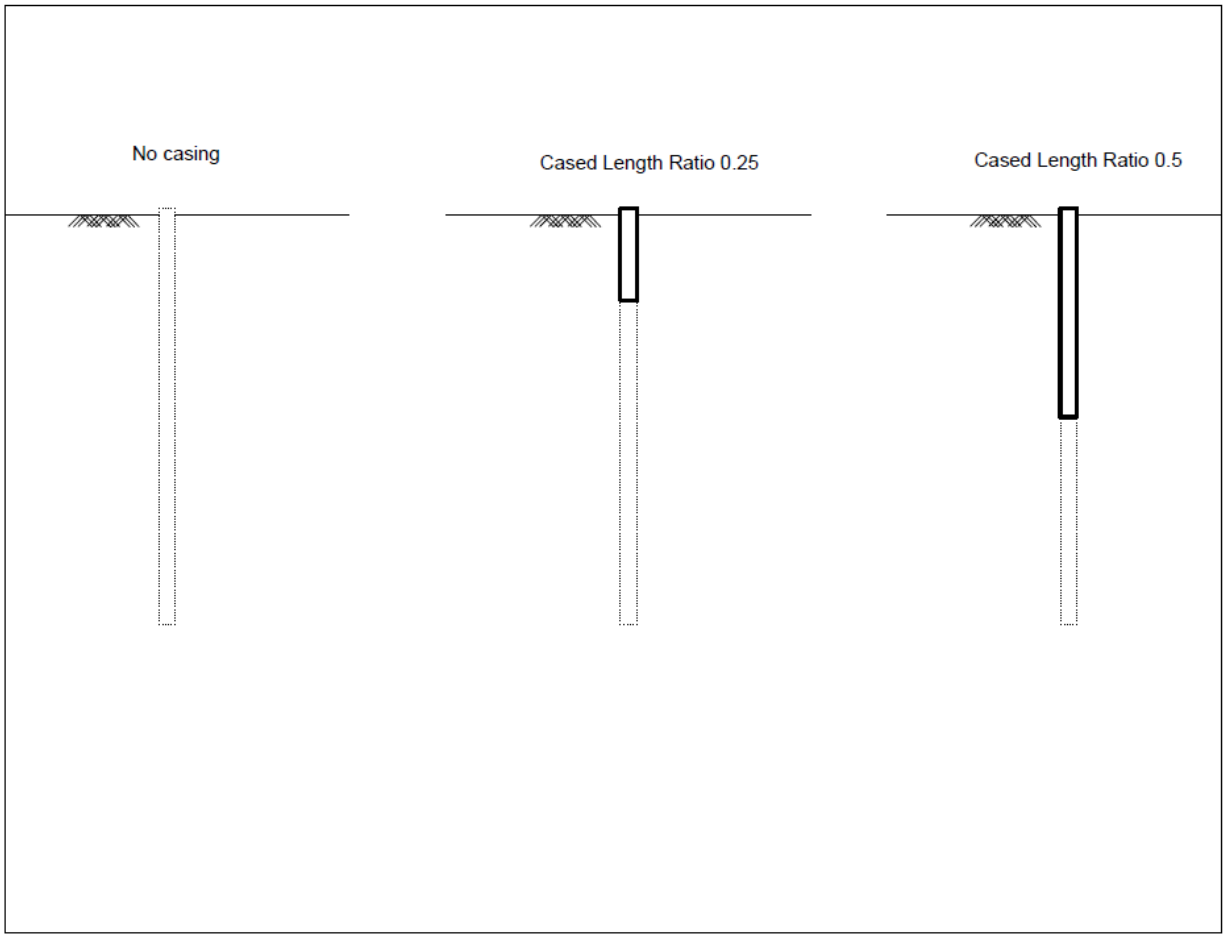

Figure 5-11. Cased length ratios 0, 0.25, and 0.5

The CLR was manipulated to observe the changes in load transfer behavior. The various CLR's used in the FEM can be seen in Figure 5-11 and Figure 5-12. Although a CLR is typically not seen to be over 0.75 it was included for comparison.

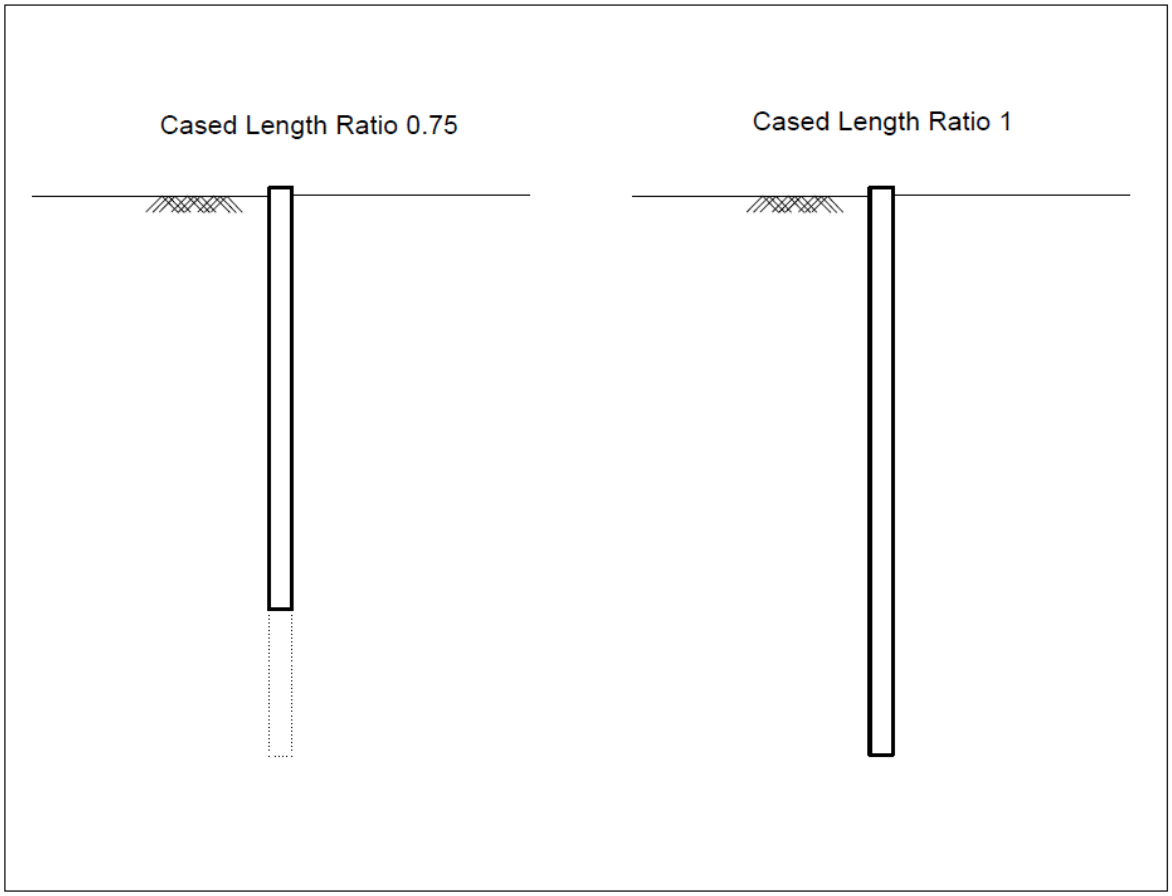

Figure 5-12. Cased length ratios 0.75 and 1

Once all of the boundary conditions, material properties, and interactions were defined gravity was imposed on the model. Below in Figure 5-13 the initial stresses in the soil can be seen. These stresses were verified using hand calculations before loading was applied.

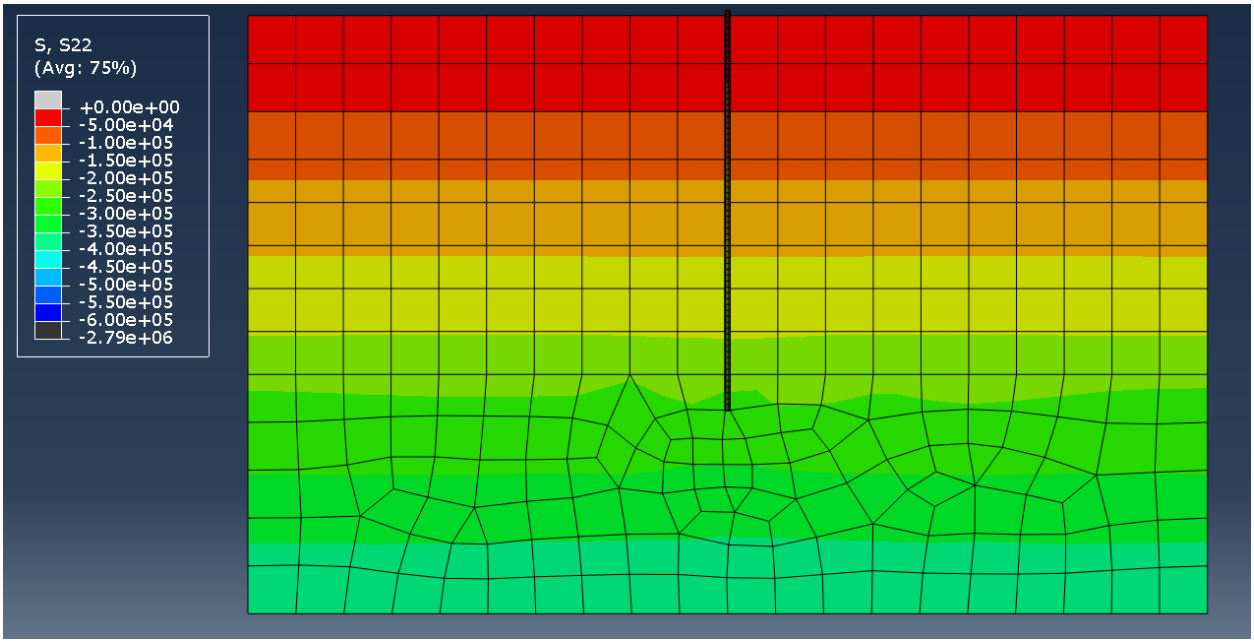

Figure 5-13. Initial soil stresses in model before loading (units of N/m^2)

Loading was then applied in the axial and lateral directions. A total of 21 models were completed comparing various casing lengths and soil conditions. Varying from no casing to full casing, lateral and axial loadings, for soil conditions consisting of sand, clay, and rock.

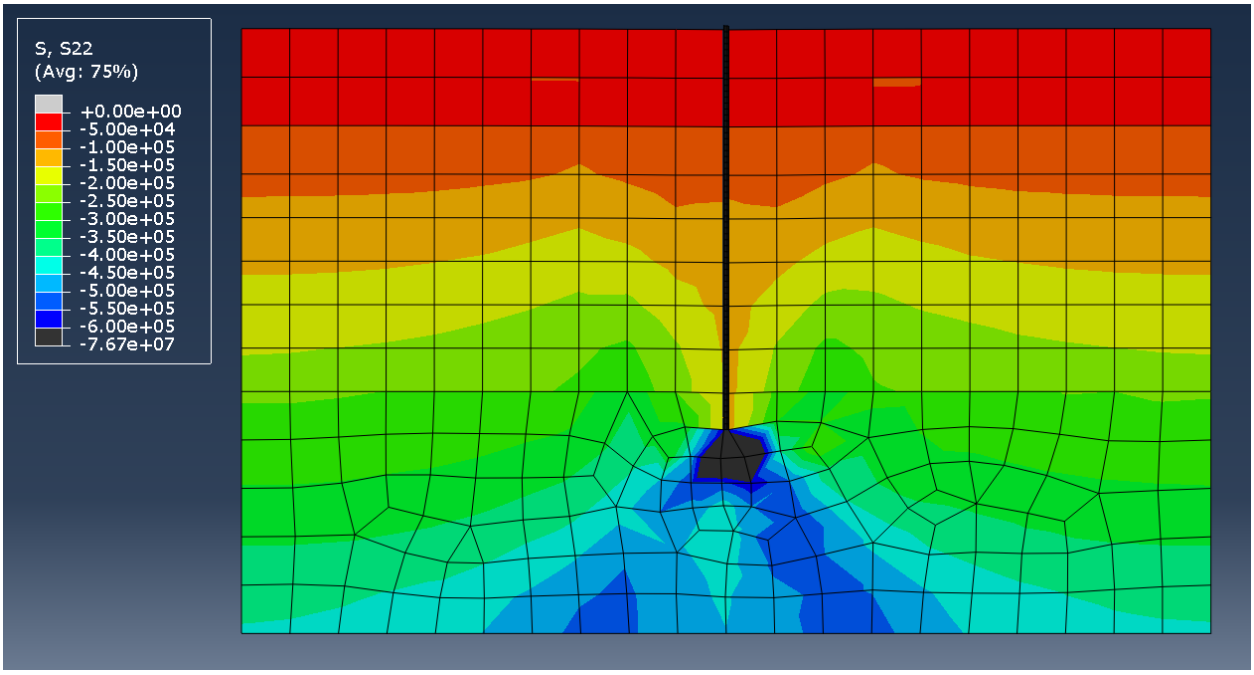

Figure 5-14. Vertical stress distribution of full cased micropile in sand while loaded (units N/m^2).

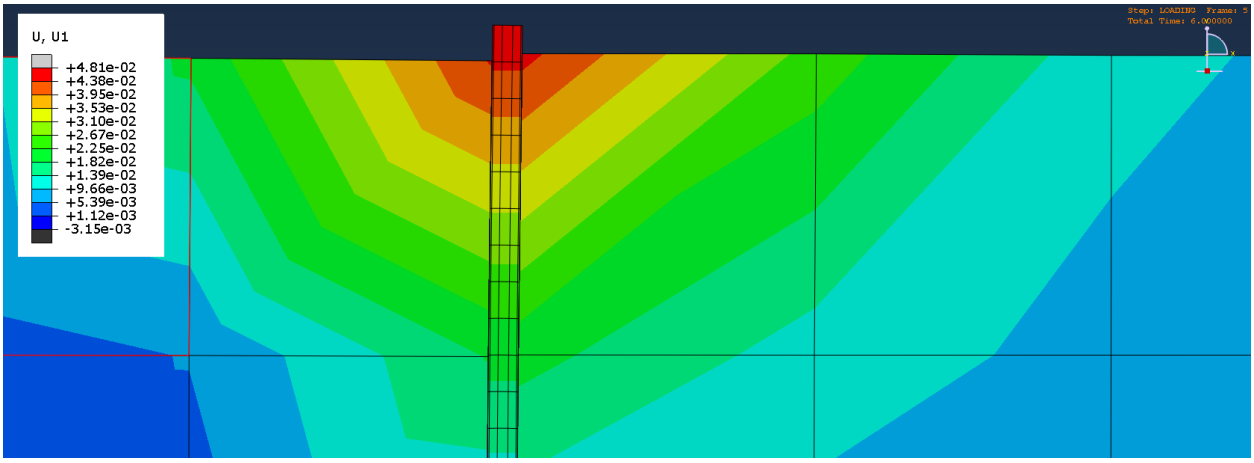

Figure 5-15. Laterally loaded fully cased micropile in sand (lateral deflection, U1, in units of meters)

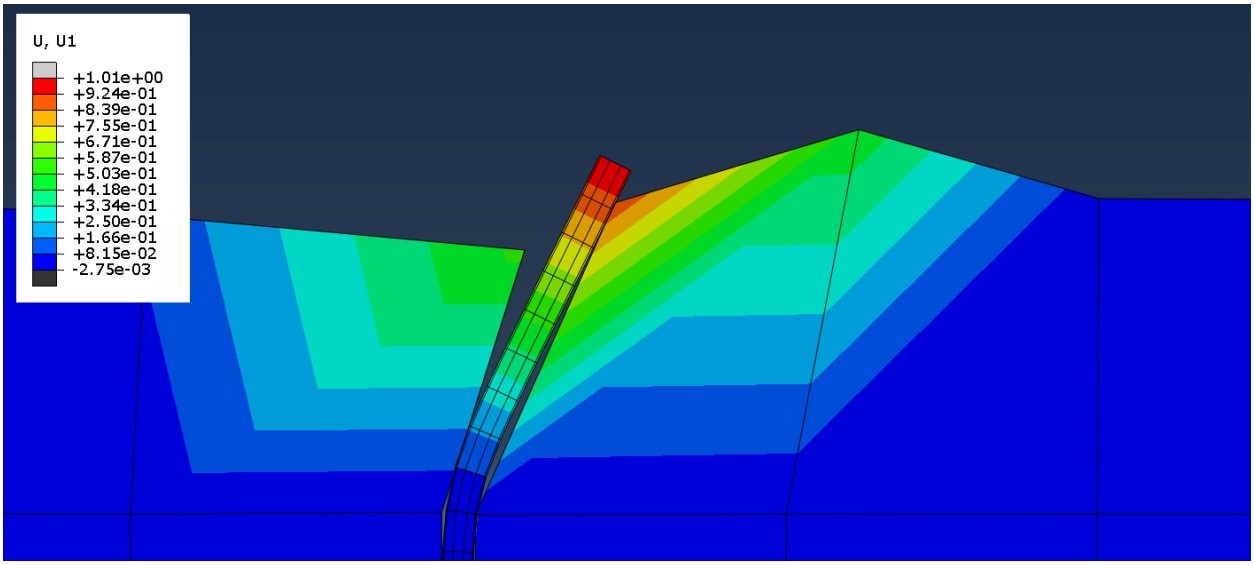

Figure 5-16. Lateral loading failure for an uncased micropile in sand (lateral deflection, U1, in units of meters)

Each of the simulated load test were loaded until plastic failure was observed. The main goal of the research was to produce load test graphs similar to those produced in the field. Each load was applied and then released showing the permanent plastic deformation in the soil-structure system. This similar load and unload procedure is typically of a micropile field load test.

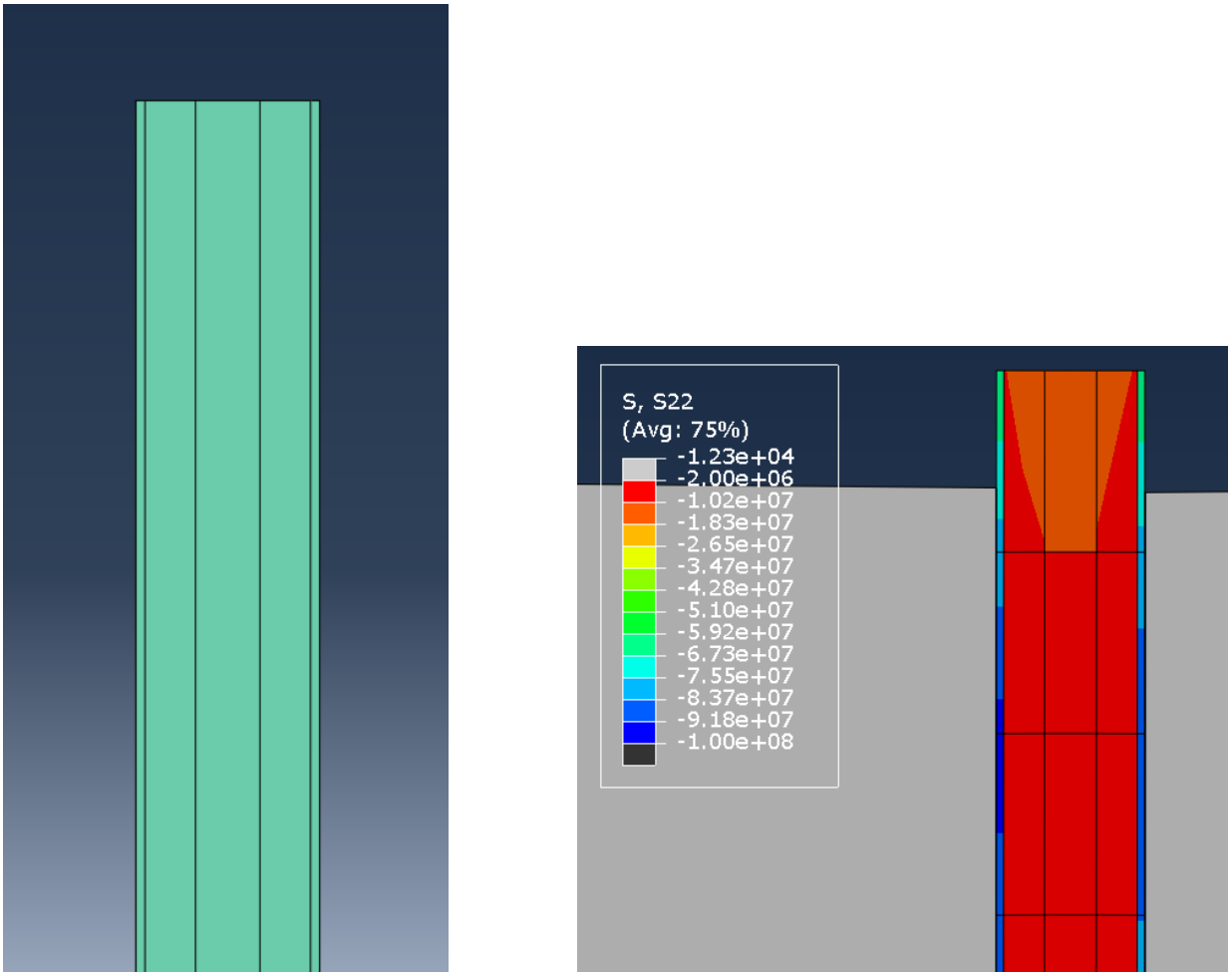

Figure 5-17. Close up of the various sections created for the micropile model and an example of stress transfer between the grout-micropile

5.3 Simulated Load Testing of the Micropile

Once the various models were simulated data was produced to show the load-deformation characteristics of the pile. Simulated vertical and lateral load tests were conducted to compare to load test results done in the field. Each load consisted of a time interval in which the load was applied and then back off to show the permanent deformation of the pile. In conclusion, 25 total load tests were conducted consisting of sand, clay, and rock. Various load tests investigated the influence of casing length on the load transfer mechanisms. Eccentric loading was also simulated and shown to produce local crushing of grout when casing in present to adequately transfer the load into the soil.

The results for the axial loads and lateral loads were placed into graphs corresponding to the soil type. Both sand and clay exhibited similar behavior when changing the casing length. A rock model was fabricated to show the capacity benefit of the micropile when casing to rock. A simulated eccentric load was also applied for a cased and uncased micropile in clay.

Once again, the availability of field load test data and the importance of field load tests for micropile design and construction led to the simulated load test setup developed by the University at Buffalo. Simulating load tests as closely as done to the field will allow for correlation between the academic research and various field tests results.

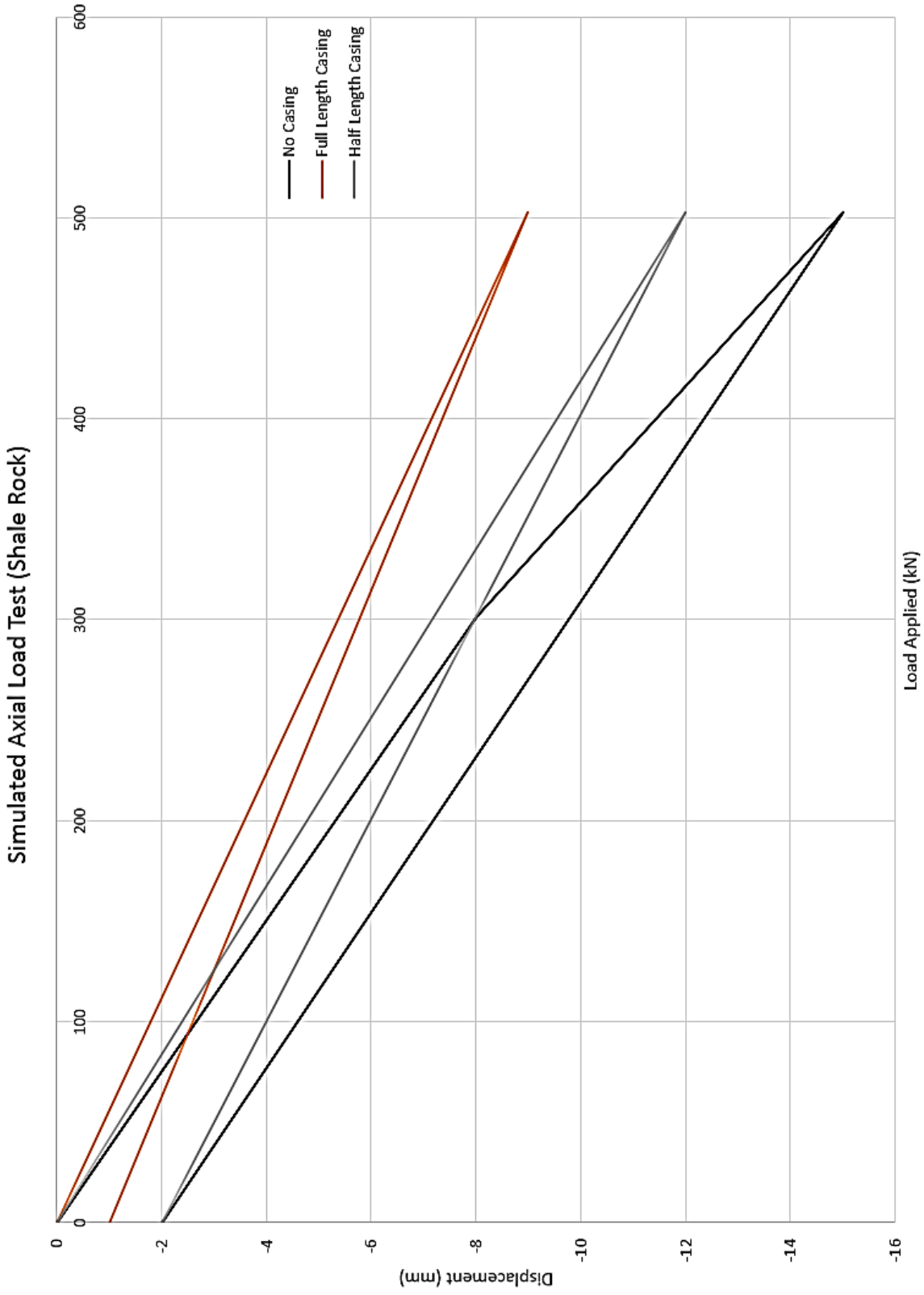

Figure 5-18. Simulated axial load tests for shale rock

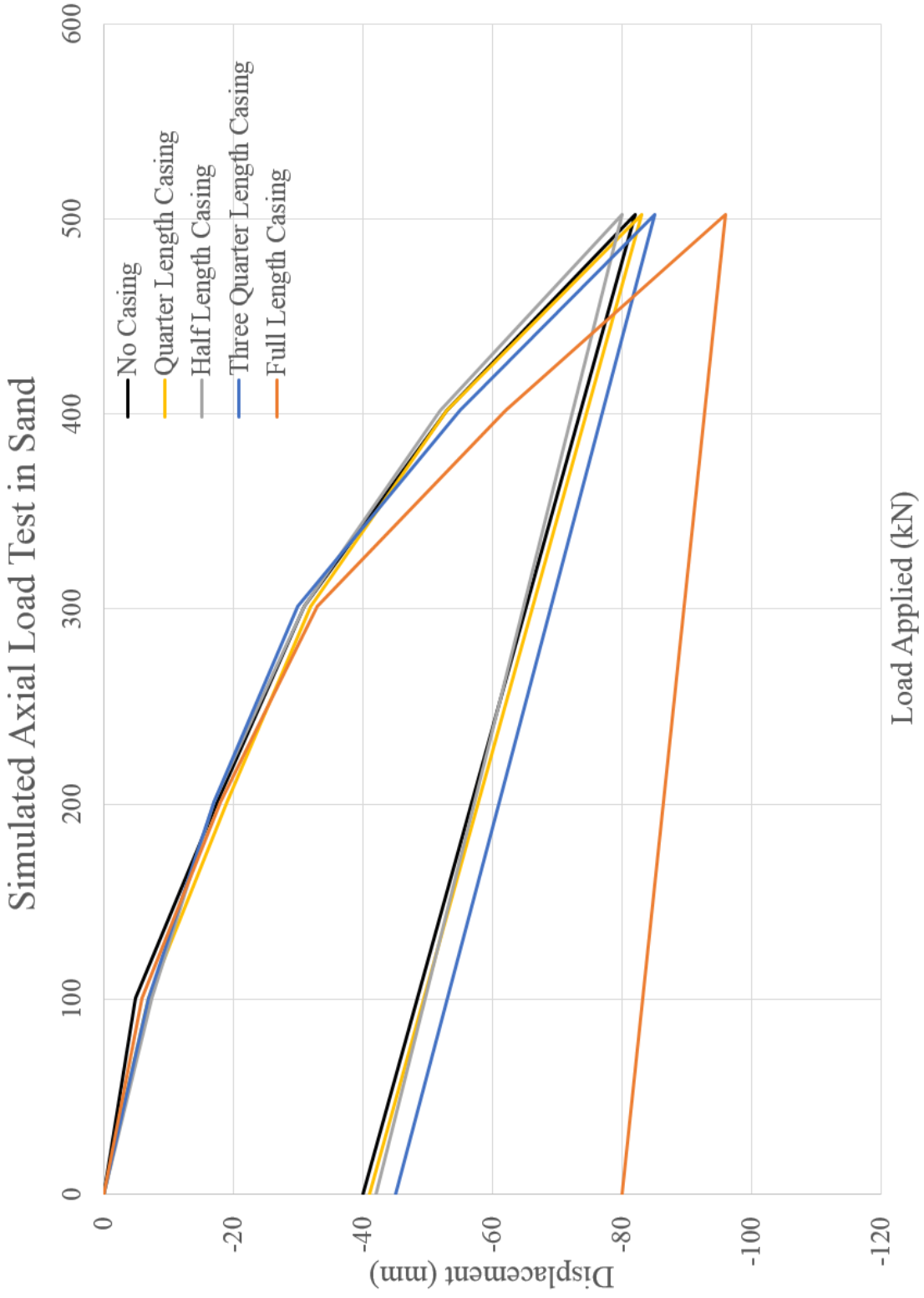

Figure 5-19. Simulated axial load test in sand

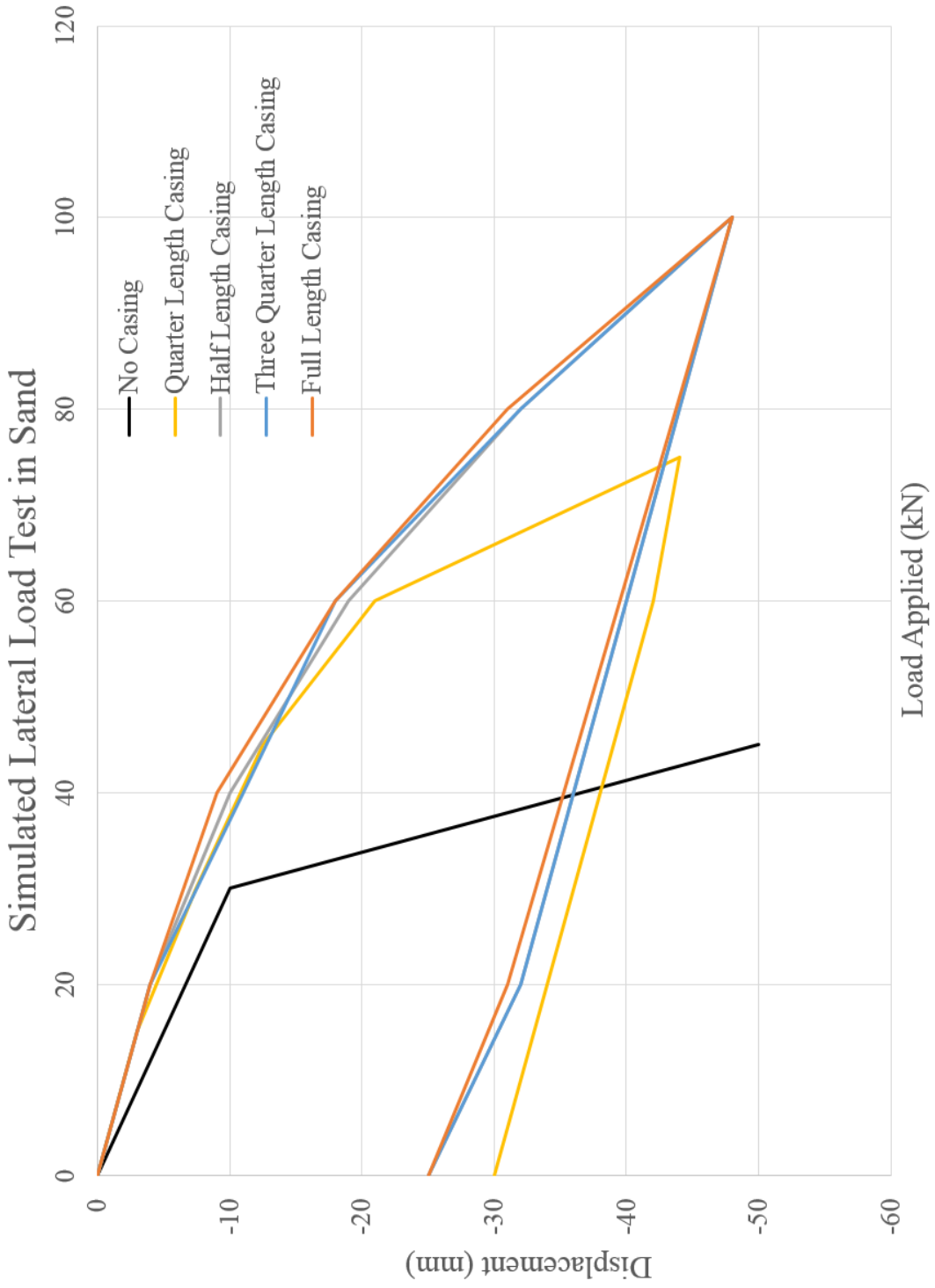

Figure 5-20. Simulated lateral load test in sand

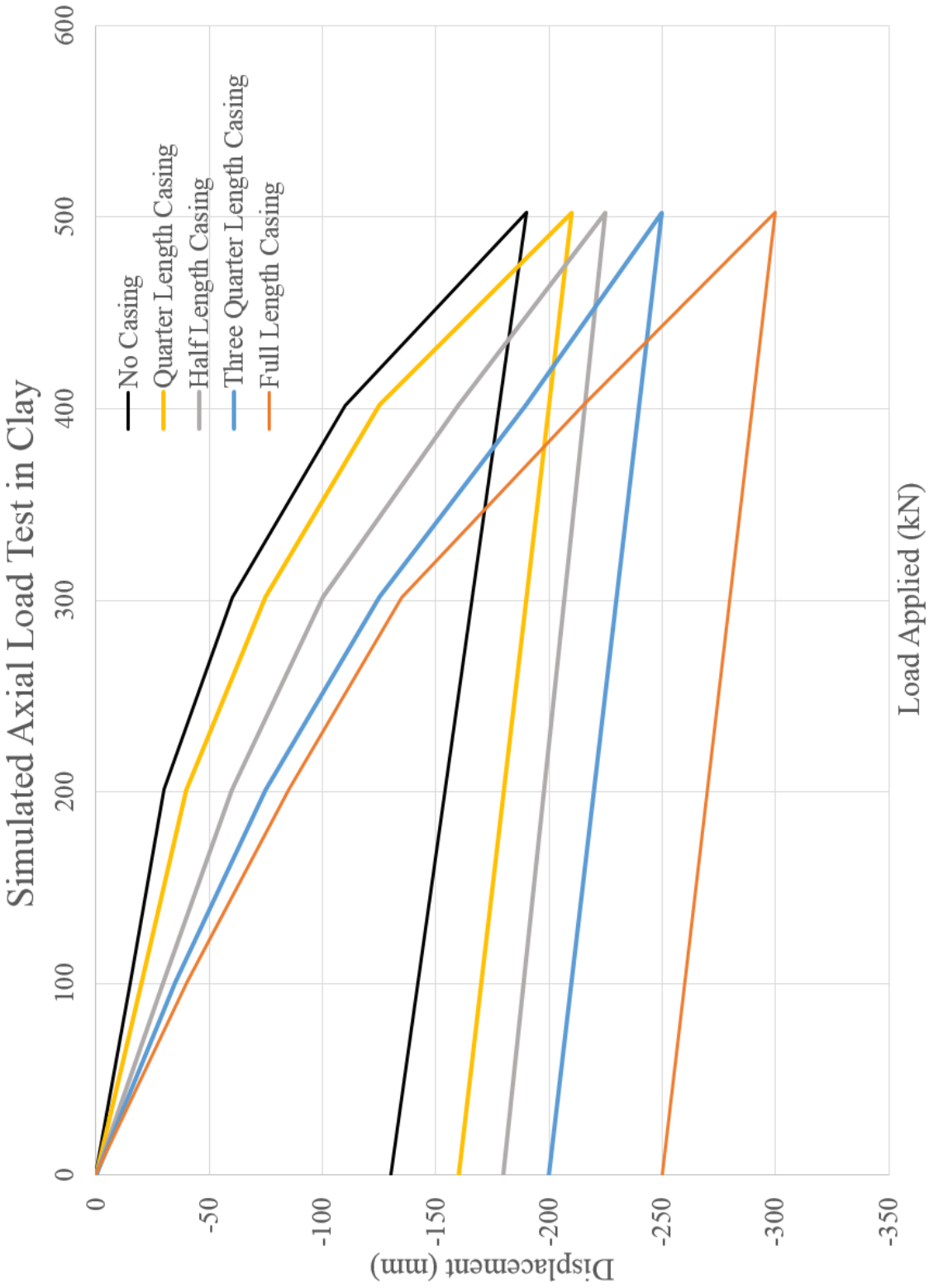

Figure 5-21. Simulated axial load test in clay

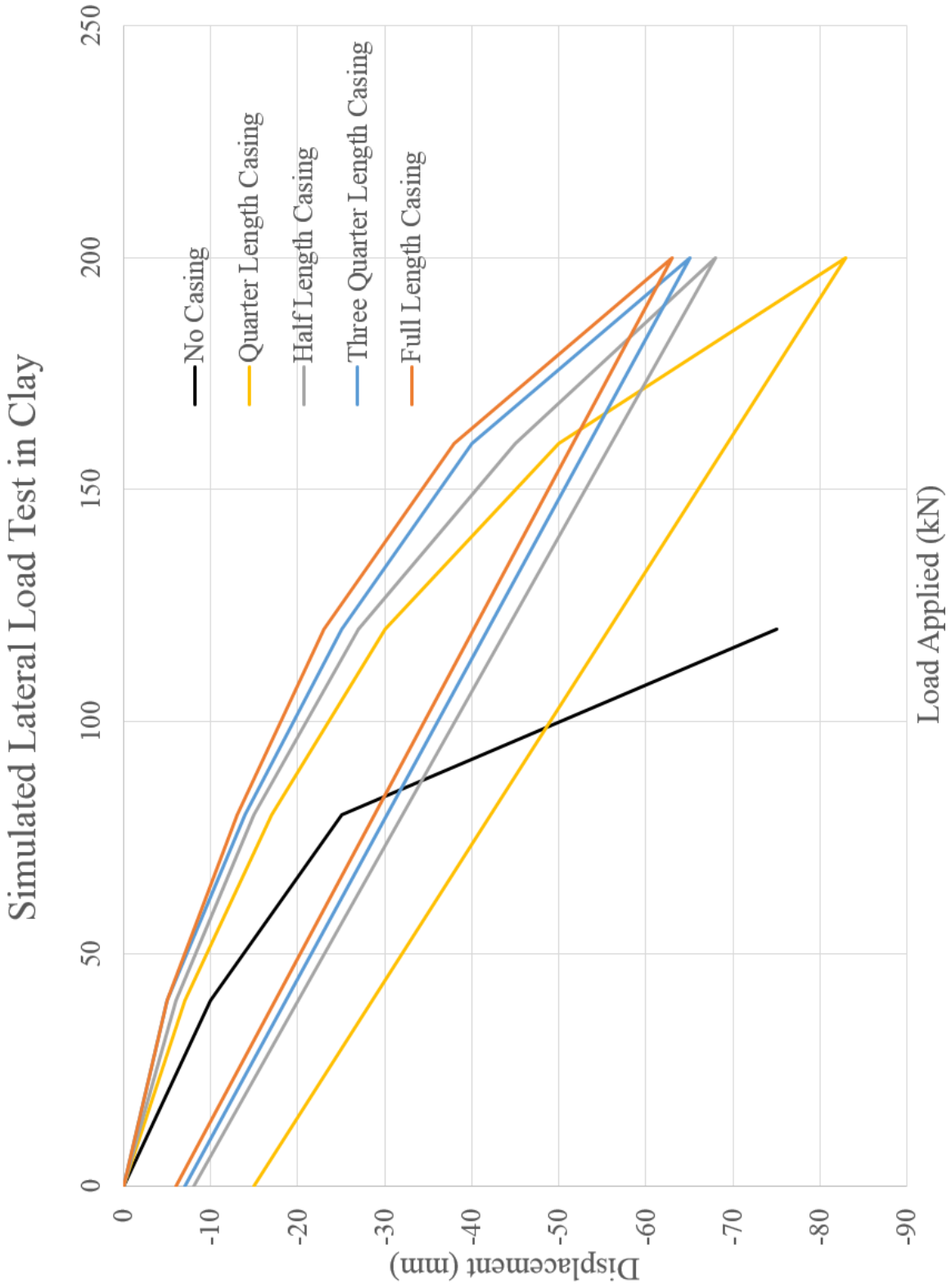

Figure 5-22. Simulated lateral load test in clay

The graphs above display a concise way to view the results from the various simulated load tests. Trends between the casing length and capacity of the micropiles are further discussed in the next section.

An additional result from the simulated eccentric load test can be seen below in Figure 5-23. A previous field load test has demonstrated crushing failure at the top of the micropile even though the axial design was considered accurate. Large loadings, large load frames, and the slenderness of the micropile can cause eccentric loads during load tests. The simulated eccentric load shows similar results as seen in the field.

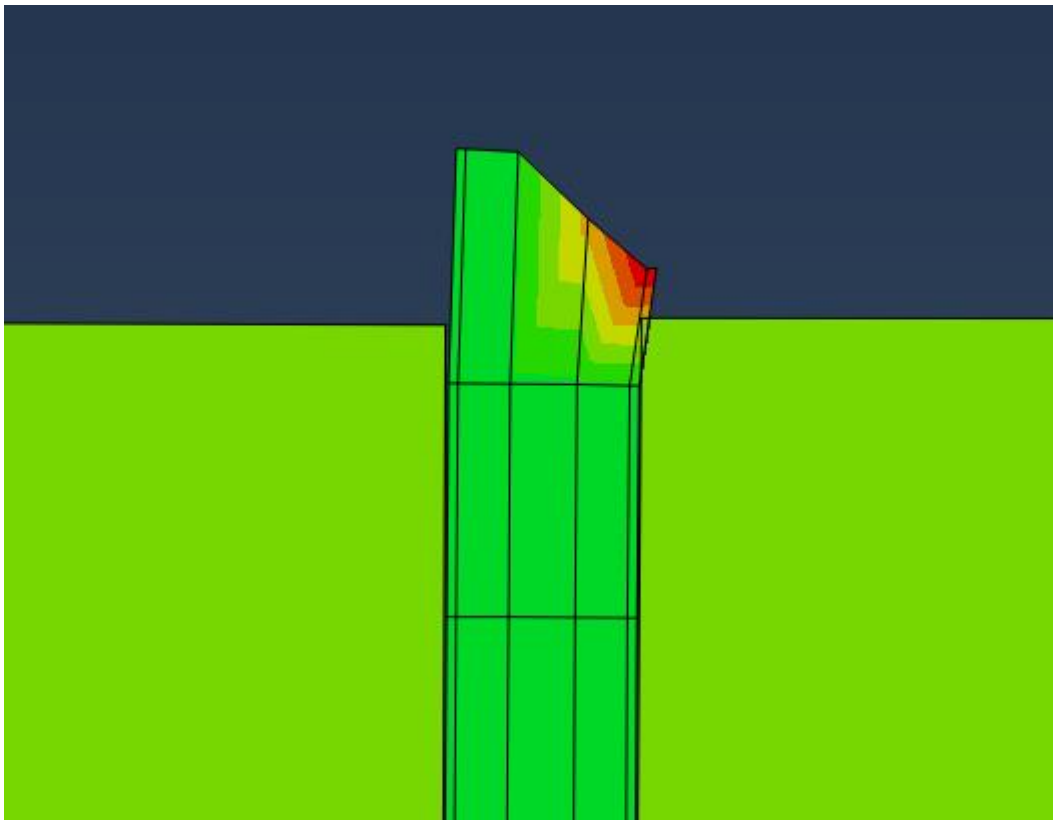

Figure 5-23. Local concrete crushing failure due to an eccentric load applied on an uncased micropile

5.4 Micropile Casing Depth Design Conclusions

When a pile is loaded, the load acting on the cross section of the micropile decreases with depth. This is due to the side friction of the micropile resisting the compression of the pile. Typical loading variations with depth can be seen in the diagrams below (Sivakugan, 2010).

For the axial case, in both sand and clay, the addition of casing length increased the deformation of the micropile when loaded. This supports the postulation and design of Dr. Lizzi using fully bonded micropiles to resist additional settlement of historic structures. The grout-soil bond mobilizes much quicker and begins to resist additional loads (Lizzi, 1982).

Recommendation #1 – Settlement Prone Structures

When dealing with settlement prone structures or instances where vertical movement is of greatest concern casing should be minimalized in clay and sand. The soil-grout bond is mobilized quicker under loading and provides better resistance to settlement (Bruce & Juran, 1997).

Recommendation #2 – Lateral Loading

It is recommended for any micropiles undergoing lateral loads to contain casing through the expected point of fixity. Any additional casing past ½ the length of the micropile has shown to have diminishing returns in terms of lateral capacity if the point of fixity is surpassed. Due to the slender nature of the micropile, the additional stiffness provided by the steel casing allows the lateral load to be adequately transferred to the soil (Reese & Van-Impe, 2011).

Recommendation #3 – High Capacity Micropiles

All high capacity micropiles, even if solely axial loads are present, are recommended to contain casing. This is to provide adequate stiffness at the pile head to transfer high loads into competent soil. During load tests, eccentric loads have been proven to develop and cause local failure at the pile head. Large test frames and small micropile diameters cause misalignment during load testing ("Micropile Installations Dutchess Rail Trail (Stage 4) Poughkeepsie, New York," 2012).

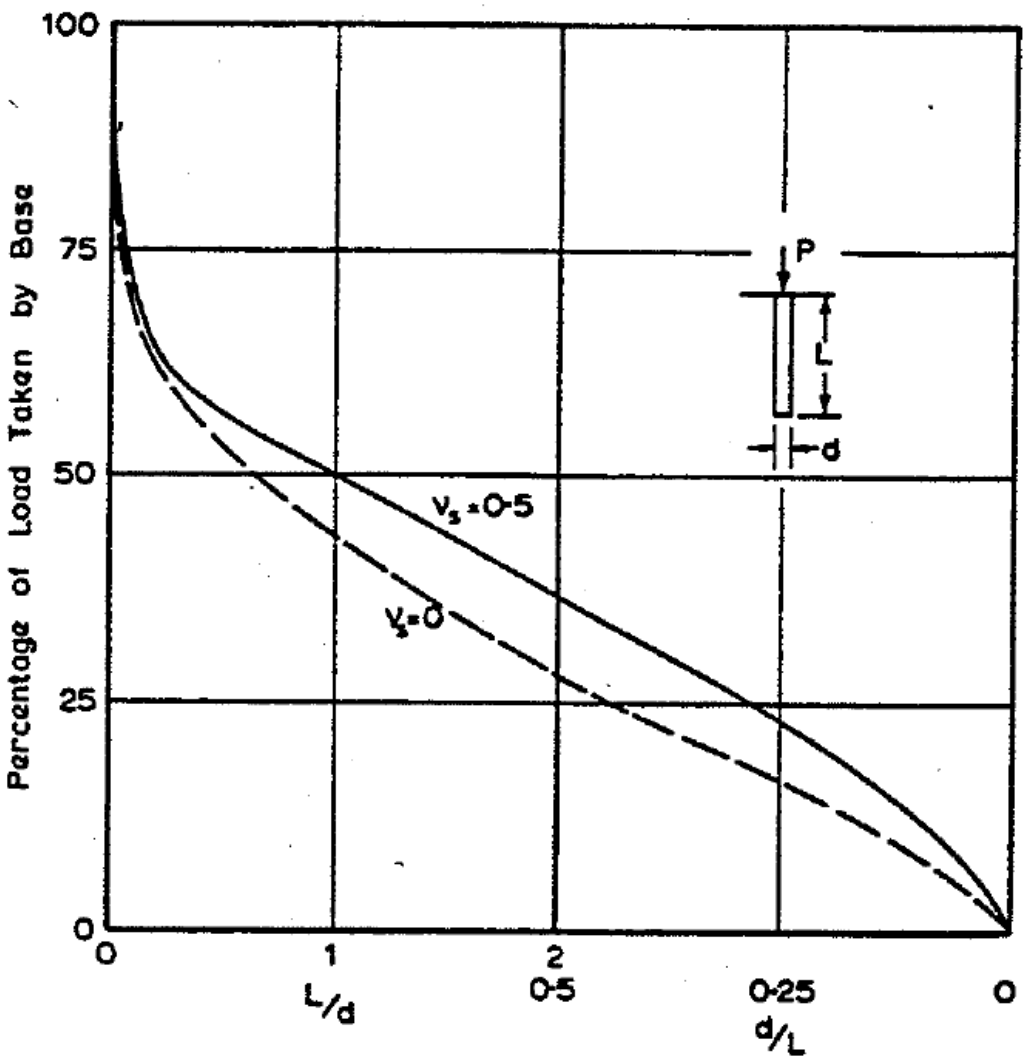

Figure 5-24. The influence of pile geometry on load transfer mechanisms (Poulos & Davis, 2006)

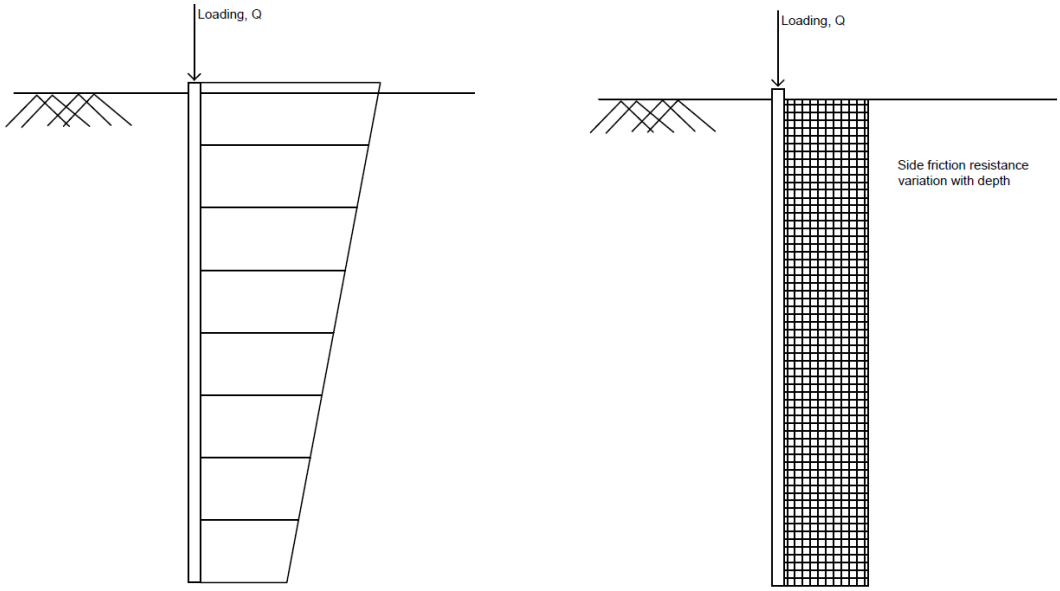

Figure 5-25. Load transfer model showing stress in the pile and correlating side friction resistance

Seen in Figure 5-24, Figure 5-25, Figure 5-26 are various load transfer mechanisms of the micropiles depending on micropile geometry and soil conditions. Micropiles are slender in nature resulting in a larger majority (90% and greater) of the load transfer occurring between the side friction of the micropile. Casing reduces this friction over a length causing the load to be transferred to deeper soil media.

Understanding and defining these load conditions using instrumented load tests and simulated load tests will aid in future engineers efficiently designing micropiles. Initial recommendations are provided and more are expected with further research into more situations.

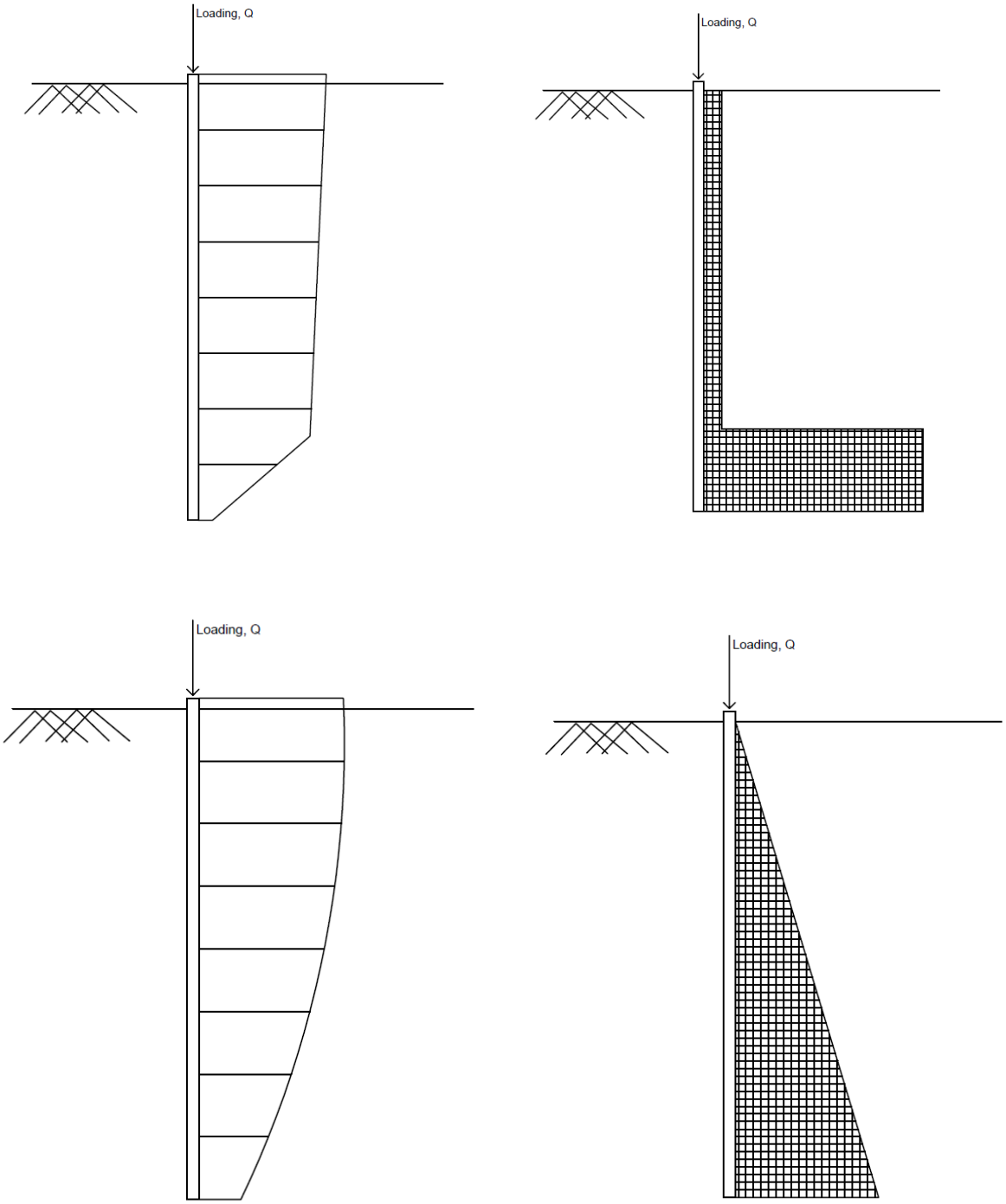

Figure 5-26. Load transfer diagrams for micropile cased to rock with rock socket (above) and micropile in sand (below)

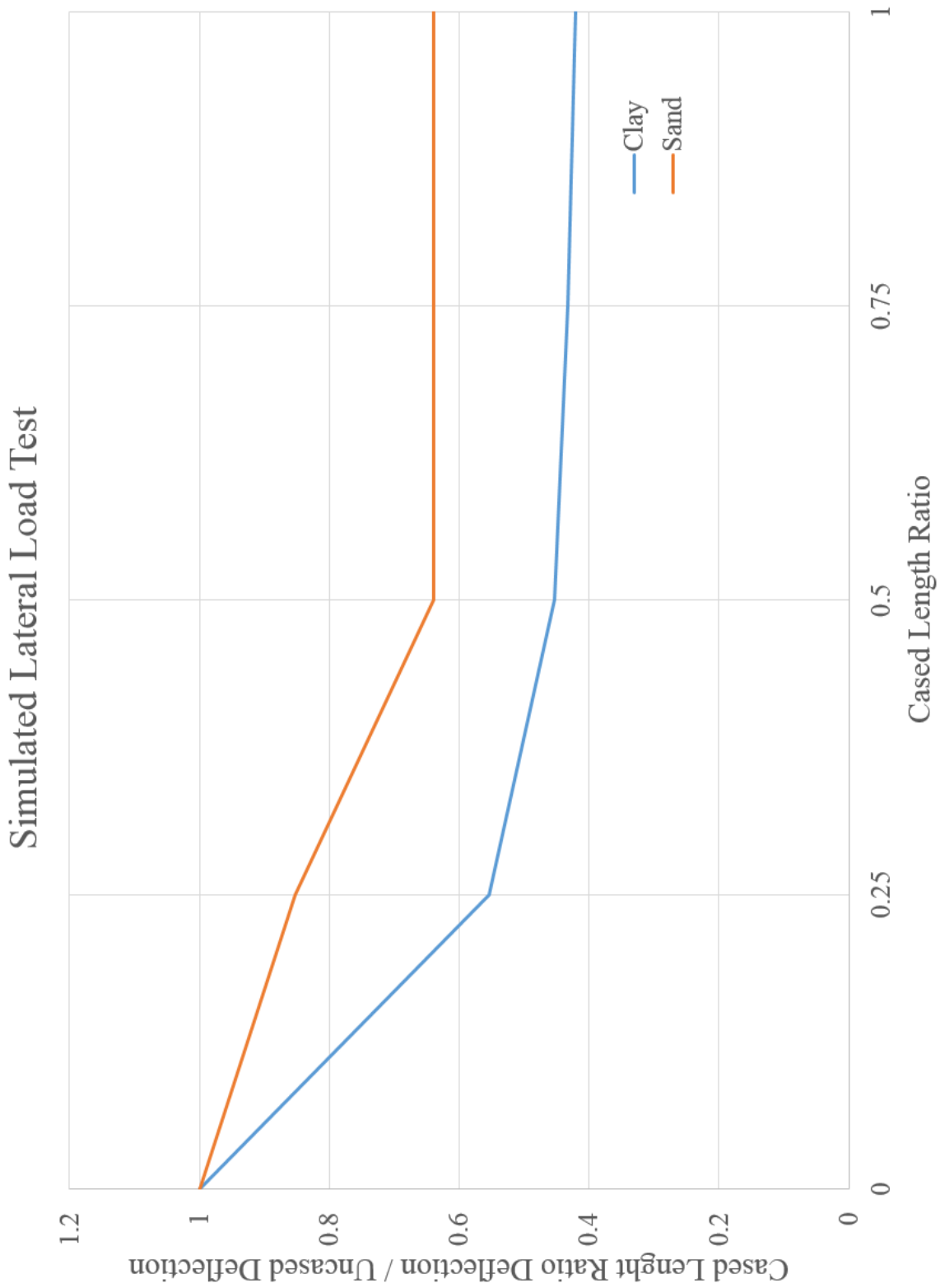

Figure 5-27. Normalized simulated lateral load test results

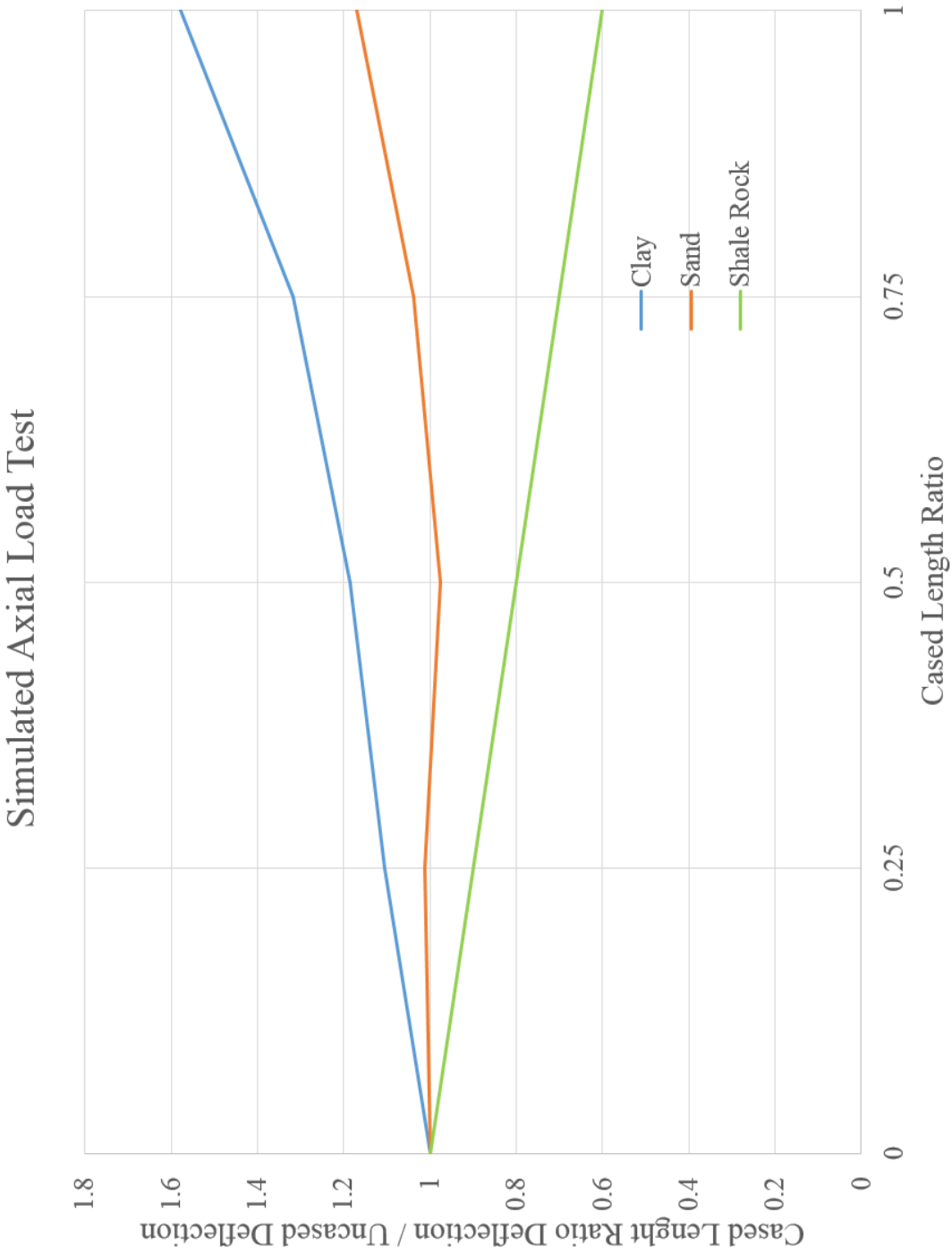

Figure 5-28. Normalized simulated axial load test results

6. Investigated Case Histories

6.1 Design-Build-Test process for High Capacity Micropiles

Dutchess Rail Trail Bridge Foundations, Poughkeepsie, New York

Innovative design methods and materials are making micropiles a cost effective solution for many foundations. However, there is a methodical design process to ensure each micropile has the capacity to support the required loading. A construction case study was performed on high capacity micropiles that were designed, constructed, and tested by Buffalo Drilling Company, Inc. The micropiles serve as the deep foundations for various abutments and piers for a bridge in Poughkeepsie, New York. The project was part of the "Rails to Trails" program interconnecting pathways used by hikers and bicyclists. Fundamental geotechnical and structural concepts combined with load test results were essential in designing each micropile effectively. Testing procedure followed the New York State Department of Transportation Geotechnical Control Procedure Static Pile Load Test Manual (GCP-18) Quick Load Test. Failed load test results of test micropiles required redesign and retesting. The failed micropiles contained a center steel pin surrounded by high strength grout. After the load test results were analyzed, it was determined failure occurred due to lack of lateral support at the top of the pile, possibly due to an induced moment during testing. Redesigning the micropiles containing steel casing, to transfer the full loading to bedrock, resulted in passing load test results. The case study outlines the design process, the construction process, and interpretation of load testing results. A combination of shale bond stress, end bearing capacity, lateral soil stability, pile stability, and side friction were analyzed to produce micropile designs. Final applied loadings for the five test micropiles that passed were 6,000 kN, 5,200 kN, 5,345 kN, 6,327 kN, and 2,000 kN respectively.

Buffalo Drilling Company, Inc. designed, constructed, and tested micropiles for the "rails to trails" project located in Poughkeepsie, New York. A new pedestrian bridge required a foundation including grouped piles at various locations. For the micropiles, a general design guideline was presented with load and placement specifications. This type of micropile project for a drilling contractor is commonly called a design-build-test contract. Meaning, the contractor designs the micropile to meet the specifications presented, and then constructs the micropiles. After construction, load tests verify the capacity of the micropiles to ensure the foundation design capability. These type of contracts offer the owner efficient construction, saving both time and money. Open communication and engineering ethics play a large role in moving the project forward. Success on these projects has increased the requests for bids concerning Design-Build micropiles.

Geotechnical soil borings were conducted prior to construction and determined the overburden soil consisted mainly of sand with some clayey silt. Bedrock was encountered at varying elevations of 3-16 meters (10-50 feet) below ground surface and was determined to be a hard to medium hard Shale. The foundation loads were decided to be transferred to the bedrock using groups of micropiles at each abutment. Various abutment foundations were placed for pedestrian bridges to connect the Dutchess Rail Trail. The Dutchess Rail Trail is a 13 mile rail trail that travels through Poughkeepsie and ends at the walkway over the Hudson. The trail is a shared use trail for both pedestrians and bicyclers.

Figure 6-1. Aerial view of completed pedestrian bridges in Poughkeepsie, New York

Boring logs B23 and B23A can be seen below. These soil borings were taken at the location of the end abutment, which is the main micropile analysis throughout the paper. The bedrock elevation changed drastically at different locations of the site. The soil was predominantly sand, with layers of silt and clay, and a till layer present before shale bedrock. Conservative geotechnical parameters design values were determined from the subsurface logs below.

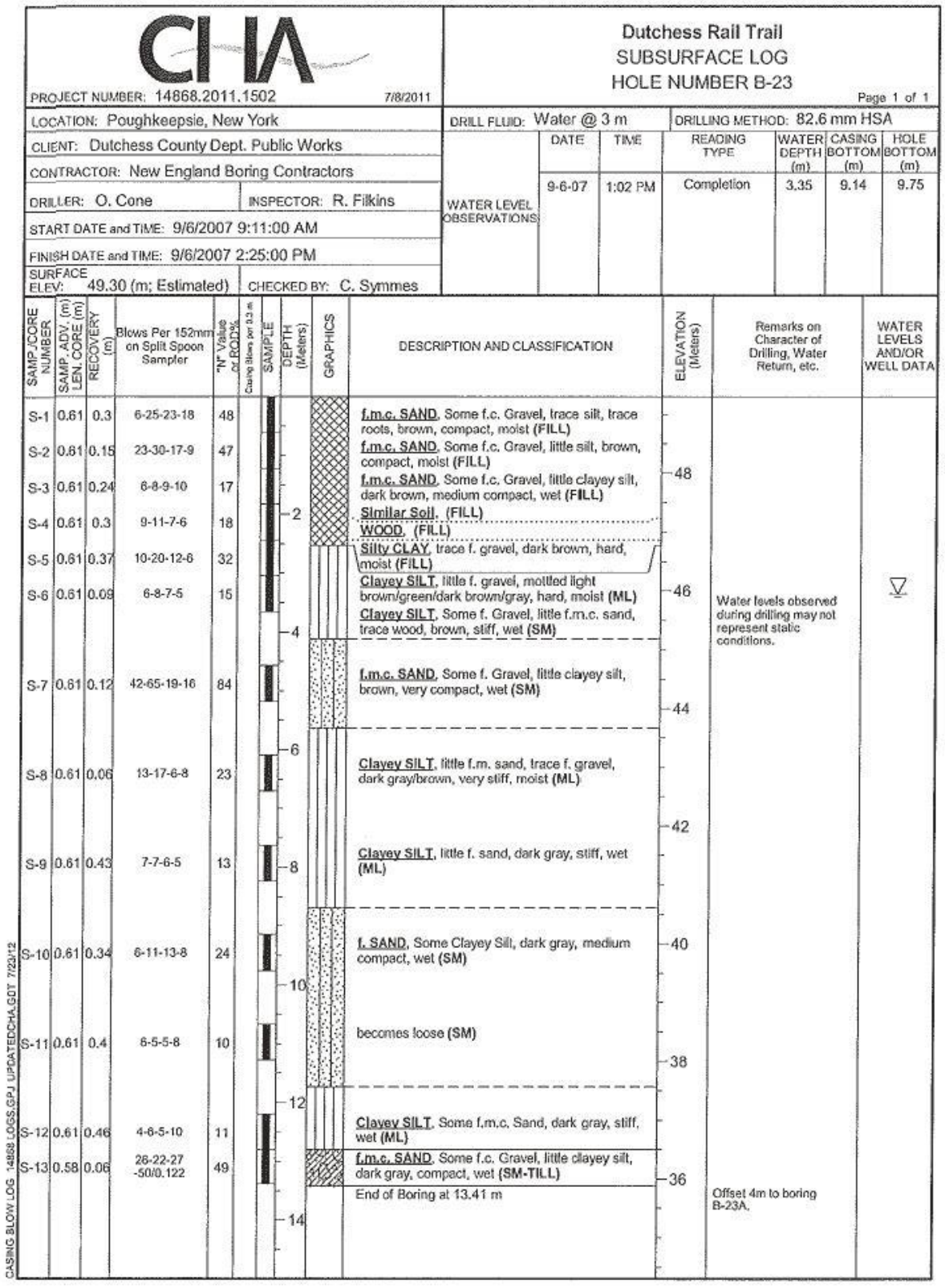

Figure 6-2. Subsurface boring logs taken at the proposed end abutment

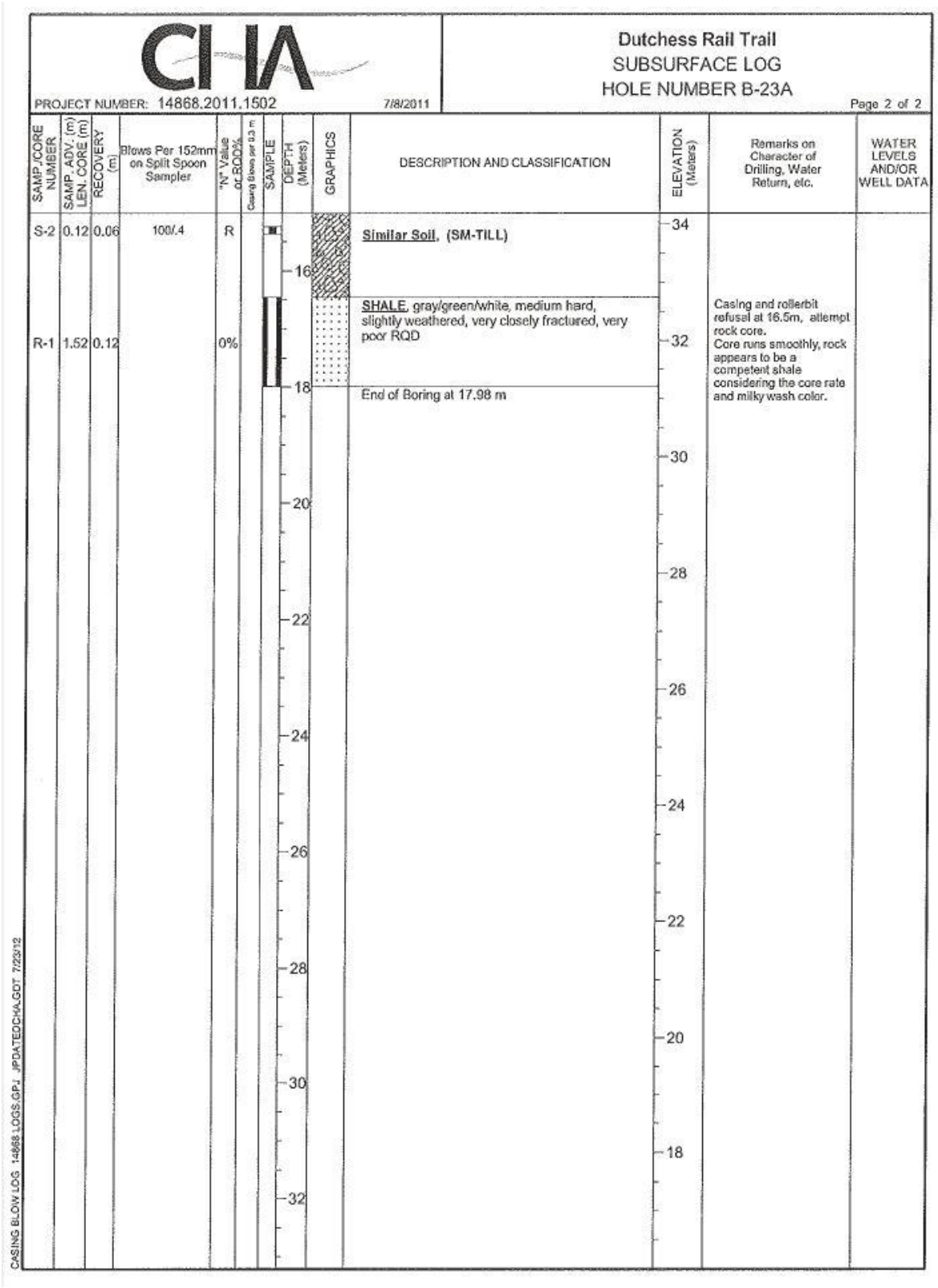

Figure 6-3. Subsurface logs at proposed end abutment showing shale bedrock

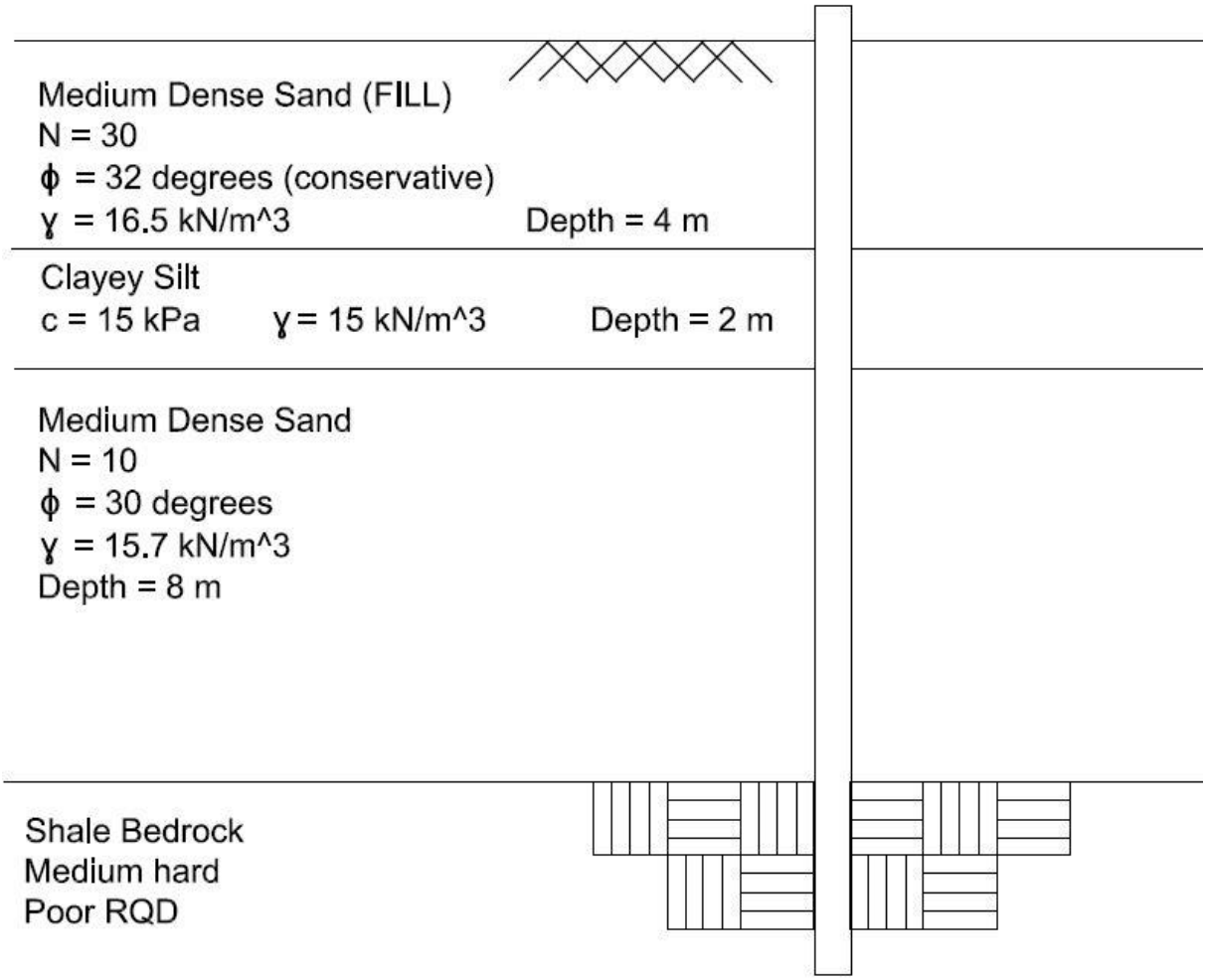

Figure 6-4. Micropile schematic and geotechnical parameters used for design

From these values the geotechnical design was done using the Bond Strength Method. The most important parameter determined for this method is the bond strength. Tables provided by the Federal Highway Administration (FHWA) contains various typical bond values for different soil types (FHWA, 2005). Using the subsurface logs, past experience, and these tables the bond values are determined to use for design.

The initial design required the following loadings for each micropile location can be seen in the table below. Capacities for the micropiles placed at each location were designed to meet these requirements. The New York State Department of Transportation Geotechnical Control Procedure Static Pile Load Test Manual (GCP-18) Quick Load Test was used to determine the service and ultimate capacity of the constructed micropiles. Utilizing this design-test process serves to ensure the capacity was sufficient for the specification as well as support the theoretical design calculations performed.

Table 6-1. Micropile required strength and service states as stated in specifications

THE MICROPILES AT THE END ABUTMENT, PIERS 1, 2, AND 3 FOOTINGS SHALL BE DESIGNED FOR THE FOLLOWING MAXIMUM AXIAL LOADS PER PILE:

		PIER 1	PIER 2	PIER 3	END ABUTMENT
COMPRESSION	MAXIMUM STRENGTH LIMIT STATE (kN)	1610	1430	1470	1740
	MAXIMUM SERVICE LIMIT STATE (kN)	1120	890	1070	1250
TENSION	MAXIMUM STRENGTH LIMIT STATE (kN)	850	490	580	630
	MAXIMUM SERVICE LIMIT STATE (kN)	320	270	230	450

THE CONTRACTOR IS MADE AWARE THAT ANY STEEL CASING LEFT IN THE GROUND, WHETHER TEMPORARY OR PERMANENT, MUST CONFORM TO THE "BUY AMERICA" PROVISIONS.

The micropiles were designed using the Bond Stress Method. The initial micropile design consisted of threaded bar and high strength grout fully bonded over the length of the micropile. These design calculations can be seen below. This design led to stability problems when the micropiles were tested resulting in load test failures seen in Figures 5 and 6. Testing procedure followed the New York State Department of Transportation Geotechnical Control Procedure Static Pile Load Test Manual (GCP-18) Quick Load Test. It was concluded that the top of the micropile

mobilized first during loading and resulted in high stress concentrations at the top of the pile. The stress concentrations caused the test micropile to fail. Due to failed load tests, the micropiles had to be redesigned and retested.

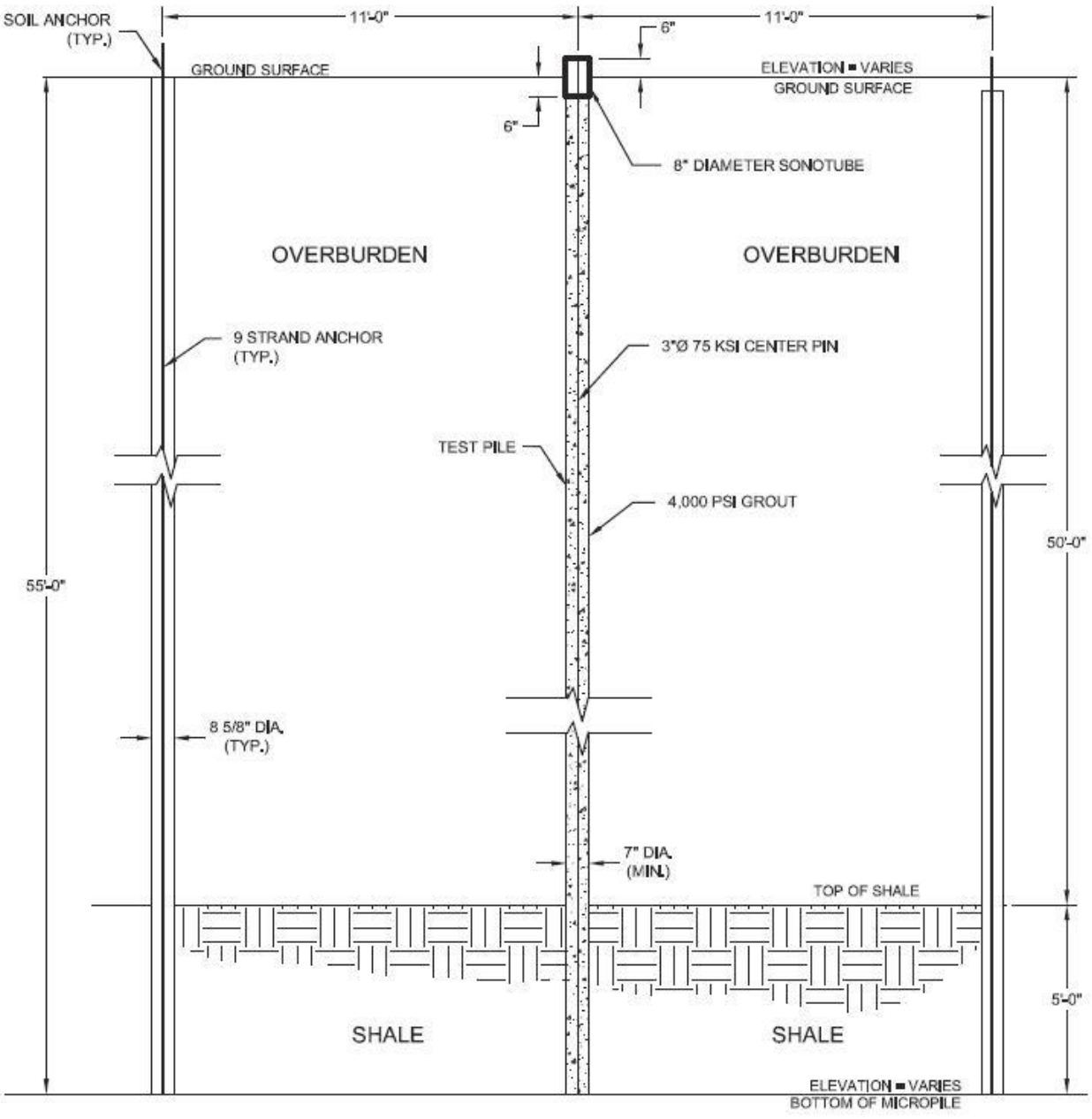

Figure 6-5. Initial uncased design which failed a load test

The End Abutment theoretical capacity will be demonstrated using the Bond Strength Method and compared to the load test results. This was the geotechnical design method used to design the micropiles. Each layer has a bond strength that corresponds to the grout-soil bond formed when injecting grout into the pile. Starting with Equation 1,

$$P_{G-allowable} = \frac{\alpha_{bond}}{FS}(\pi D_b L_b) \quad \text{(Eq. 6.1)}$$

The known parameters are:

α_{bond} = Bond Strength, 500 kPa (80 psi) for shale rock, 100 kPa (15 psi) for Sand with some silt, and 50 kPa (5 psi) for Silt and Clay with some sand.

D_b = Diameter of Micropile 0.178 m

L_b = Length of Bond, 4 m for top sand (fill), 2 m for the clay layer, 8 m for the bottom sand layer, and 1.5 m for the shale rock socket

FS = 1 for ultimate capacity

$$P_{G-allowable\,(no\ casing)} = 671\ kN\ (sand) + 419\ kN\ (shale) + 56\ kN\ (clay) = 1146\ kN \quad \text{(Eq. 6.2)}$$

Structural axial capacity of the micropile was calculated to be much larger than the applied loading and should not be a factor. Thus, soil skin friction failure was expected. Previous studies verified the top of the micropile mobilizes first and may have failed before transferring the load to the rest of the pile. In this case, the result was failure in the micropile. Since it was assumed the load never

reached the bond zone in the bedrock for the initial design, added casing was expected to effectively transfer the load to the shale bedrock("Micropile Installations Dutchess Rail Trail (Stage 4) Poughkeepsie, New York," 2012).

When analyzing the structural components of the micropile, the combination of steel and grout determines the axial capacity. Compression design can be calculated by the following basic equation.

$$Q_w = g\, f_c^1\, A_c + s\, f_y A_y \qquad \text{(Eq. 6.3)}$$

Where:

Q_w = allowable design axial load

g and s = partial factors depending on material (depends on ASD or LRFD method)

f_c^1 = unconfined compressive strength of grout

A_c = area of micropile grout

f_y = yield stress of reinforcing steel

A_y = area of steel reinforcement

For the initial design including grout with a steel rod, the structural capacity was determined below. The structural miropile capacity was determined from a drilled hole diameter of 7 inches, 28 grout strength of 5000 psi, and a 3 inch diameter 75 ksi steel rod placed in the center. This structural design was the same for each micropile.

$$Q_{w\,(no\ casing)} = g\, f_c^1\, A_c + s\, f_y A_y = 584\ kips\ \ or\ \ 2{,}600\ kN \qquad \text{(Eq. 6.4)}$$

The calculated allowable structural axial capacity was greater than the service load of the micropiles, however structural failure was occurring during load testing.

Figure 6-6. Micropile load test setup

Figure 6-7. Pier 3 (left) and End Abutment (right) test micropiles after load test failure

For each separate location a test micropile was required to verify design. Since the specifications required the micropile be tested in compression, soil anchors were required on either side of the test pile to resist the resulting upward load from the jack. The soil anchors can be seen in Figure 6-5. A picture of the load test set up can be seen in Figure 6-6. During the load test, deflection readings were recorded and the integrity of the micropile observed.

It was determined that in order to successfully transfer the loading to the bedrock casing was required. The Bond Stress Method calculations and the structural calculations both change. Due to the lack of bond between steel-soil the resistance between these two materials is not considered. This makes, theoretically, all of the loading transferred to the shale bedrock. In order to account for this the rock socket was increased to 6.5 meters into the shale. The final geotechnical and structural capacity for the cased micropiles was determined to be 1817 kN all contributed to the shale rock socket..

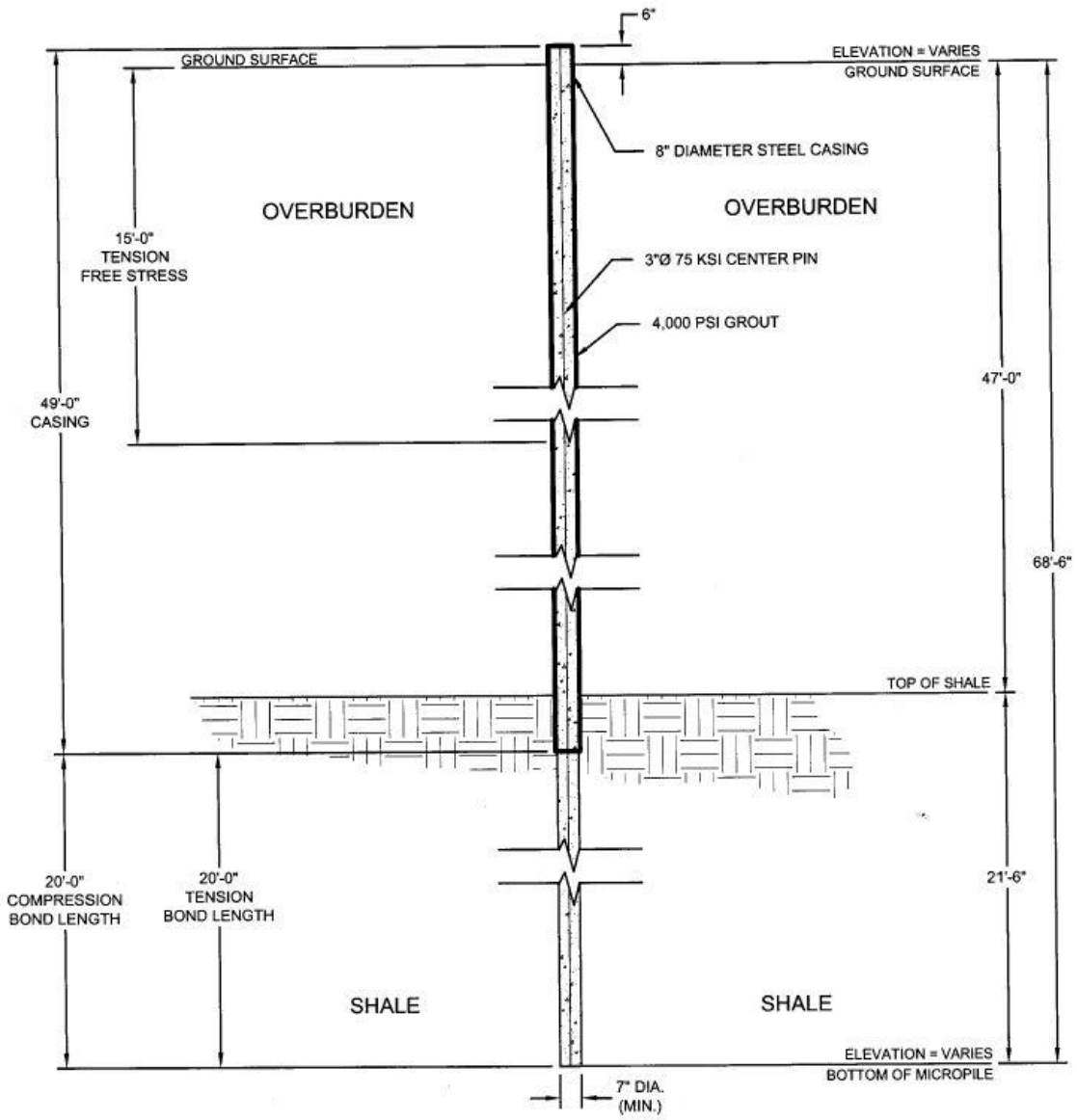

Figure 6-8. Final design for the end abutment that consisted of steel casing down to bedrock

Adding 8-5/8" steel casing with a thickness of ½" allowed for additional structural capacity.

With the steel casing of 50 ksi the structural capacity of the micropile becomes:

$$Q_{w(casing)} = g\, f_c^1\, A_c + s\, f_y A_y = 1126\ kips\ \ or\ \ 5{,}010\ kN \qquad \text{(Eq. 6.5)}$$

This change in structural design allowed the micropiles to be tested without structural failure. Even with an additional moment, the added steel casing will withstand the added stress and transfer the load to competent soil stratum below. Verification from passed load tests allowed for the construction of production micropiles. Many phone calls and open communication lines were essential through the testing process. Keeping everyone that was involved informed of what was going on made the redesign successful. The final design of the End Abutment followed by passing load tests can be seen below.

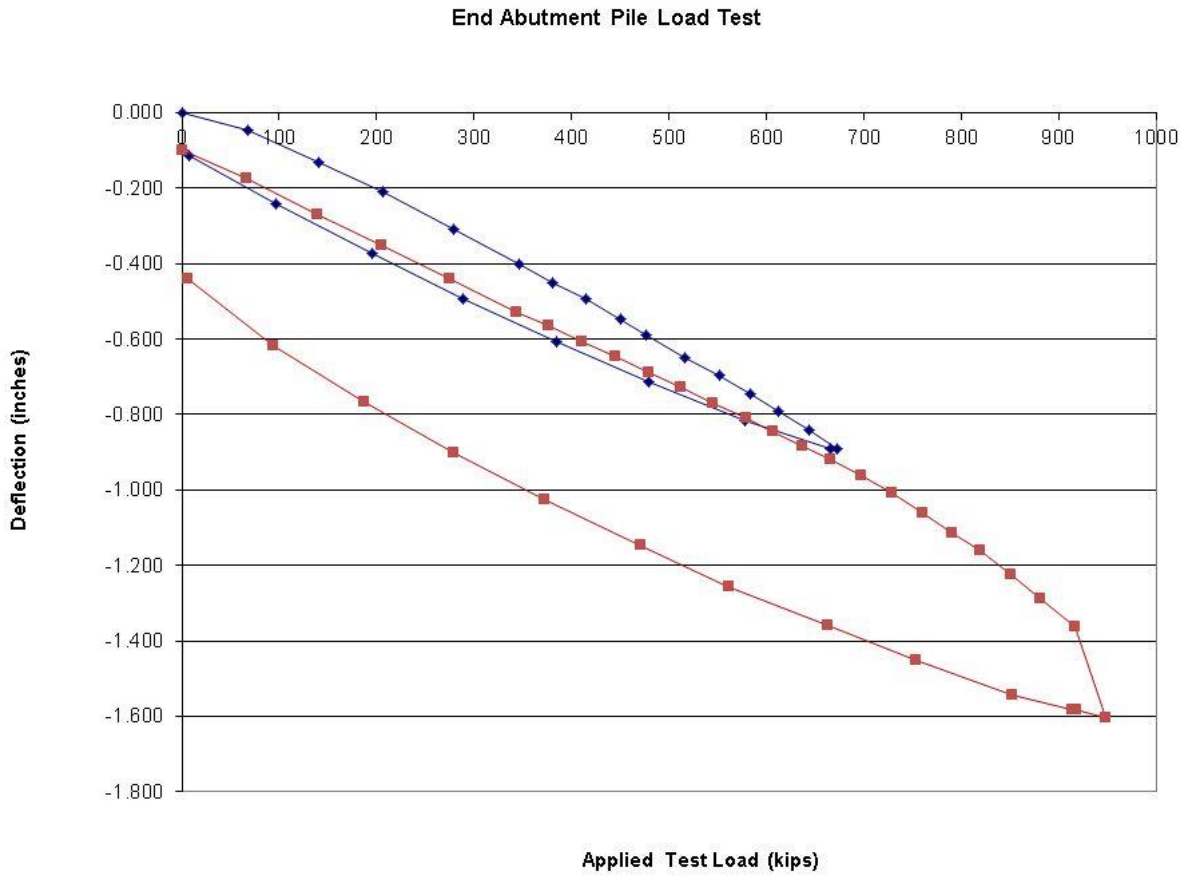

Figure 6-9. Successful load test for the End Abutment micropile

This case study presents the process involved with design, build, and test micropiles. Load tests ensure the micropile can withstand the designated load. When failed load tests occur, redesign is necessary. The outcome of this project provided the owner with sufficient micropiles for the design, and reinforces the necessity for micropile load tests. Final applied loadings for the five test micropiles that passed were 6,000 kN, 5,200 kN, 5,345 kN, 6,327 kN, and 2,000 kN respectively. Buffalo Drilling Company, Inc. is investigating the possible causes of the load test failures, from design to construction methods, to prevent load test failures in the future.

Conclusions from the case study are as follows:

- Load testing techniques must be precise for high capacity micropiles
- Load testing scenarios may differ from actual applied service loads (fixed head vs. free head condition)
- Micropile load transfer mechanisms vary based on design and geotechnical parameters. Current micropile design theories, such as the Bond Stress Method, don't fully investigate these components.
- Structural and geotechnical components need soil-structure-interaction consideration
- Eccentric loadings can induce a moment at the micropile head
- A combination of rod, casing, and grout are needed for most high capacity micropile applications to successfully transfer the load to competent soil stratums

Design-build-test micropile project success is dependent on open communication and active discussion among parties involved.

6.2 Micropile Underpinning of Existing Structure

Hartwick College Cambell Fitness Center, Oneonta, New York

A retaining wall design for Hartwick College was being done next an existing building. It was expected when soil is removed from the excavated side of the wall, the lateral pressure from the building will act on the wall. Instead of designing the retaining wall to hold the building surcharge load, it was decided that a portion of the building foundation would be underpinned by micropiles. This allowed for the retaining wall beam design to remain consistent throughout the wall and easily stay within the required 0.25 inch max deflection at the top of the retaining wall. The soil encountered on site was a silty sand. The foundation of the building was underpinned using 4 micropiles and connected using plates. It was imperative that when drilling was concluded and grouting was to begin, that the pressurized grout was given sufficient time to seep into the surrounding soil to fill in any possible voids around the micropile and under the structure. The micropiles were successful in stabilizing the building and were economical as opposed to designing the retaining wall to hold the surcharge load of the building ("Micropile Installations Hartwick College Campbell Fitness Center Oneonta, New York," 2013).

Figure 6-10. Picture of Hartwick College retaining wall with the building that was underpinned

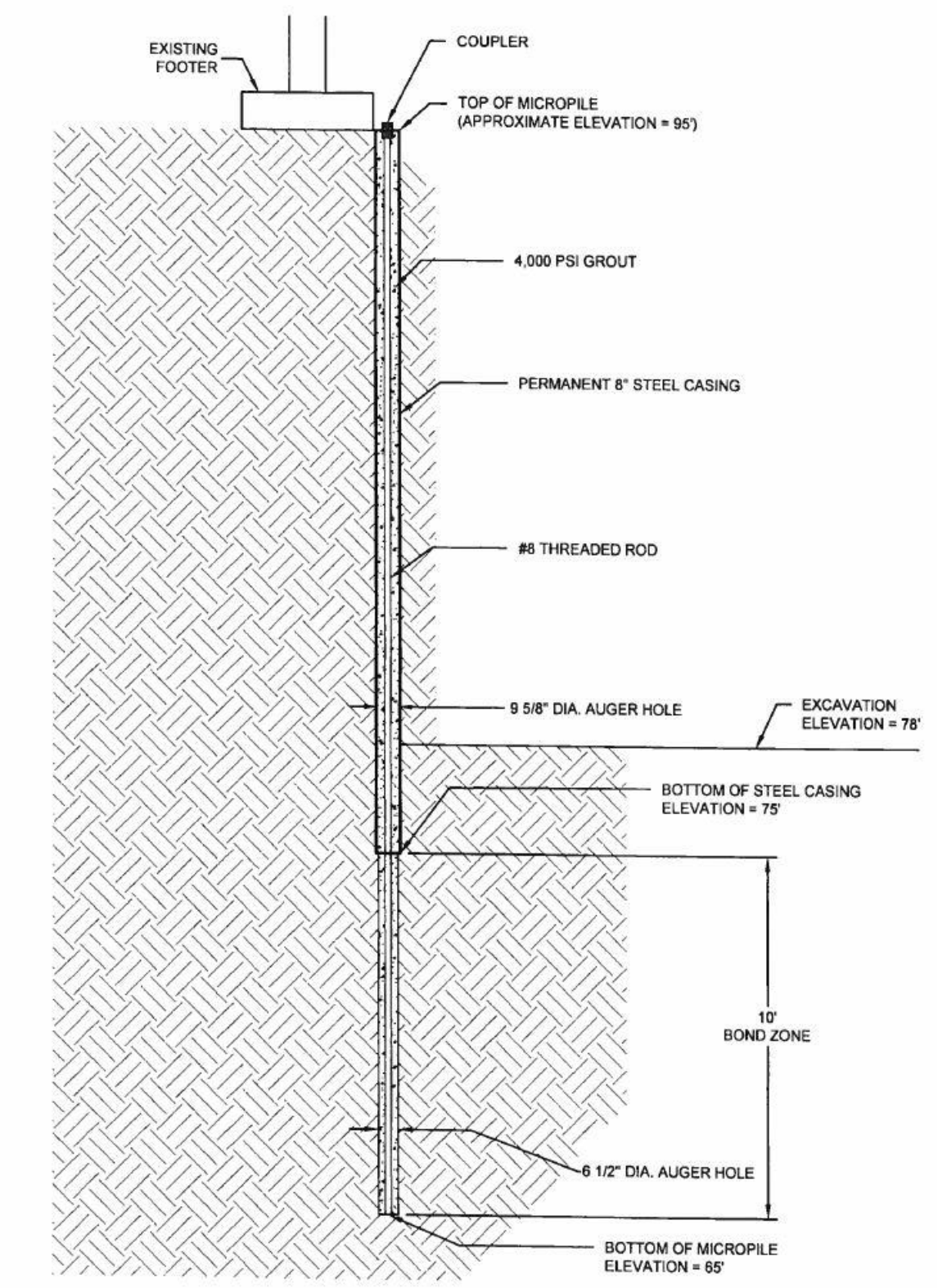

Figure 6-11. Schematic of micropile used to underpin the building foundation. Required design load of 40 kips.

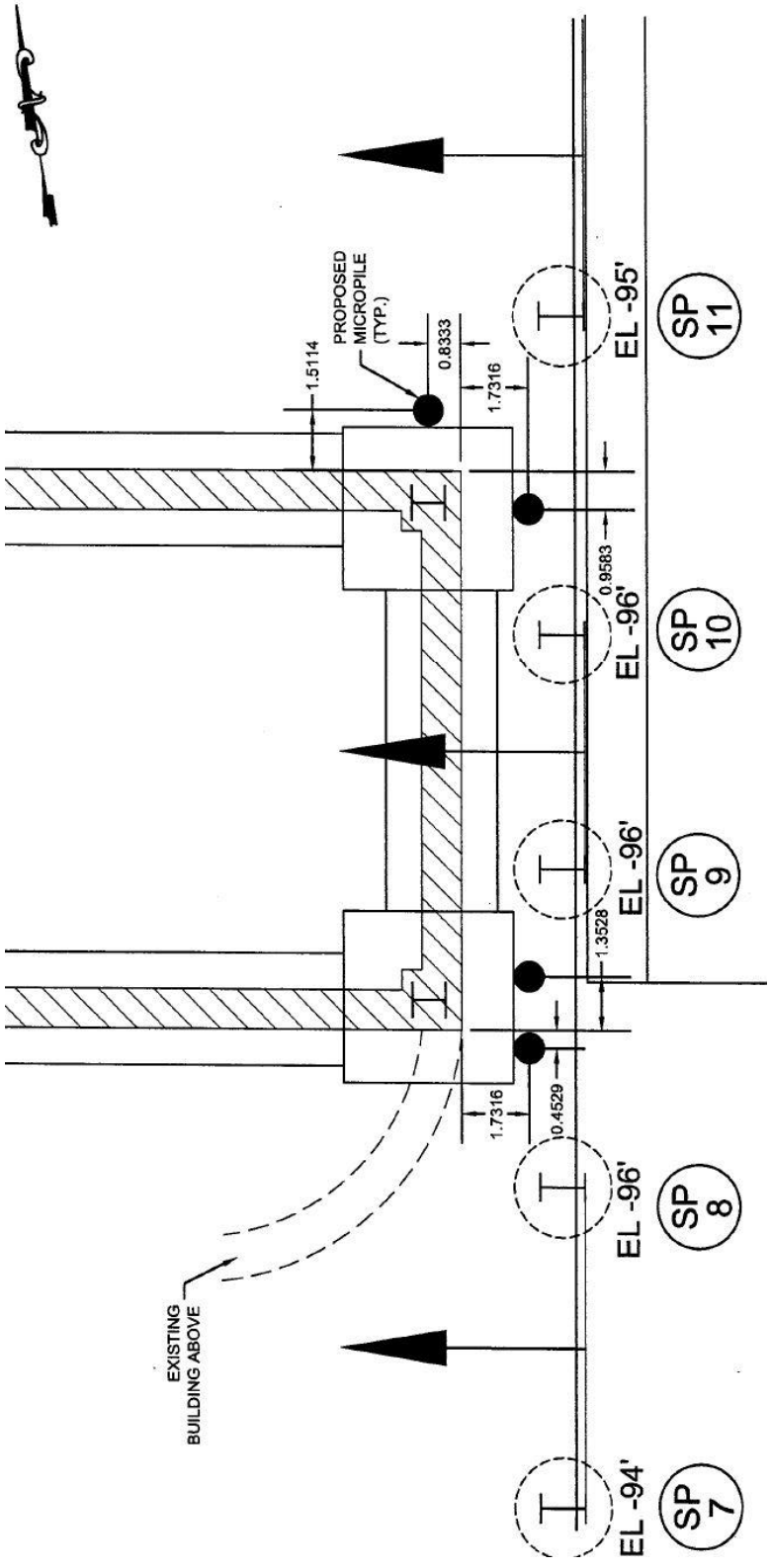

Figure 6-12. Schematic showing the close proximity of the underpinned part of the building to the proposed retaining wall

6.3 Underpinning a Dormitory to Remedy Differential Settlement

Suranaree University of Technology, Thailand

A student dormitory Suranivet 9 part of Suranaree University of Technology (SUT) experienced differential settlement years after construction. Located in Thailand, SUT was constructed on a varying soil profile across the site. There are generally two types of soil present on the site. The top layer, 0-3 meters in depth, consisted of clayey sand. This clayey sand was low to moderate strength. Laboratory tests also revealed that the clayey sand was greatly affected by water content. High strength silty clay underlay the clayey sand. Engineers concluded the varying depth of the clayey sand, along with water presence from rain and the other building systems, resulted in a differential settlement. The settlement profile varied from 20.8 cm to 0.0 cm. This differential settlement caused additional stress on many of the building components causing cracking and damage. Failure was observed in many critical structural components such as beams, columns, and piers. The dormitory initially began construction in 1990 and was open for students in 1993. The dormitory was then closed in 2001 due to the cracks observed on structural members. It was stated the floor unevenness was very noticeable and cracks along walls were progressing quickly. In 2003 it was decided that underpinning the structure was the ideal solution to remedy the differential settlement. Underpinning was completed in September 2004 (Horpibulsuk, Kumpala, & Katkan, 2008).

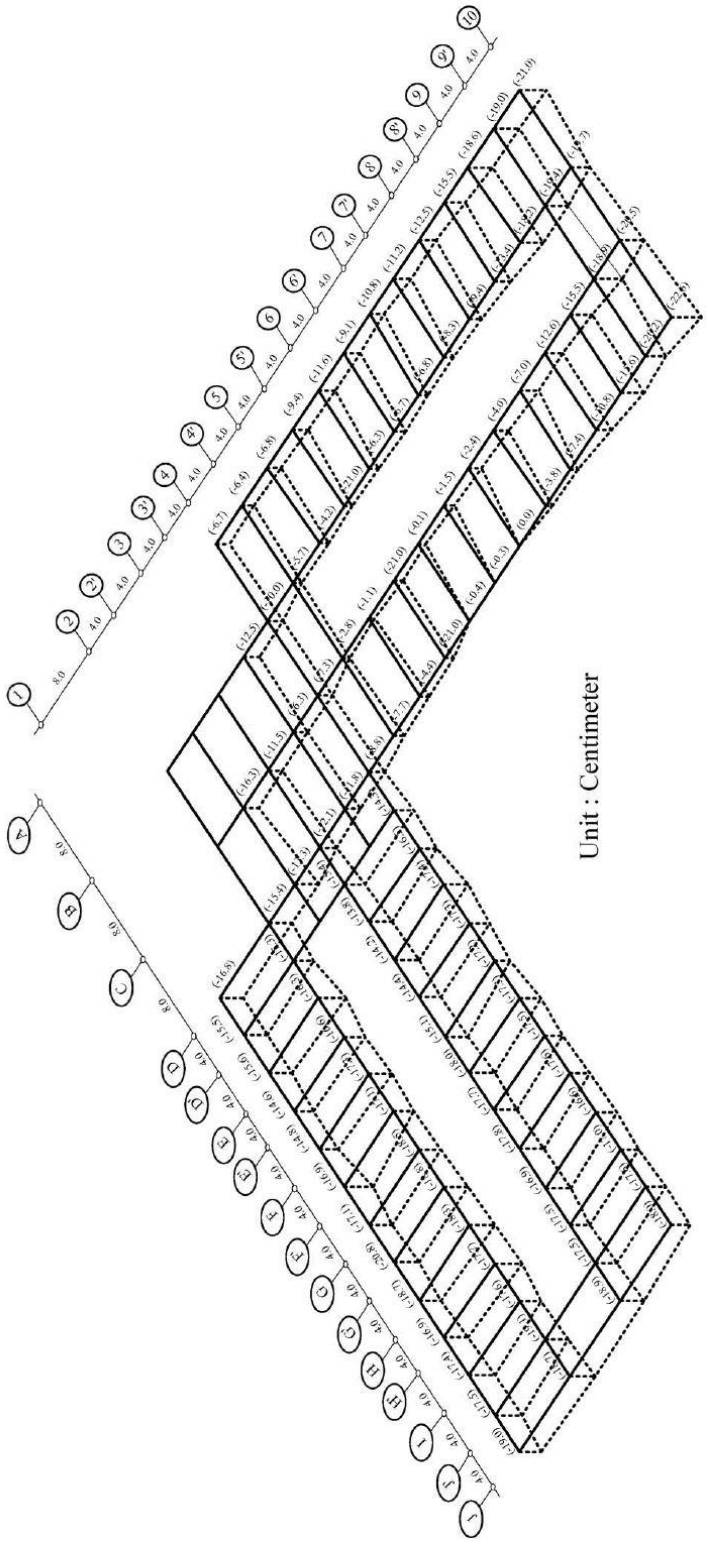

Figure 6-13. Settlement profile of prior to underpinning Dormitory Suranivet 9 (Horpibulsuk et al., 2008)

The underpinning design consisted of 10.0, 12.5, and 15.0 cm diameter micropiles which ranged in length from 7.0 to 10.0 meters. It was determined by laboratory testing that the underlying silty clay was viable for the micropile design. Each footing was designated a number of micropiles, depending on the design load.

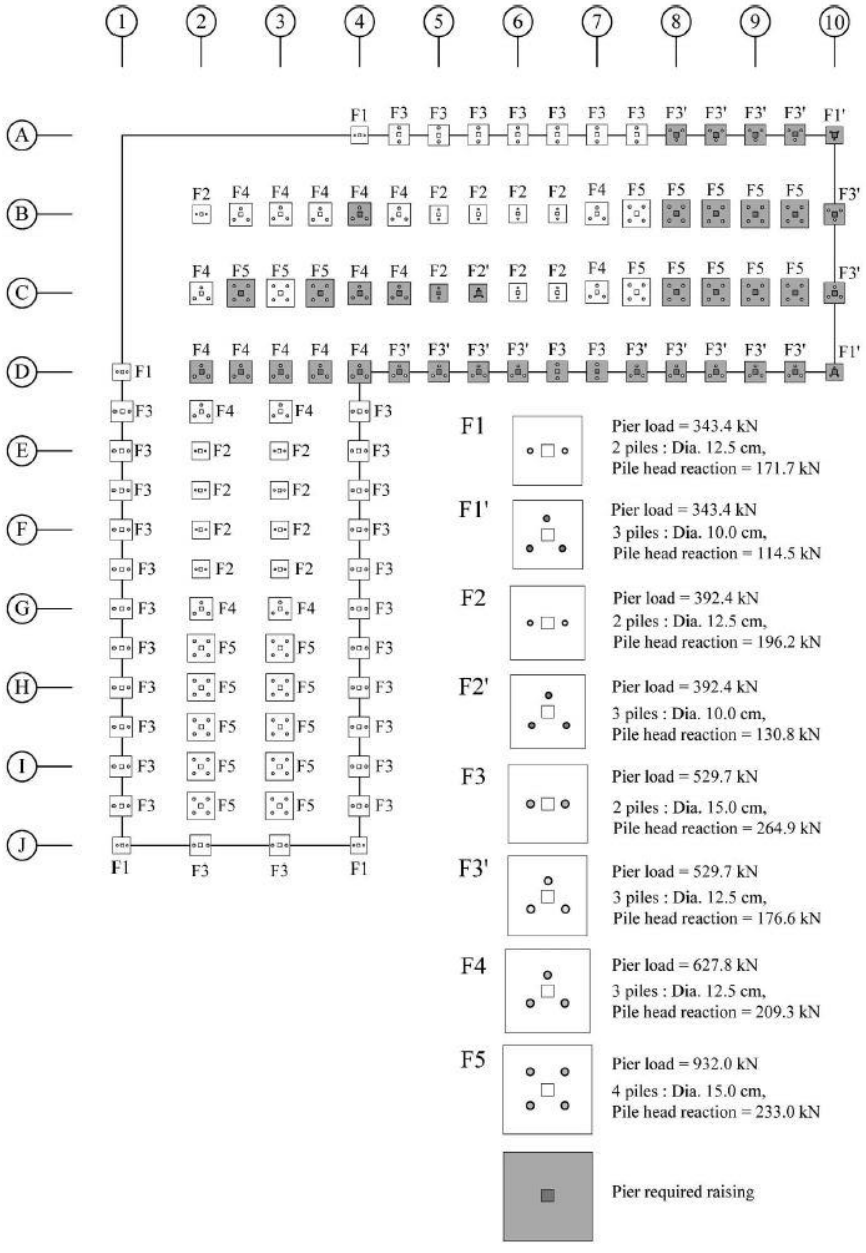

Figure 6-14. Plan view of underpinned foundations for Dormitory Suranivet 9 (Horpibulsuk et al., 2008)

The micropiles are arranged as symmetric as possible not to allow any moment on the concrete footing. Every pile was underpinned to unify the building. Some of the concrete piers with extensive settlement, needed to be jacked up prior to connection with the micropiles. A diamond bit was used to drill the boreholes, which were spaced at least 3 times the diameter from each other to reduce the group effect pile settlement (Horpibulsuk et al., 2008). A year after the underpinning, very small settlement values were recorded. The low settlement recordings display the success of the micropile underpinning. This supports that using micropiles to underpin structures experiencing differential settlement is effective.

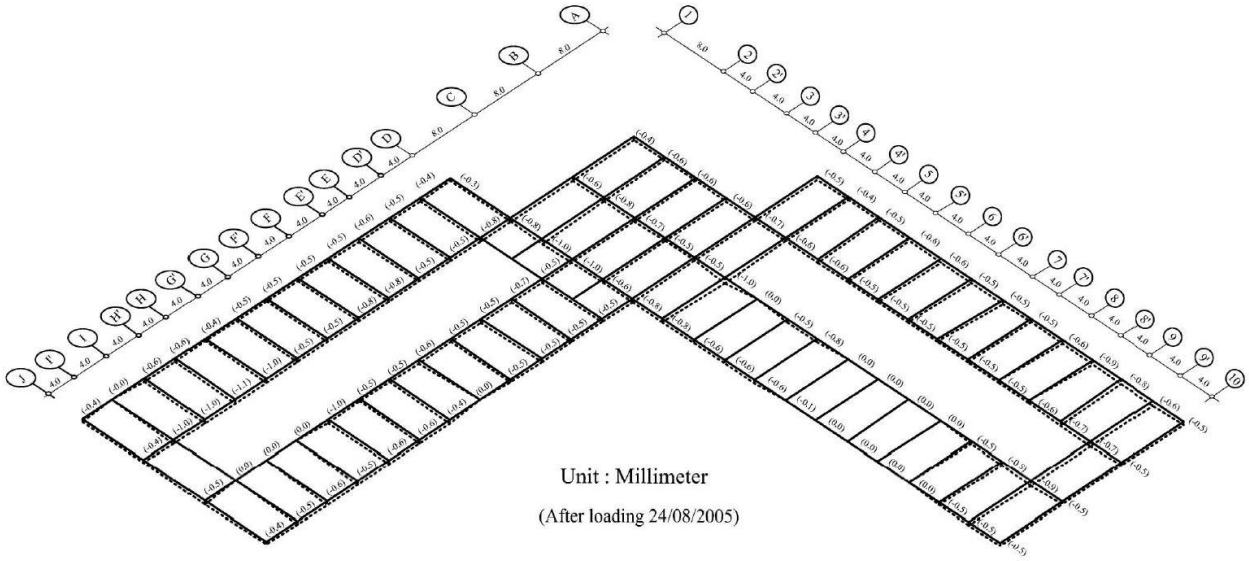

Figure 6-15. Settlement profile of Dormitory Suranivet 9 after underpinning foundation and one year of service (Horpibulsuk et al., 2008)

7. Conclusions and Future Research

In conclusion micropile design depends on the combined knowledge from geotechnical investigation and various design methods. Field load tests provide essential data to ensure a current design is satisfactory for the loads specified. Axial and lateral micropile design mobilize different load transfer mechanisms into the soil. Axial load testing utilizes skin friction and end bearing resistance. Micropiles, due to their slender nature depends largely on skin friction for capacity.

Currently, the bond stress method is the most accepted design methodology. However, this design method fails to incorporate the change in load transfer mechanisms for various cased length ratios. Steel casing has lower bond values to soil that grout. Therefore fully boned micropiles are mobilized faster and better suited for settlement mitigation. Casing provides both lateral capacity and ensures axial loadings are correctly transferred to competent soil stratum. Simulated load testing has shown that casing adds lateral capacity due to additional pile head stiffness. Normalized capacity graphs developed from the FEM has supported that casing past the point of fixity for lateral loads is critical. However, casing passed the point of fixity provides diminishing returns for capacity.

Due to the slender nature of the micropile, load transfer behaviors can be difficult to quantify. Additional understanding of micropile load transfer behavior can limit the amount of field load testing required saving the project owner time and money. Various cross sections, connections, and geologic conditions used for the micropile need to be investigated to further progress the benefits from micropile construction.

Additional research is required to determine design methods that provide engineers with the tools necessary to efficiently implement micropiles. We have discussed future research exploring the micropile load transfer behavior associated with cyclic loadings, pile cap connections, casing joints, bridge retrofitting, slenderness ratios, and for use as structural fuses. Micropiles are going to continue to rapidly grow due to the ageing infrastructure in the U.S. requiring bridge retrofits and replacements. Micropiles are one of the most promising emerging technologies related to the foundation industry.

8. References

Aschenbroich, H. Using Anchor Foundations in Difficult Soil Conditions. *North American Wind Power*.

ASTM. (1994). Standard Test Method for Piles Under Static Axial Compressive Load (pp. 11). PA: American Society for Testing and Materials.

ASTM. (1995). Standard Test Method for Piles Under Lateral Loads (pp. 15). West Conshohocken, PA: American Society for Testing and Materials.

Bruce, D., & Juran, L. (1997). Drilled and Grouted Micropiles: State-of-Practice Review, Volume I-IV. McLean, Virginia: U.S. Department of Transportation: Federal Highway Administration.

Cadden, A., & Gomez, J. (2002). Buckling of Micropiles: A review of historic research and recent experiences. *ADSC*, 19.

Canadian Foundation Engineering Manual, 3rd Edition. (1992). Canadian Geotechnical Society.

Elaziz, A. Y. A., & Naggar, M. H. E. (2015). Performance of Hollow Bar Micropiles under Monotonic and Cyclic Lateral Loads. *American Society of Civil Engineers, Journal of Geotechnical and Geoenvironmental Engineering*, 11.

FHWA. (2005). Micropile Design and Construction: Reference Manual. Washington, D.C.: U.S. Department of Transportation.

Geotechnical Control Procedure: Static Pile Load Test Manual. (2015). Albany, New York: State of New York Department of Transportation.

Grove Road Bridge Replacement. (2014). Essex County Department of Public Works: Schoder River Associates.

Helwany, S. (2007). *Applied Soil Mechanics with ABAQUS Applications*: John Wiley and Sons.

Horpibulsuk, S., Kumpala, A., & Katkan, W. (2008). A Case History on Underpinning for a Distressed Building on Hard Residual Soil Underneath Non-Uniform Loose Sand. Tokyo: Japenese Geotechnical Society.

Houlsby, G. T. (1991). HOW THE DILATANCY OF SOILS AFFECTS THEIR BEHAVIOUR (pp. 30). European Conference on Soil Mechanics and Foundation Engineering.

Hussin, J., & Cook, C. (2010). Fast-Track Installation of Micropiles to Resupport Settled Florida SR-60 Bridge End Bents. *Transportation Research Record 2202*, 5.

Larsson, K., & Jog, D. (2014). Performance of Micropiles Used to Underpin Highway Bridges. *American Society of Civil Engineers, Performance of Constructed Facilities*(28), 16.

Lindeburg, M. (2012). *Civil Engineering Reference Manual for the PE Exam, 13th Edition*. Belmont, California: Professional Publications, Inc.

Lizzi, F. (1982). *The Static Restoration of Monuments*. Venetia, Pennsylvania: International Society of Micropiles.

Luna, R., Dixon, D., Kershaw, K., & Siegel, T. (2015). Monitoring Micropile Foundations of Bridge during Construction *IFCEE 2015* (pp. 878-889): American Society of Civil Engineers.

Micropile Installations Dutchess Rail Trail (Stage 4) Poughkeepsie, New York. (2012). Buffalo, New York.

Micropile Installations Hartwick College Campbell Fitness Center Oneonta, New York. (2013). Buffalo, New York.

Monopole Reinforcement and Retrofit Project. (2014). North Smithfield, Rhode Island: Crown Castle.

Mosher, R. L., & Dawkins, W. P. (2000). *Theoretical Manual for Pile Foundations*: US Army Corps of Engineers, Engineer Research and Development Center.

NYSDOT. (2015). Geotechnical Engineering Manual: Micropile Inspector Guidelines (pp. 29). Geotechnical Engineering Bureau.

Poulos, H. G., & Davis, E. H. (2006). *Elastic Solutions for Soil and Rock Mechanics*. University of Sydney: Centre for Geotechnical Research.

Reese, L., & Van-Impe, W. (2011). *Single Piles and Pile Groups Under Lateral Loading*. London, UK: CRC Press.

Scott, R. (1981). *Foundation Analysis*. Englewood Cliff, New Jersey: Prentice-Hall.

Seo, H., Prezzi, M., & Salgado, R. (2013). Instrumented Static Load Test on Rock-Socketed Micropile. *Journal of Geotechnical and Geoenvironmental Engineering, 139*(12), 2037-2047. doi: 10.1061/(ASCE)GT.1943-5606.0000946

Shong, S., & Chung, F. C. (2003). Design and Construction of Micropiles. Kuala Lumpur, Malaysia: Gue and Partners Sdn Bhd.

Sivakugan. (2010). *Geotechnical Engineering: A Practical Problem Solving Approach*. Fort Lauderdal, Florida: J. Ross Publishing.

Splitstone, D., Stonecheck, S., Dodson, R., & Fuller, J. (2010). Birmingham Bridge Emergency Repairs: Micropile Foundation Retrofit. *ASCE*(GeoFlorida), 9.

9. Appendix

Bridge Replacement 1016020 U.S. Route 20 over kinderhook creek
Micropile Test
Brainard, New York
Rensselaer County

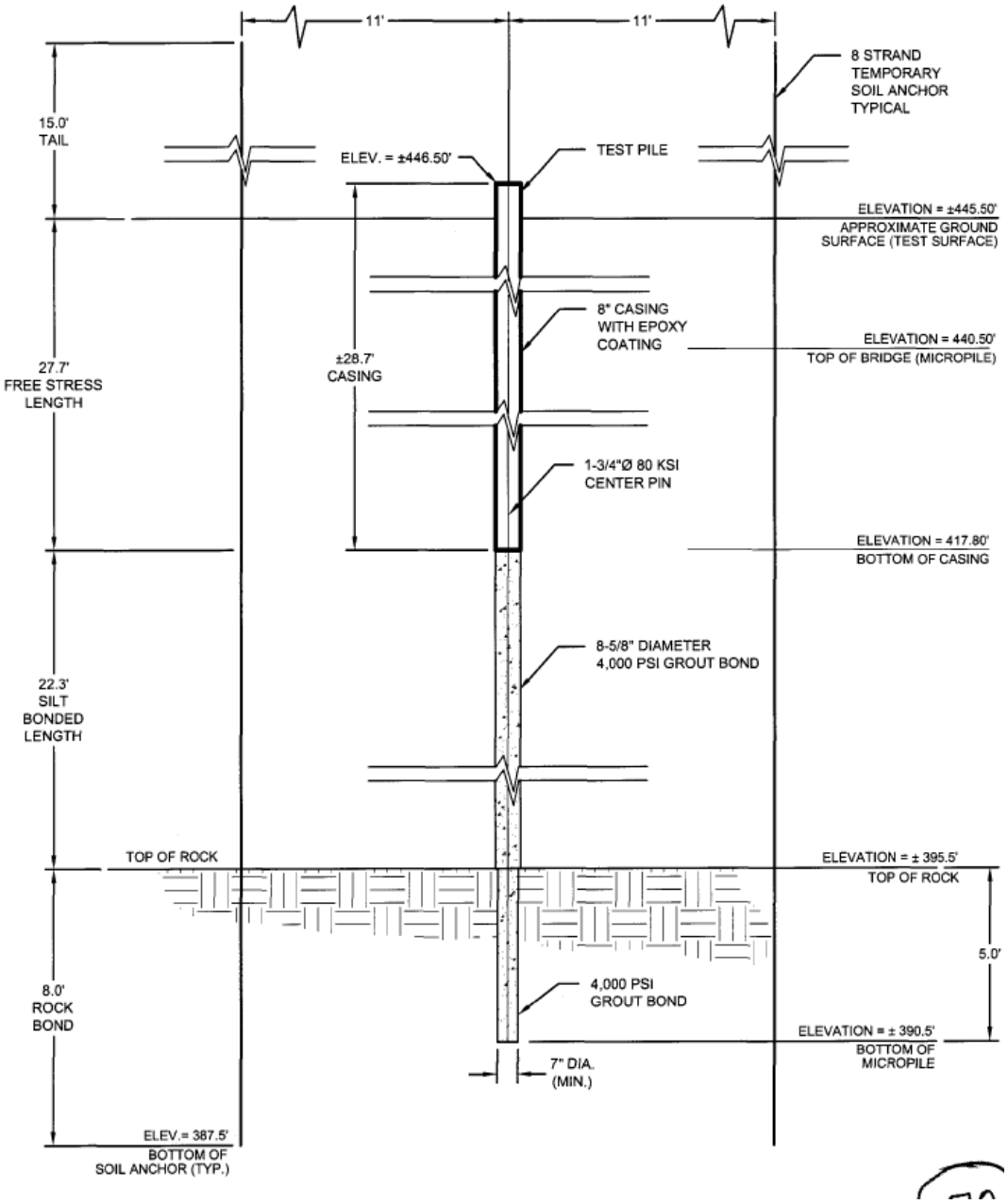

Figure 9-1. Test micropile layout BIN 1016020

BRIDGE 1016020
BEGIN ABUTMENT

SM 282 E 12/02

STATE OF NEW YORK
DEPARTMENT OF TRANSPORTATION
GEOTECHNICAL ENGINEERING BUREAU
SUBSURFACE EXPLORATION LOG

PSN 11987 BORNUM 19
REGION 1
COUNTY RENSSELAER
PIN 1BOW.00.101
PROJECT CRITICAL BRIDGES OVER WATER PROGRAM
ACTUAL COORDINATES (N) 1,336,283.080 (E) 753,624.110 DATUM NAD83
DATE START 16-NOV-2013 DATE FINISH 20-NOV-2013

HOLE DN-B-22
LINE BL
STA
OFFSET ft
SURF. ELEV. 498.65
DEPTH TO WATER SEE NOTE

CASING O. D. 3 1/2 in I. D. 3 in WT OF HAMMER-CASING lb HAMMER FALL-CASING in
SAMPLER O. D. 2 in I. D. 1 3/8 in WT OF HAMMER-SAMPLER 140 lb HAMMER FALL-SAMPLER 30 in

CASING BLOWS/ft	DEPTH ft BELOW SURFACE	SAMPLE NO.	BLOWS ON SAMPLER in 0/6 6/12 12/18 18/24	MOIST. CONT. (%)	DESCRIPTION OF SOIL AND ROCK
	0.0				(0.00) Concrete
		J1	5 9 10	10%	(1.00) Brown Gravelly SAND ,Silty (W-NPL)
	5.0				
		J2	12 18 16	11%	(5.00) Brown Sandy GRAVEL ,Silty (W-NPL)
	10.0				
		J3	8 6 3	14%	(10.00) Brown Sandy SILT ,Gravelly (W-NPL)
	15.0				
		J4	15 47 55	6%	(15.00) Red-Brown Silty GRAVEL ,Sandy (W-NPL)
		B1			(17.40) Run #1 Drilled from 17'5" To 20'0" BOULDER REC. 7.2" 23.1% 3 Pieces and cobbles NW SINGLE TUBE
	20.0				
		J5	35 62	7%	(20.00) Red-Brown Silty GRAVEL ,Sandy (W-NPL)
		B2			(21.00) Run #2 Drilled from 21'0" To 25'0" BOULDER REC. 10.8" 22.5% 2 Pieces and cobbles NW SINGLE TUBE
	25.0				

TOP OF MICROPILE EL 489.70

8" CASING 28.5' TOTAL

30

The subsurface information shown here was obtained for design and estimate purposes. It is made available so that users may have access to the same information available to the State. It is presented in good faith. By the nature of the exploration process, the information represents only a small fraction of the total volume of the material at the site. Interpolation between data samples may not be indicative of the actual material encountered.

CONTRACT CONTRACTOR

DRILL RIG OPERATOR D.Okosky
SOIL & ROCK DESCRIPTION H.MacNeil
REG GEOTECHNICAL ENGINEER Michael A. Novak
DATE APPROVED 07-JAN-2014
RESIDENT ENGINEER
STRUCTURE NAME B.I.N. 1016020
Rt. 20 / Kinderhook Creek, Rm 2161
SHEET 1 OF 4 HOLE DN-B-22

Figure 9-2. Geotechnical boring for BIN 1016020

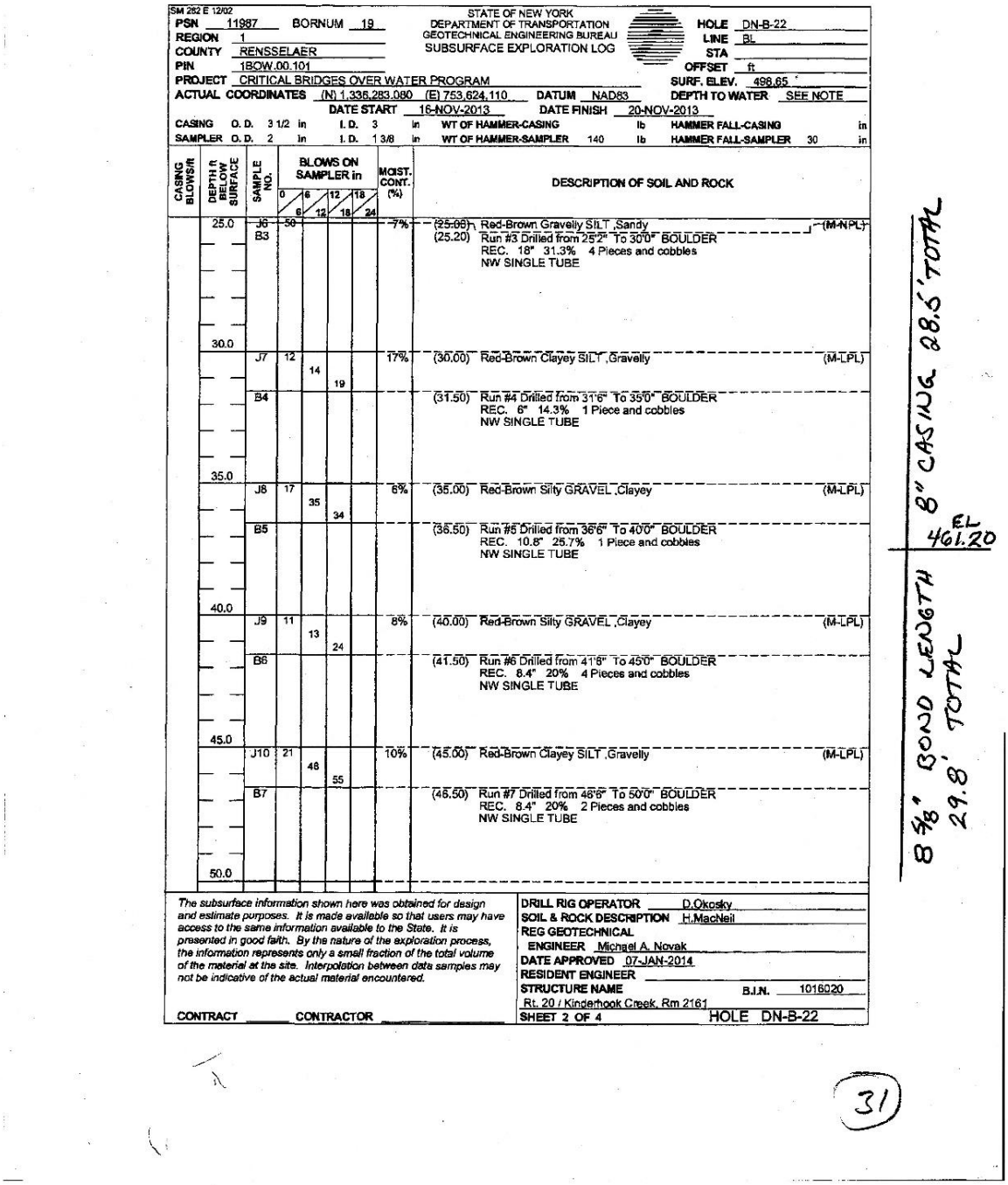

SM 282 E 12/02

PSN 11987 BORNUM 19
REGION 1
COUNTY RENSSELAER
PIN 1BOW.00.101
PROJECT CRITICAL BRIDGES OVER WATER PROGRAM
ACTUAL COORDINATES (N) 1,336,283.080 (E) 753,624.110 DATUM NAD83
DATE START 16-NOV-2013 DATE FINISH 20-NOV-2013

STATE OF NEW YORK
DEPARTMENT OF TRANSPORTATION
GEOTECHNICAL ENGINEERING BUREAU
SUBSURFACE EXPLORATION LOG

HOLE DN-B-22
LINE BL
STA
OFFSET ft
SURF. ELEV. 498.65
DEPTH TO WATER SEE NOTE

CASING O. D. 3 1/2 in I. D. 3 in WT OF HAMMER-CASING lb HAMMER FALL-CASING in
SAMPLER O. D. 2 in I. D. 1 3/8 in WT OF HAMMER-SAMPLER 140 lb HAMMER FALL-SAMPLER 30 in

CASING BLOWS/ft	DEPTH ft BELOW SURFACE	SAMPLE NO.	BLOWS ON SAMPLER in (0/6, 6/12, 12/18, 18/24)	MOIST. CONT. (%)	DESCRIPTION OF SOIL AND ROCK
	25.0	J6	50	7%	(25.00) Red-Brown Gravelly SILT ,Sandy (M-NPL)
		B3			(25.20) Run #3 Drilled from 25'2" To 30'0" BOULDER REC. 18" 31.3% 4 Pieces and cobbles NW SINGLE TUBE
	30.0	J7	12 (14/19)	17%	(30.00) Red-Brown Clayey SILT ,Gravelly (M-LPL)
		B4			(31.50) Run #4 Drilled from 31'6" To 35'0" BOULDER REC. 6" 14.3% 1 Piece and cobbles NW SINGLE TUBE
	35.0	J8	17 (35/34)	6%	(35.00) Red-Brown Silty GRAVEL ,Clayey (M-LPL)
		B5			(36.50) Run #5 Drilled from 36'6" To 40'0" BOULDER REC. 10.8" 25.7% 1 Piece and cobbles NW SINGLE TUBE
	40.0	J9	11 (13/24)	8%	(40.00) Red-Brown Silty GRAVEL ,Clayey (M-LPL)
		B6			(41.50) Run #6 Drilled from 41'6" To 45'0" BOULDER REC. 8.4" 20% 4 Pieces and cobbles NW SINGLE TUBE
	45.0	J10	21 (48/55)	10%	(45.00) Red-Brown Clayey SILT ,Gravelly (M-LPL)
		B7			(46.50) Run #7 Drilled from 46'6" To 50'0" BOULDER REC. 8.4" 20% 2 Pieces and cobbles NW SINGLE TUBE
	50.0				

The subsurface information shown here was obtained for design and estimate purposes. It is made available so that users may have access to the same information available to the State. It is presented in good faith. By the nature of the exploration process, the information represents only a small fraction of the total volume of the material at the site. Interpolation between data samples may not be indicative of the actual material encountered.

CONTRACT CONTRACTOR

DRILL RIG OPERATOR D.Okosky
SOIL & ROCK DESCRIPTION H.MacNeil
REG GEOTECHNICAL ENGINEER Michael A. Novak
DATE APPROVED 07-JAN-2014
RESIDENT ENGINEER
STRUCTURE NAME B.I.N. 1016020
Rt. 20 / Kinderhook Creek, Rm 2161
SHEET 2 OF 4 HOLE DN-B-22

8" CASING 28.5' TOTAL
EL 461.20
8 5/8" BOND LENGTH 29.8' TOTAL

31

Figure 9-3. Geotechnical boring for BIN 1016020 (cont 1)

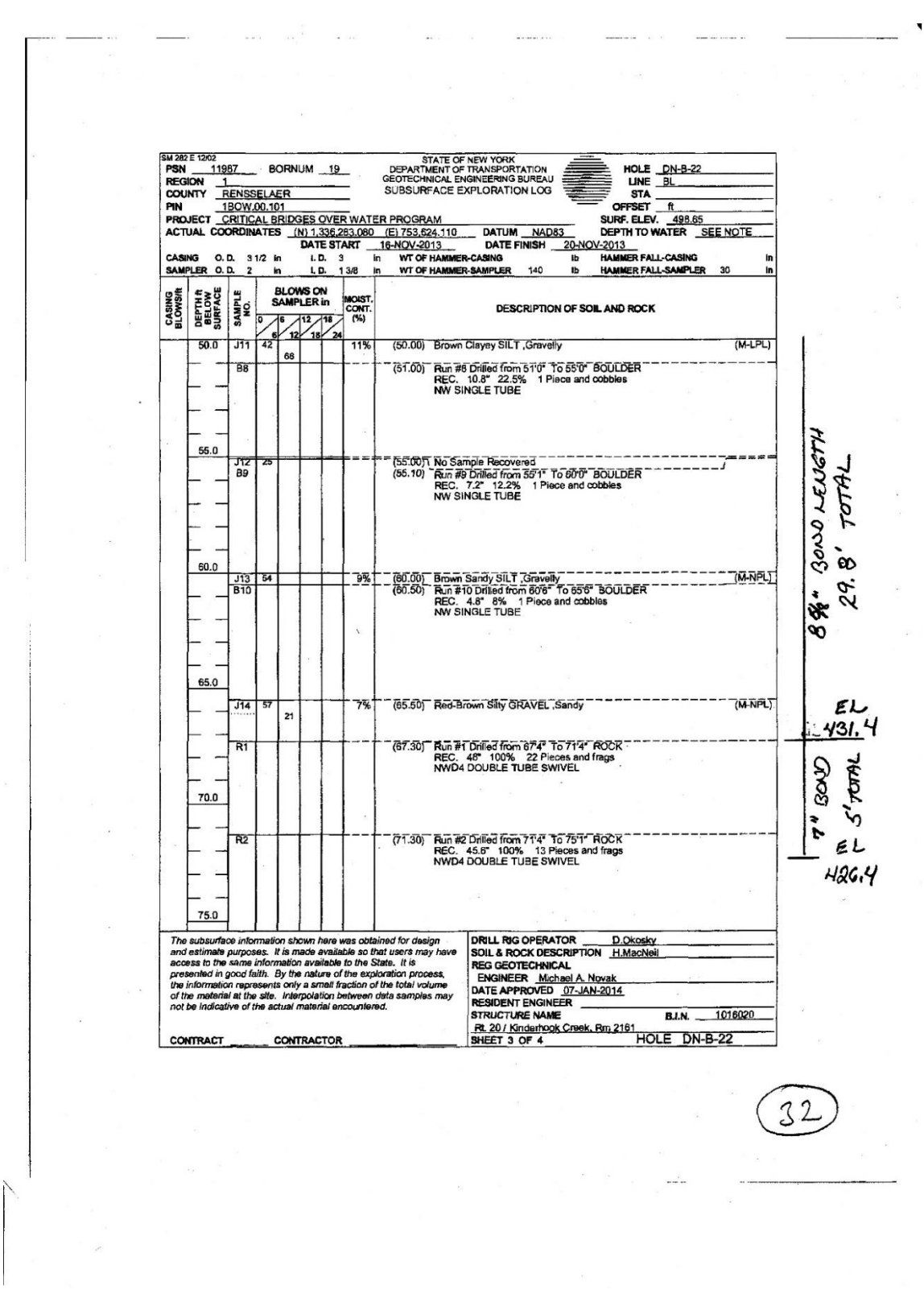

SM 282 E 12/02

STATE OF NEW YORK
DEPARTMENT OF TRANSPORTATION
GEOTECHNICAL ENGINEERING BUREAU
SUBSURFACE EXPLORATION LOG

PSN 11987 BORNUM 19
REGION 1
COUNTY RENSSELAER
PIN 1BOW.00.101
PROJECT CRITICAL BRIDGES OVER WATER PROGRAM
ACTUAL COORDINATES (N) 1,336,283.080 (E) 753,624.110 DATUM NAD83
DATE START 16-NOV-2013 DATE FINISH 20-NOV-2013

HOLE DN-B-22
LINE BL
STA
OFFSET ft
SURF. ELEV. 498.65
DEPTH TO WATER SEE NOTE

CASING O. D. 3 1/2 in I. D. 3 in WT OF HAMMER-CASING lb HAMMER FALL-CASING in
SAMPLER O. D. 2 in I. D. 1 3/8 in WT OF HAMMER-SAMPLER 140 lb HAMMER FALL-SAMPLER 30 in

CASING BLOWS/ft	DEPTH ft BELOW SURFACE	SAMPLE NO.	BLOWS ON SAMPLER in (0/6, 6/12, 12/18, 18/24)	MOIST. CONT. (%)	DESCRIPTION OF SOIL AND ROCK
	50.0	J11	42 (6/12: 68)	11%	(50.00) Brown Clayey SILT ,Gravelly (M-LPL)
		B8			(51.00) Run #8 Drilled from 51'0" To 55'0" BOULDER REC. 10.8" 22.5% 1 Piece and cobbles NW SINGLE TUBE
	55.0	J12	25		(55.00) No Sample Recovered
		B9			(55.10) Run #9 Drilled from 55'1" To 60'0" BOULDER REC. 7.2" 12.2% 1 Piece and cobbles NW SINGLE TUBE
	60.0	J13	54	9%	(60.00) Brown Sandy SILT ,Gravelly (M-NPL)
		B10			(60.50) Run #10 Drilled from 60'6" To 65'6" BOULDER REC. 4.8" 8% 1 Piece and cobbles NW SINGLE TUBE
	65.0	J14	57 (21)	7%	(65.50) Red-Brown Silty GRAVEL ,Sandy (M-NPL)
		R1			(67.30) Run #1 Drilled from 67'4" To 71'4" ROCK REC. 48" 100% 22 Pieces and frags NWD4 DOUBLE TUBE SWIVEL
	70.0	R2			(71.30) Run #2 Drilled from 71'4" To 75'1" ROCK REC. 45.6" 100% 13 Pieces and frags NWD4 DOUBLE TUBE SWIVEL
	75.0				

8 3/4" BOND LENGTH 29.8' TOTAL
EL 431.4
7" BOND 5' TOTAL
EL 426.4

The subsurface information shown here was obtained for design and estimate purposes. It is made available so that users may have access to the same information available to the State. It is presented in good faith. By the nature of the exploration process, the information represents only a small fraction of the total volume of the material at the site. Interpolation between data samples may not be indicative of the actual material encountered.

CONTRACT CONTRACTOR

DRILL RIG OPERATOR D.Okosky
SOIL & ROCK DESCRIPTION H.MacNeil
REG GEOTECHNICAL ENGINEER Michael A. Novak
DATE APPROVED 07-JAN-2014
RESIDENT ENGINEER
STRUCTURE NAME B.I.N. 1016020
Rt. 20 / Kinderhook Creek, Rm 2161
SHEET 3 OF 4 HOLE DN-B-22

32

Figure 9-4. Geotechnical boring for BIN 1016020 (cont 2)

SM 282 E 12/02

STATE OF NEW YORK
DEPARTMENT OF TRANSPORTATION
GEOTECHNICAL ENGINEERING BUREAU
SUBSURFACE EXPLORATION LOG

PSN 11987 BORNUM 19 HOLE DN-B-22
REGION 1 LINE BL
COUNTY RENSSELAER STA
PIN 1BOW.00.101 OFFSET ft
PROJECT CRITICAL BRIDGES OVER WATER PROGRAM SURF. ELEV. 498.65
ACTUAL COORDINATES (N) 1,336,283.080 (E) 753,624.110 DATUM NAD83 DEPTH TO WATER SEE NOTE
DATE START 16-NOV-2013 DATE FINISH 20-NOV-2013

CASING	O. D.	3 1/2 in	I. D.	3 in	WT OF HAMMER-CASING	lb	HAMMER FALL-CASING	in
SAMPLER	O. D.	2 in	I. D.	1 3/8 in	WT OF HAMMER-SAMPLER	140 lb	HAMMER FALL-SAMPLER	30 in

CASING BLOWS/ft	DEPTH ft BELOW SURFACE	SAMPLE NO.	BLOWS ON SAMPLER in (0/6, 6/12, 12/18, 18/24)	MOIST. CONT. (%)	DESCRIPTION OF SOIL AND ROCK
	75.0	R3			(75.10) Run #3 Drilled from 75'1" To 77'2" ROCK REC. 25.2" 100% 7 Pieces and frags NWD4 DOUBLE TUBE SWIVEL

BOTTOM OF HOLE AT 77.20 ft

Automatic hammer used
Wash water added at ground level
Rollerbit ahead between samples J-1 through B-1
Drilled casing between samples
Sampler blows for samples J-6 were 50 blows for 2.4in of penetration
Sampler blows for samples J-12 were 25 blows for 1.2in of penetration
Sampler blows for samples J-13 were 54 blows for 6.0in of penetration
Sampler blows for samples J-14 were 21 blows for 1.2in of penetration
Driller noted Rollerbit ahead from 16.5ft to 17.4ft switched to NWST casing
Driller noted no recovery for sample J-12 from 55.0ft to 55.1ft
Driller noted refusals at 17.4ft, 25.2ft, 55.1ft, 60.5ft, and 66.1ft
Driller noted rollerbit ahead from 66.1ft to 67.3ft

DATE	TIME	DEPTH ft			ARTESIAN HEAD HEIGHT ABOVE GROUND	FILLED WITH WATER AT END OF DAY
		HOLE	CASING	WATER		
18-Nov-13	09:15	40.00	40.00	12.40		
19-Nov-13	08:00	65.50	65.50	10.00		
20-Nov-13	08:00	75.10	65.50	11.90		

The subsurface information shown here was obtained for design and estimate purposes. It is made available so that users may have access to the same information available to the State. It is presented in good faith. By the nature of the exploration process, the information represents only a small fraction of the total volume of the material at the site. Interpolation between data samples may not be indicative of the actual material encountered.

CONTRACT CONTRACTOR

DRILL RIG OPERATOR D.Okosky
SOIL & ROCK DESCRIPTION H.MacNeil
REG GEOTECHNICAL ENGINEER Michael A. Novak
DATE APPROVED 07-JAN-2014
RESIDENT ENGINEER
STRUCTURE NAME B.I.N. 1016020
Rt. 20 / Kinderhook Creek, Rm 2161
SHEET 4 OF 4 HOLE DN-B-22

37

Figure 9-5. Geotechnical boring for BIN 1016020 (cont 3)

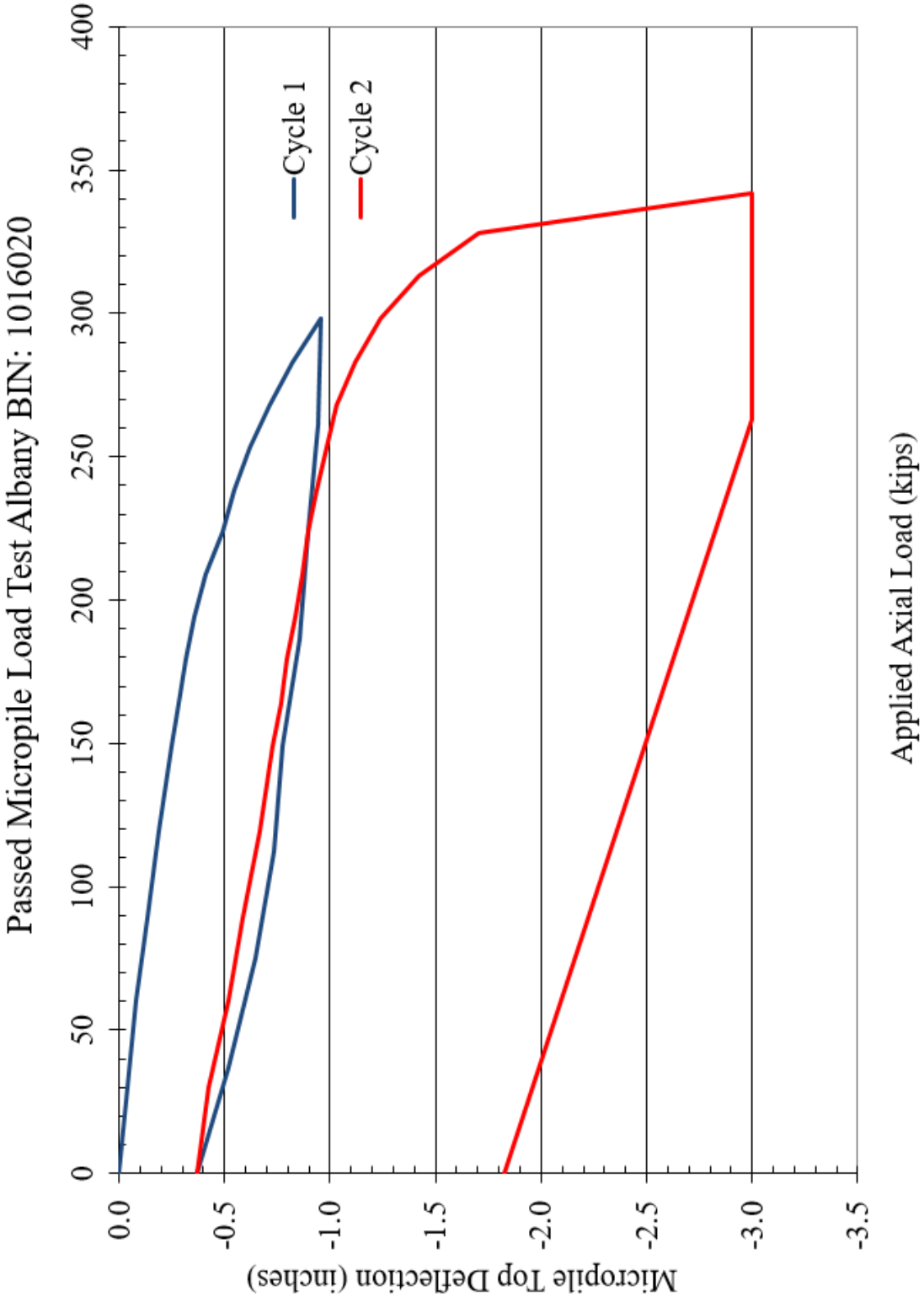

Figure 9-6. Micropile field load test results for BIN 1016020 with CLR = 0.48

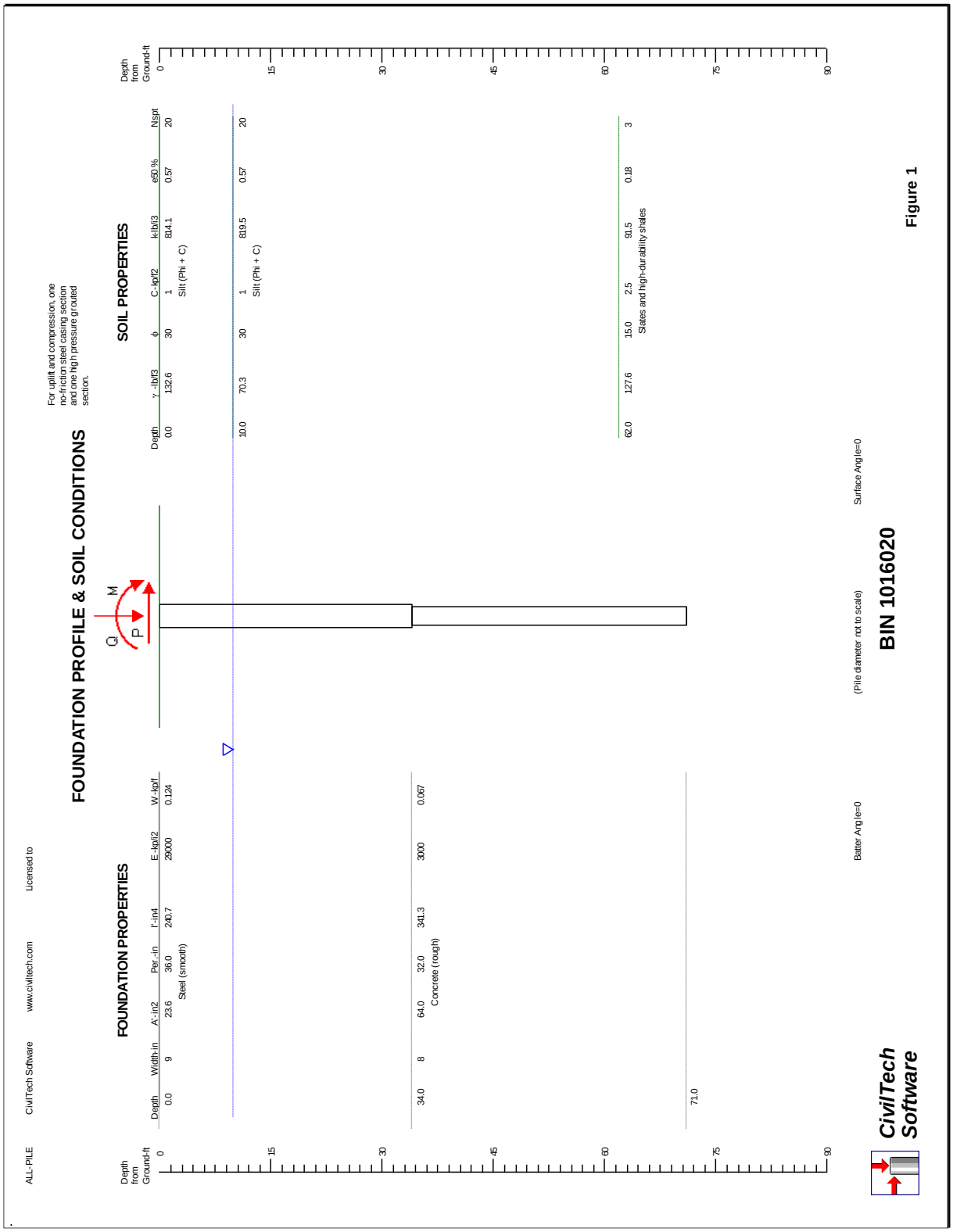

Figure 9-7. All-Pile design results for BIN 1016020

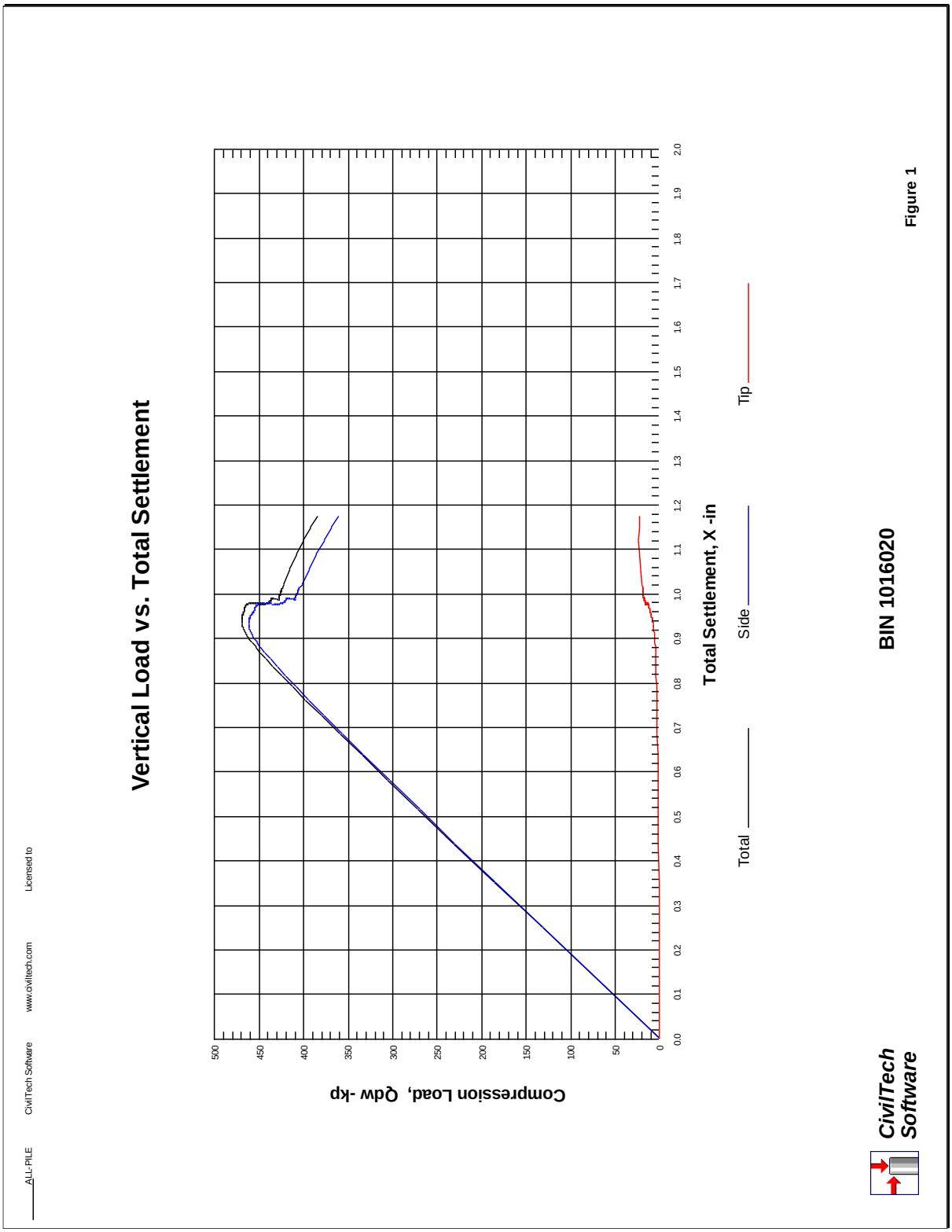

Figure 9-8. All-Pile design results for BIN 1016020 (cont 1)

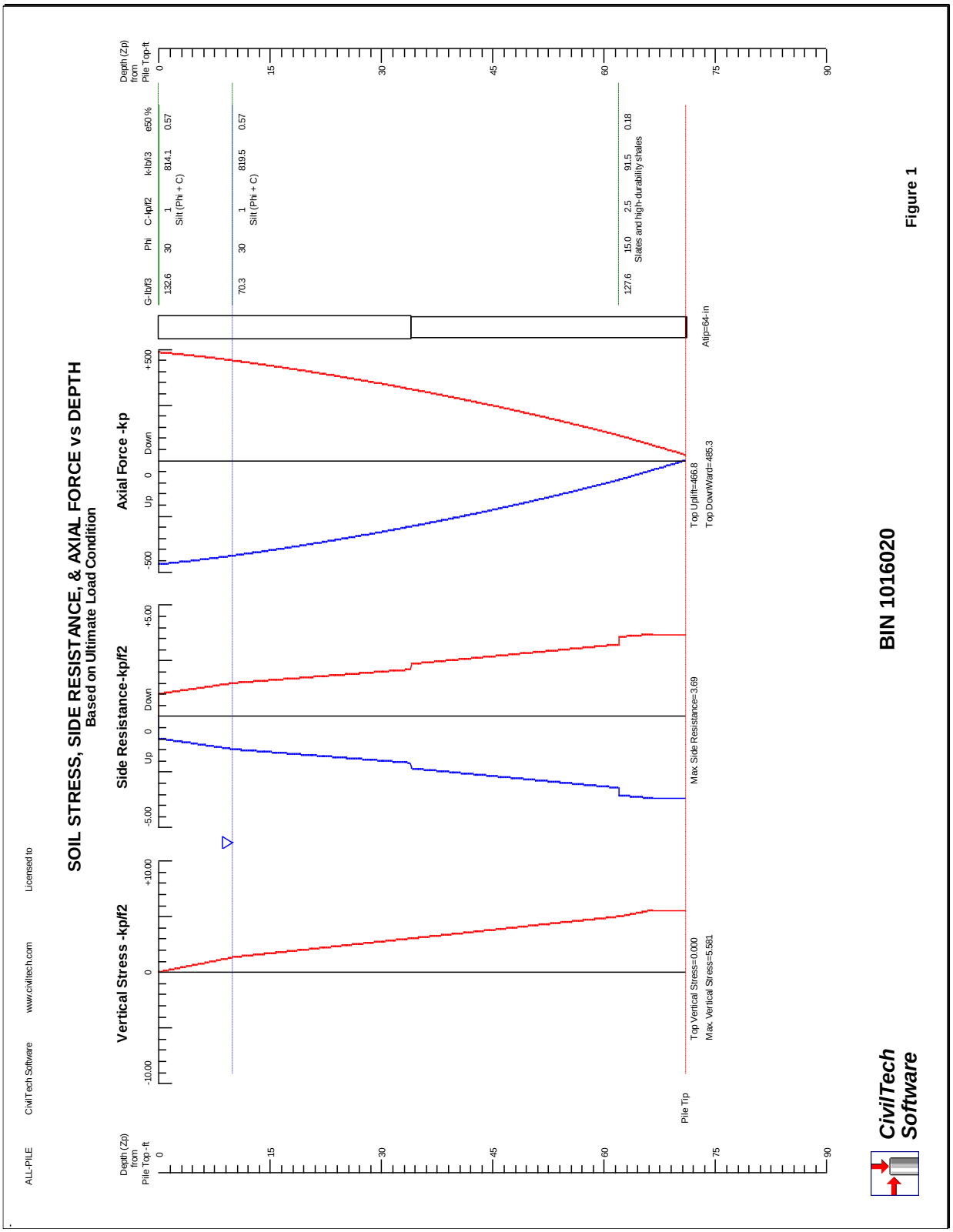

Figure 9-9. All-Pile design results for BIN 1016020 (cont 2)

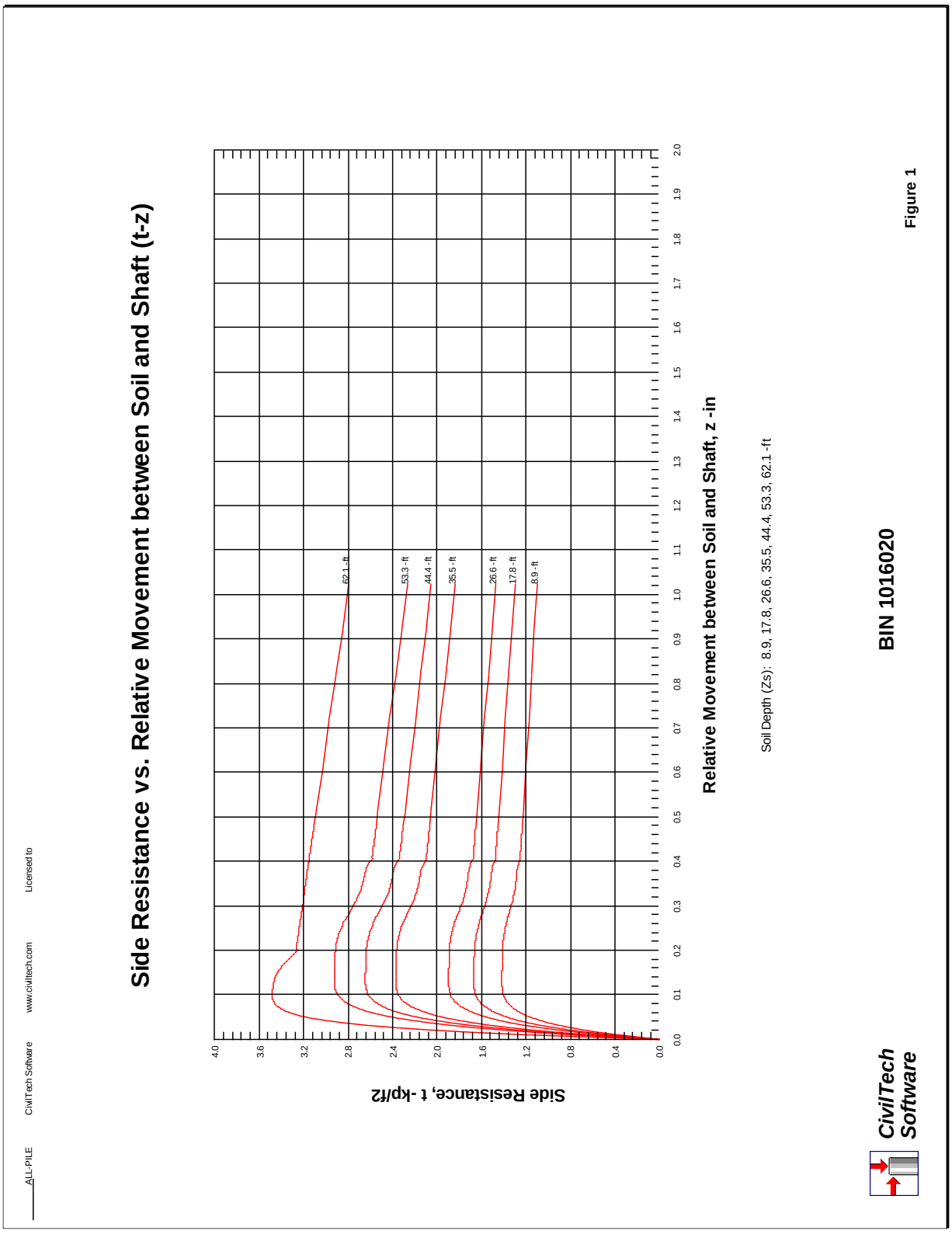

Figure 9-10. All-Pile design results for BIN 1016020 (cont 3)

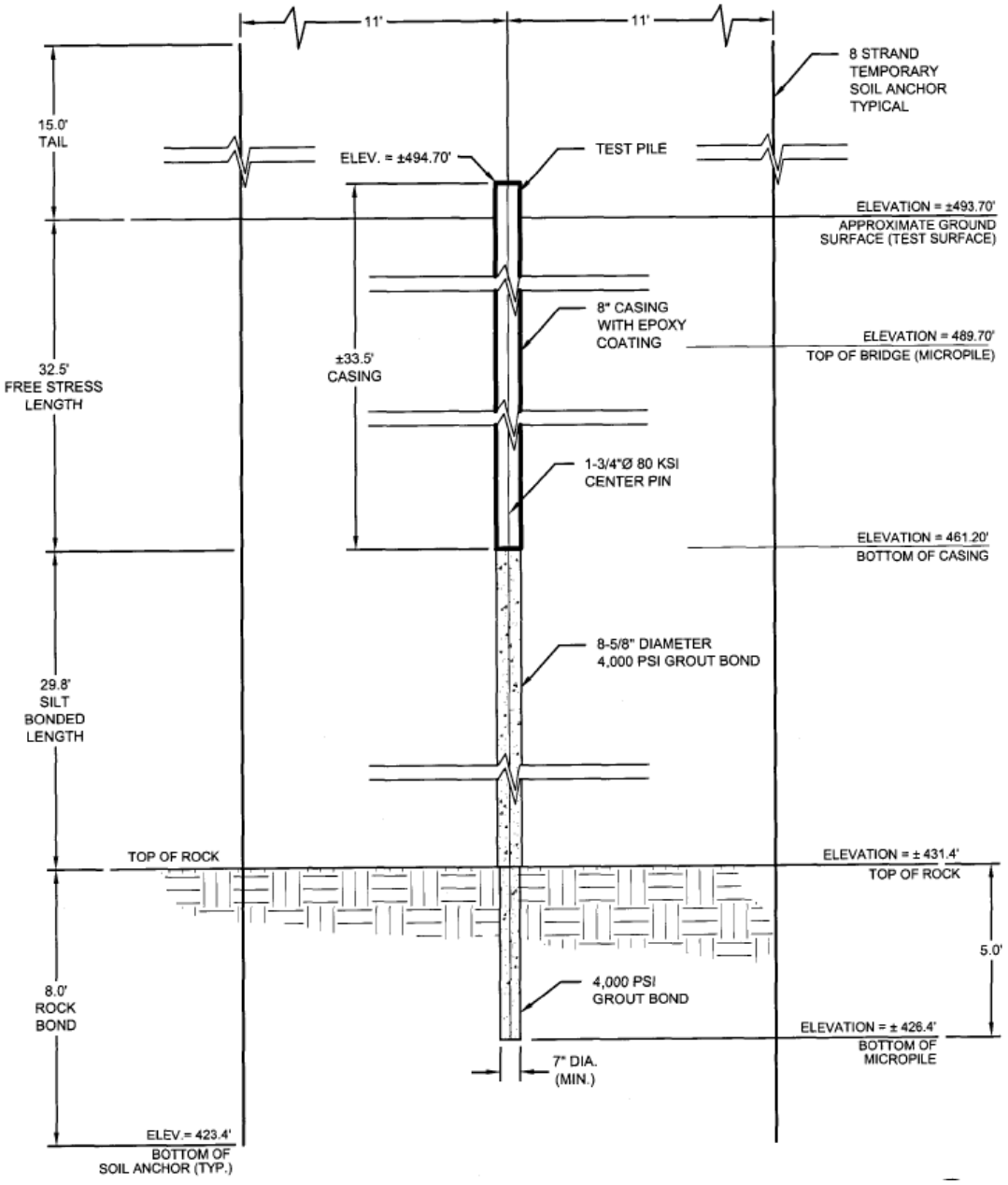

Figure 9-11. Test micropile layout for BIN 1016000

BRIDGE 1016000
BEGIN ABUTMENT

SM 282 E 12/02

STATE OF NEW YORK
DEPARTMENT OF TRANSPORTATION
GEOTECHNICAL ENGINEERING BUREAU
SUBSURFACE EXPLORATION LOG

PSN 11987 BORNUM 11
REGION 1
COUNTY RENSSELAER
PIN 1BOW.00.101
PROJECT CRITICAL BRIDGES OVER WATER PROGRAM
ACTUAL COORDINATES (N) 1,335,340.900 (E) 749,200.270 DATUM NAD83
DATE START 02-NOV-2013 DATE FINISH 05-NOV-2013

HOLE DN-B-18
LINE BL
STA
OFFSET ft
SURF. ELEV. 451.35
DEPTH TO WATER SEE NOTE

CASING O. D. 3 1/2 in I. D. 3 in WT OF HAMMER-CASING lb HAMMER FALL-CASING in
SAMPLER O. D. 2 in I. D. 1 3/8 in WT OF HAMMER-SAMPLER 140 lb HAMMER FALL-SAMPLER 30 in

CASING BLOWS/ft	DEPTH ft BELOW SURFACE	SAMPLE NO.	BLOWS ON SAMPLER in 0/6 6/12 12/18 18/24	MOIST. CONT. (%)	DESCRIPTION OF SOIL AND ROCK
	0.0				(0.00) Concrete
		J1	4 7 11	9%	(1.00) Brown Sandy GRAVEL ,Silty (W-NPL)
	5.0	J2	7 4 6	9%	(5.00) Brown Silty GRAVEL ,Sandy (M-NPL)
	10.0	J3	3 4 5	7%	(10.00) Brown Sandy GRAVEL ,Silty (W-NPL)
	15.0	J4	7 15 44	4%	(15.00) Brown/Gray Sandy GRAVEL ,Silty (W-NPL)
		B1			(16.50) Run #1 Drilled from 16'6" To 20'0" BOULDER REC. 20.4" 48.6% 5 Pieces and cobbles NW SINGLE TUBE
	20.0	J5	29 22 30	8%	(20.00) Red-Brown Gravelly SILT ,Sandy (W-NPL)
		B2			(21.50) Run #2 Drilled from 21'6" To 25'0" BOULDER REC. 13.2" 31.4% 6 Pieces and frags NW SINGLE TUBE
	25.0				

TOP OF MICROPILE EL. 440.50

8" CASING 20.7' TOTAL

The subsurface information shown here was obtained for design and estimate purposes. It is made available so that users may have access to the same information available to the State. It is presented in good faith. By the nature of the exploration process, the information represents only a small fraction of the total volume of the material at the site. Interpolation between data samples may not be indicative of the actual material encountered.

CONTRACT CONTRACTOR

DRILL RIG OPERATOR D.Okosky
SOIL & ROCK DESCRIPTION H.MacNeil
REG GEOTECHNICAL ENGINEER Michael A. Novak
DATE APPROVED 07-JAN-2014
RESIDENT ENGINEER
STRUCTURE NAME B.I.N. 1016000
RT. 20 / KINDERHOOK CREEK RM 2152
SHEET 1 OF 4 HOLE DN-B-18

29

Figure 9-12. Geotechnical boring for BIN 1016000

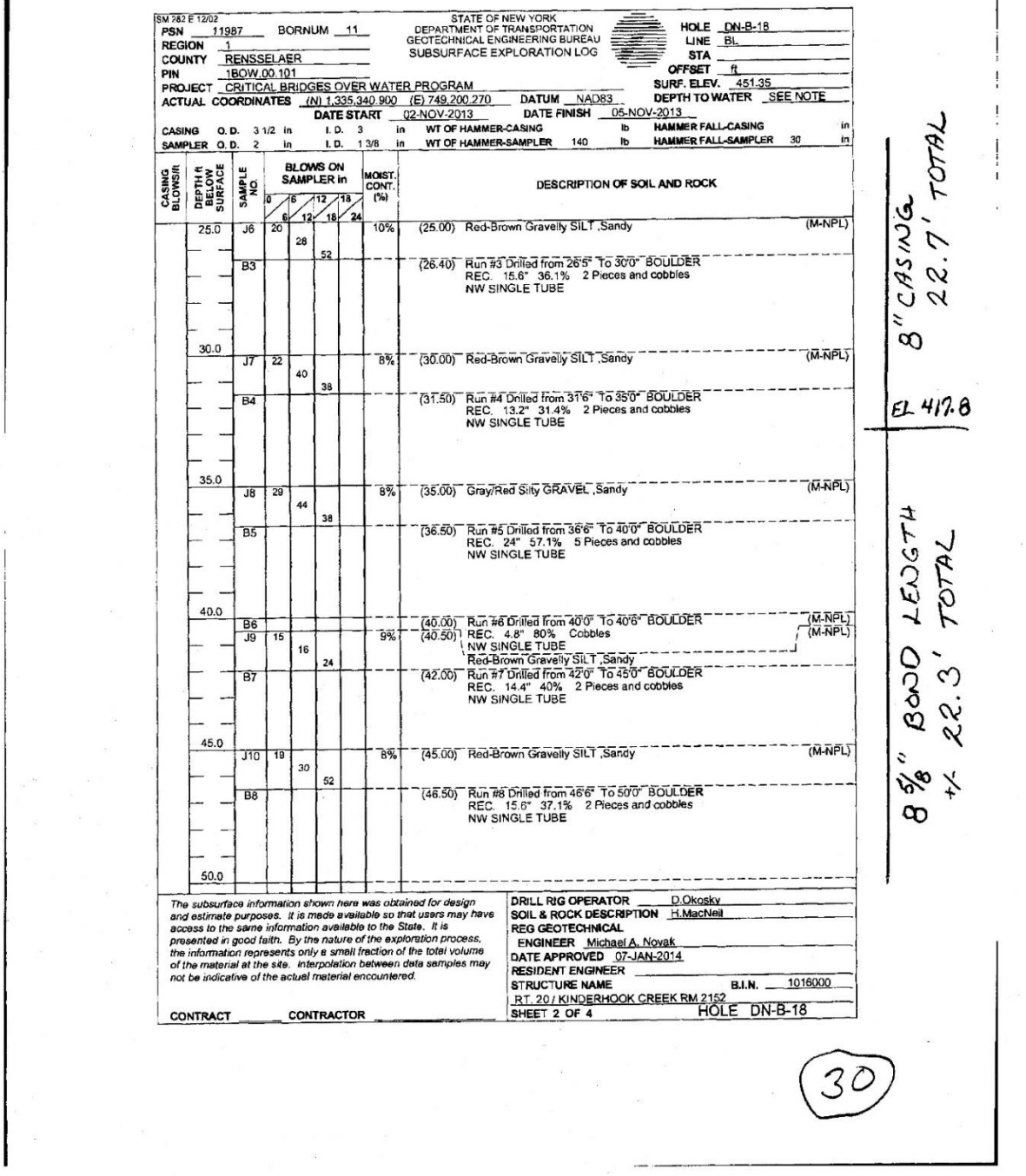

STATE OF NEW YORK
DEPARTMENT OF TRANSPORTATION
GEOTECHNICAL ENGINEERING BUREAU
SUBSURFACE EXPLORATION LOG

SM 783 E 12/02

PSN 11987 BORNUM 11
REGION 1
COUNTY RENSSELAER
PIN 1BOW.00.101
PROJECT CRITICAL BRIDGES OVER WATER PROGRAM
ACTUAL COORDINATES (N) 1,335,340.900 (E) 749,200.270 DATUM NAD83
DATE START 02-NOV-2013 DATE FINISH 05-NOV-2013

HOLE DN-B-18
LINE BL
STA
OFFSET ft
SURF. ELEV. 451.35
DEPTH TO WATER SEE NOTE

CASING O. D. 3 1/2 in I. D. 3 in WT OF HAMMER-CASING lb HAMMER FALL-CASING in
SAMPLER O. D. 2 in I. D. 1 3/8 in WT OF HAMMER-SAMPLER 140 lb HAMMER FALL-SAMPLER 30 in

CASING BLOWS/ft	DEPTH ft BELOW SURFACE	SAMPLE NO.	BLOWS ON SAMPLER in 0-6 / 6-12 / 12-18 / 18-24	MOIST. CONT. (%)	DESCRIPTION OF SOIL AND ROCK
	25.0	J6	20 / 28 / 52	10%	(25.00) Red-Brown Gravelly SILT ,Sandy (M-NPL)
		B3			(26.40) Run #3 Drilled from 26'6" To 30'0" BOULDER REC. 15.6" 36.1% 2 Pieces and cobbles NW SINGLE TUBE
	30.0	J7	22 / 40 / 38	8%	(30.00) Red-Brown Gravelly SILT ,Sandy (M-NPL)
		B4			(31.50) Run #4 Drilled from 31'6" To 35'0" BOULDER REC. 13.2" 31.4% 2 Pieces and cobbles NW SINGLE TUBE
	35.0	J8	29 / 44 / 38	8%	(35.00) Gray/Red Silty GRAVEL ,Sandy (M-NPL)
		B5			(36.50) Run #5 Drilled from 36'6" To 40'0" BOULDER REC. 24" 57.1% 5 Pieces and cobbles NW SINGLE TUBE
	40.0	B6			(40.00) Run #6 Drilled from 40'0" To 40'6" BOULDER (M-NPL)
		J9	15 / 16 / 24	9%	(40.50) REC. 4.8" 80% Cobbles (M-NPL) NW SINGLE TUBE Red-Brown Gravelly SILT ,Sandy
		B7			(42.00) Run #7 Drilled from 42'0" To 45'0" BOULDER REC. 14.4" 40% 2 Pieces and cobbles NW SINGLE TUBE
	45.0	J10	19 / 30 / 52	8%	(45.00) Red-Brown Gravelly SILT ,Sandy (M-NPL)
		B8			(46.50) Run #8 Drilled from 46'6" To 50'0" BOULDER REC. 15.6" 37.1% 2 Pieces and cobbles NW SINGLE TUBE
	50.0				

8" CASING 22.7' TOTAL
EL 417.8
8 5/8" BOND LENGTH +/- 22.3' TOTAL

The subsurface information shown here was obtained for design and estimate purposes. It is made available so that users may have access to the same information available to the State. It is presented in good faith. By the nature of the exploration process, the information represents only a small fraction of the total volume of the material at the site. Interpolation between data samples may not be indicative of the actual material encountered.

CONTRACT CONTRACTOR

DRILL RIG OPERATOR D.Okosky
SOIL & ROCK DESCRIPTION H.MacNeil
REG GEOTECHNICAL ENGINEER Michael A. Novak
DATE APPROVED 07-JAN-2014
RESIDENT ENGINEER
STRUCTURE NAME B.I.N. 1016000
RT. 20 / KINDERHOOK CREEK RM 2152
SHEET 2 OF 4 HOLE DN-B-18

30

Figure 9-13. Geotechnical boring for BIN 1016000 (cont 1)

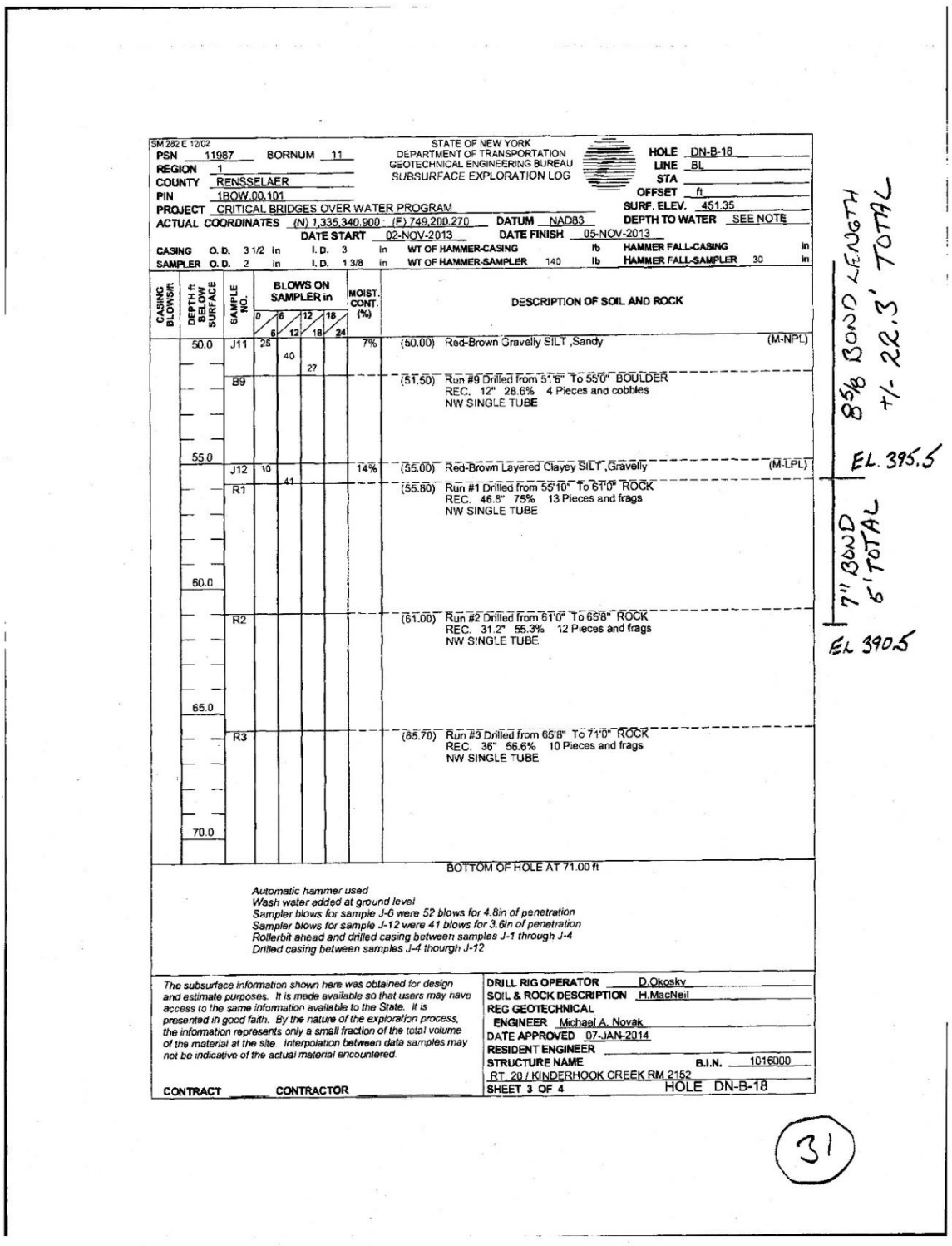

SM 282 E 12/02

STATE OF NEW YORK
DEPARTMENT OF TRANSPORTATION
GEOTECHNICAL ENGINEERING BUREAU
SUBSURFACE EXPLORATION LOG

PSN 11987 BORNUM 11
REGION 1
COUNTY RENSSELAER
PIN 1BOW.00.101
PROJECT CRITICAL BRIDGES OVER WATER PROGRAM
ACTUAL COORDINATES (N) 1,335,340.900 (E) 749,200.270 DATUM NAD83
DATE START 02-NOV-2013 DATE FINISH 05-NOV-2013

HOLE DN-B-18
LINE BL
STA
OFFSET ft
SURF. ELEV. 451.35
DEPTH TO WATER SEE NOTE

CASING O. D. 3 1/2 in I. D. 3 in WT OF HAMMER-CASING lb HAMMER FALL-CASING in
SAMPLER O. D. 2 in I. D. 1 3/8 in WT OF HAMMER-SAMPLER 140 lb HAMMER FALL-SAMPLER 30 in

CASING BLOWS/ft	DEPTH ft BELOW SURFACE	SAMPLE NO.	BLOWS ON SAMPLER in 0/6 6/12 12/18 18/24	MOIST. CONT. (%)	DESCRIPTION OF SOIL AND ROCK
	50.0	J11	25 40 27	7%	(50.00) Red-Brown Gravelly SILT ,Sandy (M-NPL)
		B9			(51.50) Run #9 Drilled from 51'6" To 55'0" BOULDER REC. 12" 28.6% 4 Pieces and cobbles NW SINGLE TUBE
	55.0	J12	10 41	14%	(55.00) Red-Brown Layered Clayey SILT ,Gravelly (M-LPL)
		R1			(55.80) Run #1 Drilled from 55'10" To 61'0" ROCK REC. 46.8" 75% 13 Pieces and frags NW SINGLE TUBE
	60.0	R2			(61.00) Run #2 Drilled from 61'0" To 65'8" ROCK REC. 31.2" 55.3% 12 Pieces and frags NW SINGLE TUBE
	65.0	R3			(65.70) Run #3 Drilled from 65'8" To 71'0" ROCK REC. 36" 56.6% 10 Pieces and frags NW SINGLE TUBE
	70.0				

BOTTOM OF HOLE AT 71.00 ft

Automatic hammer used
Wash water added at ground level
Sampler blows for sample J-6 were 52 blows for 4.8in of penetration
Sampler blows for sample J-12 were 41 blows for 3.6in of penetration
Rollerbit ahead and drilled casing between samples J-1 through J-4
Drilled casing between samples J-4 thourgh J-12

The subsurface information shown here was obtained for design and estimate purposes. It is made available so that users may have access to the same information available to the State. It is presented in good faith. By the nature of the exploration process, the information represents only a small fraction of the total volume of the material at the site. Interpolation between data samples may not be indicative of the actual material encountered.

CONTRACT CONTRACTOR

DRILL RIG OPERATOR D.Okosky
SOIL & ROCK DESCRIPTION H.MacNeil
REG GEOTECHNICAL ENGINEER Michael A. Novak
DATE APPROVED 07-JAN-2014
RESIDENT ENGINEER
STRUCTURE NAME B.I.N. 1016000
RT. 20 / KINDERHOOK CREEK RM 2152
SHEET 3 OF 4 HOLE DN-B-18

8⅝ BOND LENGTH +/- 22.3' TOTAL
EL. 395.5
7" BOND 5' TOTAL
EL 390.5

31

Figure 9-14. Geotechnical boring for BIN 1016000 (cont 2)

SM 282 E 12/02

PSN 11987 BORNUM 11

REGION 1

COUNTY RENSSELAER

PIN 1BOW.00.101

PROJECT CRITICAL BRIDGES OVER WATER PROGRAM

ACTUAL COORDINATES (N) 1,335,340.900 (E) 749,200.270 DATUM NAD83

DATE START 02-NOV-2013 DATE FINISH 05-NOV-2013

STATE OF NEW YORK
DEPARTMENT OF TRANSPORTATION
GEOTECHNICAL ENGINEERING BUREAU
SUBSURFACE EXPLORATION LOG

HOLE DN-B-18

LINE BL

STA

OFFSET ft

SURF. ELEV. 451.35

DEPTH TO WATER SEE NOTE

CASING	O. D.	3 1/2	in	I. D.	3	in	WT OF HAMMER-CASING	lb	HAMMER FALL-CASING	in
SAMPLER	O. D.	2	in	I. D.	1 3/8	in	WT OF HAMMER-SAMPLER 140	lb	HAMMER FALL-SAMPLER 30	in

CASING BLOWS/ft	DEPTH ft BELOW SURFACE	SAMPLE NO.	BLOWS ON SAMPLER in (0-6 / 6-12 / 12-18 / 18-24)	MOIST. CONT. (%)	DESCRIPTION OF SOIL AND ROCK

Driller noted rollerbit ahead to 16.5ft would not progress switched to NWST casing

~~*Driller noted refusal at 55.8ft*~~

DATE	TIME	DEPTH ft HOLE	DEPTH ft CASING	DEPTH ft WATER	ARTESIAN HEAD HEIGHT ABOVE GROUND	FILLED WITH WATER AT END OF DAY
04-Nov-13	07:45	36.50	35.50	18.00		
05-Nov-13	07:32	61.00	55.50	17.40		

The subsurface information shown here was obtained for design and estimate purposes. It is made available so that users may have access to the same information available to the State. It is presented in good faith. By the nature of the exploration process, the information represents only a small fraction of the total volume of the material at the site. Interpolation between data samples may not be indicative of the actual material encountered.

CONTRACT CONTRACTOR

DRILL RIG OPERATOR D.Okosky

SOIL & ROCK DESCRIPTION H.MacNeil

REG GEOTECHNICAL ENGINEER Michael A. Novak

DATE APPROVED 07-JAN-2014

RESIDENT ENGINEER

STRUCTURE NAME B.I.N. 1016000

RT. 20 / KINDERHOOK CREEK RM 2152

SHEET 4 OF 4 HOLE DN-B-18

32

Figure 9-15. Geotechnical boring for BIN 1016000 (cont 3)

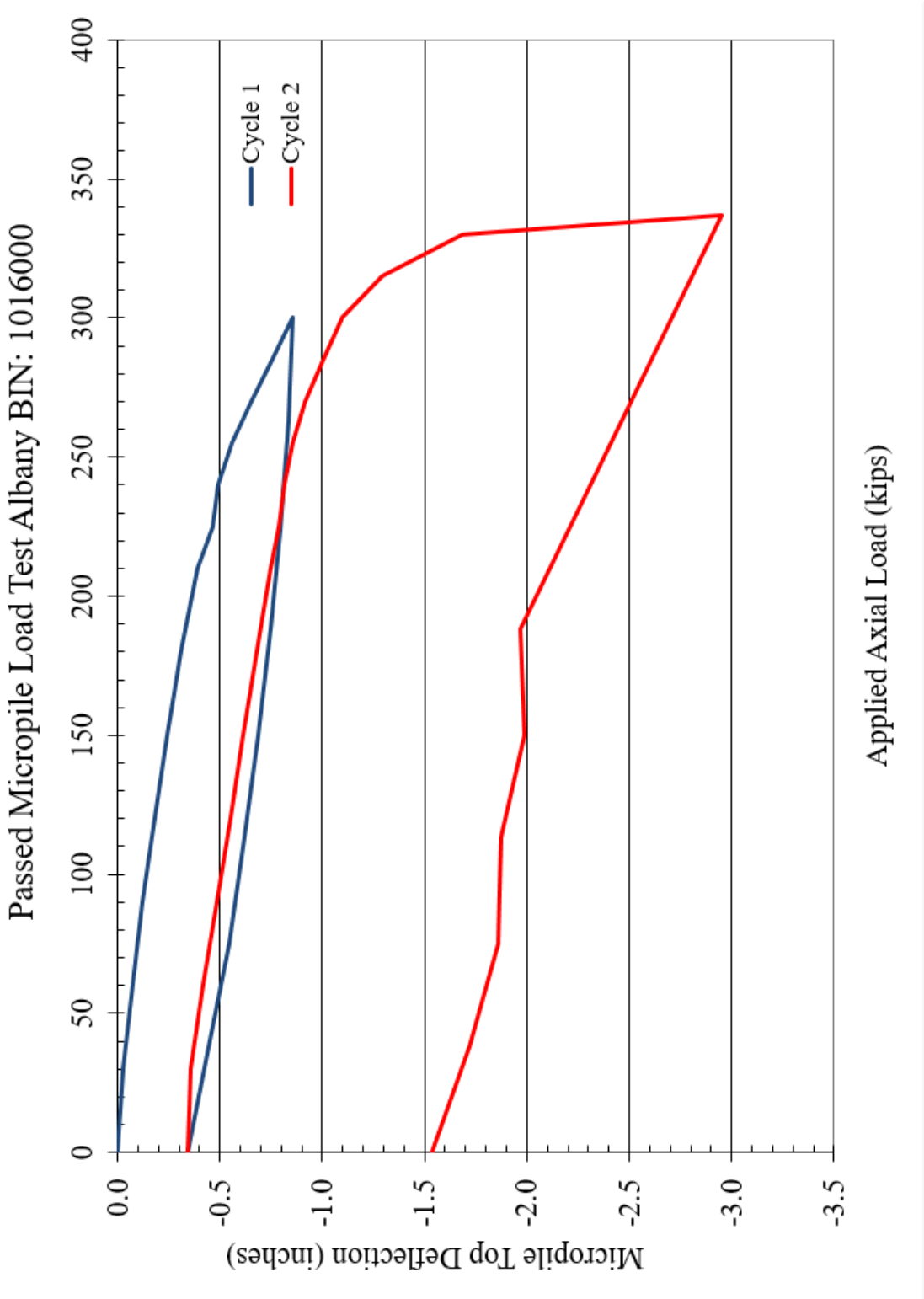

Figure 9-16. Micropile field load test results for BIN 1016000 with CLR = 0.46

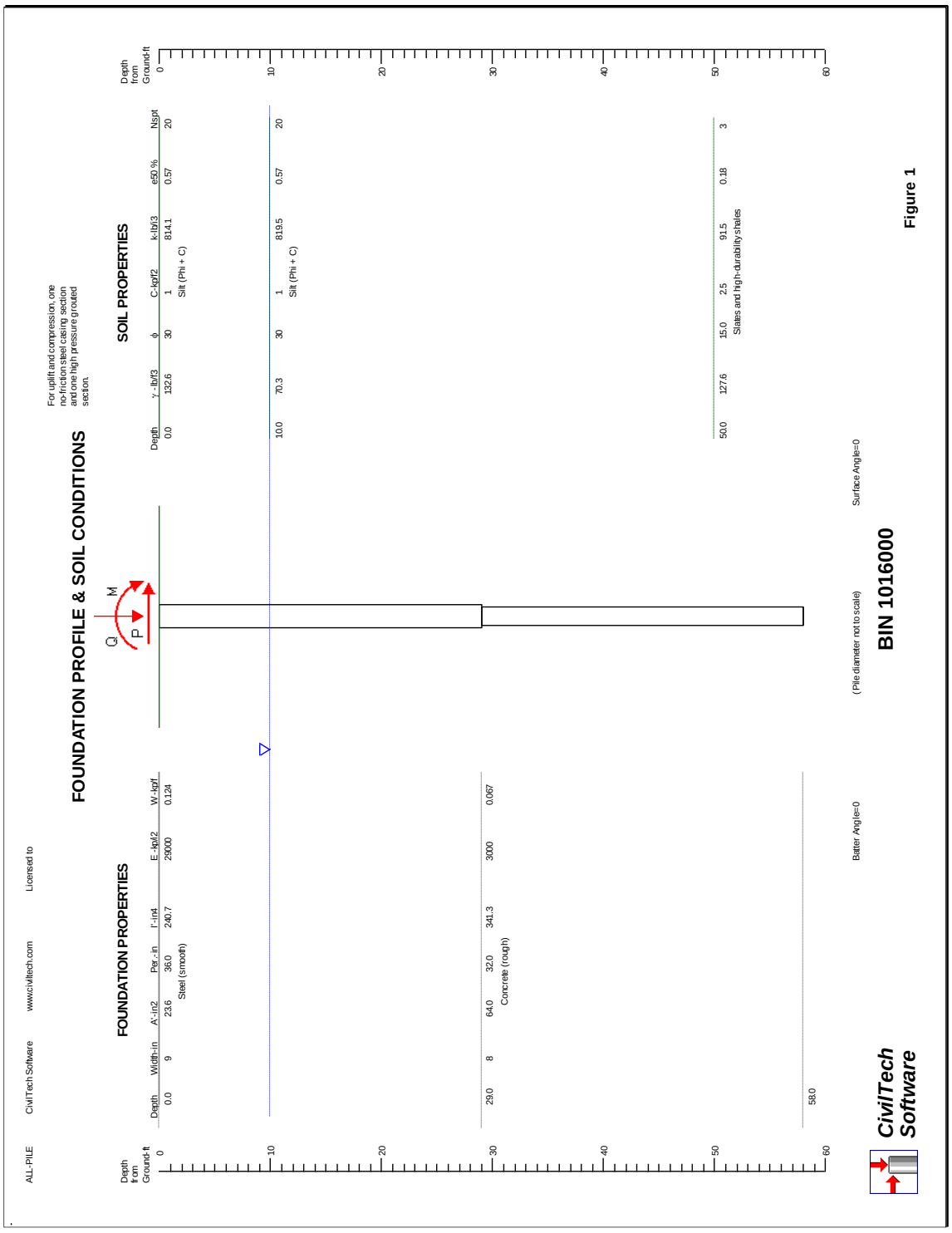

Figure 9-17. All-Pile design results for BIN 1016000

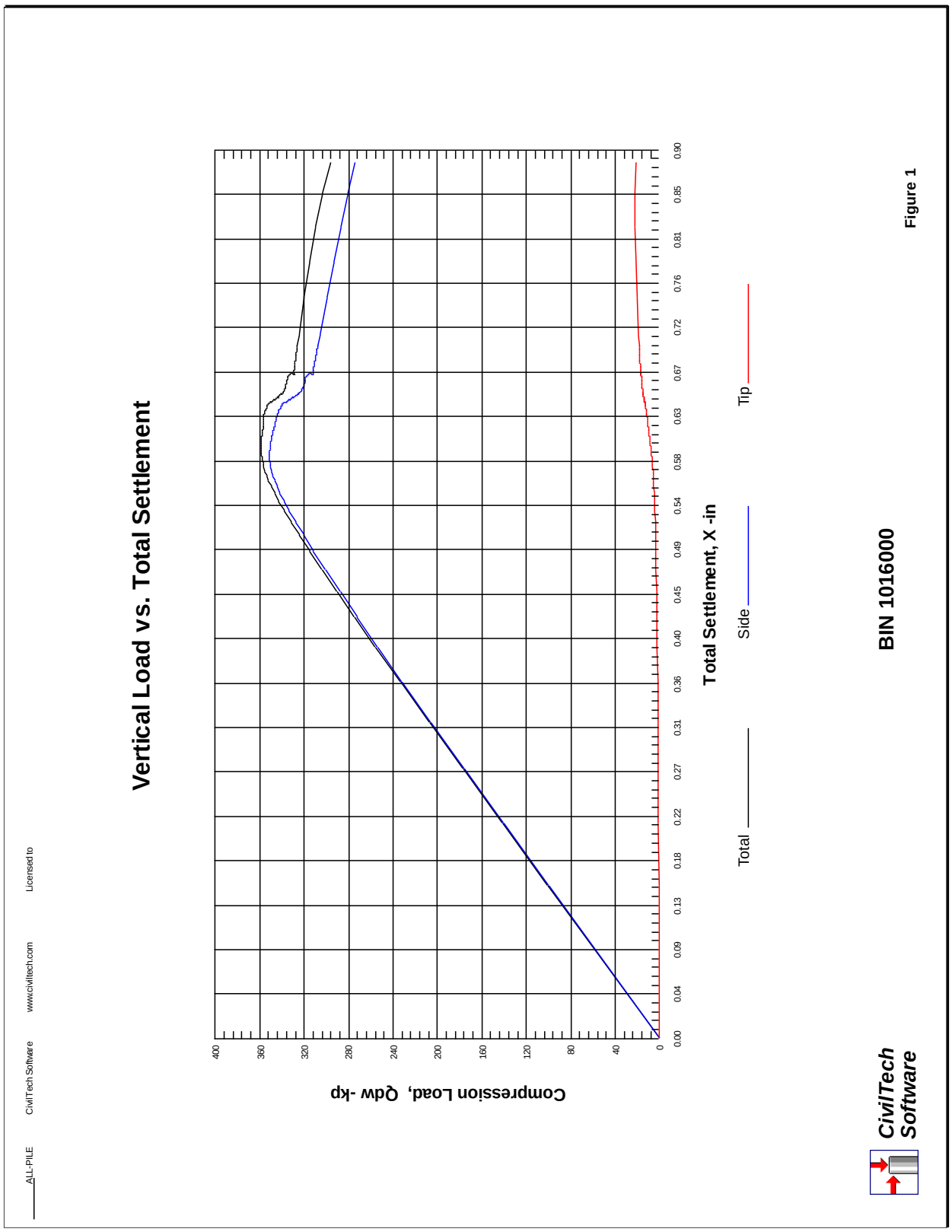

Figure 9-18. All-Pile design results for BIN 1016000 (cont 1)

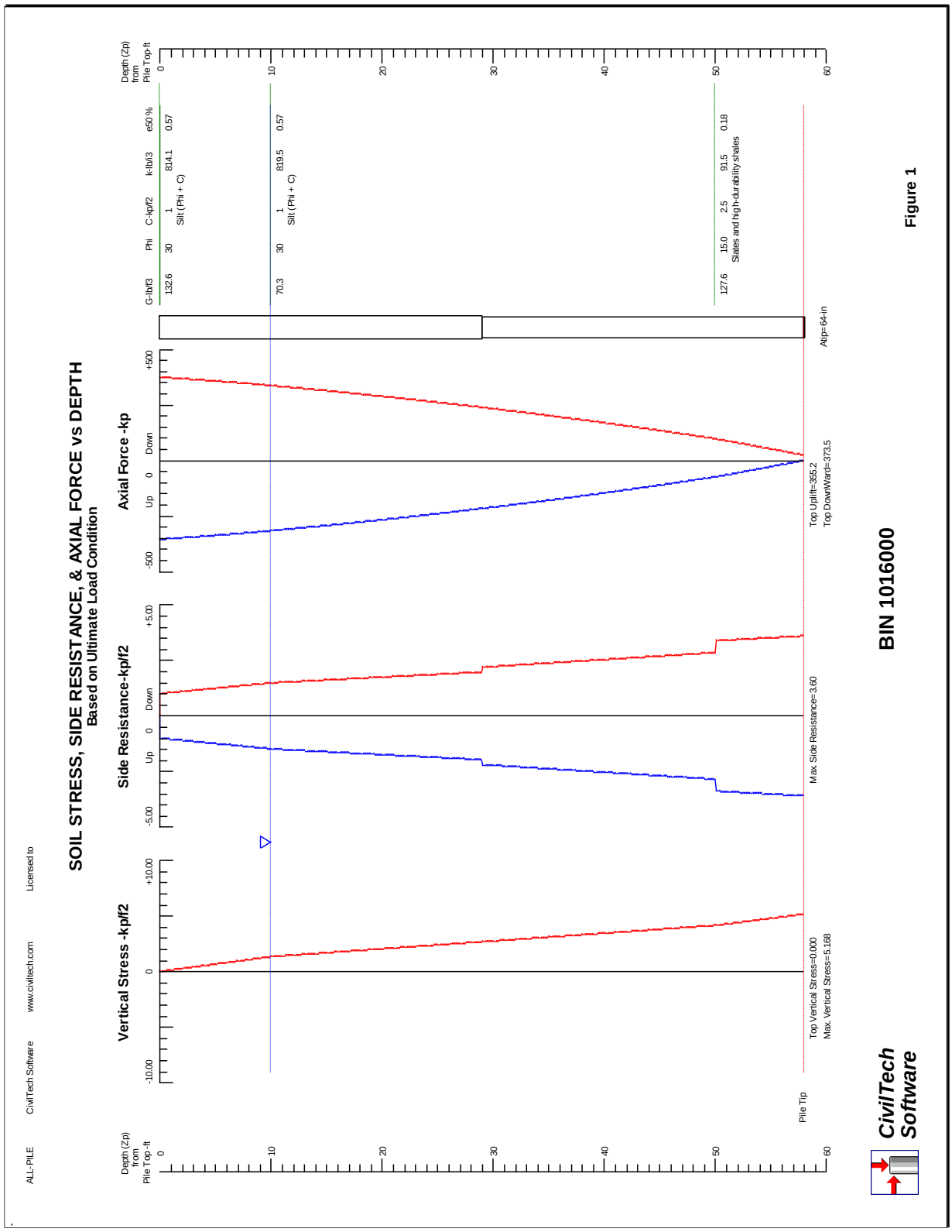

Figure 9-19. All-Pile design results for BIN 1016000 (cont 2)

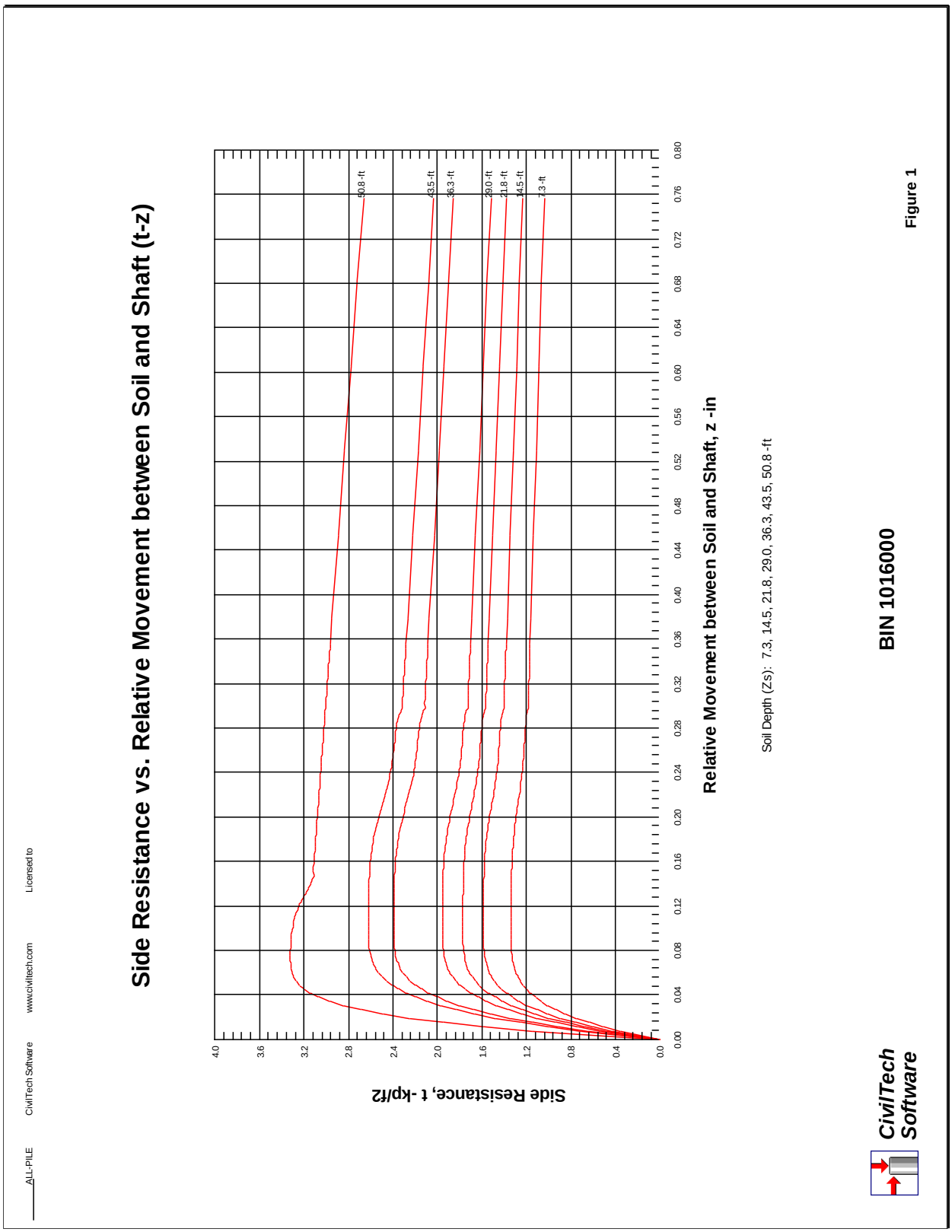

Figure 9-20. All-Pile design results for BIN 1016000 (cont 3)

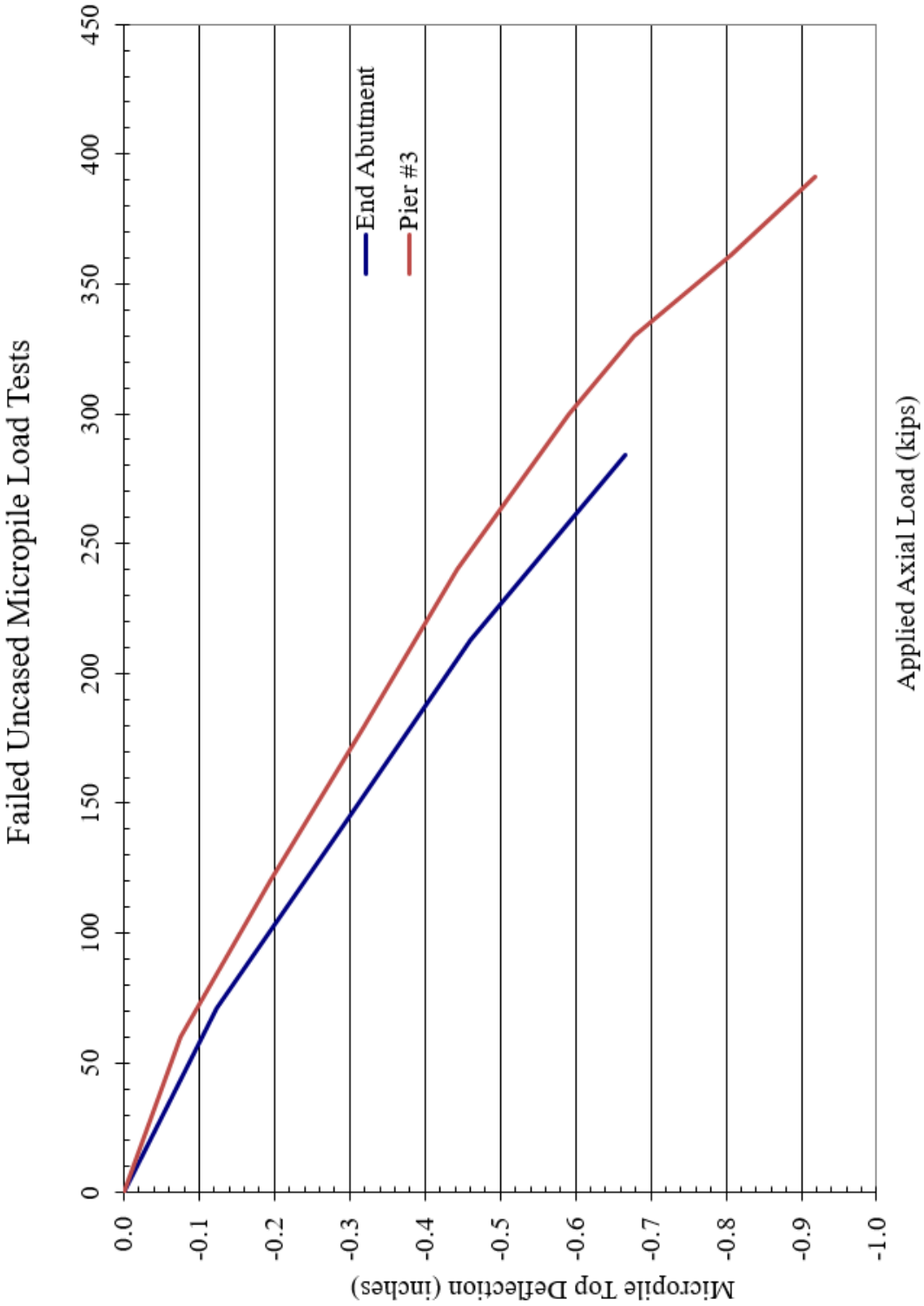

Figure 9-21. Failed high capacity micropile load tests with CLR = 0

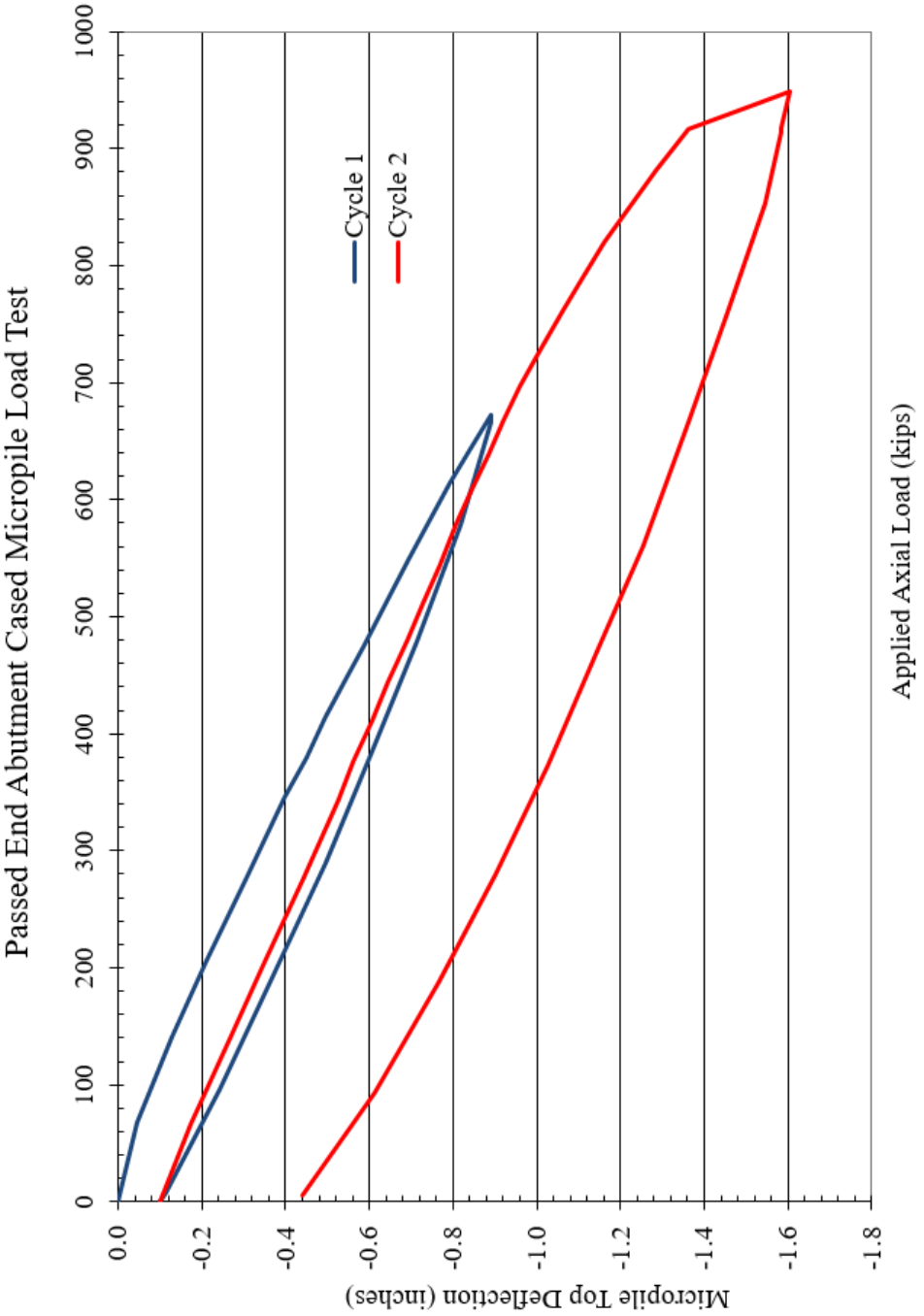

Figure 9-22. End abutment passed micropile load test with CLR = 0.71

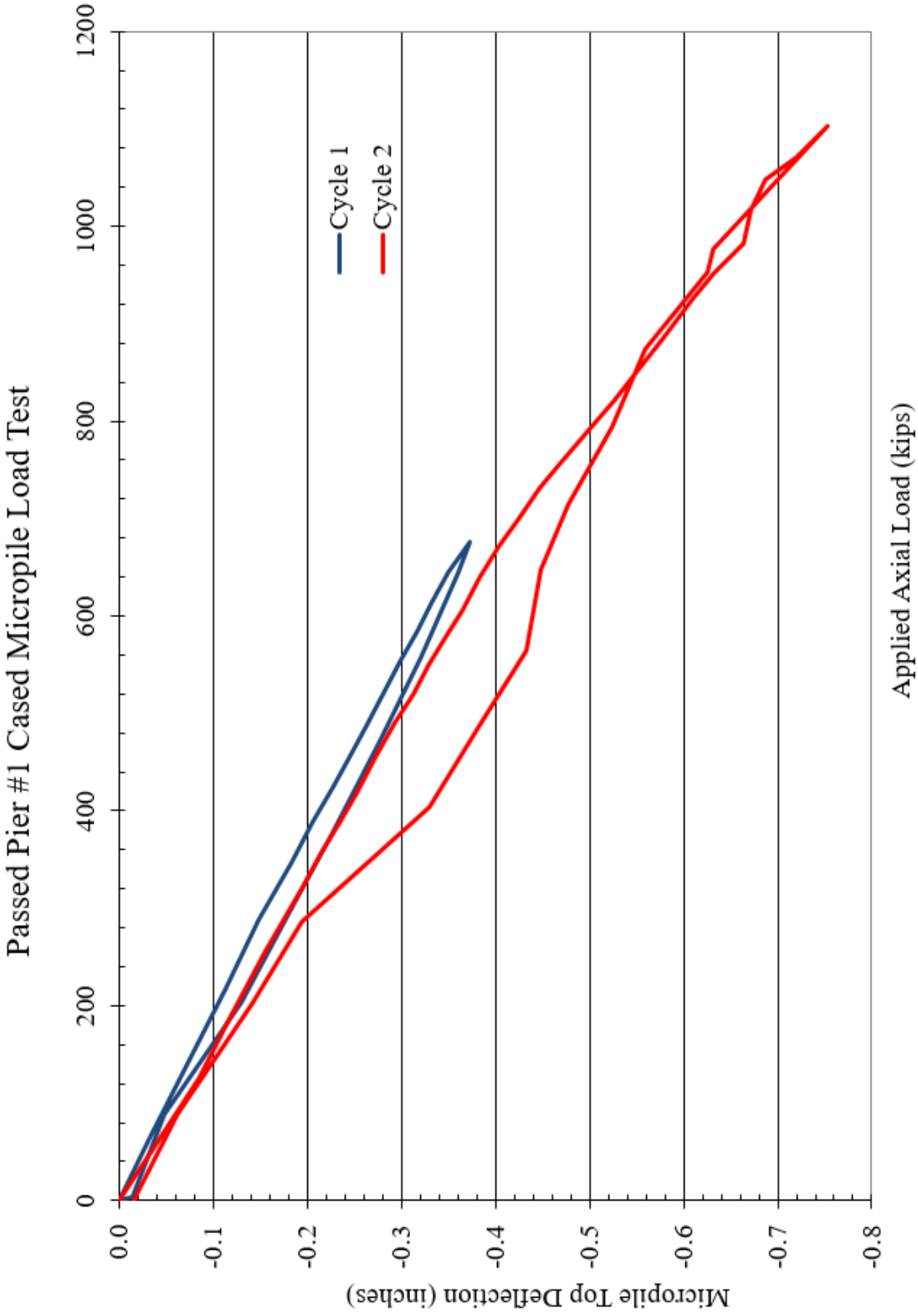

Figure 9-23. Pier passed micropile load test with CLR = 0.5

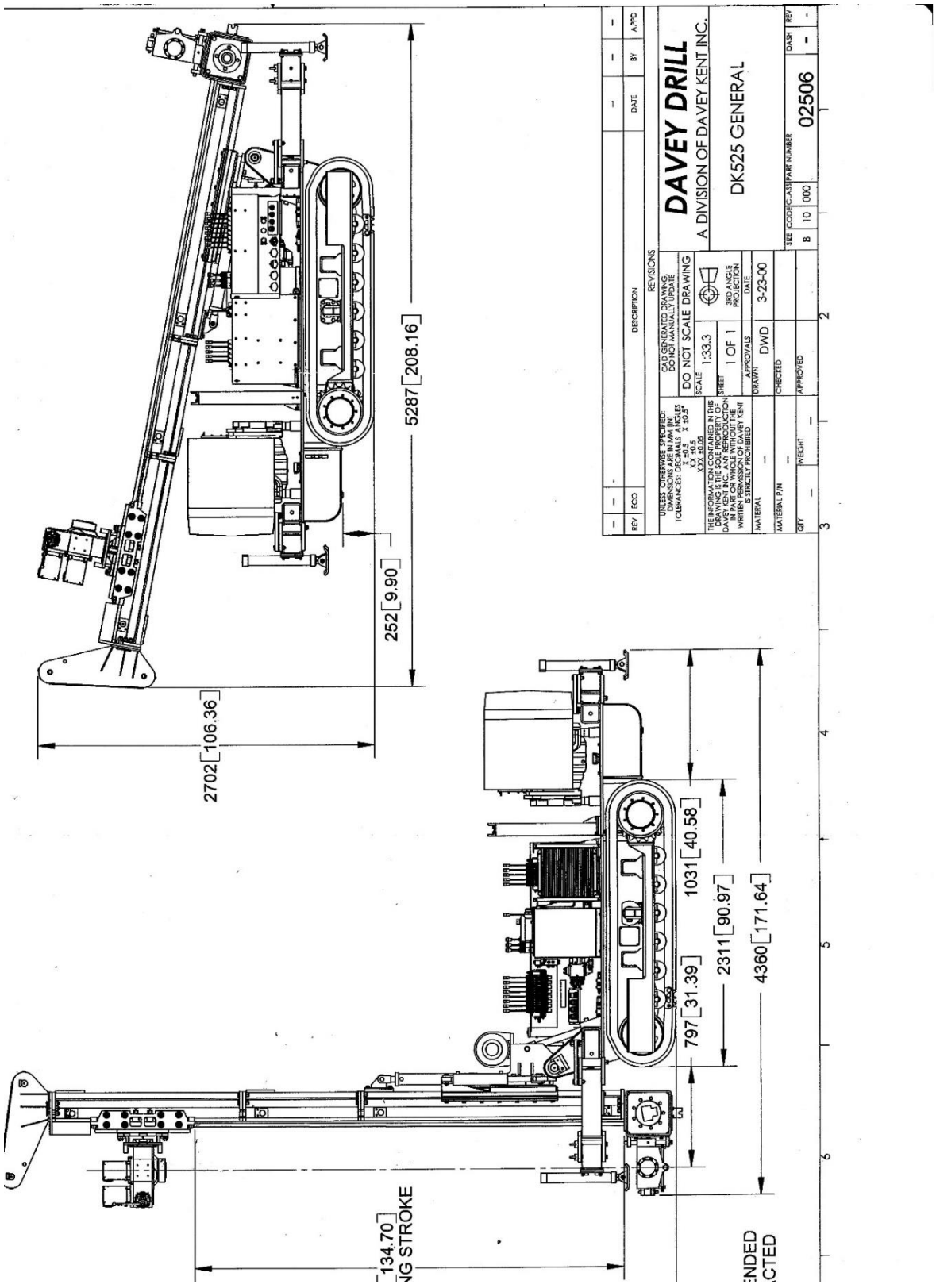

Figure 9-24. Typical micropile drill rig

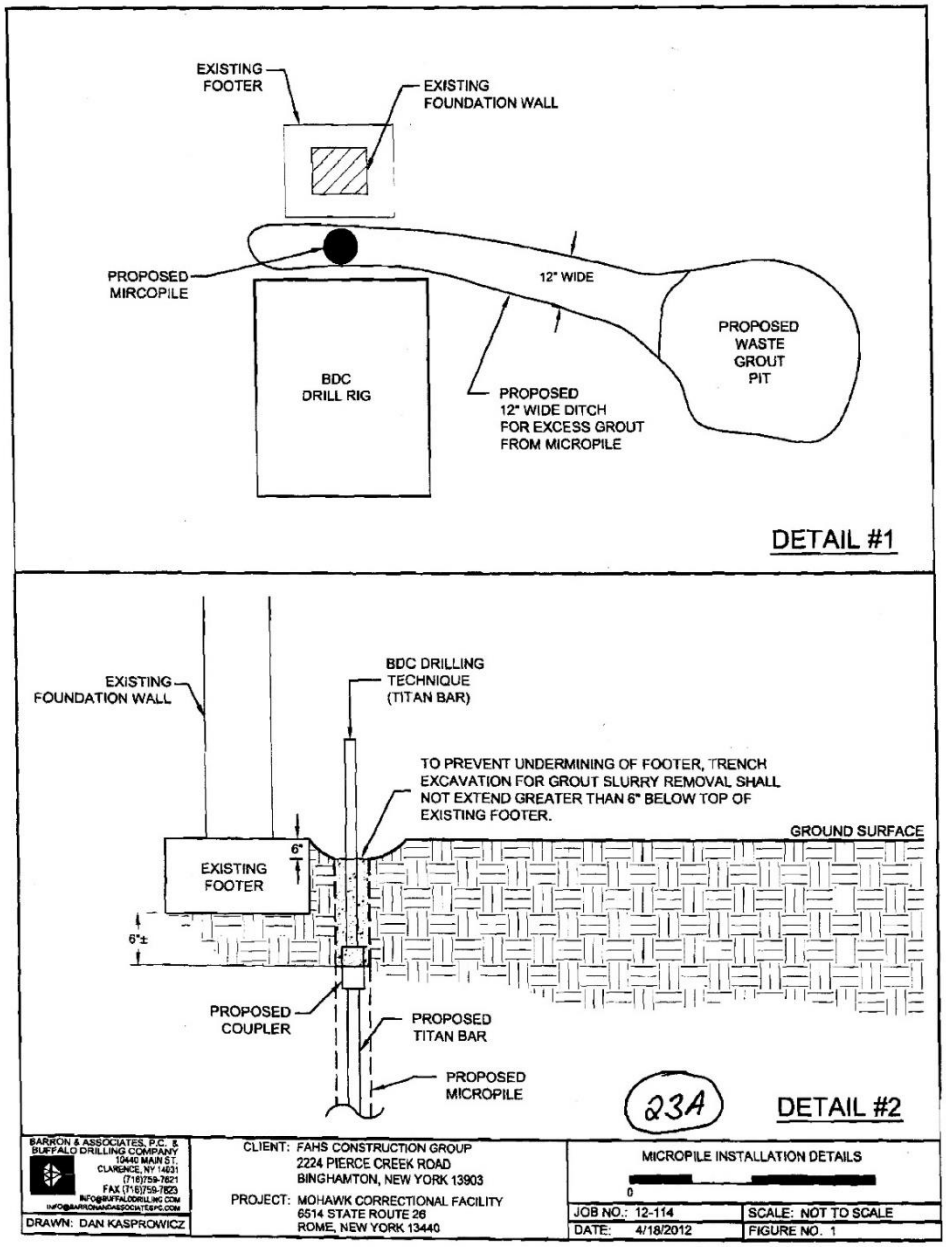

Figure 9-25. Micropile retrofit procedure

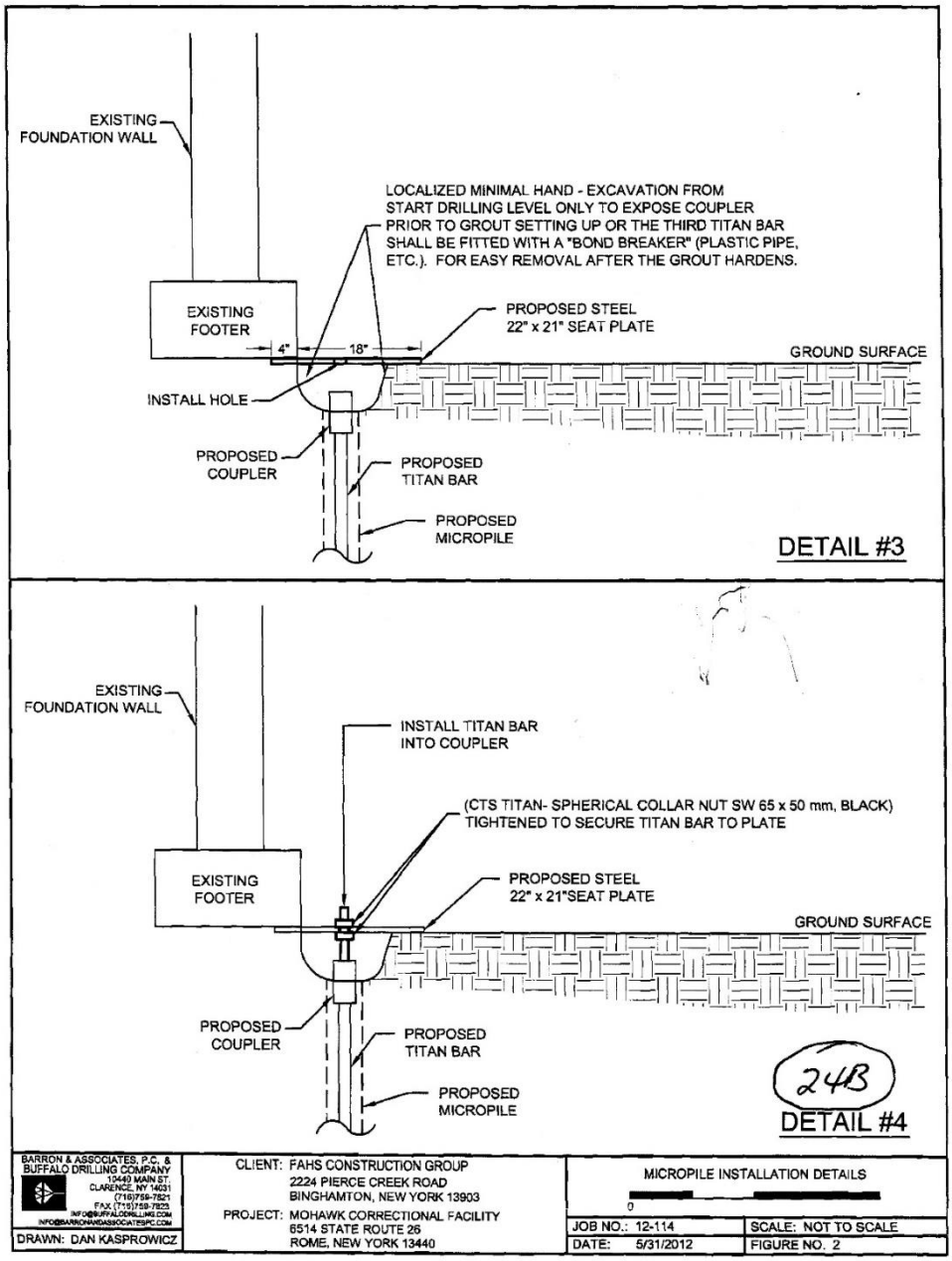

Figure 9-26. Micropile retrofit procedure (cont 1)

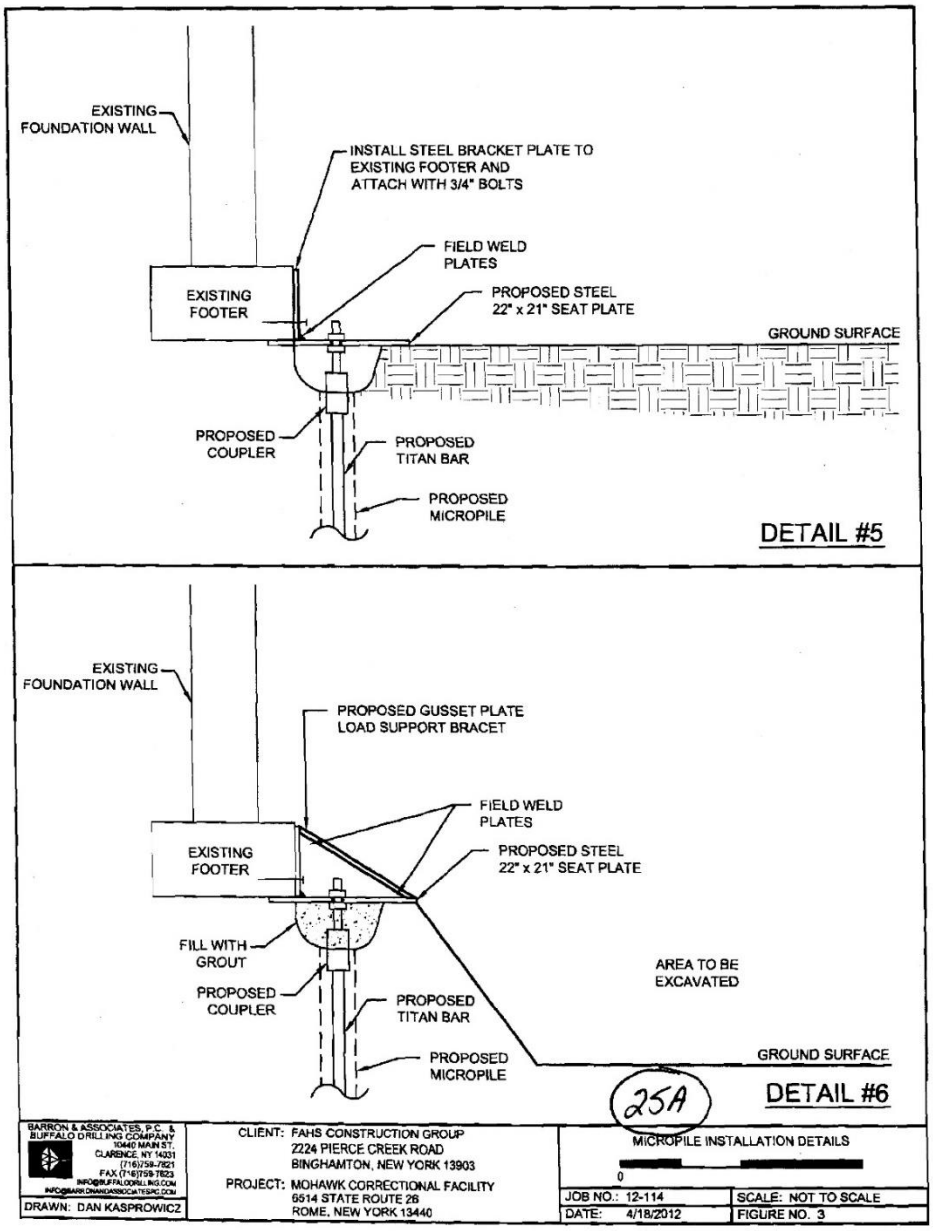

Figure 9-27. Micropile retrofit procedure (cont 2)

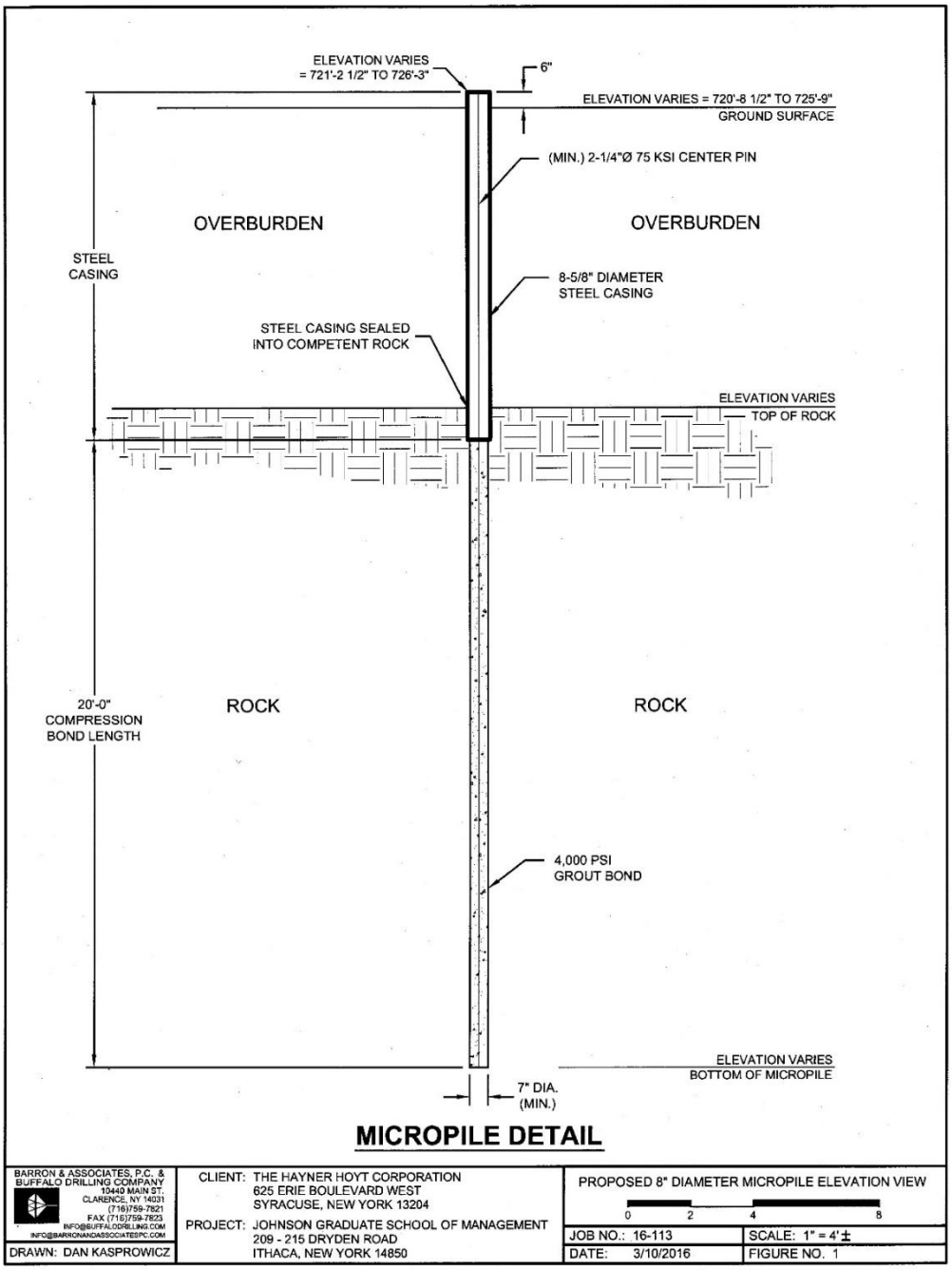

Figure 9-28. High capacity micropile design example with a CLR varying with rock elevation

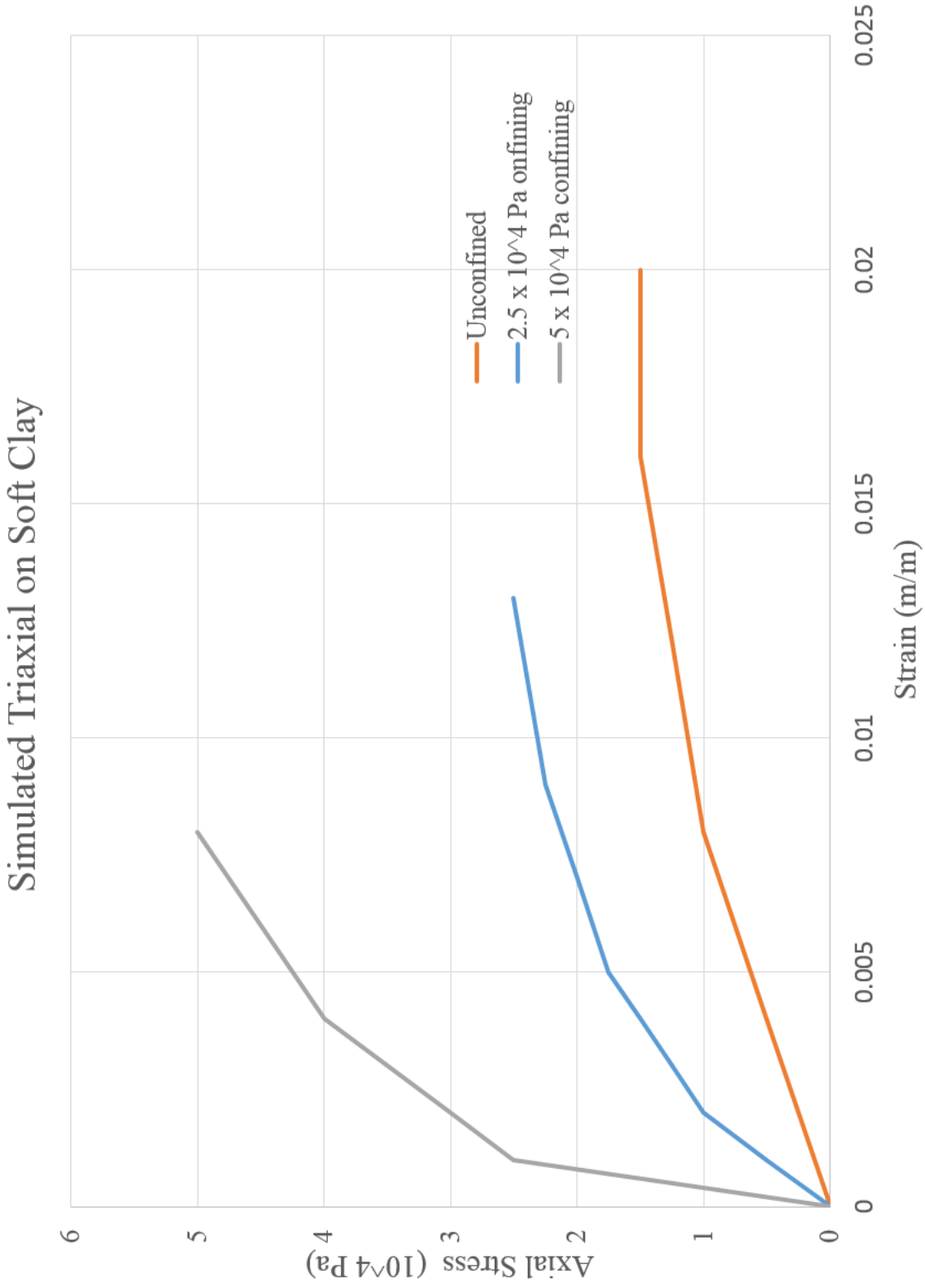

Figure 9-29. Simulated triaxial test results for soft clay

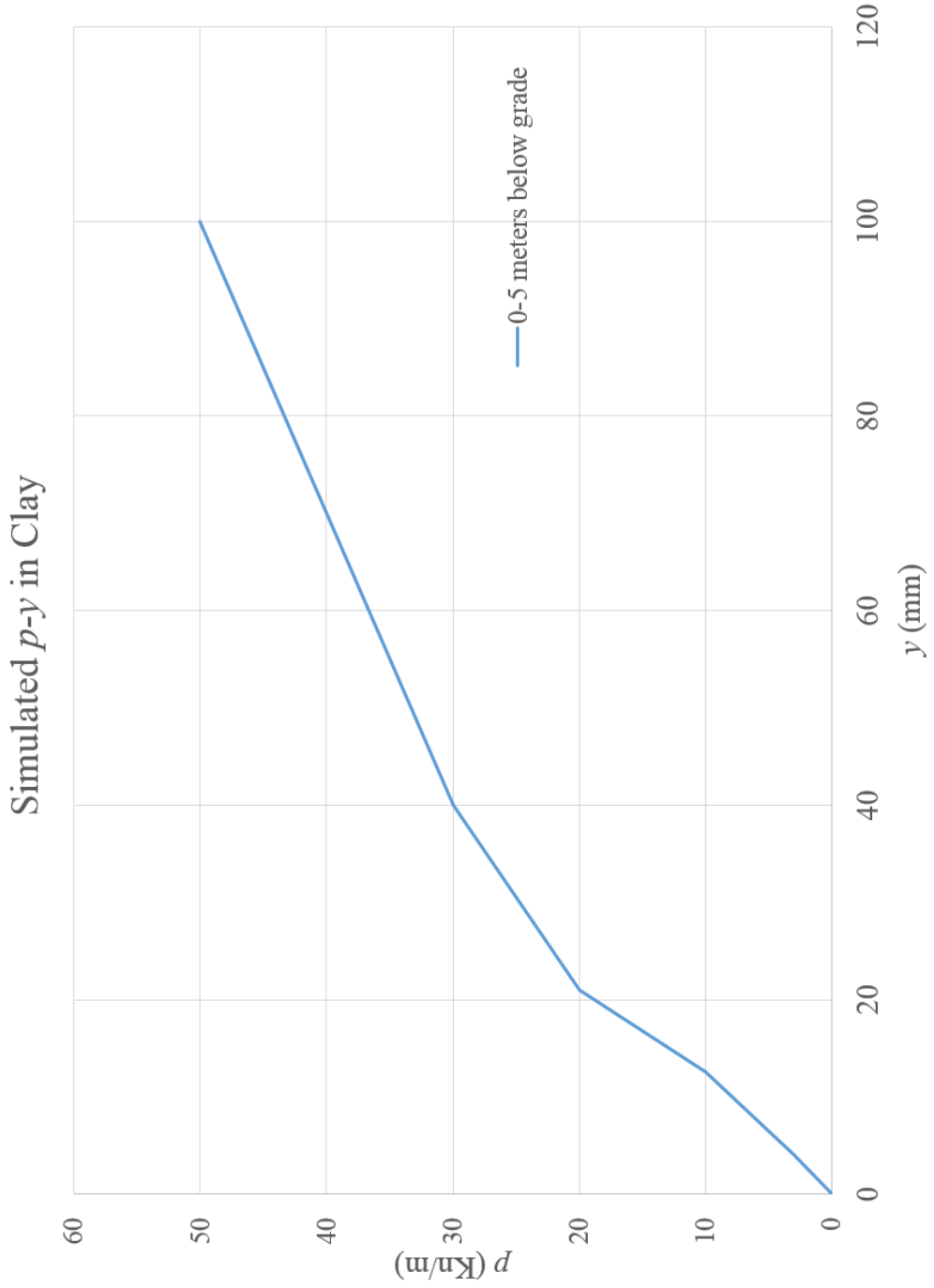

Figure 9-30. *P-y* curve generated from clay used in model

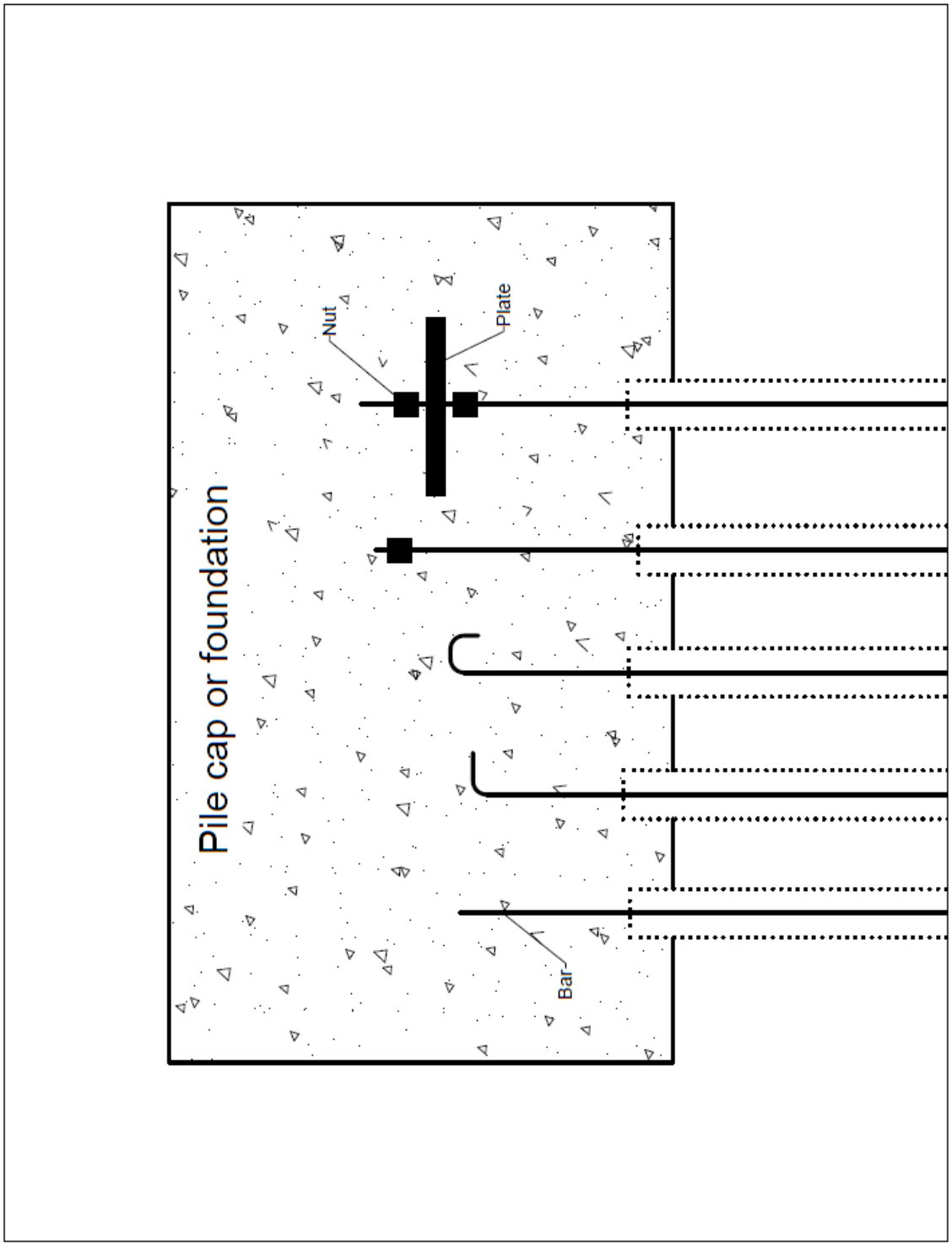

Figure 9-31. Typical micropile connections

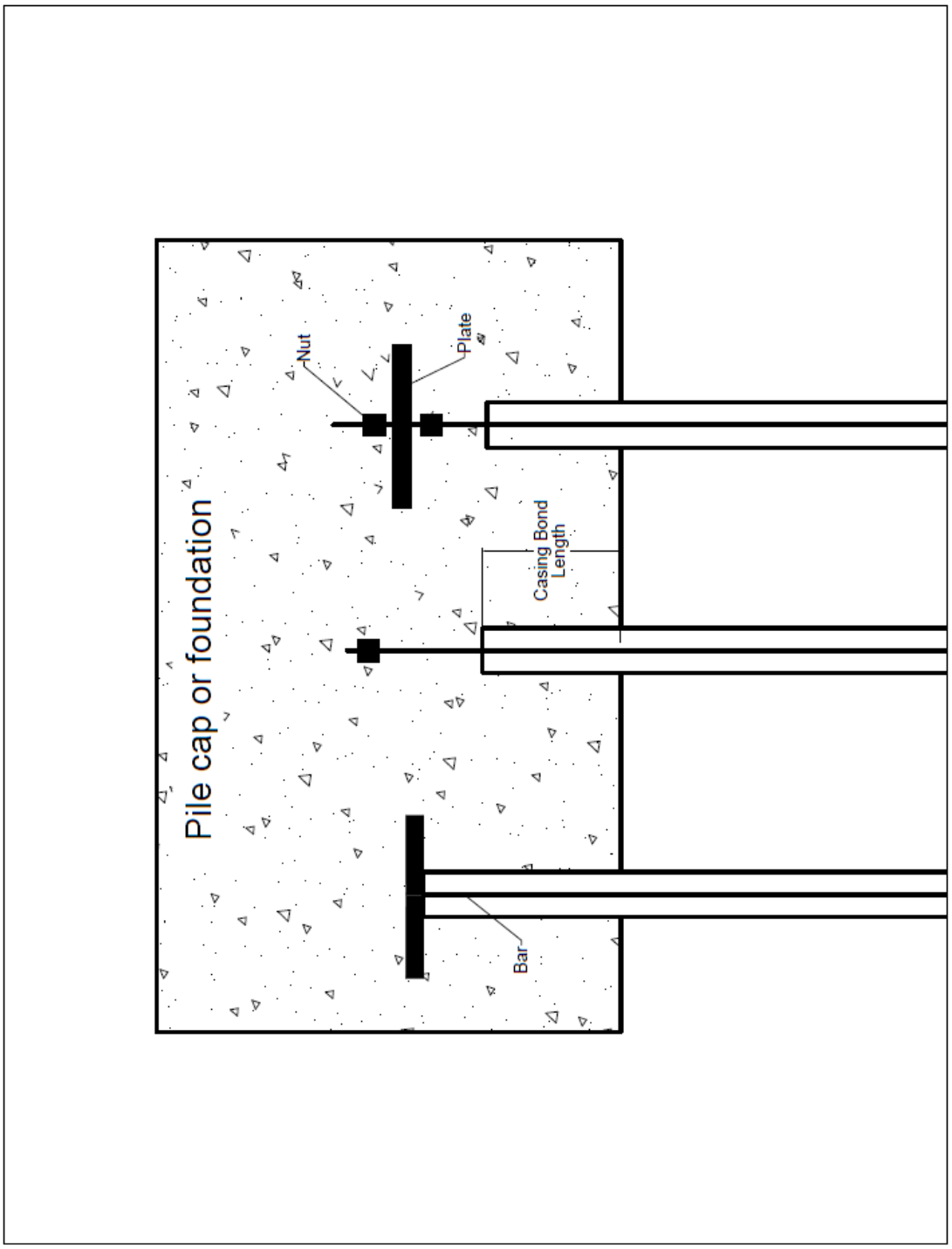

Figure 9-32. Typical high capacity micropile connections

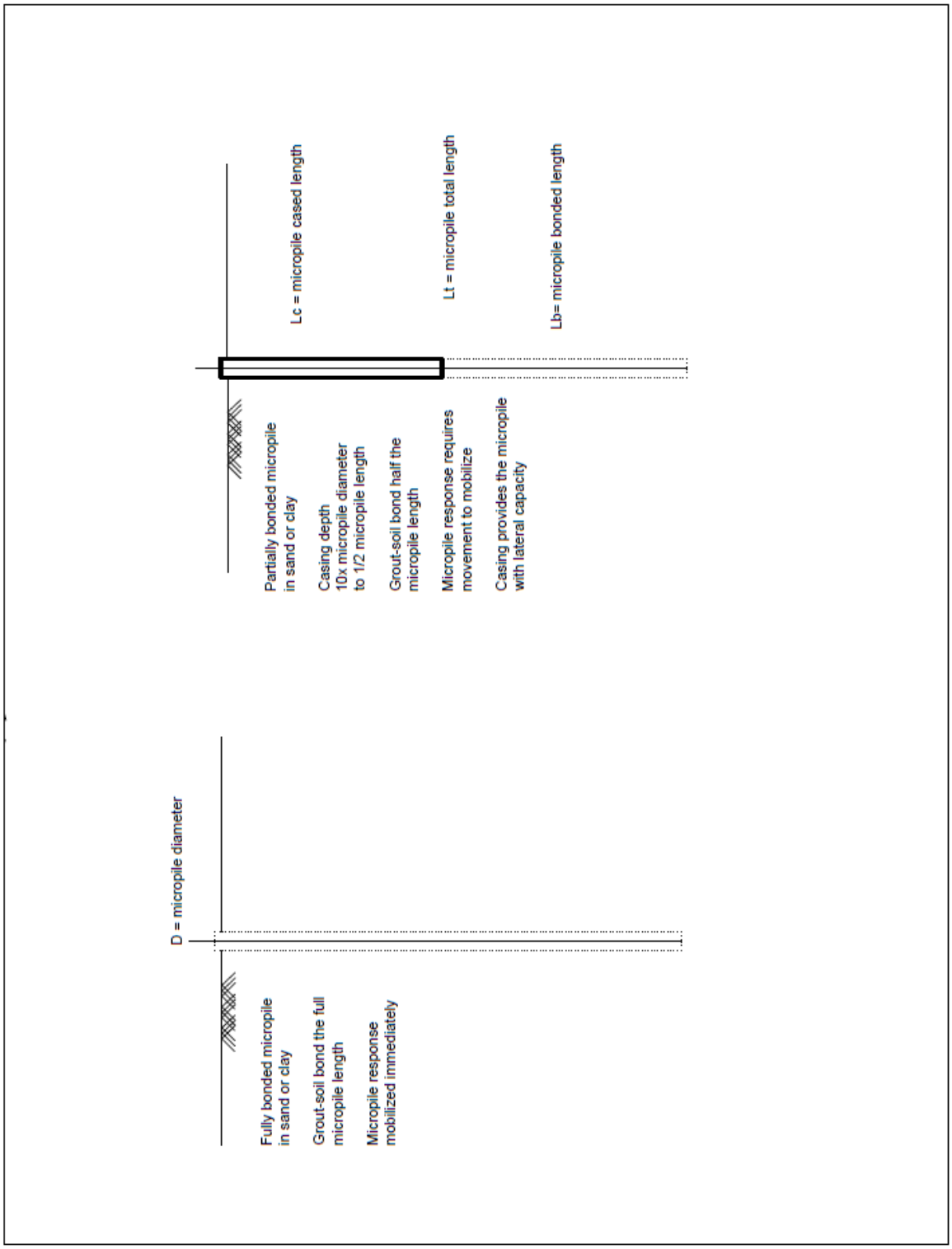

Figure 9-33. Comparison of fully bonded and partially bonded micropiles

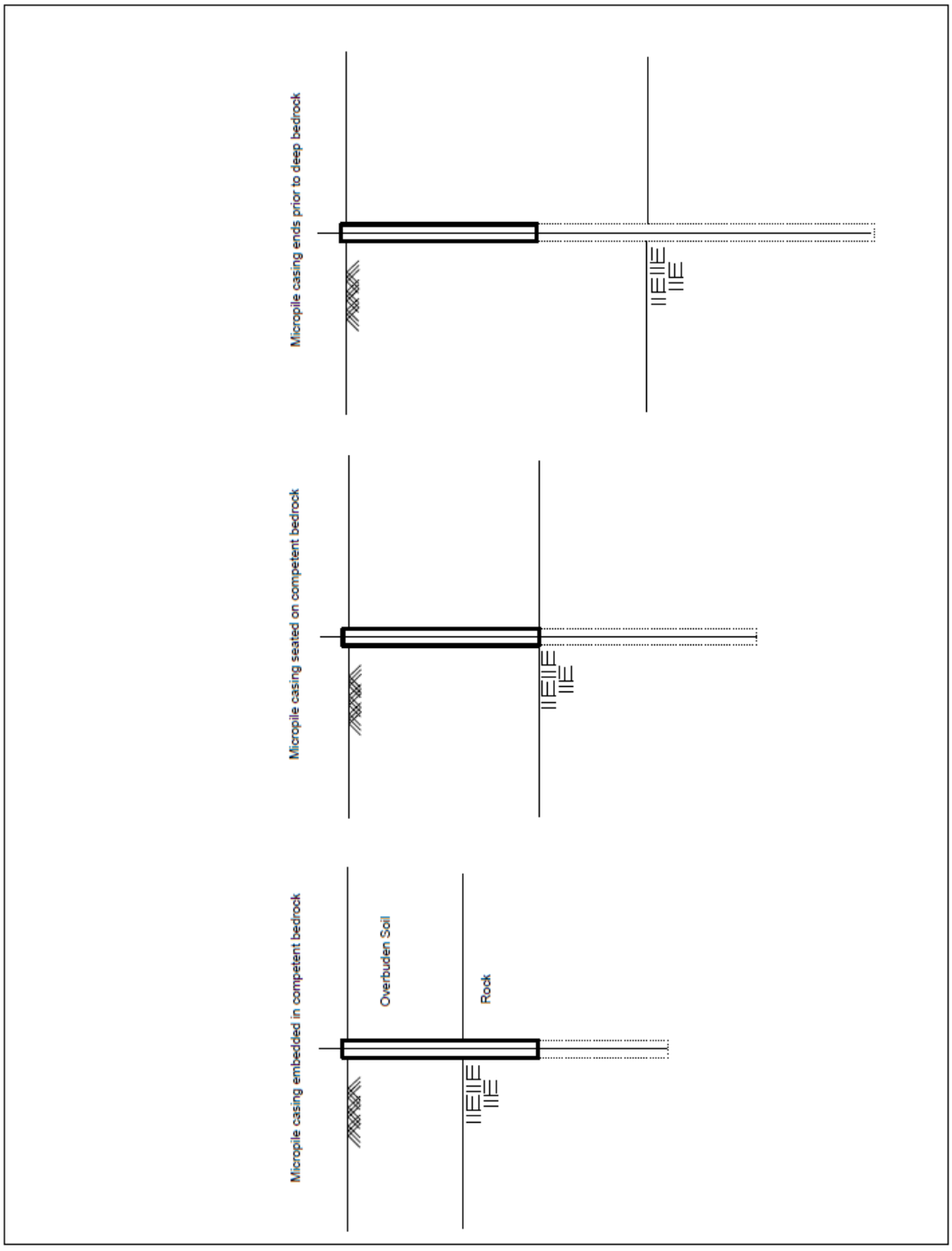

Figure 9-34. Various casing configurations when rock is present

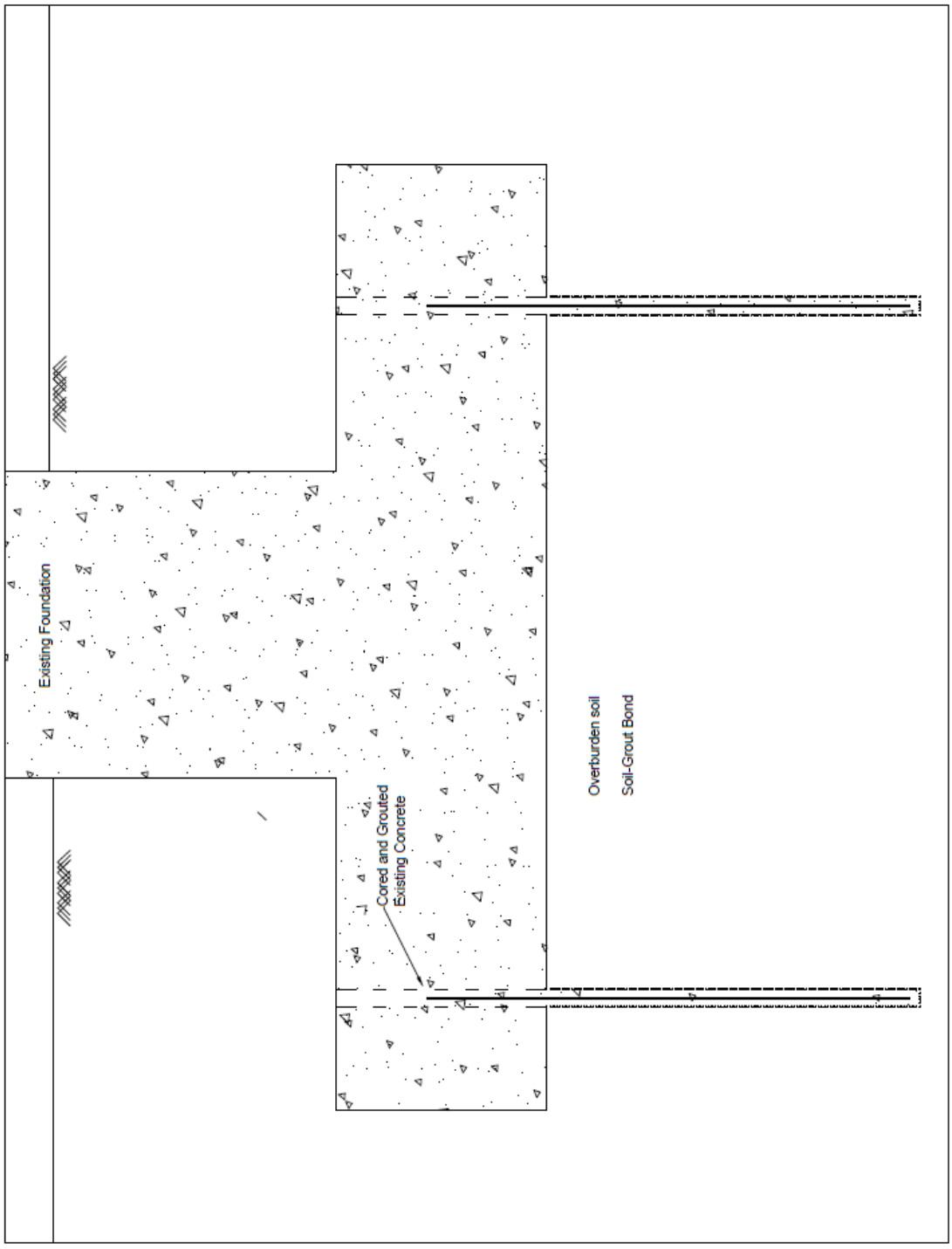

Figure 9-35. Micropile retrofit of existing foundation

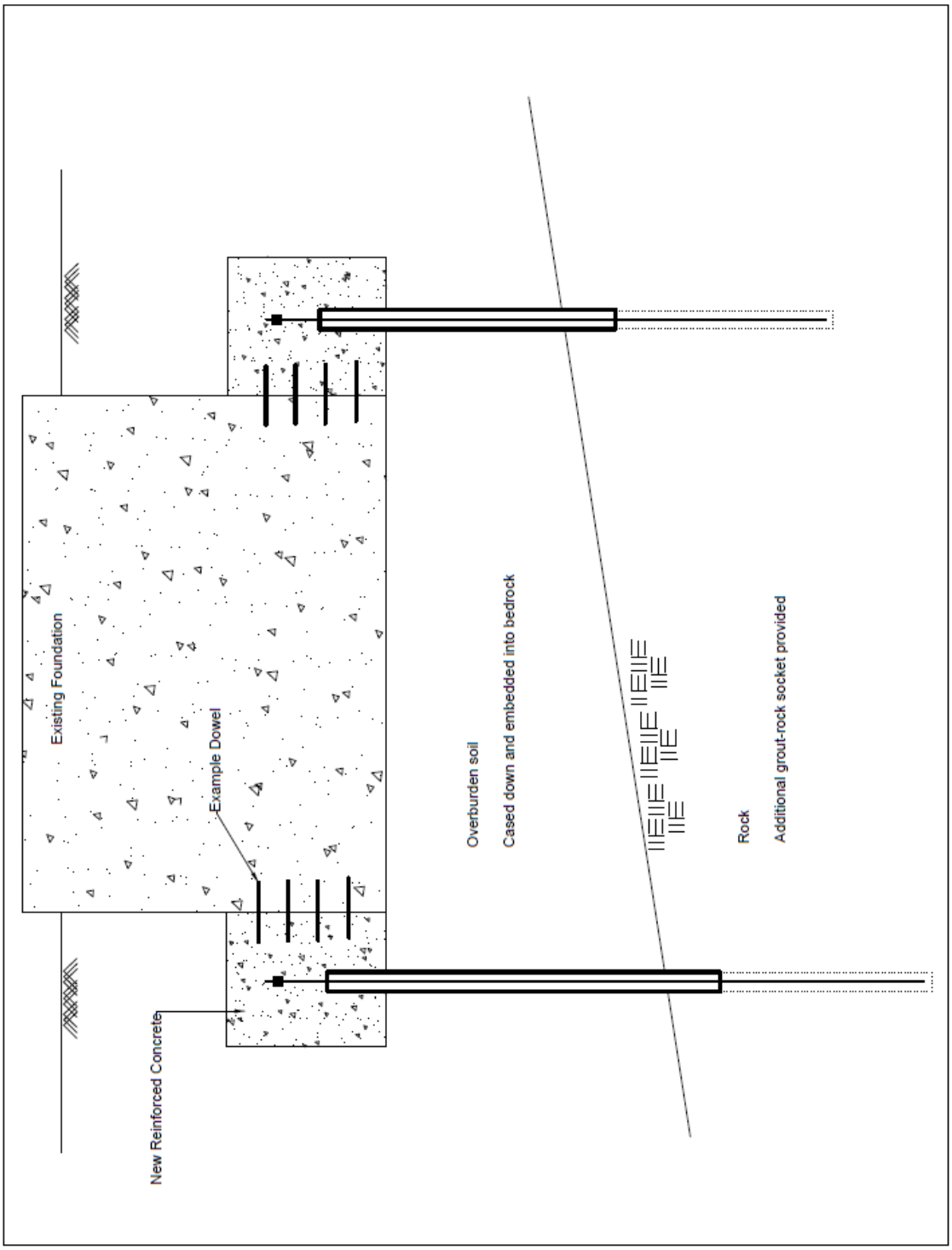

Figure 9-36. Micropile retrofit of an existing bridge foundation with rock present

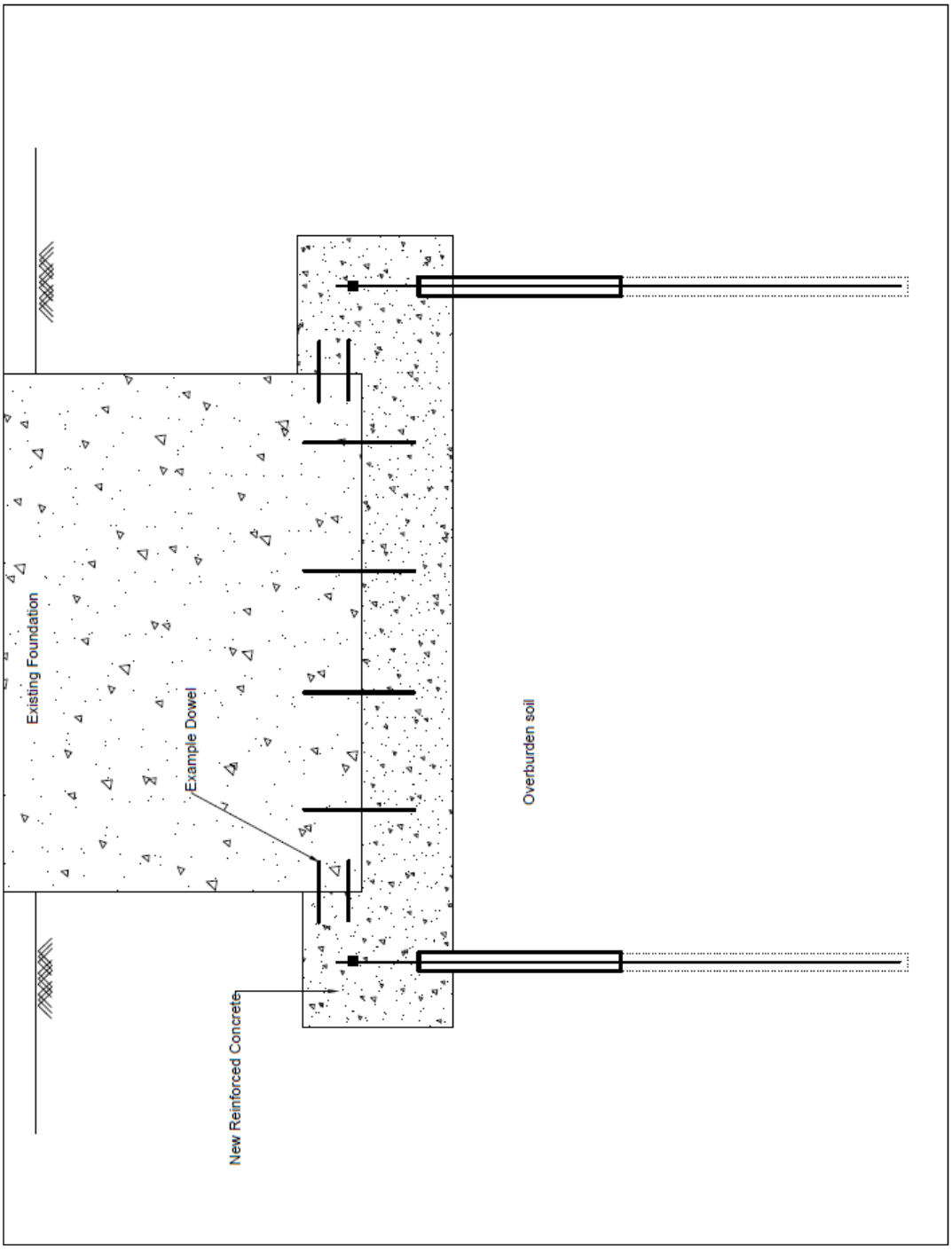

Figure 9-37. Micropile retrofit with partially bonded design

Finite Element Model Hand Calculations
Bond Stress Method, Beta Method, and Alpha Method

CLR = 0
Sand Model

Beta Method

$\boldsymbol{\beta 1} = 0.2$
$\boldsymbol{\beta 2} = 0.3$
$\boldsymbol{\beta 3} = 0.4$

$$fs1 = 0.2\pi\ (0.22m)(4m)\left(28\frac{kN}{m^2}\right) = 15.5\ kN \quad \text{(Eq. 9.1)}$$

$$fs2 = 0.3\pi\ (0.22m)(7m)\left(110.25\frac{kN}{m^2}\right) = 160\ kN \quad \text{(Eq. 9.2)}$$

$$fs3 = 0.4\pi\ (0.22m)(5.5m)\left(212.6\frac{kN}{m^2}\right) = 323\ kN \quad \text{(Eq. 9.3)}$$

$$Ft = fs1 + fs2 + fs3 = 498.5\ kN \quad \text{(Eq. 9.4)}$$

$$Qp = (0.11m)^2\ \pi\ \left(260.75\frac{kN}{m^2}\right)(10) = 99\ kN \quad \text{(Eq. 9.5)}$$

$$Q = Qp + Ft = 597.5\ kN \quad \text{(Eq. 9.6)}$$

Bond Stress Method

$$P1 = 10psi\ (\pi)(8.625\ in)(157.5\ in) = 42.7\ kips \quad \text{(Eq. 9.7)}$$

$$P2 = 15psi\ (\pi)(8.625\ in)(275.5\ in) = 112\ kips \quad \text{(Eq. 9.8)}$$

$$P3 = 20psi\ (\pi)(8.625\ in)(216.5\ in) = 117.3\ kips \quad \text{(Eq. 9.9)}$$

$$Pt = P1 + P2 + P3 = 272\ kips \quad \text{(Eq. 9.10)}$$

CLR = 0.5
Sand Model

Beta Method capacity remains the same. Capacity based on soil type.

Bond Stress Method

$$P1 = 0 \quad \text{(Eq. 9.11)}$$

$$P2 = 15psi\ (\pi)(8.625\ in)(137.75\ in) = 56\ kips \quad \text{(Eq. 9.12)}$$

$$P3 = 20psi\ (\pi)(8.625\ in)(216.5\ in) = 117.3\ kips \quad \text{(Eq. 9.13)}$$

$$Pt = P1 + P2 + P3 = 173.3\ kips \quad \text{(Eq. 9.14)}$$

CLR = 0
Clay Model

Alpha Method

$\alpha 1 = 1$
$\alpha 2 = 0.83$
$\alpha 3 = 0.56$

$$fs1 = 1\ (25\ kPa)(0.22m)(\pi)(4m) = 69\ kN \quad \text{(Eq. 9.15)}$$

$$fs2 = 0.83\ (50\ kPa)(0.22m)(\pi)(7m) = 201\ kN \quad \text{(Eq. 9.16)}$$

$$fs3 = 0.56\ (100\ kPa)(0.22m)(\pi)(5.5m) = 213\ kN \quad \text{(Eq. 9.17)}$$

$$Ft = fs1 + fs2 + fs3 = 483\ kN \quad \text{(Eq. 9.18)}$$

$$Qp = 9\ (0.11m)^2\pi\ (100\ kPa) = 34.2\ kN \quad \text{(Eq. 9.19)}$$

$$Q = Ft + Qp = 517.2\ kN \quad \text{(Eq. 9.20)}$$

CLR = 0.5
Clay Model

Alpha Method

$$fs1 = 0.5\ (25\ kPa)(0.22m)(\pi)(4m) = \ 34.5\ kN \qquad \text{(Eq. 9.21)}$$

$$fs2 = 0.415\ (50\ kPa)(0.22m)(\pi)(7m) = \ 100\ kN \qquad \text{(Eq. 9.22)}$$

$$fs3 = 0.56\ (100\ kPa)(0.22m)(\pi)(5.5m) = \ 213\ kN \qquad \text{(Eq. 9.23)}$$

$$Q = Ft + Qp = 381.7\ kN \qquad \text{(Eq. 9.24)}$$